Investigating the neuroprotective function of TLDc proteins

Daria M. Svistunova

Somerville College
Department of Physiology, Anatomy and Genetics

University of Oxford



Supervisors: Professor Peter L. Oliver
Professor Dame Kay E. Davies

Thesis submitted for the degree of Doctor of Philosophy

Trinity Term 2019

Abstract

Investigating the neuroprotective function of TLDc proteins

Daria M. Svistunova
Somerville College, University of Oxford

Submitted for the degree of Doctor of Philosophy, Trinity Term, 2019

A recent World Health Organisation Global Burden of Disease study reports a yearly increase in the prevalence of neurodegenerative diseases, with more than 100 million people worldwide expected to be living with dementia by 2050. These disorders represent a range of neurological conditions characterised by selective neuronal cell death; no effective treatments have been developed, with the available therapy only able to reduce the symptoms in some cases. Although etiology of neurodegenerative diseases is not well understood, some common pathological features are shared between them, including protein aggregation and oxidative stress. Identification of the molecular mechanisms underlying these processes would therefore deepen our understanding of the disease pathogenesis and help in the search for new therapeutic targets. Members of a conserved protein family (TLDc) have been shown in recent years to protect neurons from oxidative insults *in vitro* and *in vivo* and play a role in oxidative stress response regulation via unknown mechanism. In addition, TLDc mutations are causative in range of neurological disorders, some characterised by neurodegeneration. Therefore, further analysis of this particular protein family may provide new insights into fundamental protective mechanisms that could be harnessed in the future.

The aim of this thesis was to investigate the mechanism of action of the TLDc protein oxidation resistance 1 (Oxr1) in oxidative stress protection and in the maintenance of neural tissue homeostasis. Using a combination of *in vitro* assays and in animal models with disruption or overexpression of *Oxr1,* I have shown that Oxr1 interacts with the potent antioxidant enzyme peroxiredoxin-2 where it regulates its post-translational modifications and oligomerisation in a brain-region specific manner. I have also for the first time discovered a molecular function of Oxr1 by showing it possesses holdase chaperone activity *in vitro*, suggesting it acts as a putative chaperone. Next, to understand the cause of neurodegeneration in the Oxr1 knockout mouse, transcriptional profiling was carried out, revealing an induction of presymptomatic neuroinflammatory markers, suggesting *Oxr1* is critical for the normal inflammatory response in the brain. I have also produced preliminary data suggesting a role for Oxr1 in autophagy. Finally, computational analysis of transcriptional activity and regulation of TLDc family members suggests high degree of functional conservation between TLDc genes and their involvement in processes throughout the body, proposing novel directions for future studies. Together, my results contribute to our understanding of the functions of TLDc genes in the CNS and the role of Oxr1 in oxidative stress protection and proteostasis.

Declaration

The work presented in this thesis was performed at the Department of Physiology, Anatomy and Genetics, University of Oxford, from 2015-2019. The laboratory work was funded by a European Research Council Consolidator Award to Peter Oliver ('PAROSIN'). All work presented was conducted by the author (Daria M. Svistunova) unless otherwise stated, and no part of this thesis has been submitted for any other degree in this or any other university or institute of learning.

Acknowledgements

I would like to thank my supervisors Professor Peter Oliver and Professor Dame Kay Davies for offering me a place in their groups and giving me an opportunity to work on this amazing and challenging project. Dear Pete, thank you for your guidance, for giving me freedom in my experiments yet steering me to the right direction, for showing me the beauty of the brain.

I also want to thank Dr Mattéa Finelli for her day-to-day supervision, her support and mentoring. Dear Mattéa, you helped me grow as a scientist and as a person, you cheered me up in the moments when nothing was working and celebrated my achievements with me. Thank you for your help with the project, with the paper and with the thesis, thank you for everything.

Thank you to Dr Esther Becker, Benjamin Edwards, Dr Andreas Koschinski for his help with HyPer experiments, and all other members of Oliver, Davies and Becker groups who helped me along these years.

Thank you to all the amazing people who became my friends – Julia, Joery, Maggie, Nesrine and Alaa. Thank you for our guest nights together, for endless chats and fruitful discussions, for all the fun we had.

Last, but not the least, I want to thank my family, my dear parents and grandparents, for their love and emotional support along the way – no matter how far from home, I never felt alone. This accomplishment will not be possible without you. Dear Grisha, thank you for being my best friend and my husband, for supporting me and believing in me, I am so grateful I have you in my life.

Table of contents

Abstract 2
Declaration 3
Acknowledgements 4
Table of contents 5
List of figures and tables 7
List of abbreviations 9
1. Introduction 12
1.1 Neurodegenerative diseases 12
1.1.1 Oxidative stress 12
1.1.2 Protein aggregation 18
1.1.3 Neuroinflammation 20
1.2 TLDc protein family 24
1.2.1 Oxidation resistance 1 27
1.2.2 Nuclear receptor coactivator 7 34
1.2.3 TBC domain family, member 24 36
1.2.4 mTOR associated protein, eak-7 homologue 39
1.2.5 C20Orf118 40
Experimental aims of the thesis 41
2. Materials and Methods 45
2.1 Animals 45
2.2 Expression constructs 48
2.3 Cell culture, transfection and treatment 48
2.3.1 Neuro2a cell line 48
2.3.2 Primary cerebellar neuron culture 49
2.3.3 Cell treatment 49
2.3.4 Immunocytochemistry 50
2.4 Protein extraction, immunoprecipitation and western blotting 50
2.4.1 SDS-PAGE 50
2.4.2 Blue Native-PAGE 51
2.5 Recombinant protein production and purification 53
2.6 In vitro activity assays 55
2.6.1 Peroxiredoxin activity assay 55
2.6.2 Holdase activity assay 55
2.7 Embryo dissecting and genotyping 56
2.7.1 Embryo dissections 56
2.7.2 Embryo DNA extraction 56
2.8 RNA preparation and qPCR reaction 57
2.8.1 cDNA sample preparation 57
2.8.2 Primers optimisation 58
2.8.3 qPCR reaction 58
2.9 Data analysis and statistics 59
3. Analysis of Oxr1 interaction with a potent antioxidant enzyme Prdx2 61
3.1 Introduction 61
3.2 Results 67
3.2.1 Oxr1 interacts with Prdx2, one of the major antioxidant enzymes in the CNS 67
3.2.2 Oxr1 and Prdx2 do not interact functionally to protect against OS-induced cell death 68
3.2.3 Oxr1 does not regulate Prdx2 antioxidant activity *in vitro* 71
3.2.4 Oxr1 and Prdx2 both prevent protein aggregation *in vitro* 73

3.2.5 A novel molecular function of Oxr1 as a holdase chaperone ... 75
3.2.6 Oxr1 modulates PTMs of Prdx2 *in vitro* and *in vivo* ... 78
3.2.7 Oxr1 modulates oligomeric state of Prdx2 *in vitro* and *in vivo* ... 81
3.2.8. Ncoa7-FL modulates Prdx2 hyperoxidation *in vitro* ... 84
3.3 Discussion ... 85
3.3.1 The mechanism and the role of TLDc proteins interaction with Prdx2 ... 85
3.3.2 The mechanisms of Prdx2 PTMs regulation by Oxr1 ... 89
3.3.3 Oxr1 is a novel putative holdase chaperone ... 94
Conclusion ... 95

4. Investigating the role of Oxr1 in brain function and homeostasis ... 96
4.1 Introduction ... 96
4.2 Results ... 99
4.2.1 Microarray transcription profiling of pre-symptomatic *Oxr1*$^{d/d}$ cerebella identifies up-regulation of microglial genes ... 99
4.2.2 Oxr1 deletion affects levels of autophagy *in vivo* ... 108
4.2.3 Oxr1 co-localizes with Golgi apparatus and is present in synapses ... 111
4.3 Discussion ... 115
4.3.1 The role of Oxr1 in neuroinflammation ... 115
4.3.2 Possible role of Oxr1 at the synapse ... 123
4.3.3 Limitations of the approach ... 125
Conclusion ... 126

5. Analysis of regulatory and functional conservation of the TLDc gene family ... 127
5.1 Introduction ... 127
5.2 Results ... 137
5.2.1 Oxr1 and Ncoa7 are potentially involved in similar pathways during development ... 137
5.2.2 Disruption of *Ncoa7-FL* expression results in deregulation of TLDc genes ... 147
5.2.3 *Ncoa7* locus deletion leads to deregulated expression of other TLDc genes ... 151
5.2.4 *Ncoa7* locus deletion does not lead to aberrant glia activation ... 153
5.2.5 *Oxr1* and *Ncoa7* are both required for successful early embryonic development ... 155
5.2.6 *Ncoa7* deletion exacerbates neuroinflammation in *Oxr1*$^{d/d}$ mouse cerebellum ... 158
5.3 Discussion ... 161
5.3.1 Evolutionary conservation of TLDc genes functions and regulation mechanisms ... 161
5.3.2 Disruption of *Ncoa7* expression leads to deregulation of other TLDc genes ... 165
5.3.3 Possible roles of *Ncoa7* in the organism ... 168
5.3.4 *Ncoa7* deletion exacerbates neuroinflammation in *Oxr1*$^{d/d}$ mouse cerebellum ... 171
5.3.5 Expression of both *Oxr1* and *Ncoa7-FL* is required for mouse embryo development ... 173
Conclusion ... 175

6. Final discussion ... 176

Appendix 1 ... 190

Appendix 2 ... 192

Appendix 3 ... 213

References ... 214

List of figures and tables

Figures

Figure 1.1 Formation of ROS from superoxide anion. 13
Figure 1.2 Factors contributing to development of neurodegeneration. 23
Figure 1.3 Domain architecture of TLDc protein family members. 24
Figure 1.4 TLDc genes expression in adult mouse brain. 25
Figure 1.5 Oxr1 isoform diversity. 29
Figure 1.6 Disease-causing mutations in TBC1D24 protein. 38
Figure 2.1 Schematic overview of *Oxr1* knockout mouse lines used in the work. 46
Figure 2.2 Schematic overview of *Ncoa7* knockout mouse lines used in the work. 47
Figure 2.3 Recombinant Prdx2 and Oxr1 production and purification. 54
Figure 3.1 Catalytic cycle of peroxiredoxin. 66
Figure 3.2 Oxr1 and Prdx2 bind in the brain, but do not have synergistic effect in cell death protection. 70
Figure 3.3 Oxr1 does not modulate Prdx2 antioxidant activity *in vitro*. 72
Figure 3.4 Presence of His6 tag affects assembly of Prdx2 HMW complexes. 74
Figure 3.5 Both Prdx2 and Oxr1 possess holdase chaperone activity *in vitro*. 77
Figure 3.6 Oxr1 modulates Prdx2 hyperoxidation *in vitro* and *in vivo*. 80
Figure 3.7 Oxr1 plays a role in the regulation of Prdx2 oligomeric state *in vitro* and *in vivo*. 83
Figure 3.8 Ncoa7-FL modulates Prdx2-$SO_{2/3}$ levels *in vitro*. 84
Figure 3.9 TLDc proteins possess canonical Prdx-binding motifs. 87
Figure 3.10 Oxr1 modulates SNO-Prdx2 levels *in vivo*. 91
Figure 4.1 Graphic overview of microarray results. 100
Figure 4.2 Validation of the microarray targets by RT-qPCR at P14, P18 and P22. 105
Figure 4.3 Comparison of expression of selected up-regulated genes in cortex and cerebellum at P18. 106
Figure 4.4 Oxr1 knockout leads to microglia activation at P22 in the cortex, hippocampus and cerebellum. 107
Figure 4.5 Oxr1 deletion affects levels of autophagy, but not lysosomes and endosomes, in the cortex. 110
Figure 4.6 Oxr1 colocalises with Golgi apparatus and is present in synapses. 114
Figure 5.1 *Oxr1* and *Ncoa7* are co-expressed in the brain. 131
Figure 5.2 Schematic overview of Ncoa7 knockout mouse lines used in the work. 136
Figure 5.3 Exon and domain composition of Oxr1 transcript variants and proteins. 139
Figure 5.4 TLDc genes transcripts and promoter activities in mouse genome. 144
Figure 5.5 Ncoa7-FL knockout leads to deregulation of other TLDc family members' expression. 150
Figure 5.6 *Ncoa7* locus deletion leads to deregulated expression of other TLDc genes. 152
Figure 5.7 *Ncoa7* deletion does not cause aberrant neuroinflammatory response. 154
Figure 5.8 Heterozygous deletion of *Ncoa7* in *Oxr1* knockout mouse exacerbates neuroinflammatory phenotype in the cerebellum at P22. 160
Figure S1. Alignment of protein sequences of TLDc domains of family members from mouse and human. 190
Figure S2. Oxr1:Prdx2 co-immunoprecipitation from cerebrum and cerebellum tissues. 191

Tables

Table 1.1. Organism-wide expression of TLDc genes in mouse organs. 26
Table 1.2 Summary of TLDc proteins structure and functions. 41
Table 2.1. Antibodies used for immunocytochemistry and western blotting. 52
Table 2.2. qPCR primers. 59
Table 4.1. List of differentially expressed genes identified by microarray. 103
Table 4.2. Gene Ontology pathway analysis of up-regulated genes. 104
Table 4.3. Relative Oxr1 expression levels in different brain cell types 116
Table 5.1. Generation of *Oxr1*$^{d/d}$*/Ncoa7*$^{del/del}$ mouse. 157
Table 5.2. Generation of *Oxr1*$^{d/d}$*/Ncoa7*$^{del/del}$ mouse. 157
Table 5.3. Generation of *Oxr1*$^{d/d}$*/Ncoa7*$^{tm1.1/tm1.1}$ mouse. 157
Table S1. Transcription factors and other DNA-binding proteins known to bind TLDc promoters regions 192
Table S2. Biological processes represented by TFs as predicted by Gene Ontology 199

List of abbreviations

5'UTR – 5' untranslated region
6-OHDA – 6-hydroxydopamine
8-OH-dG – oxidized deoxyguanosine
Aβ – amyloid β
Abra – actin-binding Rho-activating protein
Actc – actin alpha cardiac muscle
AD – Alzheimer's disease
AhR – aryl hydrocarbon receptor
ALPL – alkaline phosphatase
ALS – amyotrophic lateral sclerosis
AMPK – AMP-activated protein kinase
APP – amyloid precursor protein
Arf6 – ADP-ribosylation factor 6
ATP6VB1 – V-type proton ATPase subunit B, kidney isoform
AtTDX – *Arabidopsis thaliana* protein tetratricoredoxin
BBB – blood-brain barrier
Bcl11b – B-cell lymphoma/leukemia 11B
C1q – complement component 1, q subcomponent
C1qa – complement component 1, q subcomponent, A chain
C1qb – complement component 1, q subcomponent, B chain
C1qc – complement component 1, q subcomponent, C chain
C20Orf118 – chromosome 20 open reading frame 118
CAGE – cap analysis gene expression
Cbfb – core-binding subunit beta
Ccl3 – chemokine (C-C motif) ligand 3
Ccl9 – chemokine (C-C motif) ligand 9
Cd68 – cluster of differentiation 68
Cdk5 – cyclin-dependent kinase 5
CGCs – cerebellar granule cells
ChIP-seq – chromatin immunoprecipitation sequencing
CIL – contact inhibition of locomotion
CK2 – casein kinase II
CLN – ceroid-lipofuscinosis neuronal protein
CNS – central nervous system
CS – citrate synthase
CSP – cysteine string protein
Ctsd – cathepsin D
Ctss – cathepsin S
Ctsz – cathepsin Z
Cx3cl1 – chemokine (C-X3-C motif) ligand 1
Cx3cr1 – chemokine (C-X3-C motif) receptor 1
DAF-16/FoxO – abnormal dauer formation protein 16/forkhead box protein O
DDX3X – DEAD-box helicase 3 X-linked
DE – differentially expressed
DJ-1 – Parkinson disease protein 7
dod-3 – downstream of DAF-16
eak-7 – enhancer of akt-1 null 7
eIF2 – eukaryotic initiation factor 2
ER – endoplasmic reticulum
ERα – estrogen receptor α
ERβ – estrogen receptor β
ERbd – estrogen receptor-binding domain
ESCs – embryonic stem cells
FcγrIIb – low affinity immunoglobulin γ Fc region receptor II
FcR – Fc receptor
FcrlS – Fc receptor-like S, scavenger receptor
FF – fully folded
FTLD – frontotemporal lobar dementia
FUS – fused in sarcoma
Gapdh – glyceraldehyde 3-phosphate dehydrogenase
Get3 – guided entry of tail-anchored proteins 3
Gfap – glial fibrillary acidic protein
GO – Gene Ontology
Gpi1 – glucose-6-phosphate isomerase
Gpx – glutathione peroxidase
GRAM – glucosyltransferases, Rab-like GTPase activators and myotubularins
Grp78 – glucose-regulated protein 78
GSH – glutathione
Gstm1 – glutathione-S-transferase Mu 1
Gstp1 – glutathione-S-transferase Pi 1
H3K4Me3 – trimethylation of histone H3 at lysine 4
HD – Huntington's disease
Hdac – histone deacetylase
HexB – hexosaminidase B
His6 – hexahistidine tag
HMW – high molecular weight
HO-1 – heme oxygenase-1

Hsc70 – heat shock cognate 70
HSF1 – heat shock factor 1
HSP – heat shock protein
Iba1 – ionized calcium-binding adapter molecule 1
IFN – interferon
Ire1 – inositol-requiring enzyme 1
Irf – interferon regulatory factor
JNK – Jun kinase
Keap1 – kelch-like ECH-associated protein 1
LAMP1 – lysosome-associated membrane protein 1
LC3 – microtubule-associated proteins 1A/1B light chain 3B
Lgals9 – lectin, galactose binding, soluble 9
LIF – leukemia inhibitory factor
LSD – lysosomal storage disorders
LU – locally unfolded
Ly86 – lymphocyte antigen 86
LysM – lysin motif
MAPT – microtubule-associated protein tau
mEAK7 – mTOR associated protein, eak-7 homologue
MPS – mucopolysaccharidosis
mtHSP70 – mitochondrial chaperone HSP70, mortalin
mtl-1 – metallothionein-1
MPTP – 1-methyl-4phenyl-1,2,3,6-tetrahydropyridine
mTOR – mechanistic/mammalian target of rapamycin
NADPH – nicotinamide adenine dinucleotide phosphate
NCL – neuronal ceroid lipofuscinosis
Ncoa7 – nuclear receptor coactivator 7
Ncoa7-B – nuclear receptor coactivator 7, short isoform
Ncoa7-FL – nuclear receptor coactivator 7, full-length isoform
NDD – neurodegenerative disease
Neurod2 – neurogenic differentiation factor 2
nGD – neuropathic Gaucher disease
NMD – nonsense-mediated decay
NMNAT2 – nicotinamide mononucleotide adenylyltransferase 2
NPC – Niemann-Pick type C
NQO1 – NAD(P)H dehydrogenase [quinone] 1
Nrf2 – nuclear factor erythroid 2 (NFE2)-related factor 2
OS – oxidative stress
Oxr1 – oxidation resistance 1
Oxr1-C – oxidation resistance 1, short isoform
Oxr1-FL – oxidation resistance 1, full-length isoform
Panx1 – pannexin1
Pax6 – paired box 6
PD – Parkinson's disease
PERK - PKR-like ER kinase
Pin1 – peptidyl-prolyl cis/trans isomerase NIMA-interacting 1
Pomc – pro-opiomelanocortin peptide
PP2A – protein phosphatase 2A
PPARγ – peroxisome proliferator-activated receptor γ
Prdx – peroxiredoxin
PTM – post-translational modification
Rab-GAP – Rab-GTPase activating protein
RARα – retinoic acid receptor α
RNA-Seq – RNA sequencing
ROS – reactive oxygen species
SGT – small glutamine-rich tetratricopeptide repeat-containing protein
SIRT2 – sirtulin-2
SLI - specific language impairment
SNAP-25 – synaptosomal-associated protein 25
SNX14 – sorting nexin 14
SOD – superoxide dismutase
SRC-1 – steroid receptor coactivator 1
SRCR – scavenger receptor cysteine-rich
STAT – signal transducer and activator of transcription
TBC – Tre2/Bub2/Cdc16
TBC1D24 – TBC domain family, member 24
TDP-43 – transactive response DNA binding protein 43 kDa
TF – transcription factor
TGN – trans-Golgi network
TLDc – Tre2/Bub2/Cdc16 (TBC), lysin motif (LysM), domain catalytic
TLR – toll-like receptor
TNFRSF11B – tumor necrosis factor receptor superfamily 11b
TNPO1 – transportin
TRβ – thyroid receptor β

Trem2 – Triggering receptor expressed on myeloid cells 2
Trx – thioredoxin
TSS – transcription start site
Tyrobp – TYRO protein tyrosine kinase binding protein
UPR – unfolded protein response
VAPB – vesicle-associated membrane protein-associated protein
Xbp1 – X-box-binding protein 1
XO – xanthine oxidase

1. Introduction

1.1 Neurodegenerative diseases

Neurodegenerative diseases (NDDs) are a heterogeneous group of neurological disorders characterized by dysfunction and subsequent degeneration of particular subpopulations of neurons. NDDs affect more than 50 million people worldwide and represent a significant burden on the healthcare system (Study, 2016, Prince et al., 2013). Neurodegeneration is an age-dependent process and therefore prevalence of NDDs is increasing globally (Prince et al., 2013). Accumulation of β-amyloid, hyperphosphorylated tau and α-synuclein, as well as loss of brain volume, neuronal death and synaptic dystrophy, signs of neurodegeneration, are observed in majority of aged people, however in the case of NDD, loss of brain connectivity typically results in significant cognitive or/and movement impairment (Elobeid et al., 2016, Wyss-Coray, 2016). Alzheimer's disease (AD), Parkinson's disease (PD), Huntington's disease (HD) and amyotrophic lateral sclerosis (ALS) are four major NDDs, accounting for 60-80% of all NDD cases (Erkkinen et al., 2018). There is no effective treatment available and existing therapies only reduce the symptoms of the disease (Chen and Pan, 2014). While the etiology of NDDs remains unclear, multiple factors are believed to play a role in the onset and progression of neurodegeneration, including oxidative stress (OS), protein misfolding and aggregation, and neuroinflammation (Gandhi and Abramov, 2012, Kumar et al., 2016, Patten et al., 2010, Ransohoff, 2016). Thus, understanding the role of these factors in the mechanisms and pathways underlying the pathogenesis of NDDs is essential for development of effective therapeutic approaches.

1.1.1 Oxidative stress

OS arises from imbalance between production of reactive oxygen species (ROS) by the cell and its ability to neutralize these toxic compounds. ROS are chemically reactive

compounds containing oxygen, including superoxide anion ($\bullet O_2^-$), hydrogen peroxide (H_2O_2) and hydroxyl radical ($\bullet OH$). The major source of ROS in eukaryotic cells is mitochondrial respiratory chain, where electron leaks in complex I and complex III result in production of $\bullet O_2^-$ (Collin, 2019). Other sources of ROS include nicotinamide adenine dinucleotide phosphate (NADPH) oxidase, xanthine oxidase (XO), cytochrome P450 and peroxisomes (Brieger et al., 2012, Collin, 2019). $\bullet O_2^-$ is considered a primary ROS as it can give rise to other types of ROS through enzyme-catalised process or via direct reaction with another molecule (Fig. 1.1), but the molecule is short-lived and is not as reactive as other species (Brieger et al., 2012, Buonocore et al., 2010). The most powerful oxidant among ROS is hydroxyl radical that readily reacts with all types of cellular molecules; H_2O_2 reacts poorly with biological molecules due to high activation energy barrier, but can be converted into $\bullet OH$ via Fenton reaction catalised by iron ions, thus possessing indirect toxicity (Collin, 2019).

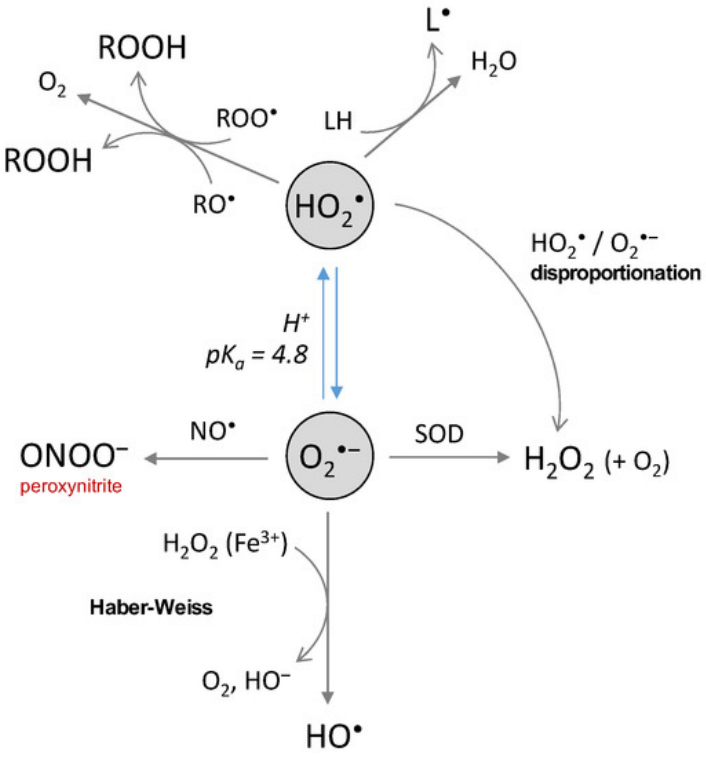


Figure 1.1 Formation of ROS from superoxide anion.
Chemical reactions between $\bullet O_2^-$ and other molecules or enzyme-catalysed reactions leading to formation of other ROS and radicals. From (Collin, 2019).

Some ROS, such as H_2O_2, act as intracellular messengers and play important roles in signal transduction, cell motility regulation and other processes (Rudzka et al., 2015, Thannickal and Fanburg, 2000). In neurons, ROS have been shown to play a vital role in synaptic plasticity, differentiation of neuron precursors and neurite outgrowth (Beckhauser et al., 2016). However, excessive accumulation of ROS may cause detrimental effects on homeostasis and cell survival. OS has been shown to be associated with oxidative DNA damage, oxidation of lipids and proteins, inactivation of enzymes, and in high concentrations ROS can even lead to activation of the apoptosis pathway (Ott et al., 2007). Therefore, numerous antioxidant mechanisms are also in place in tissues and cells to neutralize excessive ROS production and prevent the oxidation of cellular components.

Endogenous antioxidants can be divided into two classes – enzymatic and non-enzymatic (Birben et al., 2012). Antioxidant enzymes represent a diverse group of proteins that can react with and neutralize various types of ROS (Birben et al., 2012). For example, widely expressed superoxide dismutase (SOD) enzymes catalyze the conversion of highly reactive superoxide radical into H_2O_2 (Miller, 2012). H_2O_2, in its turn, is scavenged by catalase, peroxiredoxins (Prdx), thioredoxin (Trx) and glutathione peroxidase (Gpx) proteins (Birben et al., 2012). Catalase is a ubiquitously expressed peroxisomal enzyme capable of H_2O_2 neutralization and detoxification of other toxic compounds, such as methanol or formate (Glorieux and Calderon, 2017). Members of the Prdx family act on reduction of H_2O_2, lipid peroxides and peroxynitrites, while thioredoxins reduce oxidized catalytic cysteine residues to revert antioxidant enzymes back to their active state (Rhee, 2016). Gpx family consists of eight members in human, all of which catalyze the reduction of H_2O_2 or lipid hydroperoxides via oxidation of glutathione molecule (GSH) (Brigelius-Flohe and Maiorino, 2013). GSH, the most abundant antioxidant molecule in the organism, is an example of non-enzymatic ROS scavengers – these molecules do not possess any

catalytic activity and neutralize reactive molecules by direct reaction (Birben et al., 2012). Non-enzymatic antioxidants include enzyme cofactors (such as GSH, selenium or coenzyme Q_{10}) or radical scavengers (such as uric acid or vitamins A, C and E) (Birben et al., 2012, Huang et al., 2005, Nimse and Pal, 2015). Some of these molecules, such as coenzyme Q_{10}, uric acid or GSH, are synthesized in the organism, while vitamins C, E and carotenoids are dietary (Bouayed and Bohn, 2010, Mironczuk-Chodakowska et al., 2018).

During OS, expression of enzymatic antioxidant proteins is regulated by nuclear factor erythroid 2 (NFE2)-related factor 2 (Nrf2) transcription factor (Ma, 2013). Under basal conditions, Nrf2 forms a complex with kelch-like ECH-associated protein 1 (Keap1), leading to its ubiquitination and degradation. In OS conditions, the interaction between Nrf2 and Keap1 is disrupted by modification of cysteine residues in Keap1 molecule, resulting in translocation of free Nrf2 into the nucleus and induction of expression of several genes, including *SOD3*, *Gpx*, *Prdx1*, *Prdx6* and other (Ma, 2013). Thus, an extensive network of antioxidant molecules and mechanisms of regulation exist to balance the formation of endogenous and occurrence of exogenous ROS to prevent OS and oxidative cellular damage.

The brain is one of the most metabolically active tissues in the human body, utilizing approximately 20% of total oxygen consumption at rest (Mink et al., 1981). Neuronal cells require high levels of O_2 for ion transporters to sustain membrane potential and for synthesis of neurotransmitters, both required for signal transmission, but display reduced antioxidant capacity compared to non-neuronal cells, such as astrocytes or microglia (Clarke and Sokoloff, 1999, Zhang et al., 2014b); therefore, neuronal cells may be exposed to especially high levels of ROS. Furthermore, as neuronal cells are post-mitotic and cannot divide, oxidative damage and excessive accumulation of ROS would lead to irreversible neuronal and tissue damage (Gilgun-Sherki et al., 2001). Studies have demonstrated that OS plays an important role in both pathogenesis and progression of many neurological

disorders and mutations in some antioxidant genes have been identified in familial forms of NDDs. For example, almost 200 different mutations in *SOD1* have been linked with approximately 20% of all familial ALS cases (Abel et al., 2013, Kiernan et al., 2011). These mutation have been shown to significantly reduce overall dismutase activity of SOD1 in patients' tissues and shorten the protein half-life, leading to an increase in ROS levels (Saccon et al., 2013). Mutations in the PD-associated protein DJ-1, a multifunctional protein acting on OS sensing and response, disrupt its protective function and account for 1-2% of early onset PD cases (Ariga et al., 2013, Pankratz et al., 2006). Multiple disease-causing mutations have been shown to disrupt protease and chaperone activities of DJ-1, rendering it unable to protect against H_2O_2-induced cell death, and also affecting its folding, dimerisation and stability (Strobbe et al., 2018). DJ-1 has also been shown to prevent degradation and ubiquitination of Nrf2 transcription factor, suggestion its mutations could disrupt this function resulting in an insufficient OS response (Raninga et al., 2017).

A detectable increase in markers of OS, such as levels of oxidized deoxyguanosine (8-OH-dG) in DNA and RNA, protein oxidation and nitration and lipid peroxidation has been reported in *post mortem* brain tissues of individuals affected by the major NDDs (Navarro-Yepes et al., 2014, Reed et al., 2009, Reed, 2011, Zhang et al., 1999). Importantly, these markers are also detected in peripheral blood and cerebrospinal fluid of patients with AD, PD, ALS and HD during the course of the disease (Andican et al., 2012, Gmitterova et al., 2018, Medeiros et al., 2016, Robelin and Gonzalez De Aguilar, 2014, Sanchez-Lopez et al., 2012, Skoumalova and Hort, 2012), as well as pre-symptomatically in mouse models of these disorders (Chang et al., 2008, Halter et al., 2010, Hartl et al., 2012). These data suggest that OS is likely to be contributing to the neurodegeneration process and play a role in the onset and/or progressions of the diseases. Given the importance of OS in the ND process, antioxidant treatment has been proposed as potential therapeutic approach for NDDs. Few

studies report positive effect after prolonged curcumin, vitamin E or coenzyme Q10 antioxidant administration in order to reduce global levels of OS in aged controls and AD and PD patients (Hishikawa et al., 2012, Kim et al., 2015, Small et al., 2018). However, such antioxidant therapies are generally considered ineffective due to a number of factors, including poor blood-brain barrier penetration (BBB), intervention at an inadequate disease stage, method of administration and bioavailability of particular formulation. BBB is a selectively permeable border between the body circulatory system and the central nervous system (CNS) (Daneman and Prat, 2015); thus, not all antioxidants that show promising results *in vitro* will reach damaged areas *in vivo*. Absence of improvement or disease progression slowing in many trials could also be due to intervention happening too late in the disease course, when cognitive and cellular changes are already irreversible, and study in patients with earlier stages will be more informative (Persson et al., 2014). Dosage of the antioxidant is also an important factor to consider – many molecules possess both anti- and prooxidant properties, and administration of excessive amount may lead to exacerbation of OS (Chakraborthy et al., 2014, Lee et al., 2019, Pearson et al., 2006, Persson et al., 2014). Moreover, as ROS are an essential part of intracellular signaling, non-specific reduction of these molecules may have detrimental effects on cellular homeostasis. Therefore, alternative approaches to modulate OS can be utilized – for instance, pharmacological or genetic regulation of expression and/or activity of endogenous antioxidant enzymes or OS response regulatory molecules can be more effective. Thus, OS is an important factor in the neurodegeneration process and is likely to play a role long before the onset of symptoms, although its exact mechanism of action in NDD progression remains unclear.

1.1.2 Protein aggregation

Formation and deposition of intra- and extracellular protein aggregates is observed in multiple NDDs (Pedersen and Heegaard, 2013). These aggregates are characteristic pathological hallmarks of each type of NDD – for example, aggregation of of α-synuclein in Lewy bodies is observed in substantia nigra in PD patients, whereas amyloid-β (Aβ) plaques and tau tangles in cortex and hippocampus are indicative of AD (Kumar et al., 2016). Aggregates of transactive response DNA binding protein 43 kDa (TDP-43) are observed in the cytoplasm of motor neurons in majority of patients with limbic-predominant age-related TDP-43 encephalopathy and both familial and sporadic forms of ALS, although mutations in this gene account for only 1-3% of familial ALS cases (Blokhuis et al., 2013, Guerrero et al., 2016, Kapeli et al., 2017, Nelson et al., 2019). The fact that the formation of such protein aggregates occurs in both sporadic and familial cases of various NDDs suggests that this process is a fundamental mechanism in pathogenesis of these disorders. Aggregation of proteins can be caused by mutations and aberrant post-translational modifications (PTMs) (Flagmeier et al., 2016, Martin et al., 2011, Moreno-Gonzalez and Soto, 2011). For example, multiple mutations in *MAPT* gene encoding for tau protein are known to cause various tauopathies such as AD and frontotemporal lobar dementia (FTLD); this protein is also aberrantly acetylated and phosphorylated, which affects its conformation, rendering it prone to aggregation (von Bergen et al., 2001, Cohen et al., 2011, Fischer et al., 2007, Goedert and Spillantini, 2000, Kontaxi et al., 2017, Simic et al., 2016, Wolfe, 2009). Interestingly, although aggregation-prone proteins are present in cells from birth, most neurodegenerative disorders do not manifest until 40-50 years of age (Bertram and Tanzi, 2005, Myers, 2004). This phenomenon might be in part due to a depletion of intracellular protein quality control system, especially chaperones, during ageing (Brehme et al., 2014).

Chaperones are a class of proteins that assist correct folding of proteins and maintain proteostasis (Calderwood et al., 2009, Mattoo and Goloubinoff, 2014). They play a role in the detection and refolding of misfolded proteins to their native state and mark aggregated proteins for proteosomal cleavage and chaperone-mediated autophagy (Calderwood et al., 2009, Mattoo and Goloubinoff, 2014). Crucially, a decrease in the global expression of chaperones and failure to up-regulate their transcription upon stress stimuli is observed in aging and disease (Brehme et al., 2014, Koga et al., 2011). For example, heat shock factor 1 (HSF1) is a transcription factor that induces the transcription of heat shock protein (*HSP*) genes that encode stress-induced chaperones (Ahn and Thiele, 2003). Expression of *HSF1* declines with ageing resulting in a reduced ability for cells to cope with proteotoxic stress arising from the presence of non-native protein species, leading to accumulation of misfolded and aggregated proteins (Koga et al., 2011). Overexpression of HSF1 and chaperones in mouse models of NDDs has been shown to be protective and to decrease aggregation-induced toxicity and neurodegeneration (Klucken et al., 2004, Pierce et al., 2013, Toth et al., 2013), suggesting that protein aggregation plays a central role in the neurodegenerative process. Moreover, mutations in chaperone genes have been associated with NDDs. For instance, mutations in mortalin, mitochondrial chaperone HSP70 (mtHSP70), have been identified in patients with PD (Burbulla et al., 2010, De Mena et al., 2009). These mutations disrupt the chaperone activity of the protein, which makes it prone to aggregation, leading to increased ROS levels in mitochondria and altered mitochondrial membrane potential (Amick et al., 2014, Burbulla et al., 2010, Goswami et al., 2012). ALS-associated pathogenic mutations have been described in the vesicle-associated membrane protein-associated protein B (VAPB), a member of endoplasmic reticulum (ER) unfolded protein response (UPR) pathway that acts to suppress the accumulation of misfolded proteins. The mutations have been shown to disrupt the anti-proteotoxic activity of VAPB leading to protein aggregation and cell death (Aliaga et al., 2013, Chen et al., 2010, Kanekura

et al., 2006). Processes of folding and clearance of misfolded proteins are now intensively studied as a promising target for therapy; approaches include blocking aggregate formation, promotion of clearance and stabilization of aggregation-prone molecules (Kumar et al., 2016). For example, induction of Hsf1-regulated genes in response to Hsp90 inhibition via injections of a novel compound offers synaptic protection in a mouse model of AD (Wang et al., 2017a). Therefore, protein misfolding and aggregation as well as impairment of protein quality control system are important factors in the pathogenesis of neurodegeneration.

1.1.3 Neuroinflammation

Neuroinflammation is an immune response process in the CNS that is mediated by astroglia and microglia. Astrocytes are the most abundant glia cell type that regulate molecular homeostasis, facilitate synapse formation and plasticity, and maintain BBB (Daneman and Prat, 2015, Verkhratsky and Nedergaard, 2018). During inflammation, astrocytes become activated, actively proliferate, secrete cytokines and chemokines and cluster around injured or inflamed regions to isolate them from healthy tissues (Cekanaviciute and Buckwalter, 2016). Microglia is the key component of the innate immunity of the CNS, motile cells that constantly survey their surroundings for signs of neural tissue damage and pathogens (von Bernhardi et al., 2016). Upon discovery of such stimuli, microglia acquire an activated phenotype, induce the expression of major histocompatibility complex II, migrate to the site of injury and secrete chemokines to attract other immune cells to repair the damage and/or clear pathogens (von Bernhardi et al., 2016). Activated microglia have been shown to also induce transformation of astrocytes into A1 neurotoxic activated form (Liddelow et al., 2017). Importantly, during ageing, microglia adopt a primed phenotype, which can lead to an uncontrolled and exaggerated

immune response in the brain (Niraula et al., 2017, Spittau, 2017). As discussed above, ageing is accompanied by elevated OS levels, protein aggregation and decay in proteostasis systems. This in-turn can trigger microglia activation and lead to chronic inflammatory reaction and further tissue damage (Raj et al., 2017). For example, analysis of a mouse model of ageing revealed that older age is associated with presence of A1 activated toxic astrocytes in the CNS as a result of microglia activation (Clarke et al., 2018).

Neuroinflammation is a factor contributing to all major neurodegenerative conditions (Heneka et al., 2015, Vivekanantham et al., 2015), however, it is still debated whether microglia activation could also play any beneficial role in NDDs (Dheen et al., 2007, Kempuraj et al., 2016, Tang and Le, 2016). For example, microglia have been shown to recognize and internalize Aβ aggregates in AD brains (Lee and Landreth, 2010); intracranial injections of anti-Aβ antibodies in multiple mouse AD models activated microglia and resulted in Aβ deposition reduction, making it an attractive target for therapy (ElAli and Rivest, 2016). In contrast, prolonged exposure of microglia to amyloid plaques results in elevated pro-inflammatory factor release, which leads to more severe inflammation and thus enhances disease progression (ElAli and Rivest, 2016). A similar pattern is observed in PD – during the early stages of the disease, microglia activation is beneficial, whereas over time pro-inflammatory cytokines secreted by immune cells amplify pro-inflammatory response and further damage the brain (Wang et al., 2015). Importantly, signs of neuroinflammation have been reported in patients with pre-symptomatic stages of AD and HD, emphasizing its potential role in NDDs onset (Janelidze et al., 2018, Lim et al., 2014, Tai et al., 2007). Moreover, rare variants in triggering receptor expressed on myeloid cells 2 (*TREM2*) have been shown to confer higher risk of developing AD, PD and ALS and cause Nasu-Hakola disease – a rare leukodystrophy characterized by progressive presenile dementia (Dardiotis et al., 2017, Jay et al., 2017). TREM2 is expressed by myeloid lineage

cells, and in the brain it is found exclusively in microglia; its expression is induced following inflammatory stimuli, promoting cell proliferation, phagocytosis and survival, and modulates inflammatory response (Jay et al., 2017). Disease-causing mutations impair maturation of the protein and its translocation to the plasma membrane, and AD-associated variants have been reported to result in reduced gene expression, conferring loss-of function (Brownjohn et al., 2018, Cheng-Hathaway et al., 2018). Thus, inflammatory response in the nervous system may contribute to the progression of NDD and, as seen pre-symptomatically, could be another contributing factor important to the neurodegeneration onset rather than just a consequence of the disease.

All the aforementioned factors are tightly interlaced in the neurodegeneration process and they most likely work in combination to contribute to the degeneration progression (Fig. 1.2). A better understanding of the molecular processes involved in OS response and clearance of toxic aggregates is essential for discovery of new therapeutic targets and early markers of NDDs. The work in this thesis focuses on one family of proteins – the Tre2/Bub2/Cdc16 (TBC), lysine motif (LysM), domain catalytic (TLDc) proteins - that has been shown to play a role in OS defence. Using a combination of cellular and mutant mouse models, the aim of this study is to understand the molecular functions of these novel proteins in the CNS.

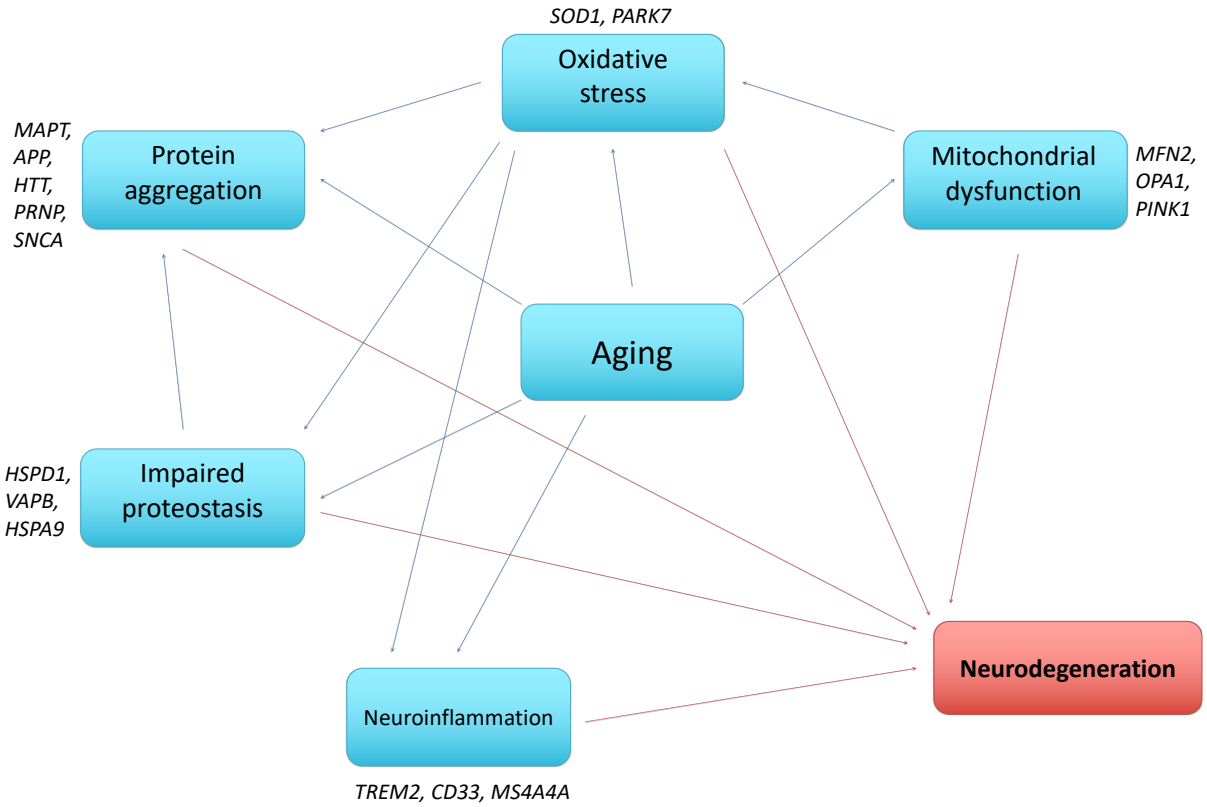


Figure 1.2 Factors contributing to development of neurodegeneration.
The neurodegeneration process is induced by an array of tightly intertwined pathological conditions and processes in the CNS, all caused by ageing or mutations. The ageing process is associated with mitochondrial dysfunction (Theurey and Pizzo, 2018), protein aggregation (Lindner and Demarez, 2009), impaired proteostasis (Labbadia and Morimoto, 2015) and OS and neuroinflammation (Barrientos et al., 2015, von Bernhardi et al., 2015). Protein aggregation has been shown to be induced by OS and impaired proteostasis (Korovila et al., 2017), and OS to result from mitochondrial dysfunction or dysregulation of antioxidant machinery (Guo et al., 2013). In case cases, these processes have also been reported to be caused by genetic mutations - gene names represent molecules, mutations in which are associated with particular ND hallmark (Bross and Fernandez-Guerra, 2016, Cenini et al., 2019, Chung et al., 2018, Freimann et al., 2013, McQuade and Blurton-Jones, 2019, Nishimura et al., 2004).

1.2 TLDc protein family

Members of the TLDc protein family are found in all eukaryotic organisms from yeast and plants to mouse and human and are characterized by their shared, highly conserved C-terminal TLDc domain (Appendix 1, Supplementary Fig. S1). In mammals, the TLDc gene family consists of five members – oxidation resistance 1 (*Oxr1*), nuclear receptor coactivator 7 (*Ncoa7*), TBC1 domain family member 24 (*Tbc1d24*), mTOR associated protein, eak-7 homologue (*mEAK7* or *Kiaa1609* or *TLDc1*) and chromosome 20 open reading frame 118 (*C20Orf118* or *TLDc2*), with some genes encoding multiple protein isoforms (Fig. 1.3) (Finelli et al., 2016).

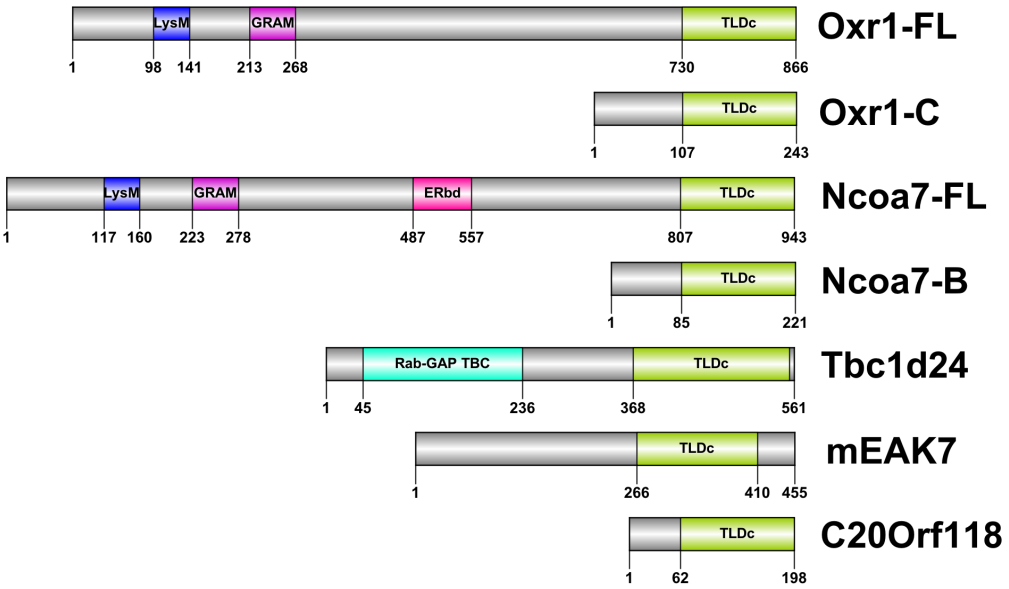


Figure 1.3 Domain architecture of TLDc protein family members.
Oxr1-FL – full-length isoform of Oxr1; Oxr1-C – short isoform of Oxr1. Ncoa7-FL – full-length isoform of Ncoa7; Ncoa7-B – short isoform of Ncoa7. TLDc: Tre2/Bub2/Cdc16), lysin motif (LysM), domain catalytic; LysM: lysine motif; GRAM: GRAM domain; ERbd: estrogen receptor binding domain; Rab-GAP: Rab-GTPase activating protein.

Oxr1, *Ncoa7* and *Tbc1d24* are highly expressed in the brain and spinal cord - high levels of all three proteins are observed in the cortex and the hippocampus, while in the cerebellum *Ncoa7* is restricted to Purkinje cells and *Oxr1* and *Tbc1d24* are found in the granule cell layer (Fig. 1.4) (Finelli et al., 2016, Tona et al., 2019). *mEAK7* is also expressed

in the hippocampus and cortex, though at a very low level, while *C20Orf118* expression is only observed in the cerebellum (Finelli et al., 2016, Pervouchine et al., 2015) (Fig. 1.4). *Oxr1*, *Ncoa7*, *Tbc1d24* and *mEAK7* are expressed in all major types of CNS cells – neurons, astrocytes, microglia and oligodendrocytes (Table 1.1) (Tabula Muris et al., 2018, Zhang et al., 2014b). TLDc proteins are also expressed in various other organs and tissues. All the TLDc proteins, except for C20Orf118, have been shown to be expressed throughout the organism (Finelli et al., 2016, Merkulova et al., 2015, Pervouchine et al., 2015, Shao et al., 2002). *Oxr1* is the most abundantly expressed TLDc gene in brain, cerebellum and testes, while *Ncoa7* displays the highest expression levels in the kidney, liver, lung and spleen samples (Finelli et al., 2016). *C20Orf118* and *mEAK7* are expressed at generally lower levels in the organism, and *C20Orf118* expression is restricted to bladder, colon, duodenum, large and small intestines, bone marrow, kidney and pancreas (Table 1.1) (Finelli et al., 2016, Pervouchine et al., 2015, Tabula Muris et al., 2018).

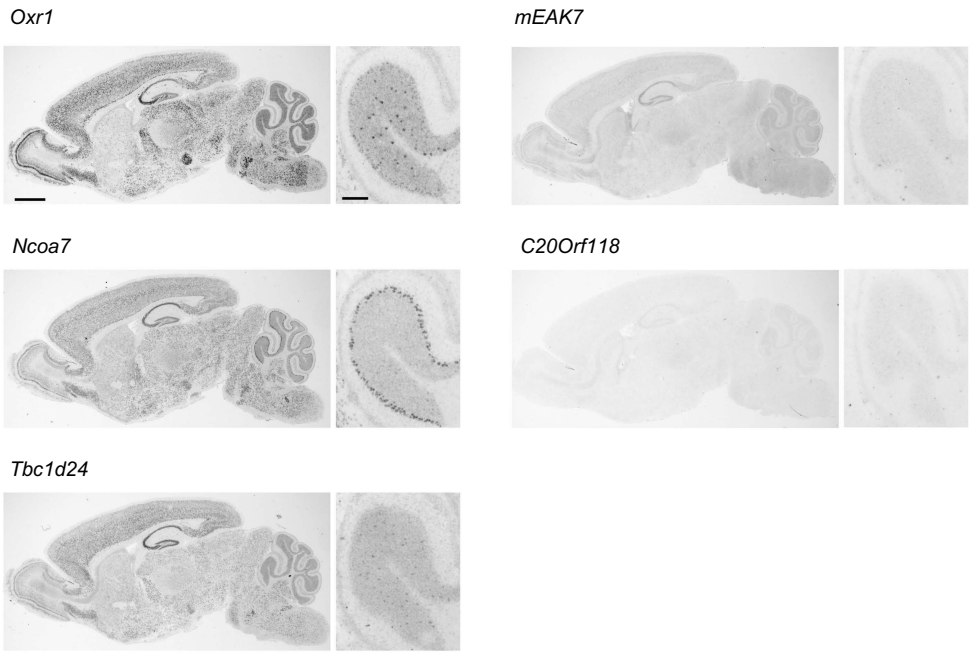


Figure 1.4 TLDc genes expression in adult mouse brain.
In situ hybridization of TLDc genes in the adult brain (left panel) and cerebellum (right panel) in wild-type male mice. Modified from Finelli et al. (2016).

Table 1.1. Organism-wide expression of TLDc genes in mouse organs.
Summary of TLDc genes expression in mouse organs and tissues based on single cell transcriptomic analysis of organs from 3-month old mice (Tabula Muris et al., 2018), RNA-Seq analysis of gene expression in brain cells (Zhang et al., 2014b) and adult organs (Pervouchine et al., 2015) and RT-qPCR and in situ hybridisation studies (Finelli et al., 2016, Liu et al., 2015, Merkulova et al., 2015, Oliver et al., 2011, Paramanik and Thakur, 2010, Sakai et al., 2017, Shao et al., 2002).

	Oxr1	***Ncoa7***	***Tbc1d24***	***mEAK7***	***C20Orf118***
CNS					
Cortex	+	+	+	+	
Cerebellum	Cerebellar granule cell layer	Purkinje cells	Cerebellar granule cell layer	+	+
Hippocampus	+	+	+	+	
Spinal cord	+	+	+	+	
Neurons	+	+	+	+	
Astrocytes	+	+	+	+	
Microglia	+	+	+	+	
Oligodendrocytes	+	+	+	+	
Other organs					
Bladder	+	+	+	+	+
Colon	+	+	+	+	+
Duodenum	+	+	+	+	+
Heart	+	+	+	+	
Kidney	+	+	+	+	+
Large intestine	+	+	+	+	+
Liver	+	+	+	+	
Lung	+	+	+	+	
Mammary gland	+	+	+	+	
Pancreas	+	+	+	+	+
Placenta	+	+	+	+	
Testis	+	+	+	+	
Thymus	+	+	+	+	
Small intestine	+	+	+	+	+

1.2.1 Oxidation resistance 1

Since its discovery *Oxr1* has been tightly linked with protection against OS. It was initially identified as a novel human gene that has the ability to reduce spontaneous mutagenesis rate in oxidation-repair defective *E.coli* mutant (Volkert et al., 2000). In *S.cerevisiae*, deletion of *Oxr1* led to increased sensitivity of yeast to H_2O_2 treatment, and, importantly, it was greater than after inactivation of oxidation repair genes, such as *ogg1*, *ntg1*, *ntg2*, *apn1* or *rad1*, suggesting *Oxr1* plays a key, potentially regulatory role in OS-protection (Volkert et al., 2000). It was later shown that expression of human *OXR1* in *Oxr1*-deficient yeast rescues the OS-sensitive phenotype, suggesting functional conservation of the protein throughout evolution (Elliott and Volkert, 2004). In *C.elegans*, *Oxr1* deletion has been reported to cause increased sensitivity to H_2O_2 and shortened lifespan, whereas further knockout of mitochondrial *Sod2* and *Sod3* extended lifespan, potentially due to up-regulation of other antioxidant enzymes (Sanada et al., 2014). Our group was the first to investigate the role of *Oxr1* in a mammalian system: we identified spontaneous *Oxr1* deletion mouse, harbouring deletion of *Oxr1* and neighbouring gene *Abra* (actin-binding Rho-activating protein) (*bella* mouse), and showed that absence of the entire *Oxr1* locus leads to apoptosis in the granule cell layer of the cerebellum, oxidative DNA damage, rapidly developing ataxia and early death at postnatal day (P)24 (Oliver et al., 2011). Cerebellar granule cells (CGCs) from these mice, when cultured, are more susceptible to OS as compared to wild-type cells, whereas over-expression of *Oxr1* can protect these cells from exogenous stress, suggesting that the level of *Oxr1* expression can modulate the sensitivity of cells to OS (Oliver et al., 2011).

Oxr1 is expressed as numerous isoforms all comprising TLDc domain; interestingly, publicly available data on Oxr1 transcripts does not report existence of corresponding transcripts to all observed protein isoforms, suggesting post-translational modification of

Oxr1 molecules or involvement of other mechanisms, such as protein splicing (Fig. 1.5). In eukaryotic organisms, different isoforms are expressed in a tissue- and cell compartment-specific manner (Fig. 1.5) (Elliott and Volkert, 2004, Finelli et al., 2016, Liu et al., 2015, Wu et al., 2016). For example, the shortest isoform, Oxr1-C, is associated with mitochondrial outer membrane, whereas the long isoform, Oxr1-FL, is cytoplasmic (Finelli et al., 2016, Wu et al., 2016). Both isoforms are observed in the spinal cord at similar expression levels, whereas in the brain and the cerebellum *Oxr1-FL* is more abundant than *Oxr1-C* (Finelli et al., 2016). *Oxr1-FL*, but not *Oxr1-C*, has been shown to be expressed in the mouse cortex at P28 and its expression to be regulated by Otx2 transcription factor, a critical regulator of embryonic and postnatal nervous system development; *Oxr1-C*, in contrast, was found to be regulated by this transcription factor in embryonic subpallium and neural retina, suggesting distinct roles of these isoforms during development (Sakai et al., 2017).

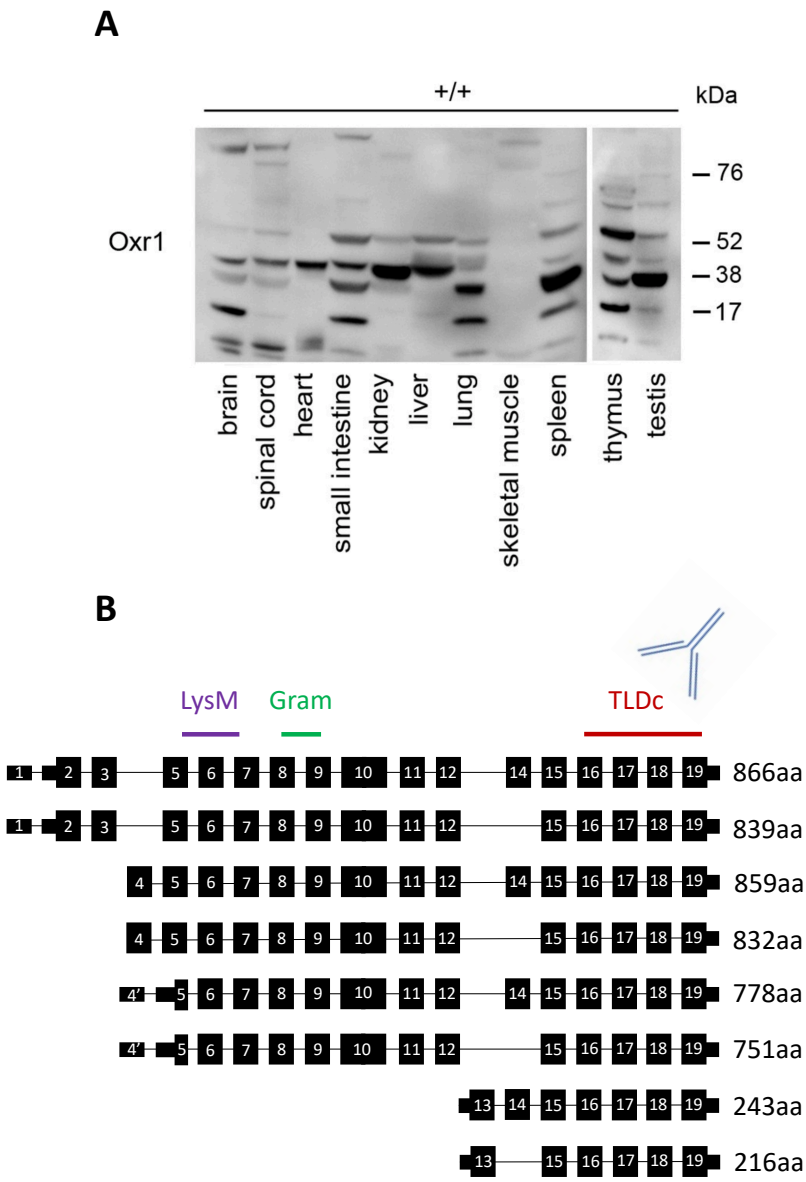


Figure 1.5 Oxr1 isoform diversity.
(A) Western blot representing Oxr1 isoforms expressed in various mouse organs. From (Liu et al., 2015). (B) Oxr1 isoforms as reported in Genome Browser based on RefSeq dataset. The location of the antibody epitope in Oxr1 molecule is shown.

All isoforms contain the TLDc domain; the two most studied, the longest and shortest, have been shown to protect against OS-induced cell death and to reduce ROS levels following oxidative treatment *in vitro* (Finelli et al., 2016). Importantly, it has been demonstrated that expression of this region alone can compensate for absence of the long isoform *in vivo* (Oliver et al., 2011), suggesting that the TLDc domain itself is essential for

protection against OS. In agreement with this, a mouse model with truncation of the TLDc domain (*Oxr1*$^{tm1a/tm1a}$ and *Oxr1*$^{d/d}$, see Materials and Methods chapter for details) were generated and the phenotype of these animals was identical to that of the original spontaneous deletion *bella* mutant, suggesting that the observed phenotype is due to absence of functional TLDc domain (Finelli et al., 2016, Finelli et al., 2018b, Oliver et al., 2011). Interestingly, Oxr1 antimutator activity in *E.coli* has been shown to be mediated by protein region outside of the TLDc domain (Murphy and Volkert, 2012). This discrepancy in mapping of the key protein region could be due to differences in prokaryotic and eukaryotic proteomes – *Oxr1* has evolved over the course of evolution in eukaryotes, meaning the mechanisms of its action are dictated by co-evolved proteins. In prokaryotes, such as *E.coli*, the genes and proteins that interact with the TLDc domain may not be present yet, thus making it unable to carry out its activity. Antimutator activity of the non-TLDc region of Oxr1 may be mediated by interaction with alternative binding partners, possibly via conserved protein folding motif mechanism, as no molecules with amino acid sequence similar to the TLDc domain have been identified among bacterial proteins. In eukaryotes this protein region may also be involved in protein's protective activity, potentially in Oxr1-FL specific functions, as it is absent from Oxr1-C (Murphy and Volkert, 2012).

The sequence of the TLDc domain is highly conserved among different species and it has been shown that mutations of a single residue can lead to dramatic decrease in protective activity (Finelli et al., 2016). However, despite the tertiary structure of the TLDc domain from zebrafish being solved in 2012 (Blaise et al., 2012), its function remains unknown, due in part to the fact that the structure does not resemble any other known protein motifs (Blaise et al., 2012). The TLDc domain was initially thought to possess enzymatic activity based on co-occurrence with TBC and LysM domains (Doerks

et al., 2002), and because TLDc domain-containing proteins appeared to be able to modulate OS, these findings suggested that it might harbour antioxidant activity. However, it has been later demonstrated that Oxr1 does not possess catalase-like or SOD1-like activities and can only react with H_2O_2 via oxidation of cysteine residues (Oliver et al., 2011, Sanada et al., 2014). Similarly to other OS-protective genes, *Oxr1* has been shown to be induced upon H_2O_2 treatment *in vitro*, and Oxr1-C is also up-regulated in response to arsenite (Dell'Orco et al., 2016, Elliott and Volkert, 2004, Finelli et al., 2016, Han et al., 2008, Volkert et al., 2008). Thus, there is clear evidence that TLDc proteins participate in the OS response and protection, but the molecular mechanisms of action of these proteins remain to be discovered.

A few studies have identified deregulation of expression of some antioxidant enzymes in *Oxr1*-deficient cells and tissues. In mosquito *Anopheles gambiae Oxr1* silencing led to significant decrease in *Gpx* and catalase mRNA levels (Jaramillo-Gutierrez et al., 2010). In human cell lines, *Oxr1* down-regulation has been shown to decrease expression of Gpx2 and heme oxygenase-1 (HO-1) enzymes, as well as p21 protein, a tumor suppressor and regulator of OS response (Yang et al., 2014). *OXR1* expression is induced in senescent cells, and this leads to increase in *GPX2*, *HO-1*, catalase, *SOD1* and *SOD2* levels, while *OXR1* knockdown down-regulated its targets (Zhang et al., 2018). In *Oxr1* knockout mice, initial analysis of antioxidant enzymes expression at the end-stage of the disease identified decrease in *Gpx1* mRNA levels (Oliver et al., 2011). Yang et. al employed RNA-sequencing (RNA-Seq) to identify genome-wide transcriptional changes caused by *OXR1* knockdown (80% at the protein level) in HeLa cells in control and OS condition (Yang et al., 2015). 807 genes were identified as being deregulated in both non-treated and H_2O_2 treated cells, including antioxidant genes, transcription factors and many members of the p53 pathway involved in cell-cycle arrest and apoptosis (Yang et al., 2015). These data are in agreement with cell

death observed in *Oxr1* knockout mouse and increase in ROS and markers of OS in absence of Oxr1. Together, these data suggest Oxr1 may act as a master regulator of expression of antioxidant genes or interact with such proteins.

To get an insight into the mechanisms that could regulate Oxr1 protective activity, a pull-down assay of binding partners was performed from neuronal Neuro-2a (N2a) cell line (Finelli et al., 2015). This led to identification of several proteins that interact with specifically Oxr1-FL or Oxr1-C, or with both (Finelli et al., 2015). Interestingly, upon H_2O_2 treatment, a number of Oxr1-C binding partners drastically increased, whereas the number of Oxr1-FL-interacting proteins did not change considerably. This suggests that Oxr1-FL and Oxr1-C have distinct functions and play different roles in the OS response (Finelli et al., 2015). Interestingly, the study has also shown that Oxr1 interacts with TDP-43 and FUS (Fused in sarcoma), proteins implicated in ALS. OXR1 has earlier been shown to be up-regulated in spinal cord of end-stage ALS patients and elevated levels of Oxr1 were also reported in pre-symptomatic hSOD1^{G93A} mouse ALS model; these data suggest that Oxr1 participates in the onset of ALS-associated pathology or is up-regulated to protect against neurodegeneration (Oliver et al., 2011). Further experiments have revealed that Oxr1 overexpression rescues mislocalisation and aggregation of some of the ALS-associated TDP-43 and FUS mutants, while some of the disease-causing mutations reduced the binding between the proteins, thus disabling the activity; *Oxr1* overexpression also restores associated mitochondrial morphology defects and mitochondrial gene splicing (Finelli et al., 2015). *In vivo*, neuronal overexpression of *Oxr1* in hSOD1^{G93A} ALS mouse model significantly extended survival, improved motor function and delayed muscle pathology and neuroinflammation (Liu et al., 2015). Recently, neuronal overexpression of *Oxr1* has been shown to improve motor performance, neuromuscular junction degeneration and muscle denervation and pathology in a distinct

ALS mouse model, TDP-43^{M337V} (Williamson et al., 2019). Moreover, *Oxr1* was reported to be down-regulated in brain tissues of PD mouse model, and its overexpression using ventricular lentiviral construct injection lead to improvement of motor symptoms, reduced apoptosis and increased number of neurons in substantia nigra (Jiang et al., 2019). Together, these data suggest that Oxr1 could be used as a target in future therapeutic approaches for various forms of ALS and other NDDs. A heterozygous nonsense mutation shortly after the start codon of *OXR1-C* isoform has been described in patients with specific language impairment (SLI), a neurodevelopmental disorder, suggesting functional importance of this isoform and its potential role in brain development (Chen et al., 2017, Kamhi and Clark, 2013), although the functional consequences of this is unknown.

OXR1 has also been shown to be protective in non-neurological conditions. Injection of OXR1-expressing mouse mesenchymal stem cells into spontaneous lupus nephritis mouse model significantly improved renal pathological changes (Li et al., 2014). Lupus nephritis is a complication of systemic lupus erythematosus caused by OS resulting from ROS production by leucocytes infiltrating the kidneys. OXR1 expression in injected cells reduced infiltration of immune cells in kidneys, renal cell apoptosis, blood urea nitrogen, proteinuria and reduced renal damage (Li et al., 2014). OXR1 protein has been shown to be significantly down-regulated in placental tissue of women with pre-eclampsia (Mary et al., 2017). Pre-eclampsia is a condition that develops after 20th week of gestation and is characterised by proteinuria, hypertension, renal insufficiency and OS (Can et al., 2014, Elliot, 2016, Mol et al., 2016). Reduction in OXR1 levels may lead to elevation of ROS levels, subsequent mitochondria damage and apoptosis observed in the condition (Dagdelen et al., 2016, Longtine et al., 2012, Zhou et al., 2017b). Together, these data suggest a strong

involvement of Oxr1 in protection against OS in various tissues and its importance for the CNS health and development, but the mechanisms of these remain unclear.

1.2.2 Nuclear receptor coactivator 7

Like *Oxr1*, *Ncoa7* is expressed under at least two isoforms – the full-length Ncoa7-FL and a shorter isoform Ncoa7-B, both possessing the TLDc domain. NCOA7-FL was first described as a brain- and kidney-specific nuclear receptor coactivator that binds estrogen receptors (ER) α and β, thyroid receptor β (TRβ), peroxisome proliferator-activated receptor γ (PPARγ), retinoic acid receptor α (RARα) and aryl hydrocarbon receptor (AhR) via non-canonical ER-binding domain and promotes expression of downstream target genes in the presence of exogenous corresponding ligands *in vitro* in cell lines (Halachmi et al., 1994, Lazennec et al., 1997, Nguyen et al., 1999, Shao et al., 2002). There is emerging evidence that estrogen plays a role in microglia inflammatory response and brain ageing, suggesting *Ncoa7* might be involved in hormonal regulation of neuroinflammation process (Villa et al., 2016, Zarate et al., 2017). In agreement with this, the interaction between Ncoa7 and ERβ has been shown to decrease with ageing in mouse cortex, when analysed by a pull-down assay, while *Ncoa7* expression to increase (Paramanik and Thakur, 2010). The exact transcriptional targets of Ncoa7 as part of a potential receptor coactivator complex remain unknown. Recently, homozygous loss of NCOA7-FL has been identified in a family with autism spectrum disorder, highlighting the importance of this protein for the CNS development and functioning (Doan et al., 2019). In addition to its wide expression in the nervous system, Ncoa7-FL is highly expressed in kidney and has been shown to play a role in kidney intercalated cells *in vivo* – deletion of the full-length isoform resulted in elevated urine pH and changes in intercalated cell morphology and size (Merkulova et al., 2018). Importantly, *Ncoa7-FL* knockout led to a significant

reduction in protein levels of several subunits of vacuolar proton pumping ATPase (V-ATPase), complementing previous work on V-ATPase interactome that has shown interaction of Ncoa7 and Oxr1 with ATP6V1B1 subunit (Merkulova et al., 2015).

The short isoform of *Ncoa7* was identified in a screen for novel ovulation-associated genes and has later been shown to be induced upon interferon β 1b (IFN-β1b) treatment *in vitro* and *in vivo*, suggesting it could play a role in the inflammatory response process (Shkolnik et al., 2008, Yu et al., 2015). In another study, *Ncoa7-B* has been identified as one of the genes induced in response to INFα in multiple cell lines and primary human monocytes and T cells, confirming its potential role in inflammation (Goujon et al., 2013). INFα pre-treatment has previously been shown to reduce HIV-1 infection in cell lines; thus, the study was performed to identify the candidate genes that could suppress viral infection (Goujon and Malim, 2010, Goujon et al., 2013). NCOA7-B has later been shown to inhibit endosome-mediated entry of viruses into the cell via regulation of V-ATPase activity and subsequent increase in acidity and protease activity, thus preventing virus particle fusion with the endosome membrane (Doyle et al., 2018). Interestingly, none of *Ncoa7* isoforms are induced upon H_2O_2 treatment, unlike *Oxr1*, although *Ncoa7-FL* is up-regulated in response to arsenite treatment, suggesting it is induced by specific types of OS (Durand et al., 2007, Finelli et al., 2016, Yu et al., 2015). On the other hand, Ncoa7-B, but not Ncoa7-FL significantly decreased OS levels in N2a neural cell line following arsenite treatment (Finelli et al., 2016). Thus, although these isoforms share conserved C-terminal TLDc domain, their functions and roles in OS response and protection differ, potentially due to absence or presence of additional domains and independent transcriptional regulation.

1.2.3 TBC domain family, member 24

Tbc1d24 has been implicated in the regulation of synaptic vesicle trafficking and development of neurons. It is known to interact with and prevent activation of ADP-ribosylation factor 6 (Arf6), a small GTPase important for membrane trafficking, and control growth and migration of neurons (Falace et al., 2014). *Tbc1d24* has been shown to play a role in neurite development *in vitro*. Primary hippocampal and cortical neurons from *Tbc1b24* heterozygous knockout mice showed reduced axonal and dendritic growth as compared to wild-type controls (Finelli et al., 2018a). *In utero* knockdown of *Tbc1d24* results in delayed radial migration of neurons and leads to impaired dendritic arborisation due to aberrant activation of Arf6 (Falace et al., 2014). *Tbc1d24* silencing has later been shown to impair axon formation in primary cortical neurons and axonal projections *in vivo*, at least partly due to excessive Arf6 activation and defective membrane trafficking at the growth cone (Aprile et al., 2019). Interestingly, knockdown of the *Tbc1d24* orthologue *sky* in flies has been shown to result in deregulated presynaptic vesicle trafficking and recycling (Fernandes et al., 2014). A recent study has also shown that Sky and orthologous proteins possess a unique lipid-binding cationic pocket essential for regulation of synaptic vesicles and Sky interaction with the cell membrane (Fischer et al., 2016). *Tbc1d24* down-regulation also resulted in decreased endocytosis and increased endosomal volume in synapses, indicating its importance in synaptic vesicle recycling (Finelli et al., 2018a). *Tbc1d24* has also been shown to be expressed in stereocilia of the inner ear in early postnatal period (P3), while it is not expressed at later stages (P7), suggesting its role in development, but not functioning of the adult sensory hair. In addition, *Tbc1d24* expression was detected in the spiral ganglion neurons of adult mice at P24 and P56 in two studies, indicating its varied roles in different systems of the inner ear (Azaiez et al., 2014, Rehman et al., 2014, Zhang et al., 2014a). Interestingly, a recent study

has demonstrated an important role for *Tbc1d24* in early embryonic development – knockdown and knockout of the gene led to disruption of neural crest cell migration in *Xenopus* embryos by blocking contact inhibition of locomotion (CIL) mechanism (Yoon et al., 2018). Tbc1d24 has been shown to interact with ephrinB2 and regulate E-cadherin recycling from plasma membrane; CIL is regulated by levels of E-cadherin on the cell surface, and in absence of Tbc1d24 E-cadherin accumulation inhibited CIL and resulted in uncontrolled cell migration (Yoon et al., 2018). These results suggest an important role of *Tbc1d24* in developmental processes.

An array of mutations and complete deletion of *TBC1D24* have been described in a range of inherited neurological disorders that are characterised by epilepsy, mental retardation, encephalopathy, microcephaly, developmental delay, hearing impairment, exercise-induced dystonia, sudden unexpected death or deafness, onychodystrophy, osteodystrophy, mental retardation and seizures (DOORS) syndrome (Afawi et al., 2013, Campeau et al., 2014, Kuroda et al., 2019, Lüthy et al., 2019, Mucha et al., 2018, Nakashima et al., 2019, Strazisar et al., 2015, Trivisano et al., 2017). Patients are usually presented with an array of symptoms caused by a single mutation, although some of the mutations cause deafness without any additional neurological phenotype, suggesting functional pleiotropy of the gene (Azaiez et al., 2014, Bakhchane et al., 2015, Rehman et al., 2014, Zhang et al., 2014a). Some patients with mutations in the gene are presented with neurodegeneration and ataxia, resembling *Oxr1* knockout mouse phenotype (Afawi et al., 2013, Banuelos et al., 2017, Corbett et al., 2010, Doummar et al., 2015, Guven and Tolun, 2013, Li et al., 2018, Oliver et al., 2011, Trivisano et al., 2017, Zhou et al., 2017a); this similarity in disease presentation highlights functional conservation of TLDc family members. On the other hand, a large proportion of patients with *TBC1D24* mutations have epilepsy and seizures, supporting protein's important role in the regulation of vesicle

trafficking, a factor that is thought to be involved in the pathogenesis of epilepsy (Casillas-Espinosa et al., 2012). Disease-causing mutations have been identified across the protein, including the TLDc domain, and there is currently no clear correlation between the position of the mutation and the disease phenotype (Fig. 1.6) (Balestrini et al., 2016). Three of these mutations affect highly conserved residues in the TLDc domain – Gly376 and Arg360 are conserved throughout the family, and Gly428 is only substituted by asparagine in MEAK7. Recently, mutations in the TLDc domain have been predicted to lead to loss in stability of its tertiary structure and affect conformation of some of the loops (Lüthy et al., 2019). Lüthy et al. have shown that the TLDc domain of Tbc1d24 acts as a ROS sensor at the synapses, promoting endocytosis and synaptic vesicles recycling upon OS conditions, and pathogenic G501R mutation or complete loss of the domain causes loss of function and inability to maintain synaptic homeostasis (Lüthy et al., 2019).

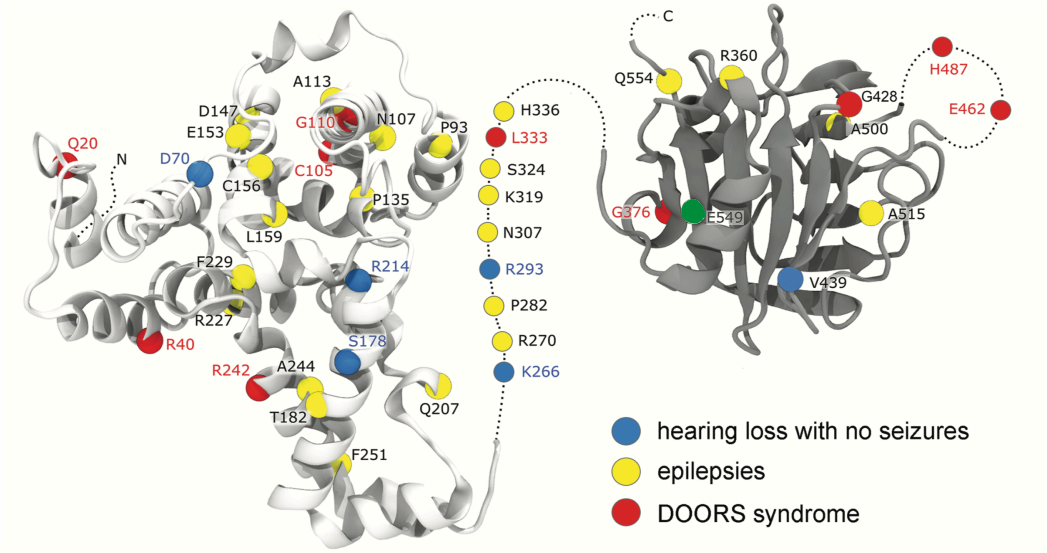


Figure 1.6 Disease-causing mutations in TBC1D24 protein.
Three-dimensional structure of TBC1D24 molecule showing location of mutations, associated with various phenotypes. TBC domain is coloured in white, TLDc domain is highlighted in grey. Additionally, highly conserved glutamic acid residue E549 is highlighted in green. Modified from (Finelli et al., 2018a).

1.2.4 mTOR associated protein, eak-7 homologue

C. elegans protein Eak-7, ortholog of mEAK7, was initially identified in a screen for genes that regulate activity of DAF-16/FoxO (forkhead box protein O) transcription factor, important for life span extension, stress resistance and physiological developmental arrest at harsh environment-induced dauer larval stage in nematoda (Alam et al., 2010, Williams et al., 2010). Eak-7 inhibits the activity of DAF-16/FoxO, thus reducing the expression of its target genes *sod-3*, *dod-3* (downstream of DAF-16) and *mtl-1* (metallothionein-1) (Alam et al., 2010). *Eak-7* null mutation in dauer-prone strain exacerbated the phenotype, leading to prolonged dauer stage and extended life span, whereas neuron-specific overexpression of *Eak-7* rescued the phenotype (Alam et al., 2010). Interestingly, *C. elegans Eak-7* mutants were also resistant to ultraviolet, heat and OS, while knockdown of *mEAK7* in mammalian neurons increased cell death upon arsenite treatment (Alam et al., 2010, Finelli et al., 2016). This suggests that Eak-7/mEAK7 is involved in OS protection, though mechanisms and effect could be cell-type- or species-specific. A recent study has shown that mammalian mEAK7 localises to lysosomes and activates the alternative mechanistic/mammalian target of rapamycin (mTOR) signaling pathway (Nguyen et al., 2018). mEAK7 recruits mTOR to the lysosome in both starved and nutrient-rich conditions, and their interaction is dependent on the TLDc domain and C-terminus of the protein (Nguyen et al., 2018). Moreover, mEAK7 has been reported to regulate cell proliferation and migration – processes known to be regulated by mTOR signaling (Holroyd and Michie, 2018, Li et al., 2016, Nguyen et al., 2018, Ryskalin et al., 2017, Wang et al., 2017b, Yang et al., 2017). These data suggest an important role for mEAK7 in the mTOR signaling and its potential involvement in the autophagy-lysosomal pathway.

1.2.5 C20Orf118

C20Orf118 is the least studied protein in the family. In tilapia fish, its ortholog TLDc2 has been shown to be differentially expressed in response to hypoxia (Li et al., 2017). The authors observed differential exon and splice junction usage in the gene in heart, gill, brain, spleen and liver tissues upon hypoxia treatment, suggesting organ-specific alternative splicing events. Interestingly, the exon that corresponds to the C-terminus of the protein is significantly up-regulated by hypoxia, suggesting shorter isoform could be induced by hypoxic treatment (Li et al., 2017).

Experimental aims of the thesis

In summary, the TLDc proteins play an important role in the development, differentiation and survival of neuronal cells, although their neuroprotective function is still not well understood (Table 1.2). Thus, the aim of this project was to dissect the fundamental mechanisms of action of the TLDc proteins by analysing possible functions and functional conservation between family members and focusing more particularly on the role of Oxr1 in OS protection and maintenance of the CNS:

- To determine the functional role of Oxr1 in the OS response by focusing on its interaction with an essential antioxidant enzyme (Chapter 3)
- To identify the early events leading to neurodegeneration in the *Oxr1* deletion mutant mouse (Chapter 4)
- To investigate the potential functional conservation, interactions and compensation between the TLDc proteins, in particular the closely-related *Oxr1* and *Ncoa7* genes, during early embryonic development and in *Oxr1* and *Ncoa7* deletion mouse models (Chapter 5)

Table 1.2 Summary of TLDc proteins structure and functions.

	Domains	Functions	Human diseases
Oxr1	Gram, LysM, TLDc	OS protection, Gpi regulation	SLI
Ncoa7	ERbd, Gram, LysM, TLDc	OS protection, v-ATPase regulation, nuclear receptor coactivator (Ncoa7-FL), inflammation (Ncoa7-B)	Autism
Tbc1d24	TBC, TLDc	OS protection, synaptic vesicle traffic regulation	Epilepsy, DOORS, deafness
mEAK7	TLDc	OS protection, mTOR regulation	
C20Orf118	TLDc	OS protection	

Chapter 3:

One of the approaches to study the function of the TLDc proteins is to identify their binding partners and analyse the effect of these interactions on functioning of the target proteins and their role in protective properties of TLDc family members. As the initial screen for Oxr1 binding partners was carried out in a neuronal cell line ((Finelli et al., 2015), see above), a more biologically relevant analysis of the TLDc proteins' binding partners *in vivo* was needed to identify and compare the interactors of all family members. A pull-down assay performed in wild-type mouse brain lysates has identified dozens of putative interactors of TLDc proteins, with approximately 15 of them common between some or all family members, suggesting a potential role for the TLDc domain itself. One of the binding partners common between the TLDc proteins was the important neuronal antioxidant enzyme peroxiredoxin 2 (Prdx2). In this chapter, utilising a combination of *in vitro* assays in cells or using purified proteins, I aimed to analyse the effect of Oxr1 on Prdx2 antioxidant and chaperone activities and then using the *Oxr1* knockout and overexpressing mice to analyse the importance of this interaction on the Prdx2 function *in vivo*.

Chapter 4:

Another approach to identify the mechanisms of *Oxr1* function is to analyse the effect of its up- or down-regulation on the expression profile of cells and tissues. Previously published studies have identified differential expression of antioxidant enzymes, transcription factors and cell cycle and apoptosis regulators in presence of *Oxr1* knock-down; however, these data were limited to cell culture systems or tissues with some endogenous Oxr1 still present. Therefore, access to the *Oxr1* knockout mouse model ($Oxr1^{d/d}$) with a well-defined neuropathological phenotype (i.e. degeneration of cells in

the granule cell layer of the cerebellum) provides an ideal opportunity to study pathways deregulated by loss of *Oxr1* that lead to neuronal cell death and to potentially identify the role of *Oxr1* in neuronal cell survival. The transcriptional changes in the cerebellum from pre-symptomatic *Oxr1*$^{d/d}$ mouse were identified using a microarray approach. After RT-qPCR validation of microarray analysis results, I went on to investigate in more detail possible involvement of Oxr1 in autophagy-lysosomal pathway, as suggested by the array of differentially expressed genes. I also performed a series of experiments to get an insight into some aspects of Oxr1 intracellular localisation in primary cerebellar neurons.

Chapter 5:

The presence of the highly conserved TLDc domain in all family members suggests a common evolutionary origin for the TLDc genes, and potentially some common functions. Therefore, I analysed any functional conservation between the TLDc genes using a computational approach to predict and compare possible pathways and processes where these genes could be involved based on experimental data on transcription factors that have been shown to bind their promoter regions. I next went on to investigate if predicted functional conservation translates into potential genetic compensation mechanisms between members of the TLDc gene family. To do this, I analysed the expression of TLDc genes and isoforms in a newly-generated *Ncoa7* deletion and Ncoa7-FL knockout mouse models; despite the loss of all isoforms of closely related *Oxr1* causing a severe neurodegenerative phenotype, preliminary data did not reveal any neurological defects or influence on survival in *Ncoa7* deficient mice, suggesting possible genetic compensation by other family members. Striking structural similarity between *Oxr1* and *Ncoa7* genes and prediction of common functions also led us to study the possible

functional overlap between them by analysing the phenotype of double knockout animals and the effect of heterozygous *Ncoa7* knockout on *Oxr1*$^{d/d}$ mouse phenotype.

2. Materials and Methods

2.1 Animals

Two distinct *Oxr1* knockout models were used in this work, both maintained on C57BL/6J background. The first one, *Oxr1*^{tm1a}, was created by insertion of the L1L2_Bact_P cassette, consisting of splice acceptor site, IRES:LacZ reporter cassette and neomycin selection marker under control of β-actin promoter flanked by FRT sites between exons 16 and 17. Additionally, adjacent exons 17 and 18 were flanked by loxP sites (Fig. 2.1) (Finelli et al., 2016). This insertion lead to disruption in the TLDc domain and expression of truncated version of all isoforms, as well as expression of β-galactosidase under *Oxr1* promoter control (Finelli et al., 2016). *Oxr1*^{tm1a} mice were crossed with ubiquitous FlpE recombinase-expressing mouse line to remove lacZ and neomycin cassettes, creating the *Oxr1*^{tm1c} allele (Fig. 2.1). *Oxr1*^{tm1c} line was subsequently crossed with a mouse line ubiquitously expressing Cre recombinase to create *Oxr1*^{tm1d} allele, resulting in removal of loxP flanked exons and premature stop codon, affecting all isoforms (Fig. 2.1) (Finelli et al., 2018b). Oxr1 Tg mice, where a full-length cDNA transgene of HA-tagged Oxr1-FL is expressed from a neuron-specific prion protein *Prnp* promoter, were maintained on a C57BL/6J background and have been described previously (Liu et al., 2015). *Ncoa7* deletion mouse (*Ncoa7*^{del}) was generated using clustered regularly interspaced short palindromic repeats (CRISPR) - CRISPR-associated protein 9 (Cas9) system on C57BL/6J background. Whole *Ncoa7* locus was removed, thus disrupting expression of all isoforms of the protein (Fig 2.2A). Mouse with a targeted deletion of *Ncoa7-FL* (*Ncoa7*$^{tm1.1}$) was generated as a part of the Knockout Mouse Project KOMP2-DTCC by insertion of ZEN-Ub1 cassette containing lacZ gene and loxP-flanked neomycin resistance gene on C57BL/6N background; this insertion resulted in deletion of a region spanning exons 2 and 3. These mice were crossed with ubiquitously Cre-recombinase expressing line to generate tm1.1

allele by excision of neomycin-resistance gene. Resulting *Ncoa7* locus has a *Ncoa7-FL* promoter-driven expression of lacZ gene and intact *Ncoa7-B* promoter and coding region (Fig. 2.2B) (Merkulova et al., 2018). All experiments were conducted in adherence with the guidelines set forth by the UK Home Office regulations, and with the approval of the University of Oxford Ethical Review Panel.

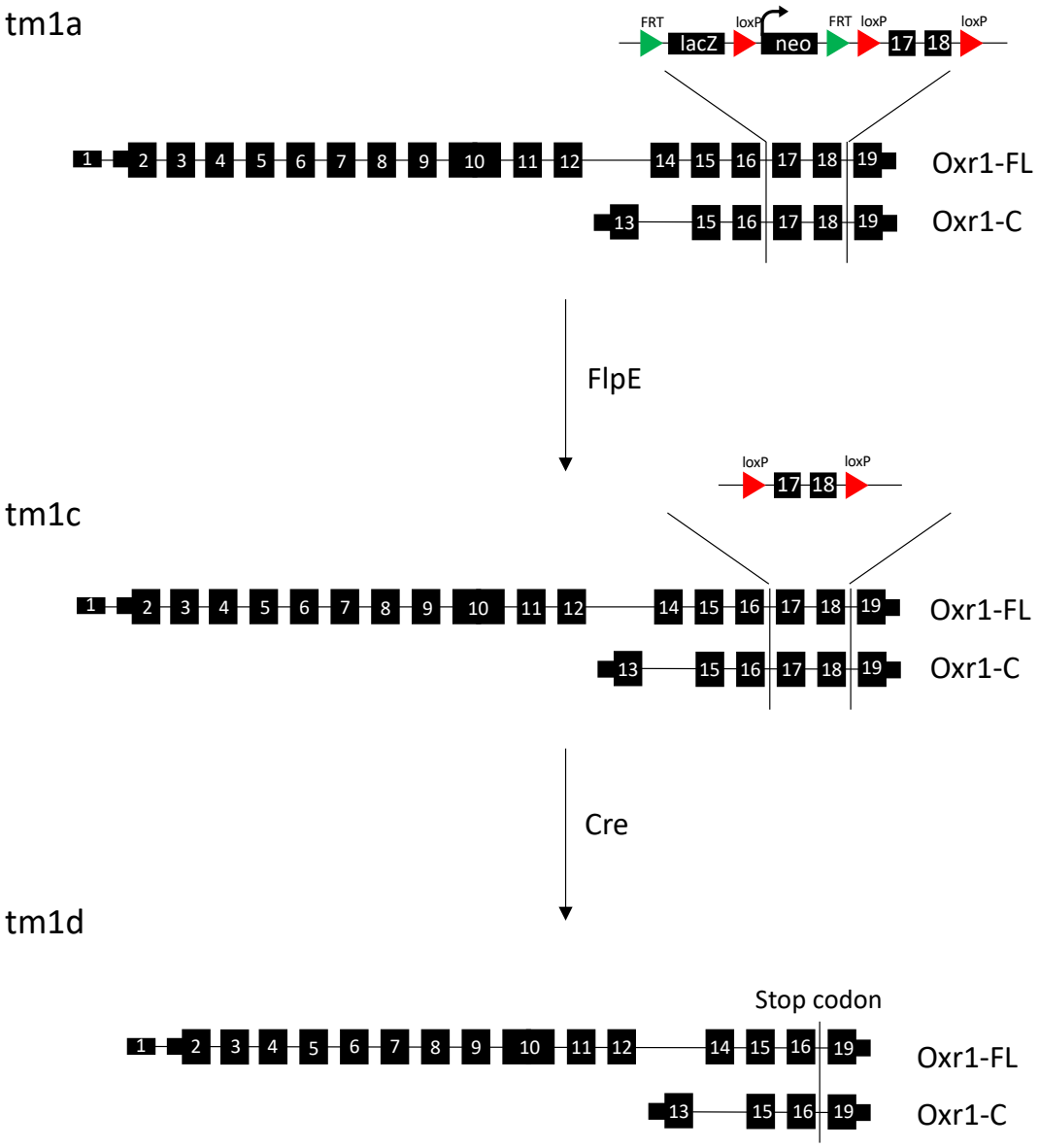


Figure 2.1 Schematic overview of *Oxr1* knockout mouse lines used in the work.
Animals carrying tm1a allele were crossed with FlpE-recombinase expressing mouse line to excise lacZ-neo cassette, thus generating tm1c allele. *Oxr1*^{tm1c} mice were crossed with Cre-recombinase expressing animals to remove loxP-flanked exons 16 and 17, creating tm1d allele. *Oxr1*^{tm1d} expressed truncated versions of all Oxr1 isoforms, and phenotypes of this line is identical to originally discovered *Oxr1* deletion mouse.

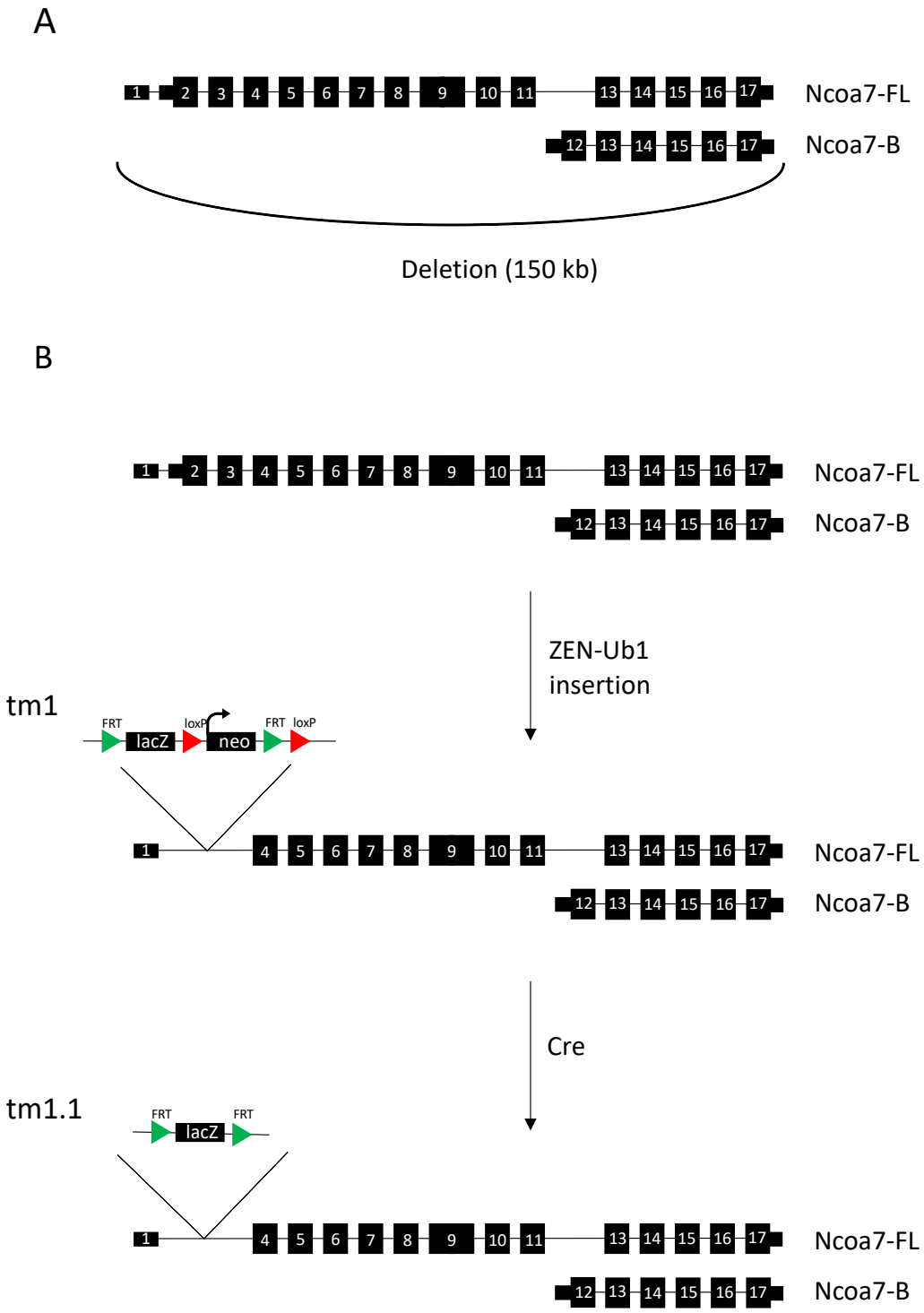


Figure 2.2 Schematic overview of *Ncoa7* knockout mouse lines used in the work.
(A) *Ncoa7*^{del} mouse was generated using CRISPR-Cas9 technology; whole *Ncoa7* locus (150 kb) was removed disrupting expression of all the isoforms. (B) *Ncoa7*$^{tm1.1}$ mouse line with disrupted *Ncoa7-FL* and preserved *Ncoa7-B* expression was generated by removal of the region spanning exons 2 and 3 and insertion of ZEN-Ub1 cassette, followed by crossing the line to ubiquitously Cre-recombinase expressing mouse line to remove neomycin-resistance gene and generate tm1.1 allele.

2.2 Expression constructs

For expression in mammalian cells, mouse *Prdx2* cDNA (NM_001317385.1) was cloned into pcDNA3.1 vector with a C-terminal Myc tag by Professor Peter Oliver. pcDNA3-Oxr1-FL-HA, pCX-Oxr1-FL-HA, pCX-Oxr1-C-HA and pcDNA3-Ncoa7-FL constructs used have been previously described (Finelli et al., 2016, Oliver et al., 2011).

For bacterial protein production, mouse *Prdx2* cDNA was cloned from a total brain cDNA extract into pET-22b vector with or without introducing thrombin cleavage site (Thr, underlined) in frame with a His_6 tag:

F1 – 5'-GAGACAT**ATG**GCCTCCGGCAACGCGCAAATC-3'

R1 – 5'-GAGACTCGAGGCTGCCACGCGGCACCAGGTTGTGTTTGGAGAAGTATTCC-3'

F2 – 5'-GAGACAT**ATG**GCCTCCGGCAACGCGCAAATC-3'

R2 – 5'-GAGACTCGAGGTTGTGTTTGGAGAAGTATTCC-3'

Mouse *Oxr1-C* (NM_001130164) was cloned from a total brain cDNA into pET-22b vector in frame with a His_6 tag:

F – 5'-GAGACAT**ATG**TCCCGTCTCTG GTATGGGAAAAAAG-3'

R – 5'- GAGACTCGAGTTCAAAAGCCCAGATTTCAATG-3'.

2.3 Cell culture, transfection and treatment

2.3.1 Neuro2a cell line

Neuro2a (N2a) cells were cultured in Dulbecco's Modified Eagle's Medium (DMEM) with GlutaMAX (Gibco) supplemented with 10% fetal bovine serum (Gibco) and 1% penicillin-streptomycin solution (Gibco) in an incubator at 37˚C in 5% CO_2 atmosphere.

Cells were seeded 24 hours prior to transfection at following densities – 5 x 10^4 cells per well for 24-well plate and 25 x 10^4 cells for 6-well plate. Cells were transfected using FuGene 6 (Promega) diluted in Opti-MEM (Gibco) according to manufacturer's protocol. FuGENE was mixed with DNA at a 3:1 µl to µg ratio.

2.3.2 Primary cerebellar neuron culture

Cerebella from P7 pups were dissected and placed in cold HBSS buffer and meninges were removed. Cerebella were incubated with trypsin (Gibco) for 15 minutes at 37°C followed by incubation with trypsin inhibitor (Gibco) for 5 minutes at room temperature. Tissues were gently triturated by pipetting and centrifuged for 5 minutes at 200rpm. Pellets were resuspended in warm culture media (DMEM supplemented by 1% fetal calf serum, 1% B27 supplement (Gibco) and 25mM KCl). Cells were seeded on glass coverslips pre-treated with poly-ornithine (Sigma) at 2 x 10^5 density. The next day, media was changed to DMEM supplemented by 1% B27 supplement (Gibco), 25mM KCl and 10µM arabinosylcytosine (Ara-C). Cells were cultured for 6 days in vitro (DIV) before conducting experiment.

2.3.3 Cell treatment

For N2a cells, 24 hours after transfection culture media was changed to media supplemented with desired treatment: for cell death assay, cells were treated with 500µM H_2O_2 for 5 hours and for Prdx2 hyperoxidation and Prdx2 oligomerisation experiments, cells were treated with 300µM H_2O_2 for 1 hour.

2.3.4 Immunocytochemistry

Cells were fixed for 10 minutes in 4% w/v paraformaldehyde (Sigma), washed with PBS three times and incubated in blocking solution (5% v/v normal goat serum (Vector Laboratories), 0.5% v/v Triton X-100 in PBS) for 1 hour at room temperature. Coverslips were incubated with primary antibodies diluted in blocking buffer overnight at 4°C. Coverslips were washed three times with PBST and incubated with secondary antibodies (Table 2.1) for 2 hours at room temperature. Coverslips were washed with PBST and mounted using DAPI Vectashield (Vector Laboratories).

A Leica TCS SP5 confocal microscope (software LAS AF v.2.7.3.9723) was used for Oxr1 co-localization analysis and Prdx2 intracellular localisation (HCX Plan Apo 63x/1.4-0.6 oil objective). Fluorescent microscope Axioplan2 Imaging (Carl Zeiss) was used for cell death assay experiment.

2.4 Protein extraction, immunoprecipitation and western blotting

2.4.1 SDS-PAGE

Tissue or cell samples were lysed in cold RIPA buffer (150mM NaCl, 0.5% w/v sodium deoxycholate, 0.1% w/v SDS, 50mM Tris pH 7.5) supplemented with protease inhibitor (Cell Signaling) and 1% v/v Triton X-100 or 1% w/v CHAPS. Tissue samples were disrupted in a tissue Precellys homogenizer (Bertin Corp.), cells were lysed by syringe trituration with a 23G needle.

Co-immunoprecipitation: For co-immunoprecipitation, equal amounts of protein extract were incubated overnight at 4°C with either Prdx2 antibody or G protein sepharose beads (Sigma) as a negative control. Prior to use, sepharose beads were

washed with RIPA buffer. The next day, protein-antibody complexes were pulled down using G protein sepharose beads for 1 hour at 4°C and prepared for gel-electrophoresis by washing away unbound proteins with cold RIPA buffer four times.

Synaptic protein extraction: Synaptic protein fraction was extracted from wild-type mouse brain using Syn-PER™ Synaptic Protein Extraction Reagent (Thermo Scientific) according to manufacturer's protocol. Briefly, whole brain tissue was homogenised in Syn-PER reagent supplemented with protease/phosphatase inhibitor (Cell Signaling) in Dounce homogenizer at 4°C. After centrifugation at 1,200×g for 10 minutes at 4°C supernatant (total protein) was transferred to a new tube and centrifuged at 15,000×g for 20 minutes at 4°C. The resulting supernatant corresponding to the cytosolic fraction was transferred to a separate tube and the synaptosome pellet was resuspended in Syn-PER™ reagent.

Protein concentration was assessed by bicinchoninic acid (BCA) assay (Novagen) and an equal amount of protein was loaded on the gels. Samples for electrophoresis were prepared by incubating with Laemmli loading buffer (Bio-Rad) supplemented with 5% v/v β-mercaptoethanol (Sigma) at 100°C for 5 minutes. Samples were run on 10%, 12.5% or 15% SDS-PAGE gels.

2.4.2 Blue Native-PAGE

Brain and cerebella tissue and cell samples were homogenized in cold PBS buffer supplemented with protease/phosphatase inhibitor (Cell Signaling) using Precellys homogenizer (for tissue samples only) and lysed by repeated freezing on dry ice and thawing (for both tissues and cells). After measuring protein concentration using BCA assay (Novagen), samples were mixed with 5x loading buffer (62.5mM Tris-HCl pH 6.8,

40% v/v glycerol, 0.01% w/v bromophenol blue) and were resolved on 10% Bis-Tris native gel.

After resolving on a gel, proteins were transferred to PVDF membrane (Amersham). The membrane was then blocked with 5% w/v skim milk in PBST for 1 hour at room temperature. For blue native-PAGE, blocking was done overnight at 4°C. The membranes were then incubated overnight with primary antibodies at 4°C. After rinsing and washing the membrane with PBST to remove excess antibody, it was incubated with secondary HRP-conjugated antibodies and signal was detected using ECL or ECL Prime Western Blotting detection kit (both Amersham) using an ImageQuant LAS 4000 (GE Healthcare).

Table 2.1. Antibodies used for immunocytochemistry and western blotting.

	Antibody dilution	**Catalog number**
Peroxiredoxin 2	1:2000 (WB), 1:300 (ICH)	10545-2-AP, Proteintech
Peroxiredoxin-$SO_{2/3}$	1:2000 (WB)	ab16830, Abcam
Oxr1	1:1000 (WB)	Custom antibody (Oliver et al., 2011)
α-synuclein	1:200 (ICH)	10842-1-AP, Proteintech
HA tag	1:2000 (WB), 1:200 (ICH)	H6908, Sigma
SNAP-25	1:500 (WB), 1:200 (ICH)	14903-1-AP, Proteintech
Golgin-245	1:250 (ICH)	sc-102565, SantaCruz
LC3	1:1000 (WB)	NB100-2220, Novus
LAMP1	1:500 (WB)	ab25245, Abcam
Rab7	1:5000 (WB)	ab50533, Abcam
Actin	1:2000 (WB)	ab8226, Abcam
anti-rabbit AlexaFlour 546	1:1000	A-11035, Thermo Fisher
anti-rat AlexaFlour 488	1:1000	A-11006, Thermo Fisher
HRP-conjugated anti-rabbit	1:10000	NA934, Amersham
HRP-conjugated anti-rat	1:10000	NA935, Amersham
HRP-conjugated anti-mouse	1:10000	NA931, Amersham

2.5 Recombinant protein production and purification

Recombinant proteins Prdx2 and Oxr1-C were produced in *E.coli* strain BL21(DE3) (Invitrogen). Expression of Prdx2-His_6 and Prdx2-Thr-His_6 was induced by 0.8mM isopropyl β-D-1-thiogalactopyranoside (IPTG) (Sigma) at OD_{600} ~ 0.7-0.8 for 5 hours at 25°C. Oxr1-C-His_6 expression was induced at OD_{600} ~ 0.8 by 0.8mM IPTG and followed by incubation on a shaker for 16 hours at 18°C. Cells were collected by centrifugation at 4,000×g at 4°C for 20 minutes and resuspended in 500mM NaCl PBS supplemented with protease inhibitor (Roche). Bacterial cells were lysed by sonication on ice and centrifuged at 18,000×g for 30 minutes at 4°C. For Oxr1-C, the procedure was repeated twice to increase protein yield. Supernatants containing recombinant His_6-tagged protein were incubated with 1ml TALON metal affinity resin (Clontech) for 1 hour at 4°C. Beads were washed with 5mM imidazole (Sigma) and protein was eluted with 500mM imidazole. Eluted fractions of samples with the highest concentration were dialysed overnight against PBS buffer at 4°C using Slide-A-Lyzer dialysis cassette (Thermo Fisher). The His_6 tag was cleaved from Prdx2-Thr-His_6 using the Thrombin CleanCleave Kit (Sigma Aldrich) at 17°C for 4 hours, as per the manufacturer's protocol. Following the tag cleavage, protein was dialysed overnight against PBS buffer at 4°C to remove Ca^{2+}. Purified proteins were analysed by Coomassie staining and western blotting with anti-Prdx2 and anti-Oxr1 antibodies (Fig. 2.3). Protein concentrations were measured using NanoDrop spectrophotometer with extinction coefficients of 21,555 $M^{-1}cm^{-1}$ for Prdx2 and 38,055 $M^{-1}cm^{-1}$ for Oxr1-C. Recombinant TBC1D24 and TLDc domain of TBC1C24 were produced and kindly provided by Professor Wyatt W. Yue (NDCM, University of Oxford). DNA fragments encoding full-length TBC1D24 (aa 1-553) and TLDc domain (aa 336-553) were

inserted into the pFB-Lic-Bse vector for insect cell expression and pNIC28-Bsa4 for bacterial expression, respectively. Recombinant TBC1D24 was expressed in Sf9 cells, while the TBC1D24 TLDc-domain was expressed in *E.coli* and purified as above, followed by size exclusion chromatography. The purity of the recombinant protein preparation was ascertained by Coomassie staining.

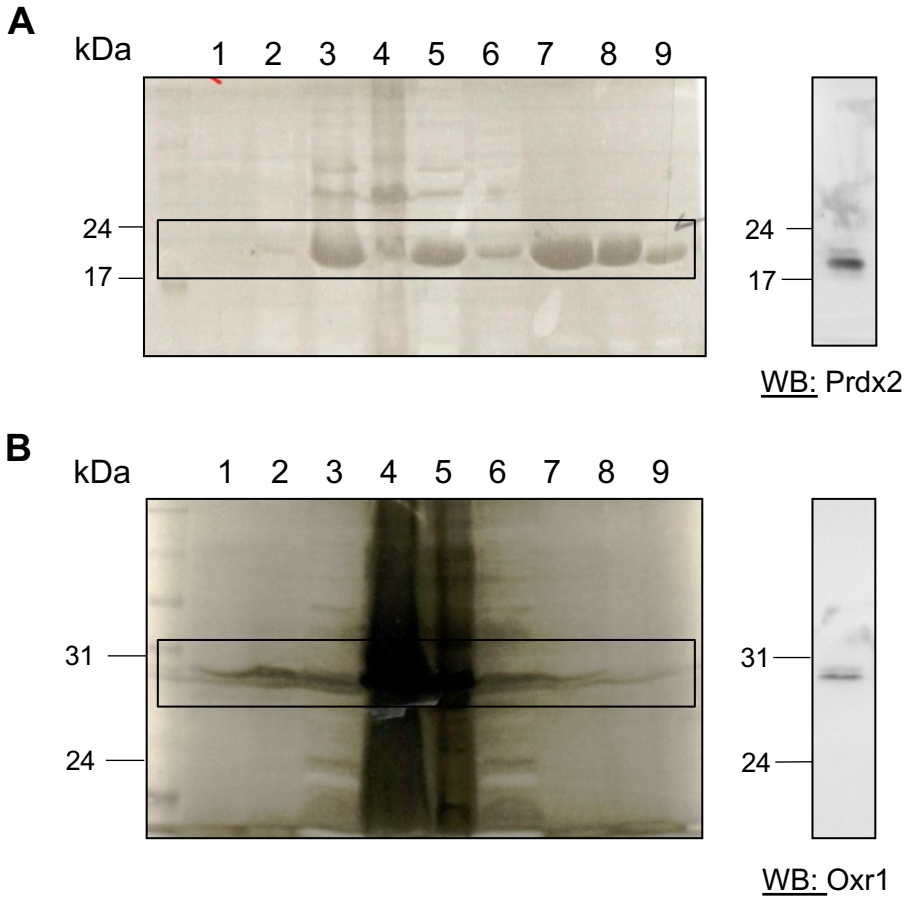


Figure 2.3 Recombinant Prdx2 and Oxr1 production and purification.
(A) Coomassie stained gel showing recombinant Prdx2 purification fractions. Lane 1 – before IPTG induction, 2 – after IPTG induction, 3 – supernatant after sonication, 4 – pellet after sonication, 5 – supernatant after beads pull-down, 6 – beads wash, 7 – beads after elution, 8 – eluted Prdx2 (non-cleaved), 9 – Prdx2 after thrombin cleavage; western blot with purified cleaved Prdx2 probed with an anti-Prdx2 antibody. (B) Coomassie stained gel showing recombinant Oxr1-C purification fractions. 1 – before IPTG induction, 2 – after IPTG induction, 3 – supernatant after sonication, 4 – pellet after 1st sonication, 5 – pellet after 2nd sonication, 6 – supernatant after beads pull-down, 7 – beads wash, 8 – beads after elution, 9 – eluted Oxr1-C; western blot of purified Oxr1-C probed with anti-Oxr1 antibody.

2.6 In vitro activity assays

2.6.1 Peroxiredoxin activity assay

Prdx2-His_6 activity was assessed using ferrous oxidation-xylenol orange (FOX) assay according to the protocol published by Nelson and Parsonage (Nelson and Parsonage, 2011). The colorimetric ferrous oxidation-xylenol orange (FOX) assay allows quantifying reduction rates of H_2O_2 by a known or putative peroxidase and is based on a reaction of a substrate with H_2O_2 in the solution that results in its oxidation and color change proportional to concentration of the peroxide. Briefly, the assay solution contained 100μM dithiothreitol (DTT, Sigma Aldrich), 50μM H_2O_2 (Sigma Aldrich), 2.2μg recombinant purified Prdx2-His_6, with 0 or 0.95μg Oxr1-C in PBS. Reaction was initiated by addition of H_2O_2 and quenched at appropriate time points with 200μl of FOX reagent (1 part of FOX A reagent (25mM ammonium ferrous sulfate (Sigma) in 2.5M H_2SO_4 (Sigma)) and 100 parts of FOX B reagent (100mM sorbitol (Sigma) with 125μM xylenol orange (Sigma) in water)). Samples were incubated at room temperature for at least 30 minutes before reading absorbance at 560nm with Fluostar Omega plate reader.

2.6.2 Holdase activity assay

In vitro holdase activity of Prdx2, Oxr1-C and TBC1D24 was assessed in chemically induced and thermally induced aggregation assays. The ability of Prdx2 and TLDc proteins to protect insulin from DTT-induced aggregation (chemically-induced aggregation) was measured as change of absorbance at 650nm at 25°C over time. The reaction was set in 150μl, solution contained 30μg insulin (Sigma), 20μg Prdx2, 22.5μg and 35μg Oxr1-C, 22.5μg TBC1D24, 22.5μg TBC1D24 TLDc domain or 15μg lysozyme in

100mM phosphate buffer (19mM NaH_2PO_4, 81mM Na_2HPO_4 pH 7.4) and was initiated by addition of DTT to a final concentration of 6.6mM.

Ability of Prdx2 and Oxr1-C to protect citrate synthase from thermally-induced aggregating was monitored by changes in absorbance at 360nm during incubation at 44°C. Reaction was set in 150µl, solution contained 10µg of citrate synthase (Sigma) and 0 or 10µg of Prdx2, Oxr1-C or both in 50mM HEPES pH 8.0.

2.7 Embryo dissecting and genotyping

2.7.1 Embryo dissections

All breedings were set up by Professor Peter Oliver. The day when a plug was observed was considered as day 0 post coitum (dpc). Pregnant mice were culled by dislocation of the neck in accordance with the Home Office's Animals (Scientific Procedures) Act 1986. Removed uteri were placed in a Petri dish containing and embryos were dissected in cold DPBS buffer (Gibco) using forceps and needles. All embryonic membranes and placenta were removed.

2.7.2 Embryo DNA extraction

Early embryos (~E6.5-E9) were lysed in lysis buffer 1 (50mM KCl, 10mM Tris-HCl pH 8.3, 2.5mM $MgCl_2$, 0.1mg/ml gelatin, 0.45% v/v NP40, 0.45% v/v Tween20) supplemented with Protease K (Thermo Fisher) overnight at 37°C. The next day, samples were incubated at 95°C for 5 minutes to deactivate protease. For older embryos (~E10-E11) embryos were lysed overnight at 37°C in lysis buffer 2 (10mM Tris pH8.0, 100mM NaCl, 10mM EDTA pH8.0, 0.5% w/v SDS) supplemented by Protease K. The next day,

solution was mixed with 5M NaCl, centrifuged for 10 minutes at 13,000×g and supernatant was transferred to a new tube. 100% ethanol was added in 1:1 ratio to the DNA-containing solution and after centrifugation DNA pellet was washed with 70% ethanol and resuspended in water.

2.8 RNA preparation and qPCR reaction

2.8.1 cDNA sample preparation

Total RNA extraction from cerebellar and cortex tissues was performed using RNeasy kit (Qiagen) as per the manufacturer protocol. Genomic DNA was eliminated with an on-column RNase-Free DNase Set (Qiagen) treatment. Briefly, cerebella were homogenized using a Precellys homogenizer in RLT buffer supplemented with β-mercaptoethanol (Sigma) and RNA was extracted according to manufacturer's protocol. Cortices were lysed with a Precellys homogenizer in TRIzol reagent (Invitrogen) and lysates were mixed with chloroform. After 3 minute incubation, samples were centrifuged for 15 minutes at 4°C and the upper phase was collected for further extraction. After addition of isopropanol, samples were incubated for 5 minutes at room temperature and centrifuged at maximal speed for 15 minutes at 4°C. Pellets were resuspended in 70% ethanol. After addition of RLT buffer extraction was followed by RNeasy kit protocol to clean the samples. Samples concentrations were measured with NanoDrop spectrophotometer and complementary DNA was synthesized from 1μg of RNA per reaction using RevertAid H Minus First Strand cDNA Synthesis Kit (ThermoFisher) according to manufacturer's protocol.

2.8.2 Primers optimisation

qPCR primers were designed using Primer3 service (http://bioinfo.ut.ee/primer3-0.4.0/). Product size range was 150-200 bp, GC content 40-60%, melting temperature 57-63˚C, size – 19-24 bp. For primer optimisation qPCR reactions were set up with different concentrations of cDNA and only primers with linear template concentration/C_t trends and single-peak melting curves were picked for further experiments.

2.8.3 qPCR reaction

qPCR reactions were set up in duplicates, each 20µl reaction contained 10µl of SYBR Green Master Mix (Applied Biosystems), 5µM forward and reverse primers and cDNA. qPCR plate design and analysis were performed in StepOne software (v. 2.3). Fold-changes were calculated using delta delta Ct method, levels of glyceraldehyde 3-phosphate dehydrogenase (*Gapdh*) mRNA were used for normalization.

Table 2.2. qPCR primers.

C1qb	F: 5'-ATAAAGGGGGAGAAAGGGCT-3' R: 5'-CGTTGCGTGGCTCATAGTT-3'
Cd68	F: 5'-TGCCTGACAAGGGACACTTC-3' R: 5'-TGGTGGCTTACACAGTGGAC-3'
Ctss	F: 5'-GACATTGCCTGACACTGTGG-3' R: 5'-GCAGTCCACCAGGTTCTGAG-3'
Fcrls	F: 5'-TGCAATGGCACAGAAAAGAC-3' R: 5'-AGGCCCAGTGCAGAAAGTAG-3'
Gapdh	F: 5'-AGAACATCATCCCTGCATCC-3' R: 5'-CACATTGGGGGTAGGAACAC-3'
Gfap	F: 5'- GCAGAAGCTCCAAGATGAAACC-3' R: 5'- CGAACTTCCTCCTCATAGATCTTC-3'
HexB	F: 5'-AATGGTCAGCCGTGGAATAG-3' R: 5'-CATAGCTGGAATGCTGTAGACG-3'
mEAK7	F: 5'-GCAGGCTGAGGTAGACAAG-3' R: 5'-CCCTCTGCATGCCGTTATAC-3'
Ly86	F: 5'-TATACTATGCCGGCCCTGTC-3' R: 5'-GGGTCCCCTGAGATTGAGTT-3'
Ncoa7-B	F: 5'-GCCCCTGGACATTCAGATT-3' R: 5'-CTGTGGGGCTGTAGGATAGG-3'
Ncoa7-FL	F: 5'-TGTCGCTACTTCACTGATGG-3' R: 5'-GCGTCTTTGATCTTCATGTG-3'
Oxr1-C	F: 5'-CCATAAATACACTCTGGTAGTGTCG-3' R: 5'-TTTGGTCGGAAAGATTCAGG-3'
Oxr1-FL	F: 5'-CAGTCGTGACTGGACAGGTTT-3' R: 5'-ATGGGCTACATCTGGAGTCG-3'
Tbc1d24	F: 5'-AATGGCCAATGAGAAAGCA-3' R: 5'-AGGGATCCAGGACCAAATG-3'

2.9 Data analysis and statistics

Western blot and microscopy images were analysed using ImageJ (v.1.51f). Statistical analyses were performed using Prism software (v.7.0b) using one-way ANOVA with

Bonferroni multiple comparison correction or unpaired t-test. Data are presented as mean ± SEM. Swiss PDB Viewer (v.4.1.1) was used for the visualization of PDB files. ChIP-Seq data was accessed at ChIP-Atlas (https://chip-atlas.org) and visualised in Integrated Genome Viewer (v.2.5.0) (Thorvaldsdottir et al., 2013). Hits with false discovery rate (FDR) less than 10^{-5} were included. Biological processes prediction was performed with Gene Ontology service (http://geneontology.org).

3. Analysis of Oxr1 interaction with a potent antioxidant enzyme Prdx2

The majority of the results presented in this chapter are published in Svistunova et al. (2018) 'Oxidation resistance 1 regulates post-translational modifications of peroxiredoxin 2 in the cerebellum' (see Appendix 2).

3.1 Introduction

TLDc proteins have been widely studied in contexts of different organisms and processes, but very little is known about their function. One of the key approaches we took to shed light on the role of the TLDc proteins was to determine their interactors; this approach provides valuable insights into the pathways or processes where these proteins are involved. The first study of the Oxr1 interactome was performed in N2a neuronal cell line in basal conditions and under OS (induced by H_2O_2 treatment) (Finelli et al., 2015). The study identified a number of binding partners of Oxr1-FL and Oxr1-C even in untreated conditions, whilst treatment with H_2O_2 increased the number of interactors for both isoforms, suggesting that they may have a function under basal conditions and that they may also acquire additional functions under OS (Finelli et al., 2015). The identified proteins were members of important pathways such as the mTOR and eukaryotic initiation factor 2 (eIF2) signaling, pre-mRNA processing, DNA repair and Nrf2-mediated OS response, the latter identified specifically for the short isoform (Finelli et al., 2015). Some of these proteins, such as Fus, vimentin, paired box 6 (Pax6) transcription factor and RNA helicase DDX3X (DEAD-box helicase 3 X-linked) were interacting with both Oxr1 isoforms (Finelli et al., 2015). Interestingly, most of the identified interactors were unique to a particular isoform, only a limited number of proteins was binding to both Oxr1-FL

and Oxr1-C, suggesting that although both isoforms may share some common functions, they may also have specific and differential roles (Finelli et al., 2015).

As the study was limited to Oxr1 and had been performed in a cell line, a much larger screen for binding partners for all TLDc proteins has since been carried out in adult wild-type mouse tissue in our laboratory by Dr Mattéa Finelli. As most of the TLDc proteins are expressed in the brain and some of them are associated with neurological and neurodegenerative phenotype when mutated or knocked out, this organ was selected to determine the TLDc protein interactome *in vivo*. This systematic analysis of the TLDc proteins' binding partners has provided clues on the potential roles for the TLDc domain, which is common between all family members, as well as identified unique functions for each TLDc protein. This study identified a small number of interactors common between all family members, suggesting common functions between the TLDc proteins (Dr Mattéa Finelli, personal communication). As all TLDc proteins have been shown to protect against OS *in vitro* and *in vivo* (Finelli et al., 2016, Oliver et al., 2011), we identified, as expected, various players of the cellular OS-defense machinery among these binding partners. In particular, among the identified proteins were antioxidant and detoxification enzymes glutathione-S-transferase Mu 1 (Gstm1), Gstp1, Prdx2 and SOD1, suggesting that TLDc proteins play a role in the cellular defense system. Prdx2 and Gstm1 could bind all family members, while Gstp1 and SOD1 interacted with Ncoa7-B and Oxr1, respectively, indicating potential specialization of Oxr1 in OS response pathways. Together, the evidence of TLDc proteins' interaction with these enzymes suggests their involvement in various aspects of ROS detoxification potentially in different cellular compartments.

Interestingly, this study also identified binding partners contributing to other cellular processes, suggesting novel functions for the TLDc proteins in addition to their OS-related role. These included transcription factors, essential metabolic enzymes and

transmembrane channels and transporters. For example, all family members were shown to interact with Gpi1, a key enzyme of the glucose metabolism pathway. Follow-up studies demonstrated that Oxr1 interacts with and regulates the function of Gpi1 (Finelli et al., 2018b). Gpi1 possesses a dual function as a glycolytic enzyme and as a cytokine that are dependent on its oligomerisation status; Oxr1-FL, but not Oxr1-C, has been shown to regulate oligomerisation of Gpi1 *in vivo* and *in vitro* and to favor formation of the monomeric cytokine form (Finelli et al., 2018b). In agreement with previously published data that Oxr1 and Ncoa7 interact with v-ATPase, all TLDc proteins were shown to bind its subunits, confirming reproducibility of the results (Merkulova et al., 2015). Ncoa7-FL was also shown to interact with various histone modification enzymes, such as histone deacetylase (Hdac) 7 or lysine-specific methyltransferase, suggesting it may act as transcription regulator via chromatin modulation. Together, these data suggest a broad range of functions carried out by TLDc proteins and presence of some conserved roles shared between all family members.

Given that so far no antioxidant activity has been described for the TLDc proteins, one of the outstanding challenges is to understand how the TLDc proteins carry out their OS-protective function. Therefore, I decided to investigate in more detail the role of the interaction between the TLDc proteins and a potent antioxidant Prdx2 in regulating activity and function of each other. Prdx2 is a ubiquitously expressed antioxidant enzyme, a member of the peroxiredoxin protein family that catalyses reduction of peroxides (Rhee, 2016). Prdxs are highly abundant enzymes constituting up to 0.2-0.8% of the total soluble protein fraction in cells and tissues (Chae et al., 1999). It has also been shown that many Prdxs react with H_2O_2 at rates comparable to catalase and Gpx, suggesting a large fraction of peroxides in the cytoplasm being reduced by Prdxs (Karplus, 2015, Parsonage et al., 2005). Prdx2 has been shown to be differentially expressed in various neurological

disorders – it is up-regulated in frontal and cerebral cortices and thalamus of patients with AD and cerebellum, temporal and frontal cortices, thalamus and caudate nucleus of people with Down's syndrome, as well as cerebral cortex of a mouse model of AD, suggesting it plays an important role in brain function (Kim et al., 2001, Krapfenbauer et al., 2003, Yao et al., 2007). Prdx2 induction is also observed in motor neurons in spinal cord sections of patients and in a mouse model of ALS (Kato et al., 2005). Together, these data suggest an important role of Prdx2 in neuronal survival. Knockout of *Prdx2* in mice leads to accumulation of ROS and oxidative DNA damage in the CA1 region of the hippocampus - similar to what is observed in in CGCs of the $Oxr1^{d/d}$ mice that carry deletion in the TLDc domain-coding region of the gene and loss of all Oxr1 isoforms (Kim et al., 2011, Oliver et al., 2011). Neuronal overexpression of Prdx2 has been shown to be protective against ischemic neuronal cell death and DNA fragmentation in mice (Gan et al., 2012). Moreover, expression pattern of *Prdx2* overlaps with that of *Oxr1* – both proteins are present in the granule cell layer of the cerebellum, as well as some regions of the cortex and olfactory bulb (Finelli et al., 2016, Goemaere and Knoops, 2012, Lein et al., 2007, Tabula Muris et al., 2018). Therefore, interaction of Prdx2 and Oxr1 was chosen for further analyses as it potentially places TLDc proteins into a central, well-characterised antioxidant pathway.

In addition to its antioxidant function, Prdx2 is also a chaperone, with its dual function being regulated by the redox state of the cell (Jang et al., 2004, Moon et al., 2005). Chaperone complexes of Prdxs can act as both holdases and foldases – two distinct classes of chaperones (Kim et al., 2009, Lee et al., 2015a, Moon et al., 2005). Holdases are a class of chaperones that bind unfolded or misfolded proteins and prevent them from further aggregation in ATP-independent manner, whereas foldases are classical chaperones that assist folding and refolding (Mattoo and Goloubinoff, 2014). The activities of Prdx2 as an

antioxidant enzyme and as a chaperone are dependent on the protein's oligomeric state (Moon et al., 2005): as homodimers and decameric rings, Prdx2 acts as an H_2O_2 scavenger, while its transition into a chaperone state is accompanied by conformational changes that lead to assembly of the high molecular weight (HMW) complexes (Moon et al., 2005). In addition, its activity and function are also regulated by various PTMs, including oxidation, phosphorylation, nitration and S-nitrosation (Chae et al., 2012, Jang et al., 2004, Jang et al., 2006, Moon et al., 2005, Randall et al., 2014). The most abundant PTM of Prdx2 is hyperoxidation of its catalytic cysteine (Cys) residues in its active site, which occurs under OS conditions (Karplus, 2015, Moon et al., 2005). The catalytic antioxidant activity is carried out by two Cys residues in each of two active centers of the complex formed by two Prdx2 molecules. Upon reaction with H_2O_2, the sulfur atom in the Cys residue is oxidised to form a sulfenic acid Prdx2-SO, which in turn forms disulfide bridge with the Cys residue in the second Prdx2 molecule and is reduced to its active state by Trx (Fig 3.1) (Karplus, 2015). In presence of high H_2O_2 levels Prdx-SO is further oxidised and forms sulfinic and sulfonic acids – Prdx2-SO_2 and Prdx2-SO_3, respectively (Fig 3.1) (Karplus, 2015, Moon et al., 2005, Veal et al., 2018). These hyperoxidised Prdx2 molecules lose antioxidant activity and assemble into HMW complexes that act as chaperones and protect proteins in the cell from OS-induced aggregation (An et al., 2011, Kim et al., 2009, Moon et al., 2005, Phalen et al., 2006, Rhee and Woo, 2011).

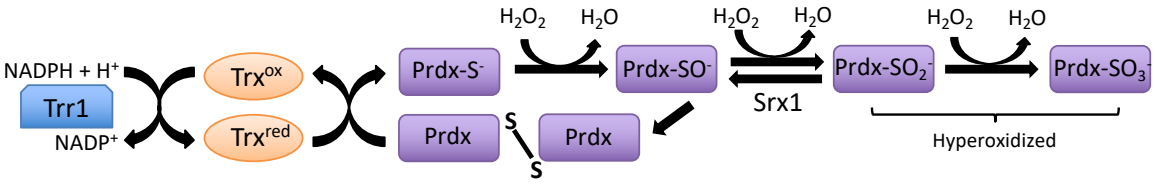


Figure 3.1 Catalytic cycle of peroxiredoxin.
Catalytic cycle of Prdx homodimer antioxidant complex includes oxidation of the Cys residue, formation of disulfide bond with the Cys residue in the second molecule and reduction of the reactive center by thioredoxin system. Excessive H_2O_2 leads to further oxidation and formation of Prdx-SO_2 and Prdx-SO_3. Modified from (Veal et al., 2018).

Ability of Oxr1 to confer protection against OS without enzymatic antioxidant activity suggest it is involved in regulation of activity or expression of other antioxidant proteins, such as Prdx2. The aim of this chapter is to investigate the role of Oxr1:Prdx2 interaction *in vitro* and *in vivo*. It will be studied, whether Oxr1 affects Prdx2 function and the mechanisms of it, and the importance of their interaction for cellular homeostasis. Experiments were performed with purified recombinant proteins as well as *in vitro* and *in vivo* using overexpressing cells and brain tissues of knockout *Oxr1*$^{d/d}$ and Oxr1 overexpressing mouse models already available in our laboratory. In particular, the role played by Oxr1 on Prdx2 PTMs, an important regulator of its activity, and its effect on Prdx2 oligomeric state *in vitro* and *in vivo*, was investigated. To study the molecular role of Oxr1 in Prdx2 function as an antioxidant and as a holdase chaperone, *in vitro* assays with recombinant proteins were performed.

3.2 Results

3.2.1 Oxr1 interacts with Prdx2, one of the major antioxidant enzymes in the CNS

To test whether Prdx2 and Oxr1 could potentially interact *in vivo*, I first analysed if they were co-expressed in neurons. To test that, I analysed the intracellular localizations of Prdx2 and Oxr1 in primary cerebellar cultures from mice overexpressing HA-tagged Oxr1-FL cDNA transgene (Oxr1 Tg) under control of neuron-specific *Prnp* promoter (Liu et al., 2015). This approach has been used because no Oxr1-specific antibodies are available for immunochemistry and we rely on tagged Oxr1 to visulalise its intracellular localization. Up to 95% of cerebellar neurons are represented by CGCs - cells where *Oxr1* is predominantly expressed in the cerebellum. Thus, although *Prnp* promoter will drive *Oxr1* expression in all neurons, CGCs will constitute the majority of them, and co-expression of Prdx2 with Oxr1-HA would indicate its co-expression with endogenous Oxr1 as well (Shepherd, 2004). Importantly, CGCs are the only cells which die in $Oxr1^{d/d}$ mouse brain, suggesting they are especially vulnerable to *Oxr1* depletion, possibly due to their overall higher vulnerability towards OS (Oliver et al., 2011, Wang and Michaelis, 2010). It makes them an attractive model to study Oxr1:Prdx2 interaction, as it could possibly shed light on the mechanisms underlying the selective neurodegeneration observed in $Oxr1^{d/d}$ mice. Prdx2 staining was observed both in the cytoplasm and the nucleus of primary cerebellar neurons, as previously described (Fig 3.2A) (Goemaere and Knoops, 2012). Full-length Oxr1-HA was present in the cytoplasm (Fig 3.2A), in agreement with previously published data (Wu et al., 2016). Importantly, all of the cells positive for Oxr1-HA protein were also expressing endogenous Prdx2, suggesting Prdx2 and Oxr1 are co-expressed in CGCs.

To validate the interaction between Oxr1 and Prdx2 identified initially by pull down assay in brain extracts, immunoprecipitation from N2a cells co-overexpressing Prdx2-Myc and HA-tagged Oxr1-FL and Oxr1-C was performed. The experiment confirmed the binding of both Oxr1 isoforms to exogenous Prdx2 (Fig 3.2B). Next, to investigate if other TLDc family members are also capable of binding Prdx2 *in vitro*, a similar experiment from cells co-overexpression Prdx2-Myc and either Ncoa7-FL-HA, Ncoa7-B-HA or Tbc1d24-HA was carried out. The experiment confirmed binding of Prdx2 to all these proteins, suggesting it is a common binding partner of TLDc family members (Fig 3.2B).

Next, to investigate whether the interaction also occurs *in vivo* in the CNS, I performed co-immunoprecipitation from mouse wild-type CNS tissue. As *Oxr1*$^{d/d}$ mouse displays cerebellar-specific neuronal loss, I investigated whether the interaction between Oxr1 and Prdx2 could be brain region-specific, which could be a potential mechanisms underlying the selective neuronal cell loss observed in the *Oxr1*$^{d/d}$ (Oliver et al., 2011). Thus, experiments with cerebrum and cerebellum were carried out separately. In the cerebrum, I observed Oxr1-FL:Prdx2 binding, confirming the interaction *in vivo* (Fig 3.2C). Interestingly, no interaction was observed in the cerebellum (Fig 3.2D). Together, these data suggest the Oxr1 interacts with Prdx2 both *in vitro* and *in vivo*, and the interaction is common between short and full-length isoforms. The data also suggest a possible brain region-specificity for this interaction.

3.2.2 Oxr1 and Prdx2 do not interact functionally to protect against OS-induced cell death

Given that I showed that Oxr1 and Prdx2 physically interact, I next investigated whether this interaction would have any consequence on their respective function. To

analyse if Oxr1 and Prdx2 could functionally interact, I first assessed whether they could affect each other's main function as protectors against OS (Finelli et al., 2016, Gan et al., 2012, Oliver et al., 2011, Zhou et al., 2016). To test this hypothesis, I used neuronal N2a cell line overexpressing either Prdx2 or one of the Oxr1 isoforms, or Prdx2 and Oxr1-FL or Oxr1-C together. Cells were treated with H_2O_2 to induce OS and cell death was assessed by counting the number of pyknotic nuclei. Consistent with our previous data, Oxr1-FL and Oxr1-C reduced the rate of cell death compared to cells expressing an empty control vector (Fig 3.2E). Prdx2 also conferred protection against OS-induced cell death, although its effect was less prominent than with Oxr1 at this dose and duration of treatment (Fig 3.2E). Interestingly, co-transfecting cells with either isoform of Oxr1 together with Prdx2 did not provide any additional protective effect (Fig 3.2E). This suggests that Oxr1 and Prdx2 do not promote each other's protective activity or have any synergistic effect to protect against OS-induced cell death.

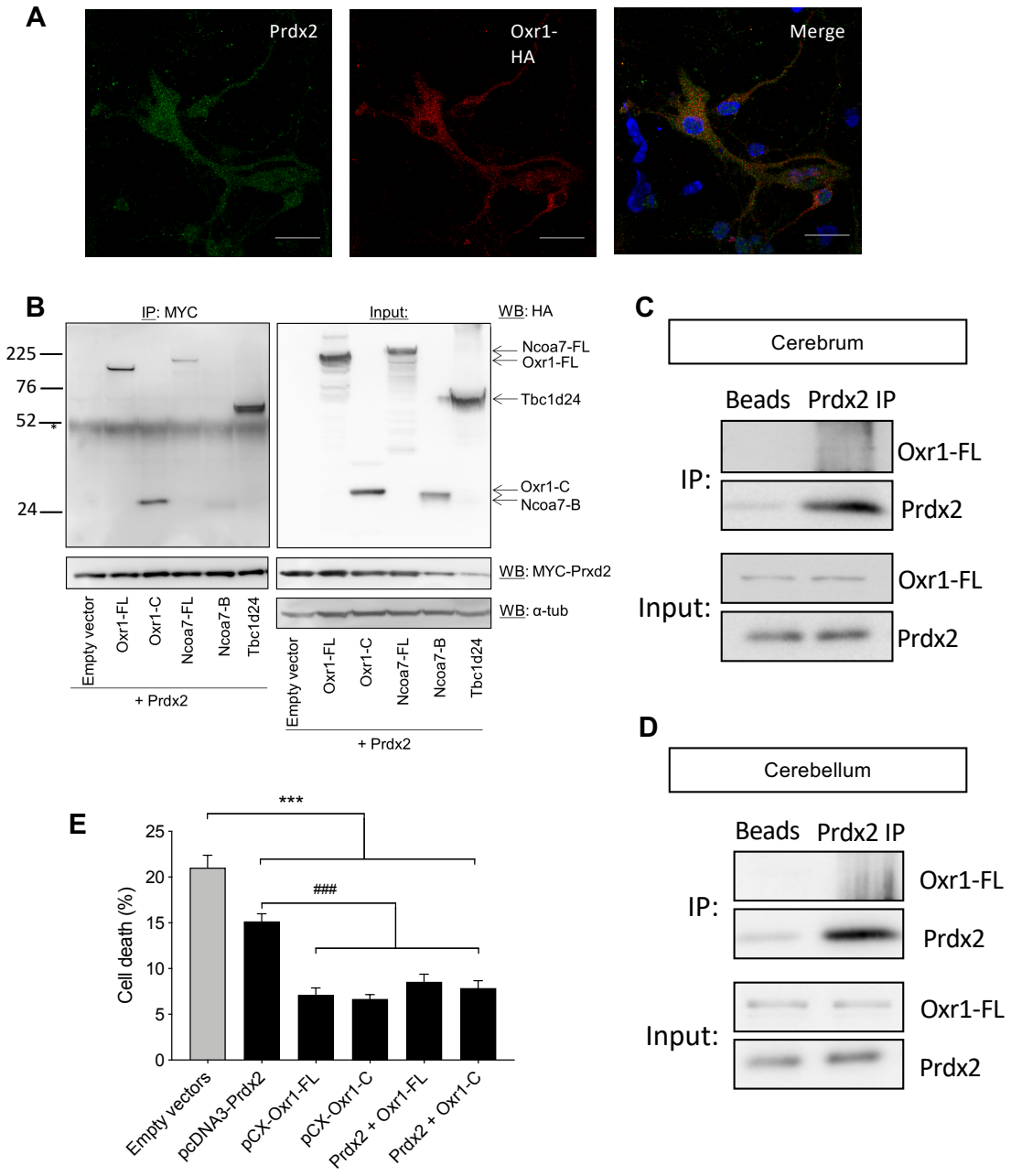


Figure 3.2 Oxr1 and Prdx2 bind in the brain, but do not have synergistic effect in cell death protection.

(A) Primary cerebellar cultures from Oxr1 Tg mice were stained for endogenous Prdx2 (green) and *Prnp* promoter-driven Oxr1-HA (red). Scale bar 25µm. (B) N2A cells were co-transfected with Prdx2-Myc and HA-tagged TLDc constructs as indicated. Results of co-immunoprecipitation using an anti-Myc antibody are shown by immunoblotting for HA (left panel). α-tubulin was used as a loading control for the input samples (right panel). The asterisk (*) represents non-specific IgG heavy chains. From Svistunova et al. (2018). (C-D) Co-immunoprecipitation of Oxr1-FL with Prdx2 from adult wild-type mouse cerebrum (C) and cerebellum (D). (E) N2A cells transfected with the indicated constructs were treated with 500µM H_2O_2 for 5 hours and cell death was quantified as the number of pyknotic nuclei. 10 fields of view per condition were quantified (N=100-150 cells per field of view). Data are represented as mean ± SEM, one-way ANOVA with Bonferroni correction, ***p<0.001 compared to empty vectors, ###p<0.001 compared to transfection with Prdx2.

3.2.3 Oxr1 does not regulate Prdx2 antioxidant activity *in vitro*

Oxr1 has been previously shown to reduce the levels of ROS *in vivo* and *in vitro*, however, so far no direct antioxidant activity has been identified, therefore it remains unclear how Oxr1 can modulate ROS levels in cells (Finelli et al., 2016, Oliver et al., 2011, Sanada et al., 2014). One hypothesis would be that Oxr1 indirectly modulates ROS levels by regulating the activity of an antioxidant enzyme, such as Prdx2. Prdx2 is an attractive target as it binds to Oxr1 *in vivo* and is a potent antioxidant that can reduce the level of ROS in cells and is highly expressed in neurons. To test this hypothesis, I quantified Prdx2 antioxidant activity in the presence or absence of Oxr1 in a cell-free assay using a peroxidase activity ferrous oxidation-xylenol orange (FOX) assay on recombinant non-His-tagged Prdx2, OXR1-FL and Oxr1-C; details for recombinant protein production and purification can be found in Materials and Methods (Chapter 2, 2.5). The purity and specificity of recombinant proteins were confirmed by Coomassie staining and western blotting with Prdx2 and Oxr1 antibodies (Chapter 2, Fig. 2.3).

As expected, Prdx2 significantly reduced H_2O_2 in this system. However, incubation of either isoform of Oxr1 alone with H_2O_2 did not lead to any decrease in H_2O_2 levels suggesting that Oxr1 does not possess a peroxidase activity *in vitro* (Fig. 3.3). Co-incubation of Prdx2 with Oxr1-C did not affect the peroxide reduction rates, suggesting that Oxr1-C does not affect Prdx2 antioxidant activity *in vitro*, at least in this cell-free assay, and Prdx2 does not act as inducer of potential Oxr1-C peroxidase activity (Fig. 3.3). These results also confirmed our previous observation that Oxr1 on its own does not possess an ability to reduce H_2O_2 in cell-free conditions (Oliver et al., 2011). Together, the results suggest that Oxr1-C does not have a major influence on Prdx2 peroxidase activity *in vitro*.

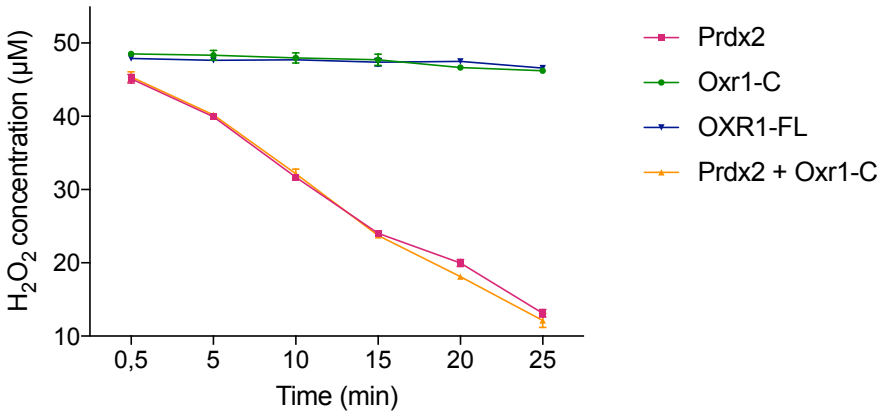


Figure 3.3 Oxr1 does not modulate Prdx2 antioxidant activity *in vitro*.
Changes in H2O2 concentration were monitored using FOX assay over 25 minutes with either recombinant purified Prdx2, Oxr1-C, OXR1-FL or Prdx2 with Oxr1-C with 50µM H2O2. (N=3-5 independent repeats).

3.2.4 Oxr1 and Prdx2 both prevent protein aggregation *in vitro*

To systematically study the potential functional interaction between Oxr1 and Prdx2, I next analysed if Oxr1 could modulate Prdx2 chaperone activity *in vitro*. Prdx2 has previously been shown to possess holdase activity (Moon et al., 2005). Thus, I analysed if Oxr1 could modulate holdase activity of Prdx2 chaperone complexes *in vitro* using recombinant proteins.

Initially, I performed the experiment using a recombinant Prdx2 tagged with a hexahistidine (His_6), as the expression vector was available in our laboratory. However, this Prdx2 unexpectedly did not display any holdase activity as opposed to previously published data (Moon et al., 2005). Based on my analysis of Prdx2 PDB structure in SwissPDB Viewer and *in silico* addition of the His_6-tag to the structure, I identified a positively charged C-terminal His_6-tag as potentially affecting Prdx2 HMW complexes assembly. The positively charged His_6-tag would be located adjacent to positively charged His_6-tag residues of another Prdx2 molecule, potentially leading to steric effect or repulsion between them; moreover, His residues have p atomic orbitals located perpendicular to the imidazole ring that can affect folding of the peptide and induce additional steric hindrance (Fig. 3.4A,B). Therefore, I subsequently produced recombinant Prdx2 with a cleavable His_6-tag (Prdx2-Thr-His), which I used for this particular assay testing its chaperone activity. Native-PAGE analysis confirmed that, as suspected, the presence of His_6-tag did indeed interfere with the assembly of Prdx2 HMW forms (Fig. 3.4C), and therefore potentially with its chaperone activity. Preliminary run of the chaperone activity assay confirmed a protective activity of non-tagged Prdx2 (not shown), therefore, it was used in further *in vitro* assays.

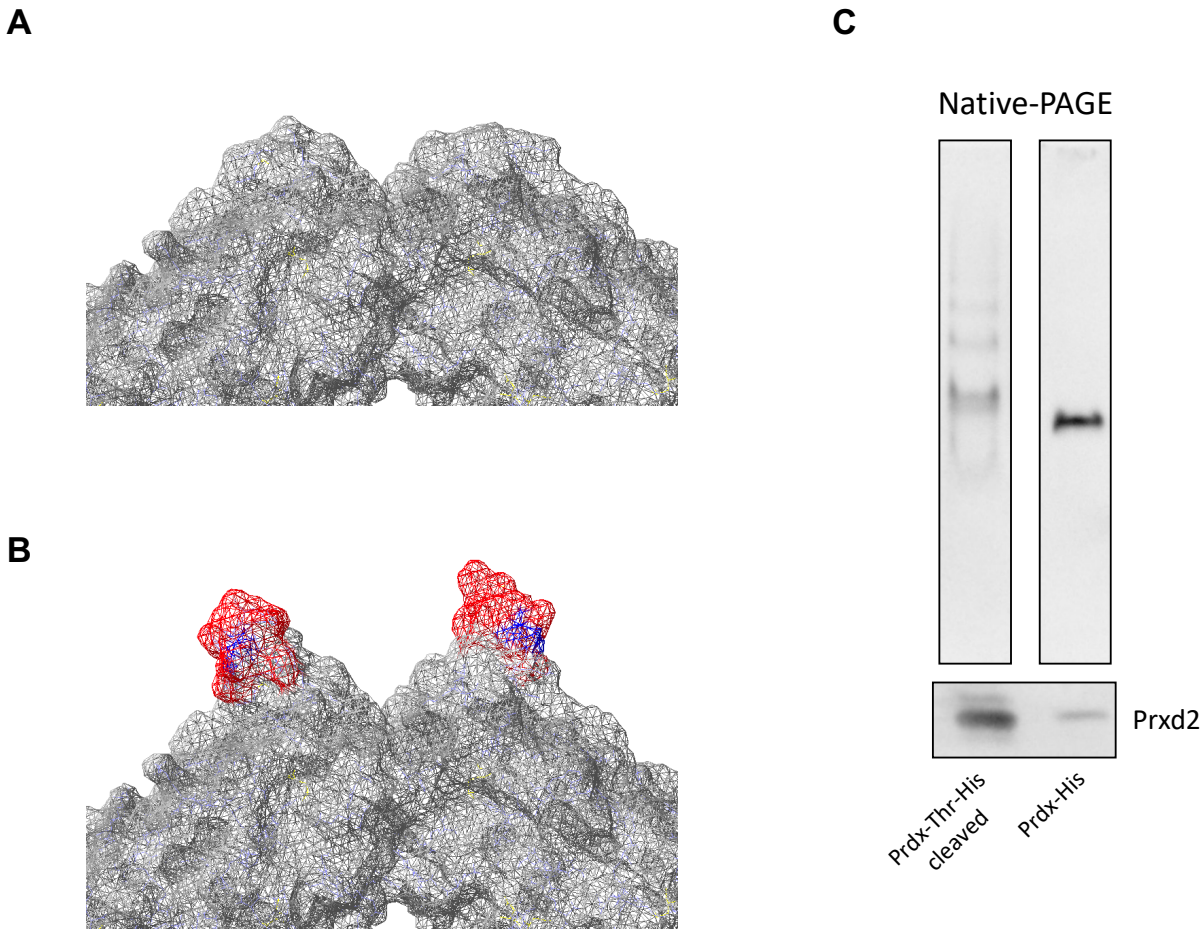


Figure 3.4 Presence of His6 tag affects assembly of Prdx2 HMW complexes.
(A) Molecular surface of untagged Prdx2 oligomer. (B) Molecular surface of Prdx2-His_6 oligomer showing positively charged histidine residues. PDB ID: 1QMV (C) Cleaved Prdx2-Thr-His and Prdx2-His_6 proteins were resolved using native PAGE and probed with anti-Prdx2 antibody. The same proteins were ran on denaturing SDS PAGE as a specificity control.

To investigate if Oxr1 can modulate Prdx2 holdase activity *in vitro* I utilized two well-established aggregation assays, one based on chemically-induced aggregation and another based on thermally-induced aggregation of the substrate protein in presence or absence of putative or known holdase chaperone. Aggregation of the substrate leads to an increase in absorbance of the solution, and activity of the chaperone is monitored as a decrease in absorbance, which corresponds to a decrease in substrate aggregation. I set up two chaperone activity assays to compare the findings between distinct experimental conditions and confirm the specificity of the obtained results. I first used an *in vitro* assay that allows the quantification of insulin aggregation induced by chemical treatment (with DTT) in presence of a known or putative holdase. As expected, Prdx2 significantly decreased the aggregation rate of insulin, whereas the control, non-chaperone lysozyme, had no effect on insulin aggregation (Fig. 3.5A). Interestingly, incubation of Oxr1-C together with Prdx2 led to further significant decrease in aggregation rate suggesting Oxr1 might be enhancing holdase activity of Prdx2 (Fig. 3.5A). Next, I utilized another holdase activity assay based on thermally-induced citrate synthase (CS) aggregation to confirm the observed result with a different substrate and to rule out the possibility that what is observed was insulin-specific. In agreement with the insulin aggregation assay, Prdx2 protected CS from aggregation and addition of Oxr1-C to the reaction enhanced holdase activity of Prdx2 and significantly reduced the aggregation (Fig. 3.5B). Together, these data suggest that Oxr1 might regulate Prdx2 holdase chaperone activity *in vitro*.

3.2.5 A novel molecular function of Oxr1 as a holdase chaperone

Surprisingly, when holdase activity assays were performed with Oxr1-C alone, I observed a significant decrease in the substrate aggregation rate in both chemically- and thermally-induced aggregation assays (Fig 3.5B,C). This result indicates that Oxr1-C

might possess holdase activity. To confirm the holdase activity of Oxr1-C, I repeated the experiment with increased amount of the protein; I expected that increasing Oxr1 concentration would lead to increase in its protective properties against protein aggregation if it was indeed a chaperone. Increasing the concentration of Oxr1-C by 1.5-fold led to a significant decrease in insulin aggregation rate, confirming Oxr1 may possess a holdase activity (Fig. 3.5C). To investigate if holdase chaperone activity is a general function of Oxr1 or is limited to its short isoform, I repeated the experiment with recombinant OXR1-FL. I observed a significant decrease in aggregation rates in the presence of OXR1-FL as compared to no-chaperone control, suggesting both Oxr1 isoforms possess novel holdase chaperone activity *in vitro* (Fig. 3.5C).

Next, to test if this chaperone activity is shared between different TLDc-containing proteins, I performed an aggregation assay with another member of the family - TBC1D24. To test whether the TLDc domain is critical for this function, I tested the holdase properties of the TLDc domain of TBC1D24. The TLDc domain of TBC1D24 shares 28% protein sequence identity and 41% similarity with Oxr1-C and includes additional 49 residues. Insulin-based aggregation assay revealed that the TLDc domain of TBC1D24 does not possess holdase activity (Fig. 3.5C). As presence of all domains of the protein may be required to carry out the protective functions, I repeated the experiment using the full-length recombinant TBC1D24. The full-length protein also did not show any protective holdase properties and did not reduced insulin aggregation rate suggesting it does not possess holdase activity (Fig. 3.5C). Thus, holdase activity is not a general property of TLDc family members and is either specific to Oxr1 or might be shared between some members of the family. Together, these data present a novel putative function for Oxr1 as a holdase chaperone.

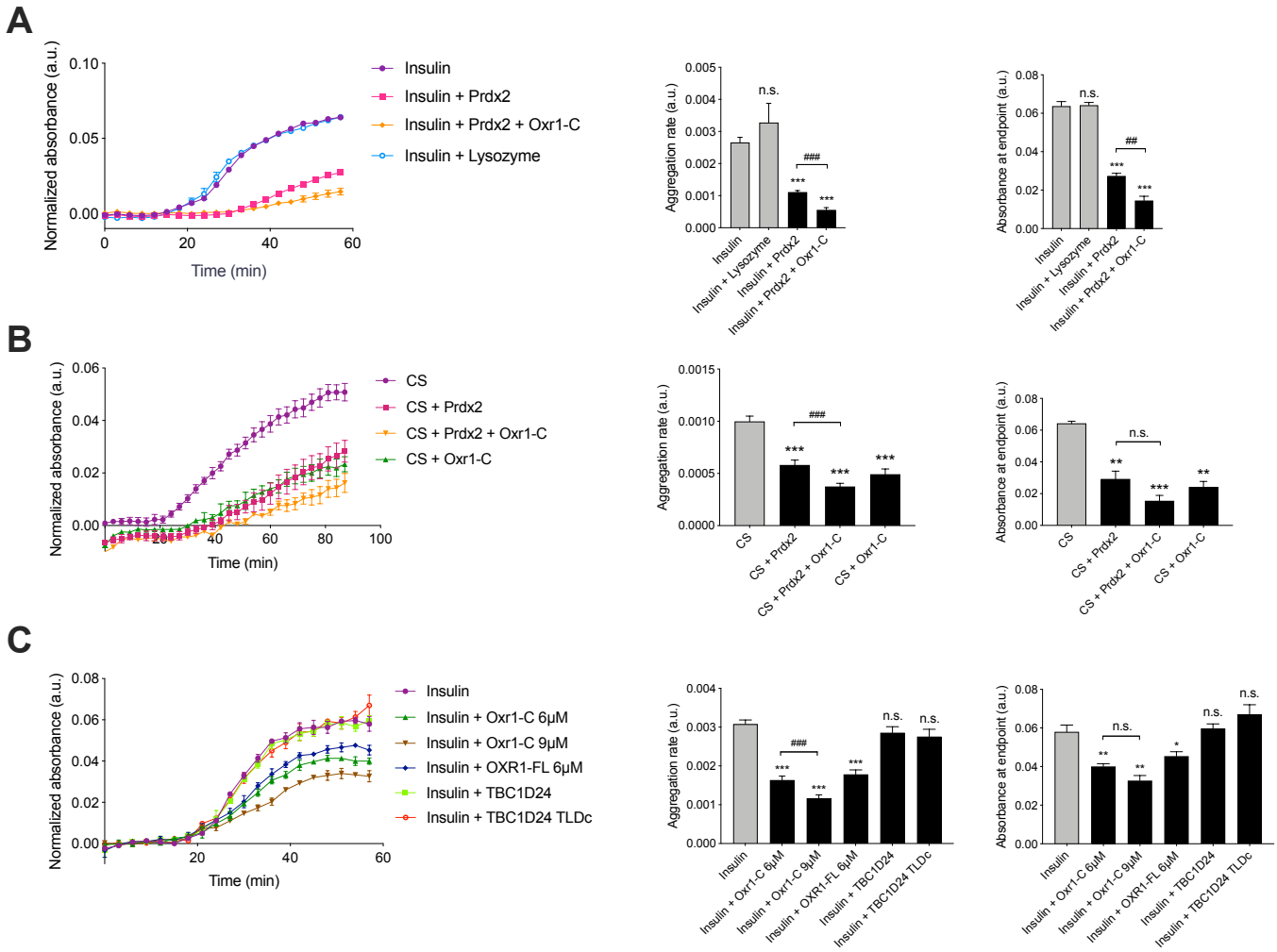


Figure 3.5 Both Prdx2 and Oxr1 possess holdase chaperone activity *in vitro*.
(A) DTT-induced insulin aggregation assay using recombinant Prdx2 and Oxr1-C with lysozyme as a negative control. Absorbance readings at 650nm were taken every 3 minutes. Quantifications for the aggregation rate and absorbance at endpoint are shown. (B) Thermally-induced CS aggregation assay using recombinant Prdx2 and Oxr1-C. Absorbance readings at 360nm were taken every 3 minutes. Aggregation rate and absorbance at end point are shown. (C) DTT-induced insulin aggregation assay using two concentrations (6μM and 9μM) of recombinant Oxr1-C or human OXR1-FL (6μM), in parallel with human TBC1D24 and the TLDc domain of TBC1D24 (TBC1D24 TLDc). Absorbance readings at 650nm were taken every 3 minutes. Quantifications for the aggregation rate and absorbance at endpoint are presented. Data are represented as mean ± SEM. N=3 independent repeats. t-test, *p<0.05, **p<0.01, ***p<0.001 as compared to insulin (B, D) or CS (C), ##p<0.01, ###p<0.001 as compared to insulin + Prdx2 (B), CS + Prdx2 (C) or insulin + Oxr1-C 6μM (D).

3.2.6 Oxr1 modulates PTMs of Prdx2 *in vitro* and *in vivo*

Acting as a functional switch for Prdx2, its activity and functions are regulated by various PTMs. Therefore, I next investigated whether Oxr1 could modulate Prdx2 PTMs. First, I analysed *in vitro* if overexpression of Oxr1 could affect the levels of Prdx2 hyperoxidation (Prdx2-$SO_{2/3}$), its main PTM, using N2a cell line overexpressing Oxr1-FL or Oxr1-C. As Prdx2-$SO_{2/3}$ was undetectable in non-treated cells (data not shown), I performed this assay in OS conditions to induce hyperoxidation of Prdx2 by treatment of cells with H_2O_2. Preliminary experiments have shown that the micromolar concentrations of H_2O_2 were the optimal conditions to induce moderate increase in levels of Prdx2-$SO_{2/3}$, allowing to measure possible effects of Oxr1 on this modification. Levels of Prdx2-$SO_{2/3}$ were assessed by western blotting and measured as a proportion of modified protein Prdx2-$SO_{2/3}$ over total Prdx2 level. In cells overexpressing Oxr1-FL, I observed a significant increase in levels of Prdx2-$SO_{2/3}$, and similar effect was present in cells overexpressing Oxr1-C (Fig. 3.6A,B). This suggests that Oxr1 can regulate Prdx2 PTMs, directly or indirectly, and this ability is shared between full-length and short isoforms.

Next, to test whether this observation holds true *in vivo*, I used brain tissue from wild-type and Oxr1 Tg overexpressing mice and analysed the levels of Prdx2-$SO_{2/3}$. As I have previously shown that Oxr1:Prdx2 interaction does not occur in the cerebellum, I decided to study if this difference in Oxr1:Prdx2 binding between brain regions translates into difference in Prdx2 PTM regulation. Thus, I performed my experiments separately in cerebrum and cerebellum. Consistent with the *in vitro* findings, I observed an increase in Prdx2-$SO_{2/3}$ levels compared to wild-type mice ($Oxr1^{+/+}$) in both brain regions (Fig. 3.6C,D). To confirm that Oxr1 does indeed modulate Prdx2 hyperoxidation, I assessed whether loss of Oxr1 would have the opposite effect on Prdx2-$SO_{2/3}$ levels. To test this, I used cerebrum and cerebellum of $Oxr1^{d/d}$ pre-symptomatic P18 animals and control

littermates. There was no change in the levels of Prdx2-$SO_{2/3}$ in *Oxr1*$^{d/d}$ cerebrum as compared to wild-type animals, whereas significant decrease was observed in the cerebellum (Fig. 3.6E,F). These data confirm that Oxr1 modulates Prdx2 PTM and suggest that it is a brain region-specific mechanism.

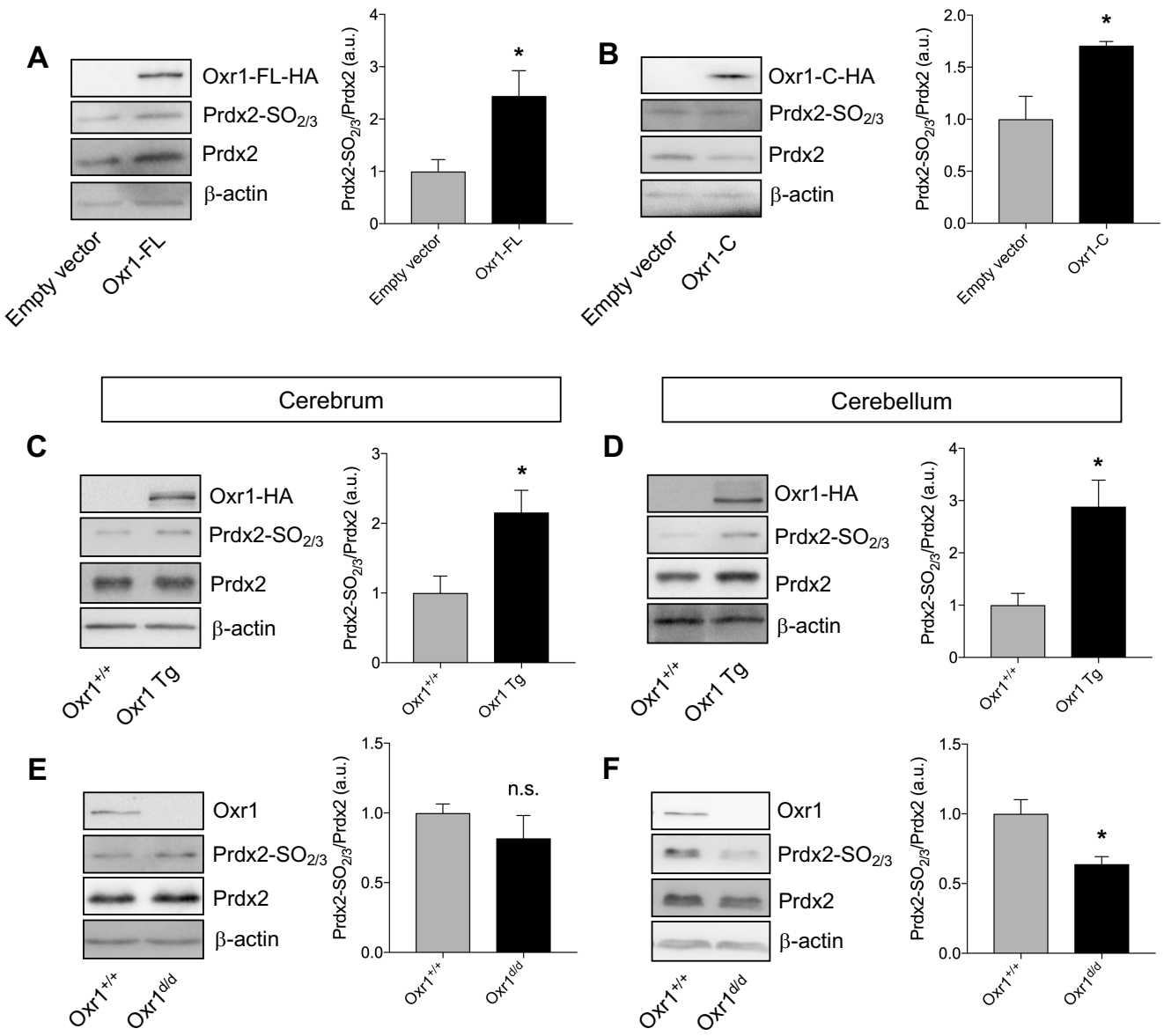


Figure 3.6 Oxr1 modulates Prdx2 hyperoxidation *in vitro* and *in vivo*.
(A-B) N2A cells were transfected with either Oxr1-FL (A) or Oxr1-C (B) and treated with 300µM H_2O_2 for 1 hour. Representative image of western blots and quantification of Prdx2 hyperoxidation is shown as the ratio of Prdx2-$SO_{2/3}$ to total Prdx2 (N=6 independent repeats for Oxr1-FL and N=3 independent repeats for Oxr1-C). (C-F) Representative westerns blots of protein extracts from an adult Oxr1 overexpressing mouse (Oxr1 Tg) (C-D) and a P18 Oxr1 knockout (*Oxr1*$^{d/d}$) mouse (E-F) from both the cerebral and cerebellar tissues, with quantification of Prdx2 hyperoxidation compared to wild-type controls (N=3-4 animals per group). β-actin was used as a loading control. Data presented as mean ± SEM, t-test, *p<0.05.

3.2.7 Oxr1 modulates oligomeric state of Prdx2 *in vitro* and *in vivo*

Next, as Prdx2 hyperoxidation plays an important role in the regulation of its HMW complexes assembly, I went on to investigate if modulation of Prdx2 hyperoxidation by Oxr1 *in vitro* leads to deregulation of its HMW complex formation, potentially altering its chaperone function. Using non-reducing native-PAGE, I first assessed the effect of Oxr1 overexpression on oligomerisation of Prdx2 in N2a cells overexpressing Oxr1-FL. Cells were treated with H_2O_2 to promote formation of HMW complexes of Prdx2 via its hyperoxidation using the same dose used previously to induce formation of Prdx2-$SO_{2/3}$. In control vector-transfected cells, I observed the presence of the dimeric form of Prdx2 with apparent molecular weight ~60kDa as well as HMW complexes of ~400kDa (Fig. 3.7A). Interestingly, in Oxr1-overexpressing cells, I observed formation of additional HMW complex of a smaller size (~250kDa), suggesting that Oxr1 affects assembly of Prdx2 oligomers *in vitro* (Fig. 3.7A).

Next, to determine whether Oxr1 also modulates assembly of Prdx2 oligomers *in vivo*, I analysed the Prdx2 oligomerisation status in Oxr1 Tg brain as compared to *Oxr1*$^{+/+}$ mice by native-PAGE. In the brain tissue from *Oxr1*$^{+/+}$ animals, Prdx2 was present as dimers and HMW complexes, and a significant increase in the abundance of HMW form was observed in Oxr1 Tg tissues demonstrating a positive correlation between Oxr1 and Prdx2 HMW levels (Fig. 3.7B). To further assess the role of Oxr1 in Prdx2 complex formation, I analysed the levels of its oligomeric forms in *Oxr1*$^{d/d}$ brain. As *Oxr1* knockout resulted in cerebellar-specific reduction in Prdx2-$SO_{2/3}$ levels, I performed independent experiments with the cerebrum and cerebellum to investigate if the brain-region specific regulation of hyperoxidation correlates with changes in Prdx2 oligomer formation. Interestingly, I observed a significant decrease in the levels of HMW complexes of Prdx2 as compared to wild-type control in the cerebrum, while levels of dimers remained

unchanged (Fig. 3.7C). Analysis of cerebellar tissue revealed similar effect of *Oxr1* knockout on Prdx2 oligomers distribution: a decrease in assembly of HMW complexes with unchanged levels of dimeric form (Fig. 3.7D). Importantly, levels of Prdx2 protein expression were not affected in Oxr1 Tg or *Oxr1*$^{d/d}$ brain tissues (Fig. 3.7 B,C,D). Together, these data suggest that Oxr1 can modulate Prdx2 oligomerisation *in vivo* and *in vitro* without affecting Prdx2 total expression levels, and this process is partially independent from modulation of its PTMs by Oxr1. The data also indicates that these processes are regulated differently in cerebrum and cerebellum, suggesting an involvement of other factors in the regulation of this process.

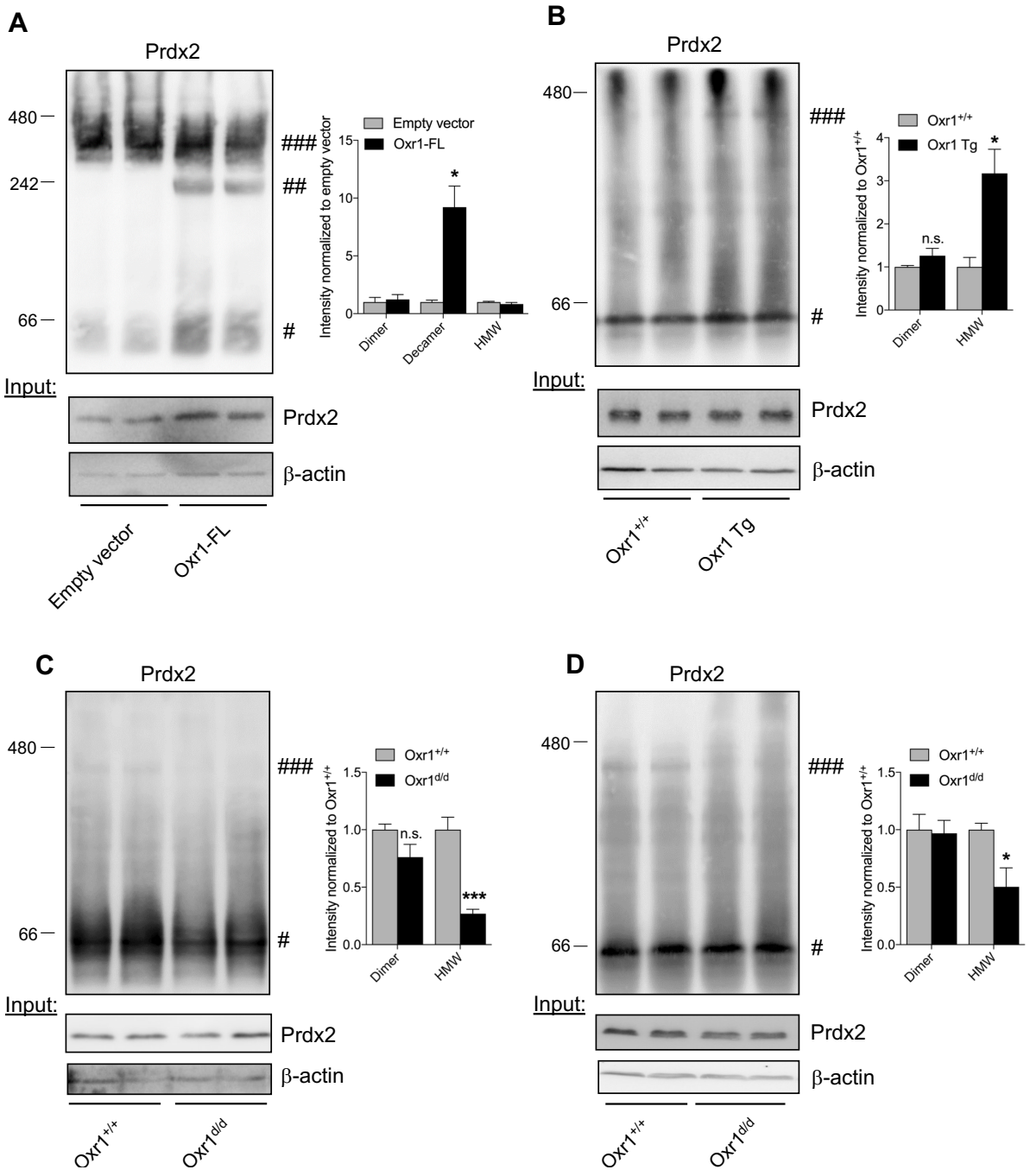


Figure 3.7 Oxr1 plays a role in the regulation of Prdx2 oligomeric state *in vitro* and *in vivo*. (A) Western blot of Prdx2 from protein extracts of N2A cells transfected with either an empty vector or Oxr1-FL and treated with 300µM H_2O_2 for 1 hour. Quantification of the HMW Prdx2 complexes (###), the Prdx2 decamer (##) and the dimer (#) is shown (N=3 independent repeats). (B) Western blot of Prdx2 from protein extracts of adult wild-type and Oxr1 Tg mouse cerebra. (C-D) Representative western blot of Prdx2 from protein extracts of P18 wild-type control (*Oxr1*$^{+/+}$) and *Oxr1*$^{d/d}$ cerebrum (C) and the cerebellum (D). Quantification of the HMW Prdx2 complexes (###) and the Prdx2 dimer (#) is shown (N=8 animals per group (C) and N=3 (B, D)). For all experiments, extracts were run on 10% Blue Native-PAGE gels and levels of Prdx2 and β-actin (input) were determined for the same samples in reducing conditions on separate gels. β-actin was used as a loading control. Data are represented as mean ± SEM, t-test, *p<0.05, ***p<0.001

3.2.8. Ncoa7-FL modulates Prdx2 hyperoxidation *in vitro*

As other TLDc family members have also been shown to interact with Prdx2, I analysed if they could regulate Prdx2 hyperoxidation in a manner similar to Oxr1. Thus, I performed a preliminary *in vitro* experiment in N2a cell line overexpressing Ncoa7-FL, a most closely related to Oxr1 family member. Interestingly, the results suggest an opposite effect of Ncoa7-FL overexpression on Prdx2-$SO_{2/3}$ levels as compared to Oxr1 (Fig. 3.8). Ncoa7-FL overexpression led to statistically significant 30% reduction in Prdx2-$SO_{2/3}$ levels as compared to empty vector-transected control cells. Together, these data suggest that ability to modulate Prdx2 hyperoxidation is shared between TLDc proteins and the mechanisms and role of it are protein-specific.

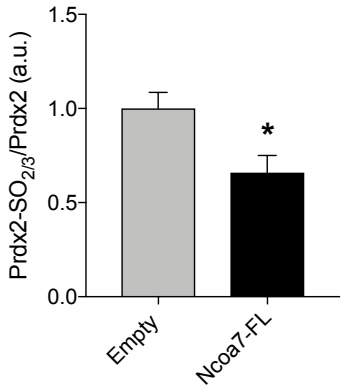


Figure 3.8 Ncoa7-FL modulates Prdx2-$SO_{2/3}$ levels *in vitro*.
N2a cells were transfected with Ncoa7-FL or empty vector and treated with 300μM H_2O_2 for 1 hour to induce Prdx2 hyperoxidation. Data presented as mean ± SEM, t-test, *p<0.05

3.3 Discussion

Since its discovery, Oxr1 has been known to confer protection against OS, but its mechanism of action was unknown (Finelli et al., 2015, Finelli et al., 2016, Oliver et al., 2011, Volkert et al., 2000, Yang et al., 2014). Oxr1 molecule has been tested for different types of antioxidant activities, such as catalase-like or Sod-like, but results of these experiments were negative, suggesting it may possess other types of antioxidant activity such as peroxidase or glutathione transferase activity, or not be itself an antioxidant enzyme. The crystal structure of the TLDc domain also did not give any clues as to other possible functions for the TLDc proteins (Blaise et al., 2012, Oliver et al., 2011, Sanada et al., 2014). Emerging evidence for a regulatory mechanism for Oxr1 neuroprotective function against OS suggested it could be through the regulation of the activity of other antioxidant enzymes, and Prdx2 was identified as a promising candidate for this role. Here, I have shown that Oxr1 interacts with Prdx2 both *in vitro* and *in vivo* and regulates its main PTM and subsequently its oligomeric state and function, suggesting it plays a role in Prdx2 functional switch between antioxidant and chaperone activities. I have also for the first time discovered a molecular function of Oxr1 protein as a putative holdase chaperone, suggesting its potential direct involvement in cellular OS-protection machinery. These exciting findings lead to a first-author publication - Svistunova et al. (2018).

3.3.1 The mechanism and the role of TLDc proteins interaction with Prdx2

Interestingly, my data suggest that Oxr1 binds Prdx2 only in the cerebrum, but not in the cerebellum. One of the possibilities is that Oxr1:Prdx2 interaction is mediated by another factor that is not expressed in the cerebellum, thus affecting their binding,

possibly making it weaker. Another option is that Oxr1:Prdx2 binding is only taking place in a limited group of neurons in the cerebellum - Oxr1 is known to be expressed in highly abundant CGCs, but it is also present in Golgi cells, that represent a much smaller proportion of cerebellar neurons (Joery den Hoed, unpublished data) (Shepherd, 2004). If Oxr1:Prdx2 interaction is, for example, limited to these cells, co-immunoprecipitation and subsequent western blotting may be not sensitive enough to detect the binding (Herculano-Houzel, 2010, Walloe et al., 2014).

Many Prdx interactors are known to share common binding motifs - CXXC, PXXP, and LXXLL (Bertoldi, 2016), and interestingly, this motif is found in Oxr1-FL; however, it is not found in its TLDc domain (Fig. 3.8). Both Oxr1-FL and Oxr1-C, an isoform almost exclusively comprised of the TLDc domain, have been shown to interact with Prdx2, suggesting a potential non-canonical recognition and binding mechanism involved in their interaction. Moreover, other TLDc family members have also been shown to interact with Prdx2, however only Tbc1d24, mEAK7 and C20Orf118 possess potential binding motifs (Fig. 3.8); thus, TLDc:Prdx2 interaction could be mediated by a non-canonical Prdx-binding motif, some elements of the tertiary structure present in the TLDc domain or through an intermediate protein.

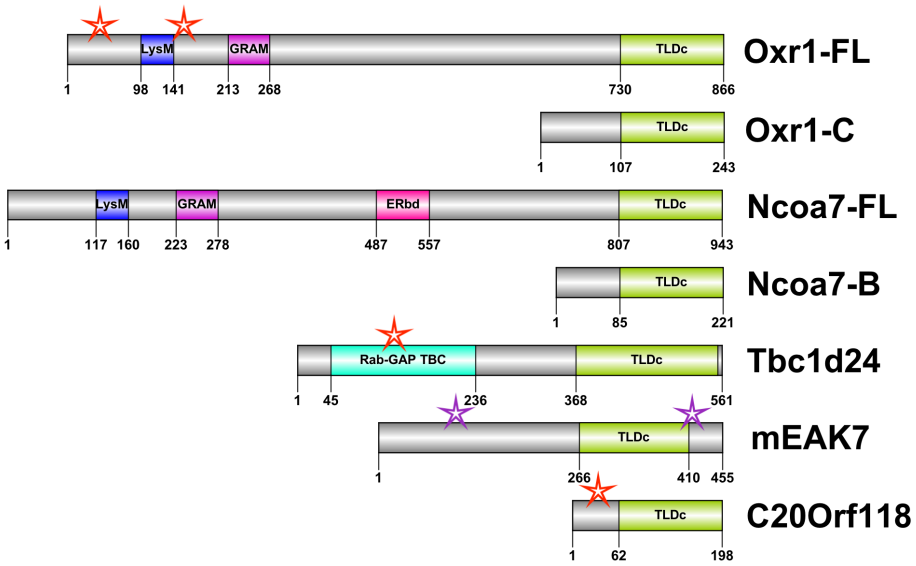


Figure 3.9 TLDc proteins possess canonical Prdx-binding motifs.
Oxr1-FL, Tbc1d24, mEAK7 and C20Orf118 possess canonical Prdx-binding motifs. Red asterisks indicate location of PXXP motifs, purple asterisks refer to LXXLL binding sites.

Binding of Oxr1 and Prdx2 suggests that Oxr1 could regulate Prdx2 activity. Similar mechanism of direct regulation of protein's function via binding has been previously described, for example, for cyclophilin A, a peptidylprolyl isomerase, that binds all PRDX family members and increases their antioxidant activity *in vitro* via direct reduction of oxidized catalytic residues (Lee et al., 2001). Here, I have shown that Oxr1-C and Oxr1-FL do not regulate Prdx2 antioxidant activity *in vitro*. This could mean that Oxr1 is either not a Prdx2 antioxidant activity-regulatory protein or that our *in vitro* experimental setup lacks some proteins or compounds essential for this interaction to occur. Importantly, there is a possibility that Oxr1 possesses some antioxidant activity, but it requires binding of other molecules to carry it out, and Prdx2 itself cannot promote it. I have also shown here that incubation of Oxr1 with Prdx2 further reduces aggregation of the substrate proteins *in vitro* as compared to Prdx2 alone; importantly, as I have shown that Oxr1 possesses holdase activity itself, it is difficult to determine whether this further increase in protective properties of the solution is due to Oxr1 modulating Prdx2 holdase activity (synergistic effect) or whether it is a combined effect of two proteins (additive effect). To

distinguish between these two possibilities, we could create an Oxr1 or Prdx2 mutant that lacks ability to bind the second protein, but still retains its holdase activity. Then, if Oxr1:Prdx2 interaction is involved in holdase activity increase, we would not observe it in experiment with disrupted interaction, whereas in the case when increase in protective activity is just a combined effect of Prdx2 and Oxr1 we should not expect to see any changes.

As the *in vitro* experiment with purified proteins revealed no regulatory activity for Oxr1 towards Prdx2 antioxidant activity, I performed a preliminary experiment that allows monitoring H_2O_2 reduction in cells in real time. The approach utilizes an exogenously expressed H_2O_2 sensor protein HyPer that changes its fluorescence properties upon oxidation by H_2O_2 (Bilan and Belousov, 2016, Mishina et al., 2013). I used primary cerebellar cultures from wild-type mice transfected with HyPer construct. Using this approach, the levels of H_2O_2 could be quantified in live cells using the reporter's fluorescence signal. Preliminary experiments proved the approach to be promising, allowing to monitor sensor fluorescence in transfected primary neurons following oxidative insults, and provided us with some potentially interesting data: different cells displayed different response to H_2O_2 treatment – while some cells successfully recovered from two consecutive treatment-recovery cycles, others died immediately after addition of H_2O_2. This observation could potentially be explained by selective vulnerability of different neuronal population to OS (Wang and Michaelis, 2010). Primary cells from *Oxr1*$^{d/d}$ and Oxr1 Tg animals can be used to study the role of Oxr1 in regulating cellular OS response capacity; use of Prdx2 inhibitor conoidin A in these experiments would help to estimate the contribution of Prdx2 activity in Oxr1-regulated ROS protection. Thus, I propose this experiment could be performed in the future to study the role of Oxr1 or other TLDc genes in the regulation of cellular response to OS.

In this chapter I have focused on Oxr1:Prdx2 interaction and its role in Prdx2 function and activity, but it remains to be investigated whether other TLDc proteins can also modulate its function. In a preliminary experiment I assessed the effect of Ncoa7-FL, the closest family member to Oxr1-FL, on Prdx2 hyperoxidation *in vitro*. Interestingly, Ncoa7-FL overexpression in N2a cells resulted in a decrease in Prdx2-$SO_{2/3}$ levels under OS conditions, suggesting Ncoa7-FL protects Prdx2 from hyperoxidation and potentially maintains its activity as an antioxidant enzyme. Importantly, both Ncoa7-FL and Prdx2 are known to localize to the nucleus, suggesting Ncoa7-FL might be regulating nucleus-specific activities of Prdx2. For example, oligomeric rings of PRDX2 have recently been shown to regulate progression of the replication fork in cells, and oxidative treatment induced PRDX2 oxidation, disassembly of oligomer complexes and replication fork slowdown (Somyajit et al., 2017). Thus, decrease in Prdx2-$SO_{2/3}$ levels in OS conditions in the presence of exogenous Ncoa7-FL could be attributed to a potential role for Ncoa7-FL in the maintenance of DNA replication via regulation of Prdx2 hyperoxidation.

3.3.2 The mechanisms of Prdx2 PTMs regulation by Oxr1

I have also shown that levels of Oxr1 modulate Prdx2 hyperoxidation – an important regulator of its activity, acting as a functional switch between its antioxidant and chaperone functions. PTMs play an important role in the regulation of the activity of all Prdxs, and their levels have been reported to be altered in NDDs. Cdk5 (cyclin-dependent kinase 5), a kinase that contributes to neurodegeneration in PD, inactivates Prdx2 via phosphorylation, thus increasing the levels of ROS and promoting cell death (Przedborski, 2007), while peptidyl-prolyl cis/trans isomerase NIMA-interacting 1 (Pin1), a Prdxs1-4 binding partner, has been shown to modulate Prdx1 peroxidase activity *in vitro* via regulation of it dephosphorylation by protein phosphatase 2A (PP2A) (Chu et al., 2013).

In addition, nitration of non-catalytic residue increases peroxidase activity of Prdx2 and protects it from hyperoxidation (Randall et al., 2014), and elevated levels of nitrated Prdx2 have been reported in early AD inferior parietal lobule samples (Reed et al., 2009).

My results show that Oxr1 regulates the levels of Prdx2 hyperoxidation *in vitro* and *in vivo*, and in our recent study we have also demonstrated that Oxr1 modulates the levels of Prdx2 S-nitrosation (SNO-Prdx2) (Svistunova et al., 2018). Both hyperoxidation and S-nitrosation are PTMs of the catalytic Cys residue that occur in oxidative or nitrosative stress conditions, and S-nitrosation of Prdx2 leads to reduced levels of Prdx2-$SO_{2/3}$ in cells (Collins et al., 2016, Fang et al., 2007, Wang et al., 2014). Both Prdx2-$SO_{2/3}$ and SNO-Prdx2 have been shown to reduce Prdx2 antioxidant activity by preventing its reaction with H_2O_2, and Prdx2-$SO_{2/3}$ is also known to promote its chaperone properties *in vitro* by favouring assembly of HMW complexes; S-nitrosation has been shown to promote holdase activity of its very close homologue PRDX1 (Chung et al., 2017, Fang et al., 2007, Moon et al., 2005). Together, these data suggest that the equilibrium between various PTMs regulates the activity and multiple functions of Prdx2. Levels of SNO-Prdx2 have been shown to be elevated in PD brain tissues, and associated with cellular vulnerability to OS (Fang et al., 2007). Interestingly, Oxr1 levels differentially modulated Prdx2-$SO_{2/3}$ and SNO-Prdx2 in cerebrum and cerebellum. In the cerebellum, Oxr1 overexpression led to significant increase in Prdx2-$SO_{2/3}$ and prominent decrease in SNO-Prdx2, while in the cerebrum SNO-Prdx2 decrease was minimal and did not reach significance and Prdx2-$SO_{2/3}$ was significantly up-regulated (Fig. 3.6C,D, Fig. 3.10A,B) (Svistunova et al., 2018). Conversely, *Oxr1* deletion caused significant decrease in Prdx2-$SO_{2/3}$ and increase in SNO-Prdx2 in the cerebellum, and non-significant decrease and increase, respectively, in the cerebrum, suggesting that regulation of Prdx2 PTMs by Oxr1 could be mediated by other

cellular factor that may differ between various brain regions (Fig. 3.6E,F, Fig. 3.10C,D) (Svistunova et al., 2018).

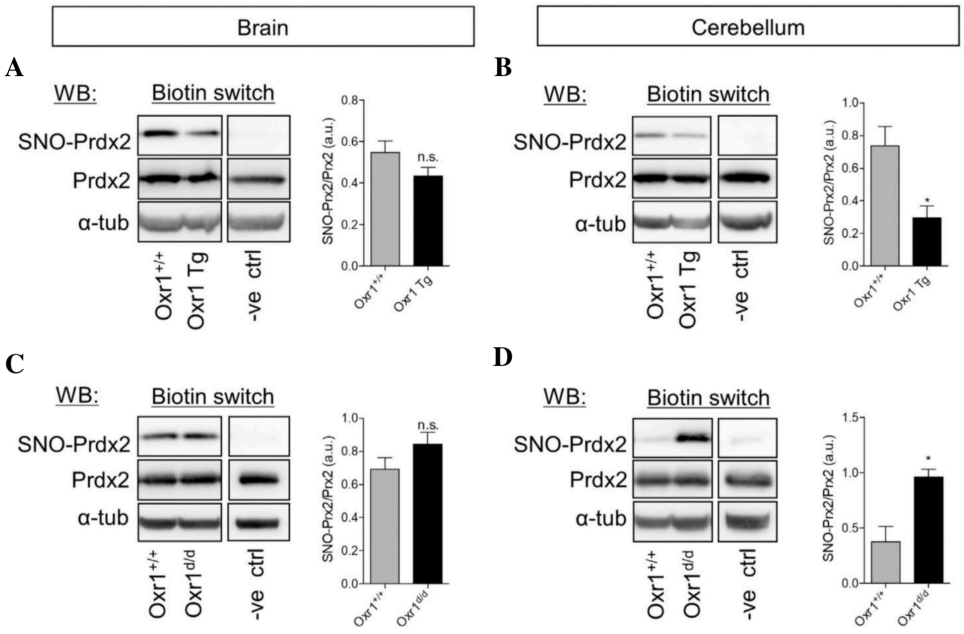


Figure 3.10 Oxr1 modulates SNO-Prdx2 levels *in vivo*.
Modified from Svistunova et al. (2018). (A-B) Representative western blots of SNO-Prdx2 levels in cerebrum (A) or cerebellum (B) from Oxr1 Tg mice and wild-type controls as determined by biotin switch. (C-D) SNO-Prdx2 levels in cerebrum (C) or cerebellum (D) from *Oxr1*$^{d/d}$ mice and wild-type controls determined by biotin switch. Quantification is shown as the ratio of SNO-Prdx2 to total Prdx2. N=3 animals per group. Data presented as mean ± SEM, t-test, *p<0.05.

During the catalysis, Prdx2 active centre adopts fully folded (FF) and locally unfolded (LU) conformations (Karplus, 2015). Oxidation of the Cys residue promotes changes in the local folding and it transits from FF to LU form (Poole et al., 2011); interestingly, it has been shown that hyperoxidation-prone Prdxs are stabilised in FF conformation allowing further oxidation and formation of Prdx-$SO_{2/3}$ (Poole et al., 2011, Veal et al., 2018). Thus, it could be that Oxr1 binding to Prdx2 stabilises its active centre in the FF state, and Oxr1 deletion leads to faster transition to LU form and thus reduced Prdx2 hyperoxidation.

Another possibility is that Oxr1 modulates binding of enzymes that subsequently modulate its PTMs to Prdx2. Acetylation is another PTM shown to regulate Prdx activity

in vivo; histone deacetylases, HDAC6 and sirtulin-2 (SIRT2), have been shown to deacetylate Prdx1 and Prdx2 in neurons *in vivo* and in cancerous cell lines (Fiskus et al., 2016, Jian et al., 2017, Parmigiani et al., 2008). In a mouse model of PD, induction of HDAC6 results in decreased acetyl-Prdx1 and acetyl-Prdx2 levels, increased intracellular ROS and cell death, while injections of HDAC6-specific inhibitor in the striatum increased acetylation levels and protected neurons from cell death, suggesting precise regulation of Prdx PTMs is required for neuronal homeostasis (Jian et al., 2017). A more detailed study in breast cancer cells has identified SIRT2 as a binding partner of Prdx1 and has shown that SIRT2 induction leads to acetyl-Prdx1 levels decrease, increase in Prdx1-$SO_{2/3}$ and HMW complexes abundance, resulting in ROS accumulation and subsequent DNA damage (Fiskus et al., 2016). As S-nitrosation and hyperoxidation PTMs compete for the same residue in Prdx2 molecule, and Oxr1 deletion causes increase in SNO-Prdx2 levels, it could be hypothesised that Oxr1 facilitates binding of specific denitrosylase and its deletion disturbs the interaction. Apparent differences between cerebrum and cerebellum could potentially be explained by expression levels of these enzymes – for example, levels of sulfiredoxin, a known Prdx2 denitrosylase, are lower in the cerebellum as compared to other brain regions (Lein et al., 2007, Sunico et al., 2016)**.** Thus, in the presence of sufficient denitrosylase, *Oxr1* knockout would not be detrimental, while in tissues with lower expression of this enzyme, absence of Oxr1 could significantly disturb the interaction between Prdx2 and PTM-regulating enzyme. Alternatively, binding of the denitrosylase could be regulated by other proteins in addition to Oxr1, and their differential expression in various brain regions could determine the outcome.

Alternatively, Oxr1 can directly modulate Prdx2 PTMs via a recently described mechanism of protein-protein transnitrosation. Protein-protein transnitrosation is a process whereby NO group is transferred from one protein to another in an enzyme-

independent manner (Nakamura and Lipton, 2013). Transnitrosation has been reported to occur between various proteins - haemoglobin and anion exchanger 1, thioredoxin and caspase-3, caspase-3 and X-linked inhibitor of apoptosis, Cdk5 and dynamin related protein 1 (Nakamura and Lipton, 2013). During our experiments, we observed Oxr1 S-nitrosation *in vitro* (Dr Mattéa Finelli, personal communication). Together with the data that *Oxr1* knockout leads to increase in Prdx2-SNO levels and *Oxr1* overexpression causes SNO-Prdx2 decrease, it is possible that Oxr1 can directly modulate Prdx2 S-nitrosation by protein-protein transnitrosation. As absence of Oxr1 leads to an increase in Prdx2-SNO, Oxr1 could act as an acceptor of SNO group and regulate Prdx2 function by balancing the ratio between Prdx2-$SO_{2/3}$ and SNO-Prdx2.

Interestingly, observed differences in Prdx2 hyperoxidation do not fully correlate with changes in HMW complexes abundance. Prdx2-$SO_{2/3}$ levels usually correlate with formation of oligomeric forms of Prdx2 (Moon et al., 2005), and in agreement with this, I observe decrease in HMW complexes and Prdx2-$SO_{2/3}$ levels in the cerebellum, while in the rest of the brain reduction in HMW complexes abundance was observed in absence of Prdx2-$SO_{2/3}$ levels changes. This suggests that diverse factors could be contributing to Prdx2 hyperoxidation and HMW complexes assembly regulation, and it potentially contributes to the cerebellar-specific *Oxr1*$^{d/d}$ mouse neurodegenerative phenotype.

Together, these data suggest it is possible that Oxr1 regulates these PTMs via regulation of interaction of other proteins with Prdx2, by affecting Prdx2 conformation or by directly transferring the PTM between proteins.

3.3.3 Oxr1 is a novel putative holdase chaperone

I have discovered a novel molecular function for Oxr1 as a putative holdase. Holdases are a class of chaperones that recognise unfolded or misfolded proteins and effectively bind them to prevent from further aggregation (Mattoo and Goloubinoff, 2014). Small heat shock proteins, a class of holdase chaperones, have been shown to bind partially folded intermediates and act as substrate pools for HSP70, a potent foldase chaperone (Garrido et al., 2012, Zwirowski et al., 2017). Many proteins have been shown to possess holdase activity in addition to their other functions – for example, yeast guided entry of tail-anchored proteins 3 (Get3), a player of post-translational delivery of proteins to ER, displays holdase activity in stress conditions (Powis et al., 2013), and 14-3-3 proteins are now believed to possess both holdase and foldase activities in addition to their regulatory roles (Sluchanko and Gusev, 2017). Therefore, Oxr1 holdase activity may be another of its multiple molecular functions and could be either constitutive or induced upon a particular stimulus. Mutations in holdase proteins have been identified in various pathological conditions. For instance, mutations in DJ-1, a multifunctional protein that possesses holdase activity and inhibits aggregation of α-synuclein, are associated with PD (Ariga et al., 2013, Pankratz et al., 2006), and mutations in α-crystallin holdase, a protein involved in cytoskeleton stabilisation, OS protection and accounting for eye lens transparency, causes cataract and cardiomyopathy (Brodehl et al., 2017, Huang et al., 2009, Patel et al., 2017). This highlights an importance of holdase chaperones in maintaining homeostasis of various tissues. Some of the holdase proteins are also known to also possess foldase activity; for example, *Arabidopsis thaliana* protein tetratricoredoxin (AtTDX) has been show to possess thioredoxin, holdase and foldase activities, and neuroprotective nicotinamide mononucleotide adenylyltransferase 2 (NMNAT2) in addition to its

enzymatic activity acts as both holdase and foldase chaperones (Ali et al., 2016, Lee et al., 2015b). This suggests that Oxr1 may also possess dual chaperone activity.

Conclusion

In this chapter I have shown an important role for Oxr1 as a regulator of Prdx2 antioxidant enzyme's PTMs and assembly of HMW complexes *in vitro* and *in vivo*. Absence of Oxr1 in *Oxr1*$^{d/d}$ tissue led to significant decrease in Prdx2 hyperoxidation in the cerebellum, but not in the cerebrum, and reduction in HMW complexes abundance in both brain regions. These changes result in loss of both antioxidant and chaperone activities by Prdx2, causing OS and increase in protein aggregation, possibly leading to CGCs death. I have also shown that Oxr1 possesses putative holdase chaperone activity, making it not just a regulator, but potentially important player of cellular OS defense machinery.

4. Investigating the role of Oxr1 in brain function and homeostasis

4.1 Introduction

As previously described, a spontaneous deletion of the entire *Oxr1* locus, including the neighbouring *Abra* gene in the original *bella* mouse leads to CGCs loss, ataxia and early death at P24-26 (Oliver et al., 2011). In more recent studies, it was confirmed that loss of all Oxr1 isoforms was responsible for this distinctive phenotype; mice with a premature stop codon introduced in the TLDc domain of Oxr1 - therefore disrupting all isoforms of the protein – produced the identical ataxic and pathological phenotype to the *bella* deletion mutant (Finelli et al., 2016, Finelli et al., 2018b, Oliver et al., 2011). The striking phenotype of cerebellar neurodegeneration in *Oxr1*$^{d/d}$ mouse suggests that Oxr1 is required to maintain cellular survival in this brain region. However, the functional role of Oxr1 and other TLDc proteins in the maintenance and protection of neuronal cells, and the reason for the selective vulnerability of cerebellar granule cells lacking Oxr1 remains elusive. Therefore, one approach to gain insight into the molecular pathways relevant to Oxr1 function is to analyse the transcriptional changes observed when *Oxr1* is knocked out or knocked down.

Considering the role of Oxr1 in OS defense, a number of studies have focused on the expression of other antioxidant genes in *Oxr1* knockdown and *Oxr1* knockout animal and cell models. In the mosquito *Anopheles gambiae,* Oxr1 was shown to regulate the invasion of *Plasmodium* parasite and to act downstream of Jun kinase (JNK) pathway; *Oxr1* silencing led to profound down-regulation of catalase and *Gpx* expression and moderate decrease in *Sod1*, Sod2 and *Sod3* transcript levels (Jaramillo-Gutierrez et al., 2010). In the original *Oxr1* knockout (*bella*) mouse, absence of *Oxr1* caused 70% reduction in *Gpx1* levels at the end-stage of the disease in the cerebellum, while levels of expression of other

tested enzymes, including catalase, *Sod1* and *Sod2*, where not changed (Oliver et al., 2011). A study on HeLa, HEK293 and 143B cell lines have shown that *OXR1* knockdown by 85% at mRNA level correlates with reduction in expression of p21 - a tumor suppressor involved in regulation of OS response via Nrf2 signaling pathway (Yang et al., 2014). Authors have also shown that *OXR1* depletion leads to a decrease in *GPX2* and *HO-1* mRNA levels, whereas catalase, *GPX1* and NAD(P)H dehydrogenase [quinone] 1 (*NQO1*) levels remained unchanged, suggesting *OXR1* positively regulates expression of selected antioxidant enzymes, partly via p21-Nrf2 mechanism (Yang et al., 2014). Later, Yang et. al performed RNA-Seq of control and H_2O_2 treated HeLa cells where OXR1 protein was knocked down by ~80% (Yang et al., 2015). In non-treated cells, 485 down-regulated and 194 up-regulated genes were identified in *OXR1* knockdown cells versus controls, while under oxidative treatment the number of down-regulated and up-regulated genes were 355 and 193, respectively (Yang et al., 2015). Among these transcripts, 420 were common between non-treated and treated conditions. Knockdown of *OXR1* resulted in deregulation of expression of p53 pathway members, a pathway that regulates cell cycle arrest, apoptosis and cell survival. Down-regulation of *OXR1* also affected expression of stress response genes and transcription factors that regulate response to cellular stress, and induced up-regulation and activation of caspase-9, a member of the apoptotic pathway (Yang et al., 2015). Importantly, in agreement with previous studies, *p21* and *HO-1* were shown to be down-regulated following *OXR1* silencing. Most recently, Zhang et al. have identified OXR1 as a novel senolytic target by showing that the gene is up-regulated in senescent cells, leading to significantly higher levels of *GPX2*, *HO-1*, catalase and *SOD1* as compared to non-senescent cells (Zhang et al., 2018). Accordingly, knocking-down *OXR1* mRNA levels by 75% caused reduction in *HO-1*, catalase, *SOD1* and *SOD2* mRNA levels in non-senescent cells by 20%, 40%, 35% and 50%, respectively, while in senescent cells, *OXR1* silencing led to downregulation of *HO-1* by 80%, catalase by 50%, *GPX2* and

SOD1 by 30%, leading to apoptosis (Zhang et al., 2018). Together, these findings suggest *OXR1* plays an important role in regulating OS defense in senescent cells by regulating the transcription of specific target genes and it was proposed that OXR1 could therefore be a novel therapeutic target for treating age-related disorders (Zhang et al., 2018). *In vivo*, neuronal overexpression of *Oxr1* delayed neuroinflammation-related transcription changes in the $hSOD^{G93A}$ mouse model of ALS; however, no clues as to the downstream pathways were gleaned from comparing wild-type and Oxr1 transgenic (neuronal over-expressing) mice, as the only differentially expressed gene was *Oxr1* itself (Liu et al., 2015). Yet these data do indicate that over-expression of Oxr1 *in vivo* (at least up to 5-fold) is safe and tolerated in mice (Liu et al., 2015). In summary, these studies suggest that the presence of Oxr1 is important for the regulation of cellular homeostasis and survival, including expression of antioxidant proteins, transcription factors and members of the key regulatory pathways, such as p53 and p21, responsible for cell cycle and its arrest, apoptosis, autophagy and OS protection, and these mechanisms are conserved among different species (Joerger and Fersht, 2016).

Therefore, in order to take an unbiased approach to transcriptomic changes in the brain that result from complete removal of *Oxr1*, microarray analysis was performed on the cerebella of $Oxr1^{d/d}$ mice and control littermates. A pre-symptomatic time point of P18 was chosen to assay transcriptional changes that precede cerebellar granule neuron loss and occur just before the development of the ataxic phenotype. The aim was to avoid confounding transcriptional signals derived from dead and dying cells and to discover any upstream gene changes that might trigger the neurodegeneration and identify pathways that represent the normal function of Oxr1. It was also interesting to investigate whether some of the de-regulated antioxidants and other p53-associated pathways observed in previous studies would be recapitulated *in vivo*.

4.2 Results

4.2.1 Microarray transcription profiling of pre-symptomatic *Oxr1*$^{d/d}$ cerebella identifies up-regulation of microglial genes

To study transcriptional changes that occur in *Oxr1*$^{d/d}$ mouse cerebellum prior to symptoms onset and cell death, total RNA was purified from whole cerebella from littermate pairs of male wild-type (*Oxr1*$^{+/+}$) and Oxr1 knockout (*Oxr1*$^{d/d}$) controls at P18. Microarray transcriptional profiling, quality control of the data and initial statistical analysis were performed by Cambridge Genomic Services. From these first analyses, only 20 genes were found to be statistically significantly differentially expressed (DE) in *Oxr1*$^{d/d}$ versus wild-type (Fig. 4.1). Interestingly, all of these genes were up-regulated in knockout tissue. Some of DE genes did not reach significance due to high variation in values and relatively small sample number (N=4 per group), although all of them were also up-regulated (Table 4.1). Expression of other TLDc family members was not affected in *Oxr1*$^{d/d}$ tissue as compared to wild-type (Table 4.1). Importantly, microarray analysis suggests unchanged expression level of *Oxr1* in *Oxr1*$^{d/d}$ cerebellum due to detection of transcribed exons upstream of premature stop codon, although absence of the functional Oxr1 protein was previously confirmed by western blotting (Finelli et al., 2018b). This highlights the limitations of transcription profile analysis by microarray technology, as it does not cover the whole gene sequence and thus does not distinguish between various isoforms (discussed in more details below).

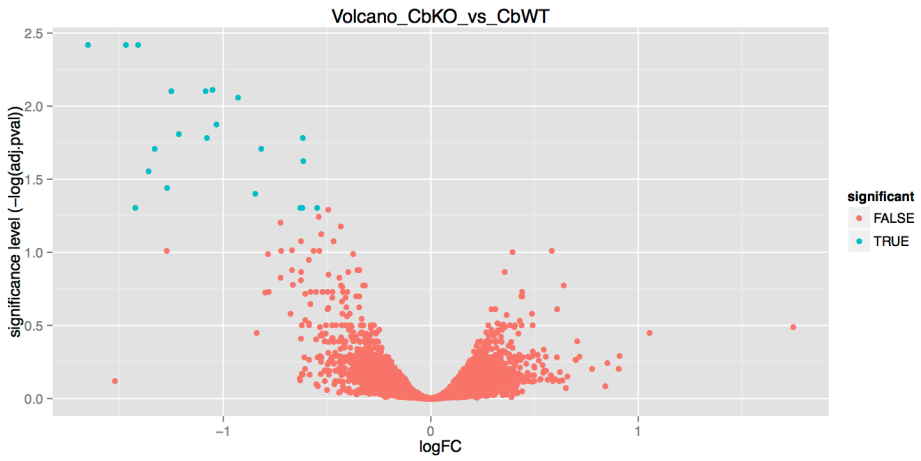


Figure 4.1 Graphic overview of microarray results.
Volcano plot representing the results of microarray analysis as logarithmic values of fold changes of gene expression in *Oxr1*$^{+/+}$ as compared to *Oxr1*$^{d/d}$ (negative values correspond to transcripts up-regulated in *Oxr1*$^{d/d}$). Blue dots correspond to transcripts significantly up-regulated in *Oxr1*$^{d/d}$ cerebellum.

Next, to predict possible pathways affected by *Oxr1* deletion, I performed Gene Ontology (GO) annotation of the DE genes. GO enrichment analysis showed that these genes are involved in general innate immune response and brain-specific inflammatory microglia activation (Table 4.2). Consistent with these data, the vast majority of up-regulated genes are highly expressed in the microglia and are present in other cells at very low levels (Tabula Muris et al., 2018, Zhang et al., 2014b). Some of the genes are also implicated in cell apoptosis, a major consequence of *Oxr1* knockout (Table 4.2). Interestingly, several DE genes are involved in synaptic pruning and negative regulation of long-term potentiation, suggesting *Oxr1* knockout may affect synaptic plasticity (Cooke and Bliss, 2006). Overall, these results suggest that loss of *Oxr1* affects neuroinflammatory response and leads to neurodegenerative processes in the cerebellum at the pre-symptomatic stage in *Oxr1*$^{d/d}$ mice.

Next, in order to confirm the expression changes identified by the microarray analysis, RNA was extracted from an independent set of age- and sex-matched male mice

at P18 for RT-qPCR. In addition, to investigate further the timing of gene deregulation, samples from P14 and P22 mice were prepared, the latter represents disease end-stage where approximately 1% of granule cells in the cerebellum are apoptotic and the mice are severely ataxic (Oliver et al., 2011). Six genes involved in inflammatory response - complement C1q subcomponent subunit A (*C1qa*), cluster of differentiation 68 (*CD68*), cathepsin S (*Ctss*), Fc receptor-like S, scavenger receptor (*FcrlS*), hexosaminidase B (*HexB*) and lymphocyte antigen 86 (*Ly86*) - were selected for further confirmation and analysis. Housekeeping gene *Gapdh* (glyceraldehyde 3-phosphate dehydrogenase) was selected as a control as microarray did not identify any changes in its expression in *Oxr1*$^{d/d}$ animals compared to wild-type.

RT-qPCR data at P18 confirmed a statistically significant up-regulation of *Cd68* and *Fcrls* and non-significant up-regulation of *C1qb*, *Ctss*, *HexB* and *Ly86* genes due to variation between samples (Fig. 4.2). Unexpectedly, the normalised fold-changes of *C1qb*, *Cd68*, *Ctss* and *Ly86* were lower than the microarray analysis data, potentially due to the technical differences between the two methods and the variation between animals (discussed below). Timecourse analysis showed further significant up-regulation of *Cd68*, *Ctss*, *FcrlS*, *HexB* and *Ly86* towards the end-stage of the disease, whereas *C1qb* expression increase at P22 compared to P18 did not reach significance (Fig. 4.2). This suggests that the pathways affected in the *Oxr1*$^{d/d}$ cerebellum become further deregulated during the course of neurodegeneration. Interestingly, *C1qb* and *HexB* were already up-regulated in *Oxr1*$^{d/d}$ cerebella at P14 (non-symptomatic stage) where no overt phenotype is observed, suggesting that deregulation of these two genes starts several days prior to symptom onset (Fig. 4.2).

Apart from the cerebellum, *Oxr1* is highly expressed in other brain regions, such as cortex, hippocampus and olfactory bulb (Finelli et al., 2016). Interestingly, pathological

analyses of various *Oxr1* knockout lines to-date had not identified any cell death in regions of the brain other than the cerebellum at end-stage. However, given the high levels of expression of *Oxr1* in the cortex, I hypothesized that the up-regulation of inflammatory markers observed in the cerebellum may also be detectable in the cortex. Therefore, I compared the expression of selected genes in the whole frontal cortex and in the cerebellum of P18 *Oxr1*$^{d/d}$ mice in parallel (Fig. 4.3). Interestingly, *C1qb*, *CD68*, *Ctss*, *HexB* and *Ly86* expression was significantly up-regulated in cortex samples, suggesting neuroinflammation in other regions of the brain where *Oxr1* is normally expressed (Fig. 4.3). *Fcrls* expression, on the other hand, was not changed in *Oxr1* deletion cortex tissue, suggesting its expression is not dependent on *Oxr1* in this brain region (Fig. 4.3).

As further confirmation that neuroinflammation occurs outside of the cerebellum in *Oxr1*$^{d/d}$ tissue at disease end-stage, Iba1 (ionized calcium-binding adapter molecule 1) immunostaining was carried out from whole brain sections at P22 (Fig. 4.4). These data show a highly significant increase in activated microglia as demonstrated by the numbers of immunopositive cells across the cerebellum as well as the cortex and hippocampus (Fig. 4.4). This suggests that *Oxr1* is essential to maintain normal neuroinflammatory responses across the brain.

Table 4.1. List of differentially expressed genes identified by microarray.
Genes, differentially expressed in *Oxr1*$^{d/d}$ as compared to *Oxr1*$^{+/+}$. Statistically significantly up-regulated genes are highlighted in grey.

Gene name	Gene symbol	Fold-change	p-value
Up-regulated in *Oxr1*$^{d/d}$			
Chemokine (C-C motif) ligand 3	*Ccl3*	3.14	0.004
CD68 antigen	*Cd68*	2.77	0.004
Leukocyte immunoglobulin-like receptor, subfamily B, member 4	*Lilrb4*	2.68	0.049
Complement component 1, q subcomponent, B chain	*C1qb*	2.66	0.004
Fc receptor-like S, scavenger receptor	*Fcrls*	2.57	0.028
CD180 antigen	*Cd180*	2.51	0.019
Cystatin F (leukocystatin)	*Cst7*	2.42	0.097
Macrophage expressed gene 1	*Mpeg1*	2.41	0.036
Lymphocyte antigen 86	*Ly86*	2.38	0.008
Complement component 1, q subcomponent, A chain	*C1qa*	2.32	0.016
TYRO protein tyrosine kinase binding protein	*Tyrobp*	2.11	0.016
Hexosaminidase B	*Hexb*	2.07	0.008
CD53 antigen	*Cd53*	2.05	0.013
Lectin, galactoside-binding, soluble, 3 binding protein	*Lgals3bp*	1.90	0.009
Complement component 1, q subcomponent, C chain	*C1qc*	1.80	0.040
Neuronal PAS domain protein 4	*Npas4*	1.79	0.356
Cathepsin S	*Ctss*	1.76	0.019
Triggering receptor expressed on myeloid cells 2	*Trem2*	1.74	0.187
Topoisomerase (DNA) II alpha	*Top2a*	1.72	0.186
Complement component 3a receptor 1	*C3ar1*	1.65	0.062
Neutrophil cytosolic factor 1	*Ncf1*	1.65	0.149
Fc receptor, IgE, high affinity I, gamma polypeptide	*Fcer1g*	1.65	0.097
Fc receptor, IgG, low affinity IIb	*Fcgr2b*	1.59	0.096
Cathepsin Z	*Ctsz*	1.55	0.049
Integrin alpha M	*Itgam*	1.54	0.084
Chemokine (C-X3-C motif) receptor 1	*Cx3cr1*	1.54	0.049
Cathepsin D	*Ctsd*	1.53	0.016

Pleckstrin	*Plek*	1.53	0.024
Chemokine (C-C motif) ligand 9	*Ccl9*	1.46	0.049
Lectin, galactose binding, soluble 9	*Lgals9*	1.45	0.097
TLDc family members			
Oxidation resistance 1	*Oxr1*	1.02	0.982
Nuclear receptor coactivator 7	*Ncoa7*	1.06	0.911
TBC1 domain family, member 24	*Tbc1d24*	0.83	0.643
mTOR associated protein, eak-7 homologue	*mEAK7*	0.97	0.967
Chromosome 20, open reading frame 118	*C20Orf118*	1.03	0.979

Table 4.2. Gene Ontology pathway analysis of up-regulated genes.
GO service was used to predict the pathway represented by statistically significantly up-regulated genes. FDR, false discovery rate.

Pathway	Genes	p-value	FDR
Astrocyte cell migration	*Ccl3, HexB*	$2.13*10^{-5}$	$2.09*10^{-2}$
Innate immune response	*C1qa, C1qb, C1qc, Ccl3, Ccl9, Cd180, Cx3cr1, Ly86*	$1.19*10^{-7}$	$3.75*10^{-4}$
Microglial cell activation involved in immune response	*Cx3cr1, Tyrobp*	$1.14*10^{-5}$	$1.38*10^{-2}$
Negative regulation of long-term synaptic potentiation	*Cx3cr1, Tyrobp*	$5.92*10^{-5}$	$4.22*10^{-2}$
Positive regulation of lipopolysaccharide-mediated signaling pathway	*Cd180, Ly86*	$3.42*10^{-5}$	$2.82*10^{-2}$
Positive regulation of neuron apoptotic process	*Ccl3, Ctsz, Tyrobp*	$5.21*10^{-5}$	$4.09*10^{-2}$
Regulation of hippocampal neuron apoptotic process	*Cx3cr1, Tyrobp*	$7.62*10^{-6}$	$1.09*10^{-2}$
Regulation of interleukin-1 beta production	*Ccl3, Cx3cr1, Tyrobp*	$2.72*10^{-5}$	$2.51*10^{-2}$
Synapse pruning	*C1qa, C1qb, C1qc*	$7.36*10^{-8}$	$3.85*10^{-4}$

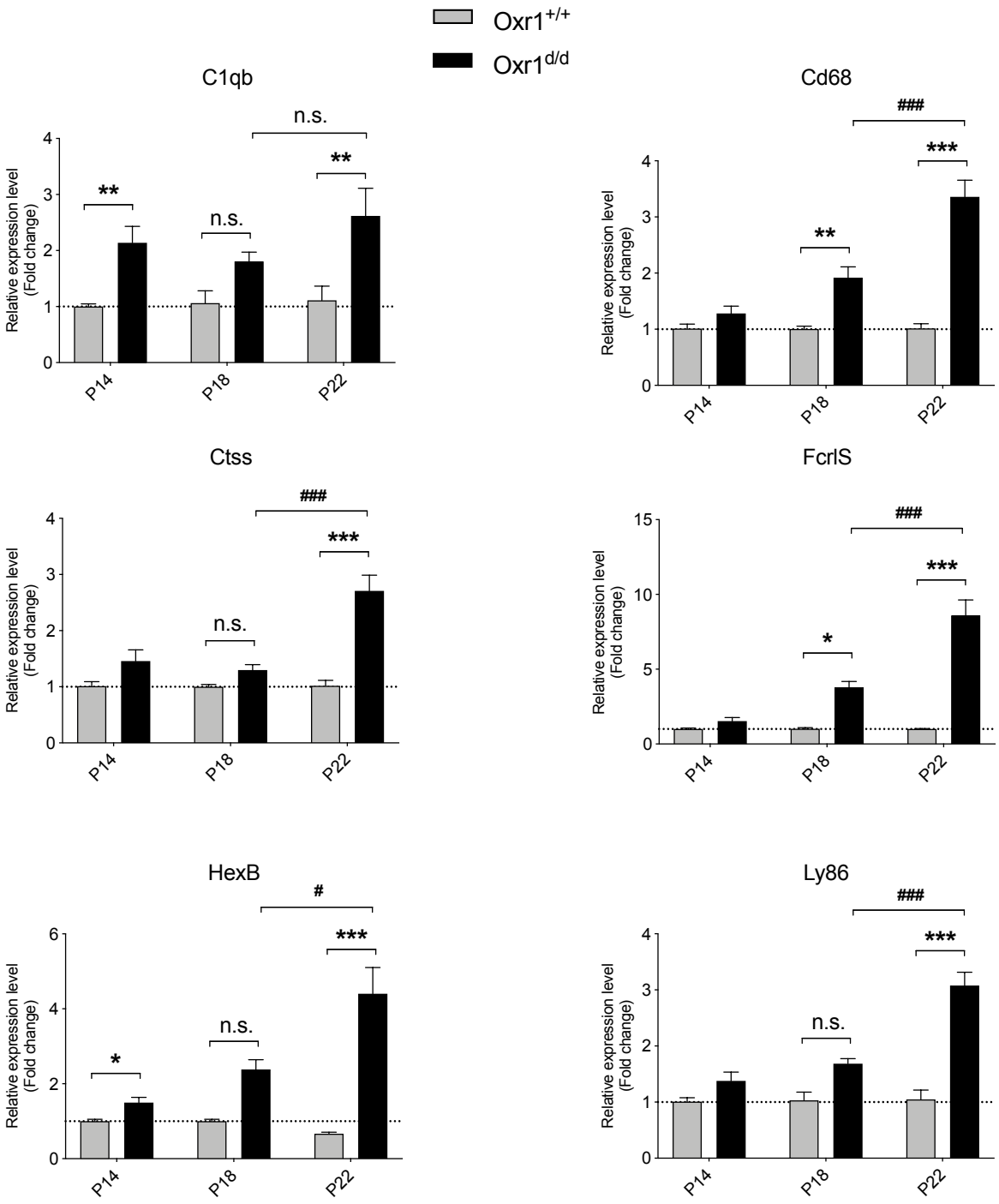


Figure 4.2 Validation of the microarray targets by RT-qPCR at P14, P18 and P22.
qPCR of selected genes expression in the cerebellum at P14, P18 and P22 time points was performed to analyse the trends of gene expression over the course of the disease. N=5 WT and KO P14 and P22 and WT P18, N=4 KO P18. t-test, one-way ANOVA with Bonferroni correction, *p<0.05, **p<0.01, ***p<0.001 as compared to corresponding wild-type sample, #p<0.05, ###p<0.001 as compared to P18 *Oxr1*$^{d/d}$.

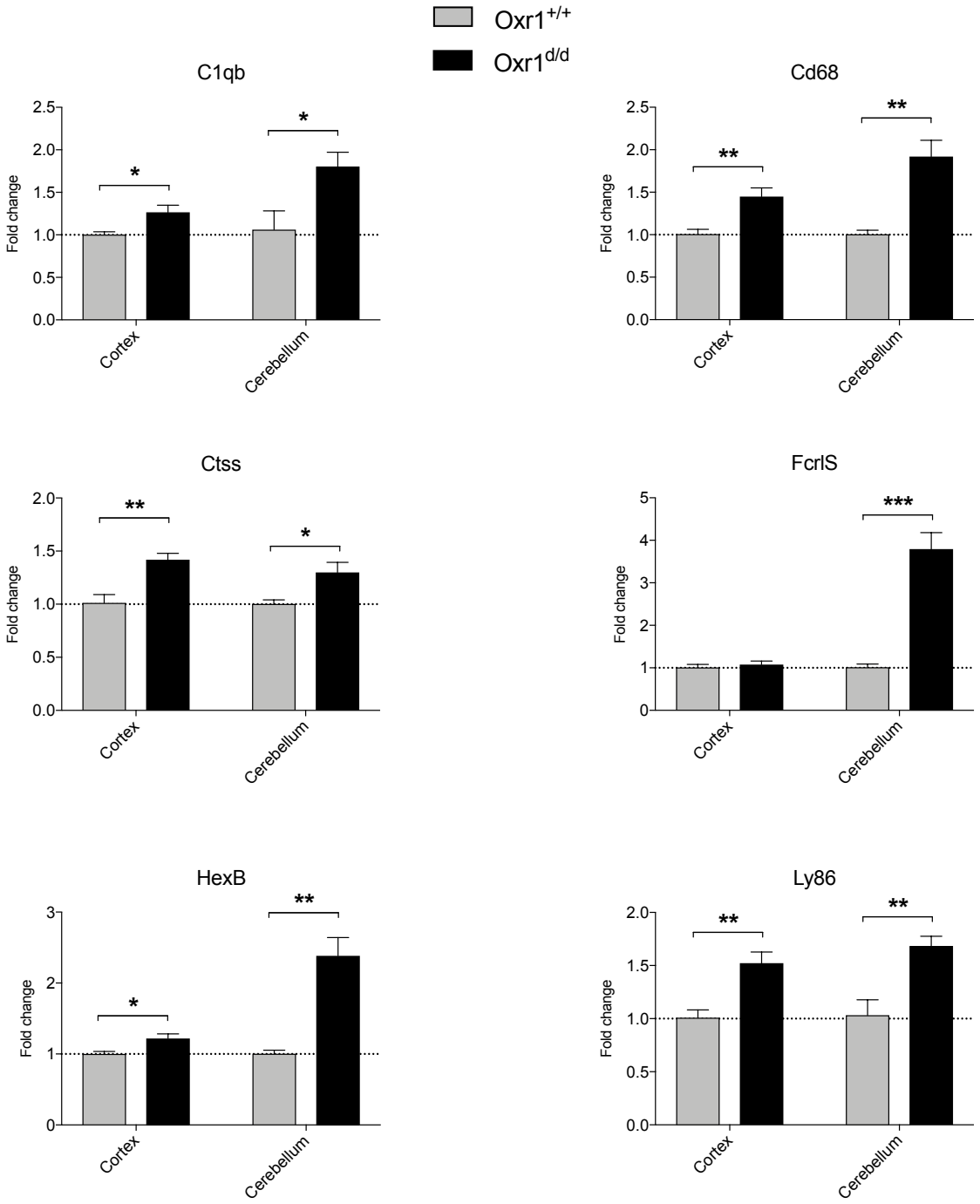


Figure 4.3 Comparison of expression of selected up-regulated genes in cortex and cerebellum at P18.

RT-qPCR analysis was performed to compare levels of up-regulation of selected genes between cortical and cerebellar tissues. N=5 for WT and KO cortex samples and WT cerebellum samples, N=4 for KO cerebellum samples. t-test, *p<0.05, **p<0.01, ***p<0.001 as compared to corresponding wild-type sample.

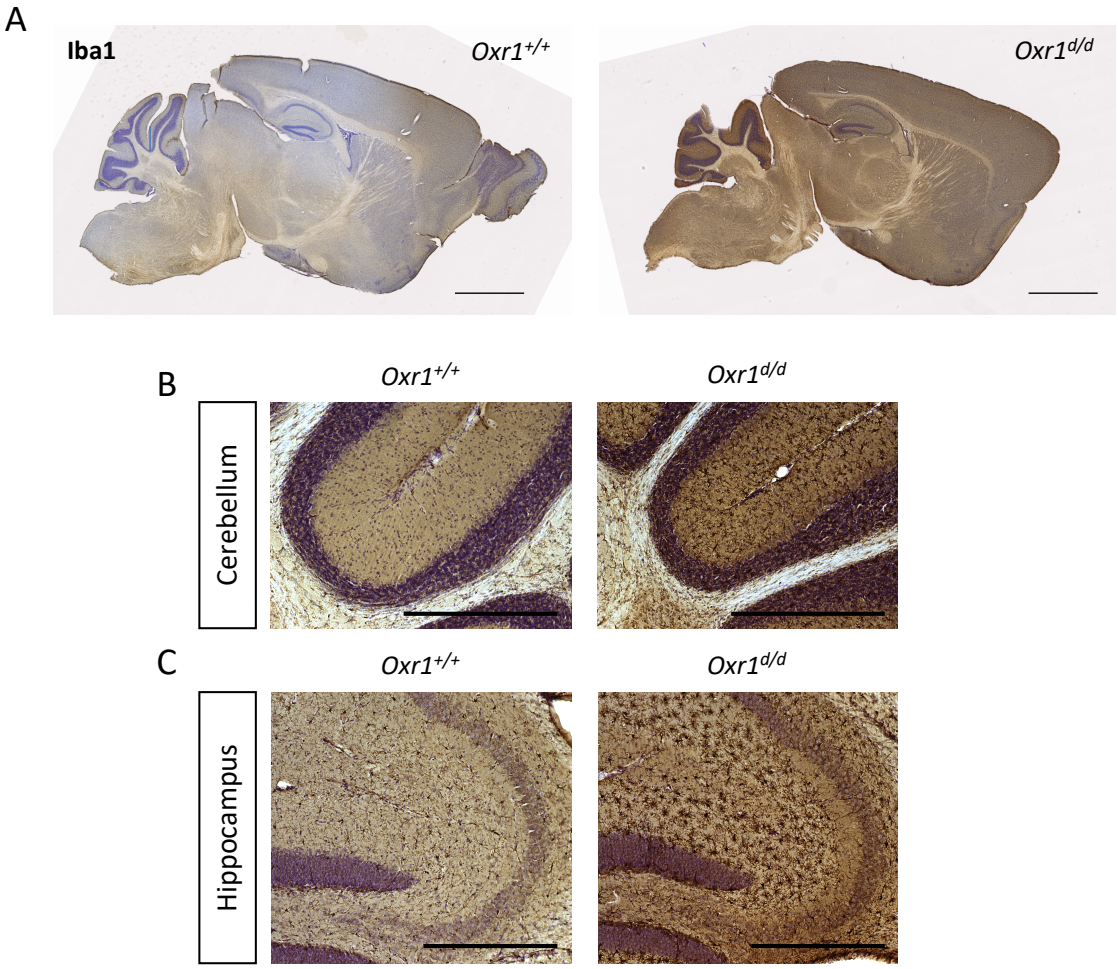


Figure 4.4 Oxr1 knockout leads to microglia activation at P22 in the cortex, hippocampus and cerebellum.

Brain sections of wild-type and *Oxr1*$^{d/d}$ mice at P22 were stained for Iba1, a marker of microglia activation. (A) Whole brain sections of wild-type and *Oxr1*$^{d/d}$ mice stained for Iba1. Scale bar 2 mm. (B) Cerebellum sections of wild-type and *Oxr1*$^{d/d}$ mice. Scale bar 0.5 mm. (C) Hippocampus sections of wild-type and *Oxr1*$^{d/d}$ mice. Scale bar 0.5 mm. (Dr Peter Oliver)

4.2.2 Oxr1 deletion affects levels of autophagy *in vivo*

As four of the genes identified as significantly deregulated in *Oxr1*$^{d/d}$, *Ctsd*, *Ctss*, *Ctsz* and *Hexb*, encode for key lysosomal enzymes, I decided to investigate the potential role of Oxr1 in the function of lysosomes. Lysosomes are membrane organelles that contain hydrolytic enzymes and are involved in the processes of breaking down and digesting intracellular and extracellular molecules (Luzio et al., 2007).

As RT-qPCR revealed similar gene expression changes in the cortex and the cerebellum, I used cortical tissues to analyse the aspects of the autolysosomal pathway, thus avoiding potential differences being derived from dead or dying cells that could be present in the cerebellum of *Oxr1*$^{d/d}$ mice. First, I assessed the levels of lysosomal marker lysosome-associated membrane protein 1 (Lamp1) in *Oxr1*$^{d/d}$ brain by western blotting. No difference in levels of Lamp1 was observed in wild-type and *Oxr1*$^{d/d}$ brain tissues suggesting Oxr1 does not have a major effect on the number of lysosomes present in the cell (Fig. 4.5).

Lysosomes play an important role in various intracellular mechanisms, including autophagy, where newly formed autophagosomes fuse with lysosomes to degrade their contents. Autophagosome maturation is associated with the recruitment of microtubule-associated proteins 1A/1B light chain 3B (LC3) protein to its membrane. In the cell, LC3 appears in two forms - LC3-I and LC3-II. LC3 is expressed as a propeptide that is cleaved to form cytoplasmic LC3-I; upon autophagy initiation, it undergoes an addition of phosphatidylethanolamine to form membrane-bound LC3-II. Thus, level of LC3-II reflects the levels of autophagy in the cell. To get an insight into the role of Oxr1 in autophagy, I analysed the levels of LC3-I and –II in P18 *Oxr1*$^{d/d}$ cerebral tissue; importantly, such post-transcriptional pathways would not be detected by transcriptomics. Interestingly, a

significant increase in the LC3-II fraction was identified in P18 *Oxr1*$^{d/d}$ tissues compared to wild-type, suggesting an increase in the number of autophagosomes in the cells lacking Oxr1 (Fig. 4.5). Importantly, levels of LC3-I were not altered indicating there is no general increase in the pool of available LC3 (Fig. 4.5).

Another pathway that delivers material to the lysosomes is endocytosis. Cells uptake fluids and small molecules from the intracellular space and form endosomal vesicles that mature to become late endosomes and fuse with lysosomes to breakdown the cargo (Vanlandingham and Ceresa, 2009). To assess if *Oxr1* deletion would affect the endosomal pathway, I analysed the levels of Rab7, a marker of late endosomes, in cerebral tissues from P18 *Oxr1*$^{d/d}$ and wild type animals. Experiment did not reveal any changes in Rab7 levels in *Oxr1*$^{d/d}$ mice as compared to control suggesting Oxr1 might not play a role in endocytosis (Fig. 4.5).

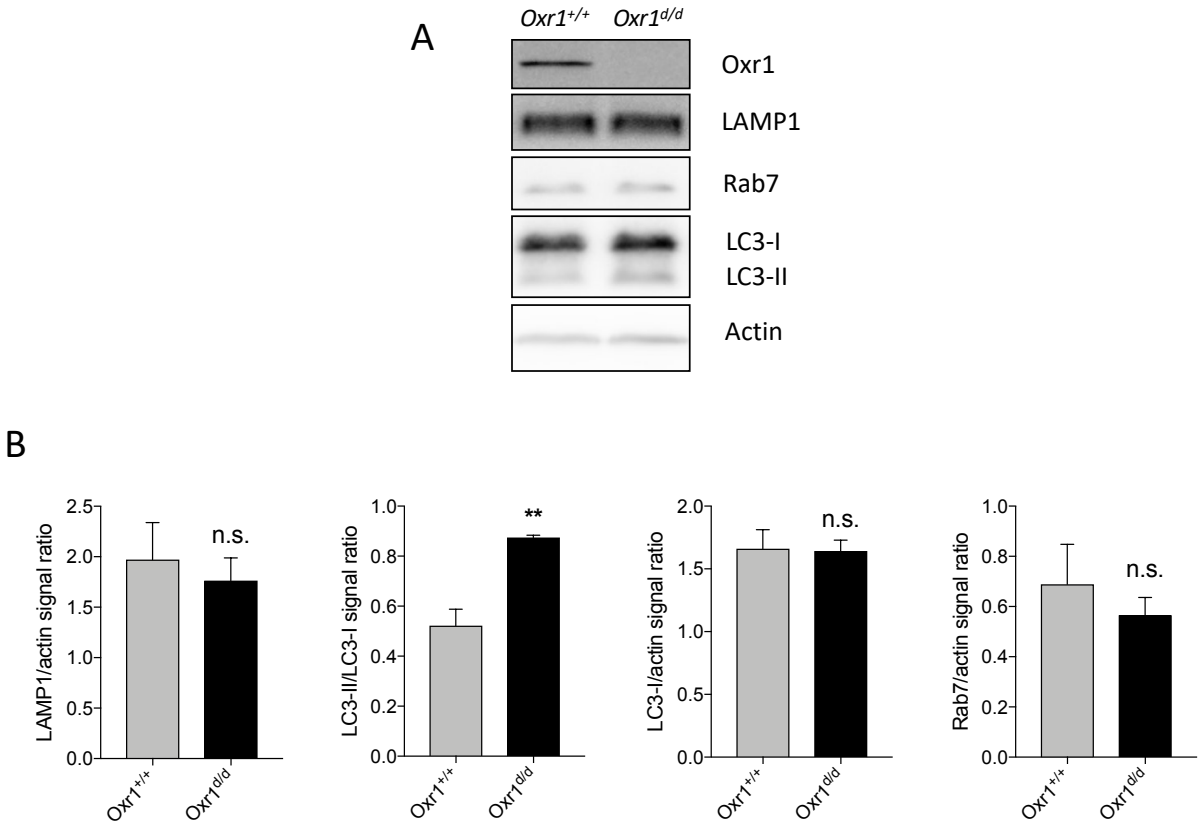


Figure 4.5 Oxr1 deletion affects levels of autophagy, but not lysosomes and endosomes, in the cortex.

(A) Representative western blot showing levels of lysosome marker Lamp1, late endosome protein Rab7 and autophagy markers LC3-I and LC3-II in *Oxr1*$^{+/+}$ and *Oxr1*$^{d/d}$ cortical tissue. (B) Statistical analysis of changes in Lamp1, Rab7 and LC3-I and LC3-II levels in *Oxr1*$^{d/d}$ tissue as compared to wild-type. (**p<0.01)

4.2.3 Oxr1 co-localizes with Golgi apparatus and is present in synapses

As I have shown that Oxr1 might play a role in autophagy process and that the microarray showed that genes implicated in lysosome function were deregulated in *Oxr1*$^{d/d}$ mice, I aimed to determine the sub-cellular localisation of Oxr1 in neuronal cells. Expression studies have unfortunately been hampered by a lack of antibodies for immunochemistry; in particular, our group has been able to validate these reagents using true Oxr1 null tissues and cell lines and found no commercial antibodies providing a reliable signal. Therefore, as a proxy for Oxr1 localisation, I performed immunostaining of Oxr1 using primary cultures from Oxr1 Tg mouse line where a long isoform of Oxr1 with a C-terminal HA-tag is expressed under the control of neuronal *Prnp*-promoter (Liu et al., 2015). First, I co-stained Oxr1 Tg primary cerebellar neurons for the trans-Golgi network (TGN) marker Golgin-245/p230 and Oxr1-HA. Golgi apparatus plays a central role in autophagy and lysosome formation by sorting newly synthesized lysosomal proteins and transporting them in budding vesicles to endolysosomes, as well as being a potential source of membrane for newly forming phagophores (Geng and Klionsky, 2010, Luzio et al., 2014). Therefore, I decided to investigate if Oxr1 is associated with Golgi apparatus. Analysis of the staining revealed partial colocalisation of Golgin-245 and Oxr1-HA suggesting it might be involved in the function of the Golgi apparatus (Fig. 4.6A). Interestingly, I also observed large Oxr1-HA-positive and Golgin-245-positive puncta along cell neurites (Fig. 4.6B). These structures resemble axonal varicosities, or boutons – swollen regions of the axon where synapses are formed, suggesting Oxr1 is present at the synapses.

Quantitative proteomic experiments from fractionated zebrafish, mouse, rat, marmoset and human brain tissues have generated several synaptic proteome datasets (Bayes et al., 2017, Koopmans et al., 2018, Roy et al., 2018). Interestingly, Oxr1 appears to

be among highly abundant proteins in synaptic and pre-synaptic density preparations, suggesting Oxr1 may be associated with synapses (discussed in more detail below). To confirm these proteomic data and investigate if these structures were indeed axonal boutons, I co-stained primary cerebellar neurons from Oxr1 Tg mouse for synaptic protein synaptosomal-associated protein 25 (SNAP-25) and Oxr1. SNAP-25 is a presynaptic protein, a component of the SNARE complex involved in the release of neurotransmitter at the synapse (Antonucci et al., 2016). Consistent with previously published data, SNAP-25 staining was observed at the membrane, and presumptive axonal varicosities were positive for SNAP-25 suggesting they are pre-synapses (Fig. 4.6C) (Gonzalo et al., 1999). Importantly, Oxr1-HA localized within SNAP-25-positive axonal varicosities, suggesting some synaptic localization (Fig. 4.6C). To further support the observation of synaptic localization of Oxr1, I carried out similar experiment using α-synuclein as an alternative synaptic marker. Alpha-synuclein is a presynaptic protein of unknown function that is thought to a play role in neurotransmission and neuronal homeostasis (Burré, 2015). Neurite varicosities were positive for α-synuclein confirming their pre-synaptic nature (Fig. 4.6D). Importantly, α-synuclein positive axonal boutons also contained Oxr1-HA (Fig. 4.6D). Together, these immunochemistry data suggest that Oxr1 localizes to pre-synapses in cultured cerebellar neurons.

Next, to examine Oxr1 localisation to synapses by an alternative approach, I performed an isolation method to enrich for the synaptic fraction from whole brain tissue of wild-type mouse followed by western blotting (Fig. 4.6E). Due to time limitations, only SNAP-25 was used as a control for efficiency of fractionation. In future experiments, additional synaptic markers, such as quisqualate receptor or *N*-methyl D-aspartate receptor subtype 2B (NMDAR2B) should be used. As expected, SNAP-25 is enriched in synaptic fraction suggesting some successful separation of fractions. These preliminary

data show that Oxr1 was found in both cytosolic and synaptosome fractions suggesting it is present in synapses. Together, these data confirm previously published synaptic proteomic data that Oxr1 is enriched at synapses and could play role in some aspects of the synaptic function.

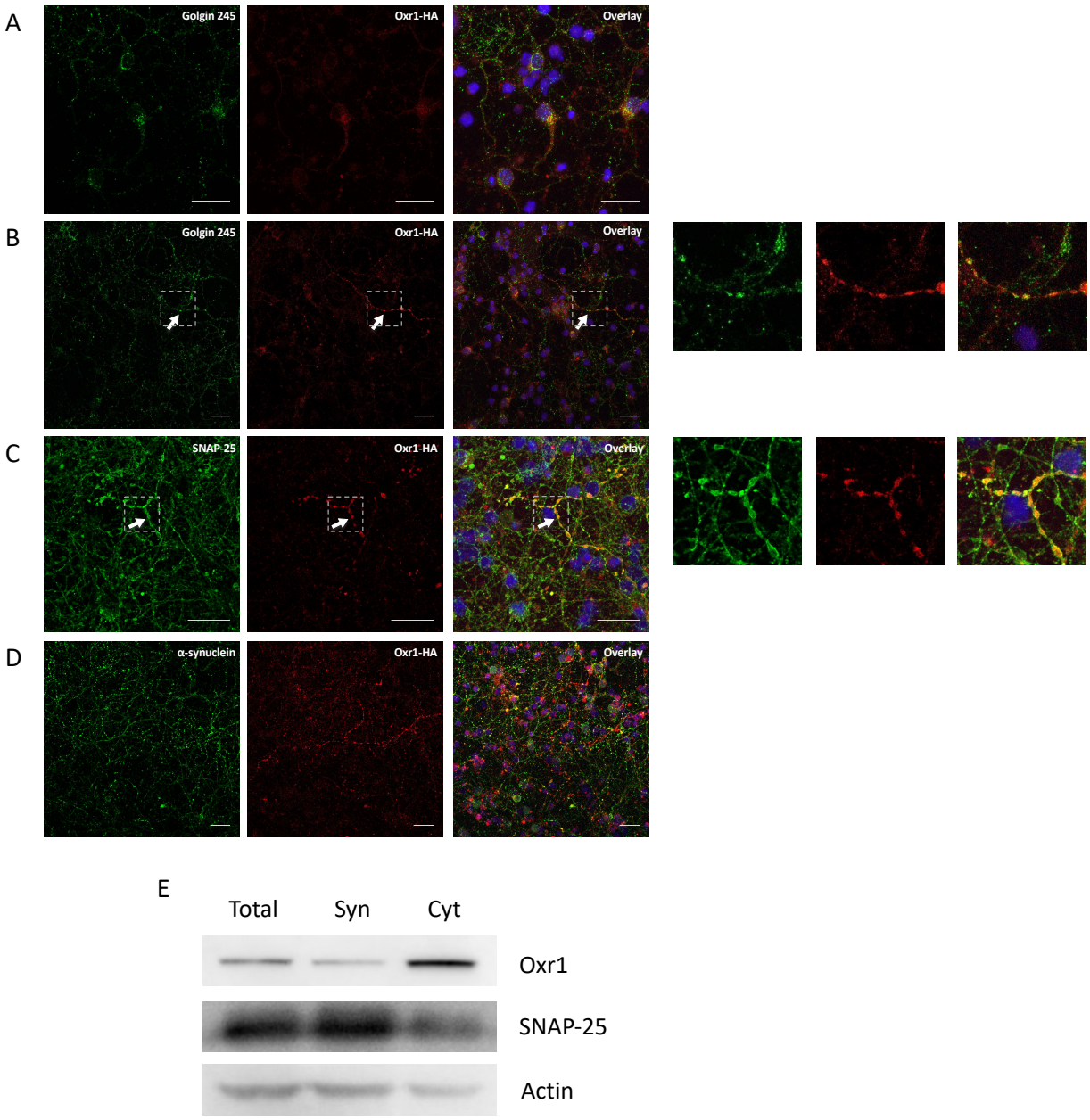


Figure 4.6 Oxr1 colocalises with Golgi apparatus and is present in synapses.
(A, B) Primary cerebellar cultures from Oxr1 Tg mice were co-stained for Oxr1-HA (red) and Golgin-245 (green). Arrows in (B) indicate boutons on neurites. (C) Primary cerebellar cultures from Oxr1 Tg mice co-stained for Oxr1-HA (red) and SNAP-25 (green). Arrows indicate a bouton with Oxr1 enclosed in a SNAP-25+ membrane. (D) Primary cerebellar cultures were co-stained for Oxr1-HA (red) and α-synuclein (green). (E) Western blotting of synaptic (Syn) and cytosolic (Cyt) fractions of a wild-type mouse brain showing presence of Oxr1 in synaptosomal vesicles. SNAP-25 used as a positive control for fractionation. Scale bar 25μm.

4.3 Discussion

4.3.1 The role of Oxr1 in neuroinflammation

Here I have shown that disruption of all isoforms of *Oxr1* in mouse leads to up-regulation of a small number of genes at pre-symptomatic stage in the cerebellum. These data were somewhat unexpected as the recent *in vitro OXR1* knockdown study in HeLa cells led to identification of many hundreds of deregulated genes, with the p53 pathway being strongly implicated. Data from the *Oxr1* KO mouse demonstrates that the biological context of the tissue to be studied is important and the role of Oxr1 may vary between cell types. A majority of the genes identified here are linked to the immune response and are highly expressed in microglial cells, a major player of neuroinflammatory reaction. For example, a 2.7-fold pre-symptomatic increase in Cd68, a macrophage marker, indicates microglia activation, suggesting it is a cause rather than a consequence of neurodegeneration in this mouse model. Importantly, Oxr1 is not only present in neurons, but is also expressed in non-neuronal cells, including astrocytes, oligodendrocytes and microglia, at varying levels, with the highest levels observed in neurons, suggesting it could directly regulate intracellular processes leading to inflammatory response in glia (details in Table 4.3 below) (Tabula Muris et al., 2018, Zhang et al., 2014b). Moreover, Oxr1 has been shown to be protective against inflammation *in vivo* – neuronal overexpression of *Oxr1* in a mouse model of ALS reduced neuroinflammatory response and 'rescued' up-regulation of multiple inflammation-related genes, including *C1q*, *Cd68* and *Ctss* (Liu et al., 2015). Consequently, it was hypothesized that Oxr1 reduces intracellular ROS levels and release of reactive molecules from damaged neurons, as well as protects them from extracellular ROS secreted by ALS mutation-bearing activated glia, thus postponing motor neuron damage, further glia activation and neuronal death (Liu et al., 2015).

Table 4.3. Relative Oxr1 expression levels in different brain cell types
The first column represents the data from RNA-Seq analysis of purified mouse cortical cells (Zhang et al., 2014b). The second column contains data of single cell RNA-Seq of purified cells mixed from various brain regions, including cerebellum (Tabula Muris et al., 2018). Percent of cells identified positive for Oxr1 transcript within given cell type is also shown. FPKM, fragments per kilobase of exon per million reads mapped; CPM, counts per million.

	FPKM (Zhang et al., 2014b)	Log-normalised CPM and percent of cells positive for transcript (Tabula Muris et al., 2018)
Astroglia	17.84±1.57	3.73, 27.08%
Bergman glia	No data	4.64, 45.00%
Endothelial cells	17.05±0.08	4.23, 35.52%
Microglia	2.97±0.48	4.31, 24.44%
Myelinating oligodendrocytes	13.91±1.15	No data
Newly formed oligodendrocytes	18.75±7.75	No data
Oligodendrocytes	No data	4.77, 70.52%
Oligodendrocyte precursor cells	22.03±5.05	4.58, 53.02%
Neurons	28.18±5.18	5.02, 67.62%

Among the genes identified by our microarray analysis, a few were implicated in microglia activation and function. TYRO protein tyrosine kinase-binding protein (Tyrobp) is known to play a role in inflammatory signaling in microglia cells (Mecca et al., 2018). Tyrobp interacts with triggering receptor expressed on myeloid cells 2 (Trem2) and this induces phagocytosis, actin cytoskeleton reorganisation and expression of chemokine receptors that promote migration towards the site of injury (Mecca et al., 2018). Trem2 expression has been shown to positively regulate expression of microglial markers, pro-inflammatory cytokines and OS and complement pathways in aged mice (Linnartz-Gerlach et al., 2018). Interestingly, Trem2 was also identified among up-regulated genes, although increase in its expression did not reach significance due to variation in expression levels across replicates (Table 4.1). In addition, Tyrobp has been shown to

inhibit pro-inflammatory signaling of toll-like receptors (TLRs), thus possessing anti-inflammatory role (Chu et al., 2008). Another up-regulated gene, CX3C chemokine receptor 1 (Cx3cr1), interacts with neuronal ligand chemokine (C-X3-C motif) ligand 1 (Cx3cl1), and their interaction also exhibits anti-inflammatory role (Lyons et al., 2009). On the other hand, chemokine (C-C motif) ligand (Ccl) 3 and 9 are pro-inflammatory molecules that attract leukocytes to the cite of inflammation (Lean et al., 2002, Reichel et al., 2009). Elevated levels of CCL3 expressed by T cells have been shown to promote peripheral T cells BBB penetration in AD patients via interaction with C-C chemokine receptor type 5 on endothelial cells (Man et al., 2007). It is worth mentioning that Ccl3 is the most up-regulated gene in the microarray analysis, suggesting that a related mechanism relevant to BBB penetration by peripheral immune cells could be taking place. Together, these data suggest that *Oxr1* deletion results in pre-symptomatic neuroinflammatory response, and its intensity may be modulated by the balance between the expression of anti- and pro-inflammatory genes.

The microarray analysis also identified up-regulation of Fc receptors (FcR). FcRs are a class of proteins that are expressed on lymphoid and myeloid cells and can bind immunoglobulin invariable Fc region, thus transmitting an activating or inhibitory signal to the cell; FcRs play a role in phagocytosis stimulation, chemokine secretion, degranulation and other processes (Getahun and Cambier, 2015, Tabula Muris et al., 2018). The increase in the levels of Low affinity immunoglobulin gamma Fc region receptor II (FcγrIIb) in *Oxr1*$^{d/d}$ tissue did not reach significance due to some variation between replicates, but it has previously been shown that it is up-regulated in AD and promotes neurotoxicity and mediates neuronal uptake of Aβ (Gwon et al., 2018, Kam et al., 2013). Another DE member of the family, Fcrls (or moFcRH2, mouse Fc receptor homolog 2), unlike other family members is not expressed in lymphoid organs and does

not have ortholog in human genome (Davis et al., 2004). This protein is highly expressed in microglia (Bennett et al., 2016, Tabula Muris et al., 2018) and has an additional domain originating from its neighboring gene - type B scavenger receptor cysteine-rich (SRCR) domain (Davis et al., 2004). Function of this unique protein is not characterized, but it may also be playing a role in regulating immune cells functioning, as other members of the family.

Complement components 1q a, b and c were also identified as significantly deregulated in *Oxr1*$^{d/d}$ cerebellum. Together they constitute the C1q complex, a part of the first component of the classical complement activation pathway (Thielens et al., 2017). C1q a, b and c are expressed in all brain cell types, with the highest levels observed in microglia, where almost 100% of cells express them, and much lower levels are observed in astrocytes, oligodendrocytes and neurons (Fonseca et al., 2017, Tabula Muris et al., 2018, Zhang et al., 2014b). Besides its important role in the complement pathway, there is emerging evidence that C1q complex is involved in the pathogenesis of NDDs. C1q is known to be up-regulated in post-mortem AD hippocampal tissues and post-mortem motor neurons from ALS patients, as well as in various mouse models of ALS at early stages of the disease (Annese et al., 2018, Lobsiger et al., 2013). C1q protects primary neurons from Aβ-induced toxicity *in vitro*, binds to Aβ and regulates its phagocytosis by microglia (Benoit et al., 2013, Kouser et al., 2015). Interestingly, elevated levels of C1q have also been shown to mediate early synapse loss in mouse models of AD via regulation of microglia (Hong et al., 2016). These data suggest dual role of the complement complex C1q in neurodegeneration process, emphasising its potential involvement in both protective and detrimental mechanisms on different stages of disease.

Microarray analysis has also identified alterations in expression of the lysosomal enzymes, cathepsins and hexosaminidase B in *Oxr1*$^{d/d}$ mice. Cathepsins are proteolytic

enzymes expressed by various cell types in the brain and are found intra- and extracellularly (Stoka et al., 2016). Cathepsins D, S and Z, which are up-regulated in *Oxr1*$^{d/d}$ cerebellum are highly expressed in microglia and have been shown to be implicated in the development of various neurodegenerative conditions. Microglia activation is associated with up-regulation and secretion of cathepsins that aggravate neuroinflammation and induce chemokine production and promote neuronal death; conversely, downregulation and inhibition of cathepsins have been shown to be neuroprotective and reduce inflammation (Gan et al., 2018, Liu et al., 2019, Lowry and Klegeris, 2018, Pislar et al., 2018). Cts up-regulation was observed in human patients with AD, PD, ALS and Lewy body dementia, as well as animal models of these disorders (Chai et al., 2018, Lowry and Klegeris, 2018, Miller et al., 2017, Pislar et al., 2018, Yelamanchili et al., 2011). Moreover, mutations in CTSD are known to cause neuronal ceroid lipofuscinosis (NCL) - progressive neurodegenerative lysosomal storage disorder characterized by dementia, seizures, visual loss and cerebral and cerebellar degeneration (Ketterer et al., 2017, Mole and Williams, 2013, Varvagiannis et al., 2018). Interestingly, secreted microglial Ctss has also been shown to play a role in the cleavage and secretion of neuronal Cx3cl1, a ligand of up-regulated Cx3cr1; release of the Cx3cl1 from neuron surface changes the effect of its interaction with receptor on microglia and is thought to be involved in pathogenesis of pain (Clark et al., 2009, Seo et al., 2016). Microarray analysis has also identified 2.4-fold non-significant up-regulation of cystatin F, an intralysosomal and -endosomal cysteine protease (i.e. Ctss and Ctsz) inhibitor, suggesting there could be compensatory interaction between these proteases' and inhibitor genes in *Oxr1*$^{d/d}$ cerebellum to balance the neurotoxic effect of cathepsins.

Importantly, up-regulation of *Cd68*, as well as *C1qb*, *Ctss*, *Hexb* and *Ly86* was also observed in the cortex of knockout *Oxr1*$^{d/d}$ mice at P18, where no cell loss occurs even at

the end stage. This indicates that *Oxr1* deletion causes generalized inflammation in the brain, but other factors, such as cell type or regional differences in expression of other genes, may contribute to the pathological outcome. Crucially, *HexB* and *C1qb* were found to be up-regulated at P14, a non-symptomatic stage in the *Oxr1*$^{d/d}$ mouse, suggesting that cellular and tissue homeostasis could be disrupted long before symptoms onset. Early up-regulation of the lysosomal enzyme *HexB* may indicate deregulation of the lysosomal function and its important role in the development of neurodegeneration in *Oxr1*$^{d/d}$ mouse model.

A number of studies have identified some or all of the genes deregulated in the *Oxr1*$^{d/d}$ cerebellum as being indicative of aged primed microglia phenotype, although direction of expression changes differs is some of them (Grabert et al., 2016, Holtman et al., 2015, Olah et al., 2018, Orre et al., 2014). Microglia priming occurs during normal ageing and in response to prolonged exposure to inflammatory stimulus, such as dying cells or aggregated proteins, and is characterized by inadequate and exaggerated immune response (Perry and Holmes, 2014). As Oxr1 is known to protect against OS and to reduce levels of OS markers, deletion of the gene will likely result in elevated levels of reactive molecules, protein damage and aggregation, as well as secretion of pro-inflammatory molecules from dying or damaged neurons; upon contact with these stimuli, microglia would become primed and further accumulation of damaged material could lead to its hyper-activation and brain tissue damage (Finelli et al., 2016, Oliver et al., 2011). Thus, microglia activation could be not a cell-autonomous effect of *Oxr1* knockout, but rather result from pro-inflammatory signaling from damaged or dying neural cells. Additionally, some of the up-regulated genes that encode receptors and other sensing molecules represent a 'microglia sensome' – a distinct transcriptomic signature of microglial cells (Hickman et al., 2013). Thus, microglia from *Oxr1*$^{d/d}$ mice could acquire 'increased

sensitivity' phenotype due to alterations in their regulation, rather than change in response to changing surroundings.

Comparison of the panel of differentially expressed genes with other mouse mutants from the literature presenting a similar cerebellar degeneration as in the *Oxr1*$^{d/d}$ mice revealed overlap with a number of lysosomal storage disorders (LSDs). Similar genes, including *C1qa*, *Ctss*, *Ctsd*, *Ctsz*, *Mpeg1*, *Tyrobp*, *Cd68*, *Cd180* and other, were shown to be up-regulated in Niemann-Pick type C (NPC) disease and neuropathic Gaucher disease (nGD) mouse models cerebella and in a mouse model of Sly syndrome (mucopolysaccharidosis [MPS] VII), suggesting that the mechanisms of neurodegeneration in these disorders could be similar to *Oxr1*$^{d/d}$ (Dasgupta et al., 2015, Liao et al., 2010, Lopez et al., 2012, Parente et al., 2012). NPC, nGD and MPS VII are inherited metabolic disorders that result from lysosomal dysfunction and are characterized by accumulation of large molecules that can not be digested, eventually leading to cell death (Ferreira and Gahl, 2017). NPC is characterized by accumulation of cholesterol and glycolipids within the cell and neurological symptoms, including cerebellar ataxia, epilepsy and tremor (Vanier and Millat, 2003), accumulation of glucosylceramide and glucosylshingosine in visceral organs and CNS is characteristic of nGD (Huang et al., 2015), while accumulation of glycosaminoglycans is observed in MPS VII leading to mental retardation and skeletal abnormalities (Montano et al., 2016). Lysosomal substrate accumulation leads to lysosomal dysfunction, leakage of organelles' contents to the cytoplasm, ER stress and cell damage, and in microglia it could trigger cell activation, leading to neuroinflammation (Bosch and Kielian, 2015). Significant overlap between DEGs identified in pre-symptomatic *Oxr1*$^{d/d}$ cerebellum and published LSDs studies suggest microglia activation observed in *Oxr1* knockout mouse model could also be resulting from lysosomal dysfunction.

Lysosomal dysfunction is observed not only in LSDs, but also in multiple other neurological conditions, including AD, PD and frontotemporal dementia (FTD) (Beck, 2016, Papadopoulos and Meyer, 2017). Mutations in various lysosomal proteins have been identified in NDDs, such as glucosylceramidase β mutation in PD, β-galactosidase variants in LSDs and GM1-gangliosidosis or disruption in presenilin 1 - a vesicular ATPase chaperone - in AD (Lie and Nixon, 2018). Importantly, disruptions in lysosome function have also been reported in cerebellar degeneration conditions, such as in sorting nexin 14 (SNX14)-associated cerebellar atrophy with ataxia, spinocerebellar ataxia type 7 and LSD mucolipidosis II (Akizu et al., 2015, Alves et al., 2014, Kollmann et al., 2012). Abnormalities in the endo-lysosomal pathway are the earliest known pathological feature of the AD brain; up-regulated lysosomal biogenesis is observed at early stages, followed by accumulation of undigested substrates, such as Aβ, lysosomal enlargement and further decline in hydrolysis, which highlights the importance of this pathway in the onset and progression of the ND process (Nixon, 2017). PD is associated with increase in number of autophagosomes and in LC3-II levels, suggesting autophagy induction (Moors et al., 2016). Interestingly, I identified an increase in LC3-II fraction in *Oxr1*$^{d/d}$ brain tissue, which suggests some deregulation of autophagic pathways in this mouse model. Importantly, one of the non-significantly up-regulated transcripts, Lgals9 (galectin-9), has recently been shown to be involved in autophagy induction via AMP-activated protein kinase (AMPK) mechanism (Jia et al., 2018). Galectin-9 senses lysosomal damage, one of autophagy induction factors, by binding exposed luminal galactosides and forms a complex with other proteins to activate AMPK, which then phosphorylates its downstream targets and activates autophagy (Jia et al., 2018). Lysosomal membrane rupture is implicated in multiple NDDs, including LSD, AD, PD and FTD (Papadopoulos and Meyer, 2017). Some of the NDD-causative mutations lead to compromised lysosomal integrity, resulting in lysosomal damage and subsequent lysophagy; interestingly,

membrane rupture has also been shown to be caused by neurotoxic protein aggregates (Papadopoulos and Meyer, 2017). Lysosomal damage would also lead to lysosomal contents leakage, leading to aberrant activation of cytoplasmic proteins, homeostatic disruption and potentially apoptosis (Papadopoulos and Meyer, 2017). Thus, increase in LC3-II in *Oxr1*$^{d/d}$ mouse at P18 could be attributed to autophagy of damaged proteins and organelles resulting from elevated OS and potential lysosomal damage. Importantly, LC3-II has also been shown to be induced in *Oxr1*$^{d/d}$ cerebellar tissues at pre-symptomatic P18 and symptomatic P22 as compared to wild-type control, meaning autophagy induction is ubiquitous in the brain of *Oxr1*$^{d/d}$ mouse (Dr Silvia Corrochano, personal communication). Interestingly, another TLDc protein, mEAK7, has been shown to localize to lysosomes and regulate mTOR alternative signaling (Nguyen et al., 2018). mEAK7 was reported to recruit mTOR to lysosomes upon nutrient treatment and promote cell migration and proliferation (Nguyen et al., 2018). mTOR is one of the key regulators of autophagy in cells – its inactivation upon starvation or other stimuli induces autophagy and expression of autophagy-related genes (Kim and Guan, 2015). Here, I have shown that loss of *Oxr1* likely leads to an induction of autophagy, and it is possible that Oxr1, like mEAK7, regulates autophagy by modulating the mTOR signaling (Maday and Holzbaur, 2016).

4.3.2 Possible role of Oxr1 at the synapse

Another observation regarding Oxr1 intracellular localization suggests its presence at synapses. Previously published proteomic datasets listed Oxr1 as a synaptic protein in mouse, human, zebrafish, marmoset and rat brains (Bayés et al., 2011, Bayes et al., 2012, Bayes et al., 2017, Koopmans et al., 2018, Roy et al., 2018). Potential role of Oxr1 at synapses is unclear, but Tbc1d24, another member of the family, is known to localize to synapses and to play role in synaptic vesicle recycling (Fernandes et al., 2014, Finelli et

al., 2018a, Fischer et al., 2016). Tbc1d24 is involved in endocytosis regulation, with its knockdown resulting in a significantly slower endocytosis rate and increased endosomal volume (Finelli et al., 2018a). Tbc1d24 has been shown to act as a potential ROS sensor via the TLDc domain and promote endocytosis and synaptic vesicle recycling in OS conditions *in vitro* (Lüthy et al., 2019). Oxr1 TLDc domain may also act as a ROS sensor, regulating other aspects of synapse functioning. For example, axon distal tip and pre-synaptic compartment are the primary sites of autophagy in neurons, where it controls proteostasis and recycling of damaged mitochondria, and the evidence for Oxr1 role in autophagy suggest it may regulate this process at synapses (Birdsall and Waites, 2018, Maday and Holzbaur, 2014, Maday and Holzbaur, 2016). Recently, Tbc1d24 has also been demonstrated to localize to clathrin-coated vesicles at the TGN, suggesting a link between possible shared functions of these two proteins (Tona et al., 2019). Co-localization of Oxr1 with Golgi apparatus can indicate its involvement in vesicle transportation within the cell and to and from the axon (Climer et al., 2018, Emperador-Melero et al., 2018, Park et al., 2011).

In Chapter 3 I have shown that Oxr1 possesses holdase chaperone activity. Chaperones constitute up to 4% of synaptic proteome, being responsible for protein folding assistance, clearance of misfolded, damaged or aggregated proteins and chaperone-mediated autophagy (Gorenberg and Chandra, 2017). Specialised chaperones are involved in a wide range of neurotransmission-specific processes at synapses – for example, CSP-Hsc70-SGT (cysteine string protein – heat shock cognate 70 – small glutamine-rich tetratricopeptide repeat-containing protein) complex regulates correct folding of SNAP-25 to enable its SNARE-associated function (Sharma et al., 2011), auxilin facilitates clathrin uncoating of synaptic vesicles (Yim et al., 2010), and chaperone NMNAT2 protects Bruchpilot, a protein essential for synaptic active zone integrity, from

ubiquitination and aggregation (Brazill et al., 2017, Wagh et al., 2006, Zang et al., 2013). Mutations in these proteins have been shown to cause axon damage, synapse degeneration and PD (Edvardson et al., 2012, Gilley et al., 2019, Wang et al., 2017c). Thus, one may hypothesise that Oxr1 participates in synaptic proteostasis capacity, and its loss leads to accumulation of toxic protein species, increase in autophagy and ultimately to neurodegeneration.

4.3.3 Limitations of the approach

Microarray analysis of transcription profiles is a widely used high-throughput method, however there are some inherent limitations regarding the data that can be obtained. Microarray technology is based on hybridization to probes on an array platform, and although arrays now contain probes for many thousands protein-coding genes and non-coding RNAs, the type used here cannot analyse the expression of alternative splicing events or previously uncharacterized genes unlike RNA-Seq (Bumgarner, 2013, Love et al., 2015, Mantione et al., 2014, Park et al., 2016). Some of the genes assayed in this chapter for qPCR validation displayed lower fold-changes as compared to the microarray result; it has previously been shown that the correlation between qPCR and microarray data is lower for genes with smaller fold-changes and depend on the source of the RNA – fresh or frozen tissue (Morey et al., 2006). Importantly, all the above-mentioned methods only give us information about RNA levels, but these do not necessarily correlate with the protein abundance (Liu et al., 2016). An example is up-regulation of the autophagy marker LC3-II that was not evident from microarray data, but was detected by western blotting.

When interpreting the results of the transcriptomic analyses I presented in this chapter, we need to bear in mind that the whole cerebellum was used for RNA extraction,

therefore generating a mixture of neuronal and glial cells transcripts. Thus, transcripts that are up-regulated in one cell type and down-regulated in another would result in no detectable changes in expression on average. Another possibility is that changes in transcription in a small group of cells were masked by a more abundant group. For example, some of the genes identified here are also expressed in neurons, but levels of expression are 1000 times lower than in microglia; even 5-fold up-regulation of these transcripts in a small group of neurons would not be detected in such mixed approach. Indeed, Oxr1 is expressed in different types of neural tissue cells and levels of expression are comparable in neuronal and glia cells (Table 4.3), suggesting its knockout could affect expression of multiple genes, possibly in a cell type-specific manner. Thus, use of purified cultures or even single-cell transcriptomics techniques would aid our understanding of the processes deregulated in *Oxr1*$^{d/d}$ brain tissue and potential role of Oxr1 in different cell types.

Conclusion

Here, I have shown that disruption of Oxr1 expression leads to a neuroinflammatory reaction in both cerebrum and cerebellum tissues and that it precedes CGCs death. Indirect evidence suggests that Oxr1 is involved in the regulation of autophagy – Oxr1 partially colocalises with the TGN and Oxr1 deletion leads to an increase in LC3-II, suggesting the phenotype of *Oxr1*$^{d/d}$ mouse could relate to lysosomal dysfunction, an avenue for future investigation.

5. Analysis of regulatory and functional conservation of the TLDc gene family

5.1 Introduction

TLDc gene family is comprised of five members in mammals, yet they differ in domain composition and localise to different compartments in the cell, which suggests they possess distinct functional roles (Durand et al., 2007, Fischer et al., 2016, Nguyen et al., 2018, Wu et al., 2016, Yoon et al., 2018). However, the fact that they all share the same highly conserved domain that confers protection against OS supports the hypothesis that TLDc proteins could share some common cellular functions and potentially compensate for the disruption of another family member (Finelli et al., 2016).

The phenomenon of compensatory up-regulation and functional substitution of a disrupted gene by a closely related family member is well documented in the literature. For example, in a zebrafish model of nemaline myopathy, disruption of the gene *actc1b* (actin alpha cardiac muscle 1b) leads to a mild phenotype due to up-regulation of paralogous actin gene *actc1a* and restoration of normal total α-actin protein levels (Sztal et al., 2018). In vomeronasal organ in mice, pannexin 1 (*Panx1*) knockout leads to induction of its homologue Panx3, thus preserving normal chemosensory processing in knockout animals (Whyte-Fagundes et al., 2018). Tamoxifen-induced loss of β-catenin in adult mouse heart led to up-regulation of mRNA and protein levels of closely related γ-catenin, with the prediction that this prevented the development of any overt phenotype (Zhou et al., 2007). The mechanism of genetic compensation is not well understood, but recent studies in zebrafish and mouse have proposed a model, whereby nonsense-mediated decay (NMD) of premature termination codon-containing mRNAs leads to alterations in epigenetic markers at transcription start site (TSS) of homologous genes and increase in their expression (El-Brolosy et al., 2019, Ma et al., 2019). Although

microarray analysis of *Oxr1*$^{d/d}$ cerebellum from Chapter 3 did not reveal any genetic compensation between Oxr1 and other TLDc family members, the possibility of such interaction cannot be ruled out, as microarray analysis does not distinguish between specific isoforms.

Based on published evolutionary analyses, *Oxr1* and *Ncoa7* are the most closely related members of the family (Durand et al., 2007, Shkolnik et al., 2008). In addition to the TLDc domain, both proteins possess LysM and Gram domains and are expressed as full-length and short isoforms from independent promoters (Fig 1.2) (Shkolnik et al., 2008, Yu et al., 2015). A comparison of *OXR1* and *NCOA7* exons sequences in human revealed overall identity of 35% between full-length isoforms and approximately 60% identity for TLDc domain-encoding exons and interestingly, an almost identical exon-intron structure, suggesting these genes emerged following duplication event (Durand et al., 2007, Shkolnik et al., 2008). In the CNS, *Oxr1* and *Ncoa7* are co-expressed in the amygdala, cerebral cortex and CA3 region of the hippocampus, whereas in the cerebellum genes are expressed in reciprocal manner – *Oxr1* transcripts are found in CGCs and Golgi cells in the granule layer, while Ncoa7 is expressed in Purkinje cell layer (Joery den Hoed, unpublished data; Fig. 5.1). Based on single-cell brain transcriptomic analysis, *Oxr1* is expressed in 50-70% of neurons and oligodendrocytes at comparable levels and approximately 25% of astroglia and microglia cells at slightly lower levels, while *Ncoa7* transcript is found in 54% of neurons, approximately 15% of oligodendrocytes and 6% and 2.7% of astroglia and microglia cells, respectively (Tabula Muris et al., 2018). At subcellular level, Oxr1-FL localizes to the cytoplasm and Oxr1-C is associated with mitochondrial outer membrane, while Ncoa7-FL displays both cytoplasmic and nuclear localization with nuclear accumulation upon hormone treatment, and Ncoa7-B is cytoplasmic (Durand et al., 2007, Finelli et al., 2016, Shao et al., 2002, Wu et al., 2016).

Together, these data suggest that *Ncoa7* and *Oxr1* could potentially share some evolutionary conserved functions and be involved in similar molecular processes based on the similarity of their domain architecture and sequence conservation, but may carry out these functions in distinct cells or cell compartments based on their expression pattern and localisation.

As well as possessing TLDc-related activities, such as protection against OS, Ncoa7 isoforms have additional functions: Ncoa7-FL possesses a non-canonical ER-binding domain and has been shown to interact with ERα, ERβ, TRβ, PPARγ, RARα and AhR nuclear receptors, naming it as a putative nuclear receptor coactivator (Halachmi et al., 1994, Nguyen et al., 1999, Shao et al., 2002). Ncoa7-FL was identified as a binding partner of these nuclear receptors by pull-down assays from cell lines and the interaction was shown to increase in the presence of receptors' agonists. Moreover, Ncoa7-FL has been shown to increase expression from ER response elements-containing promoter when co-expressed with ERα as compared to ERα-only transfected cells upon estrogen treatment; similar results were obtained for TRβ, PPARγ and RARα receptors with corresponding ligands (Shao et al., 2002). The shortest isoform (NCOA7-B) is induced upon interferon treatment in multiple sclerosis patients' blood cells as well as human astrocytoma, fibrosarcoma and other cell lines and human primary T cells and monocytes (Goujon et al., 2013, Yu et al., 2015). Recently, NCOA7-B has been shown to inhibit endosome-mediated virus entry via increased vesicular acidification and promotion of degradation of endocytosed material (Doyle et al., 2018). As such, due to their differing sizes, activation and domain content, these Ncoa7 isoforms are likely to have specific, independent functions.

Other members of the nuclear receptor coactivator (Ncoa) family have been shown to play key regulatory roles in transcriptional regulation in various organs and processes;

therefore, it is possible that Ncoa7-FL may possess similar functions. For example, *Ncoa1* (*SRC-1*, steroid receptor coactivator 1) knockout leads to delayed Purkinje cell development and moderate motor learning deficit (Nishihara et al., 2003); *Ncoa1* deficiency also led to reduced estrogen-induced uterine growth, smaller testes and underdevelopment of mammary glands, all due to impaired response of tissues to steroid hormones (Walsh et al., 2012). *Src-1* knockdown in the hippocampus leads to down-regulation of synaptic protein expression, decreased CA1 synapse density and disrupted spatial learning and memory, suggesting this protein is an integral part of hippocampal synaptic plasticity regulation (Bian et al., 2018). In a recent study, Src-1 has also been shown to be involved in the regulation of energy metabolism and food intake – knockout or obesity-associated mutations led to reduced expression of Pro-opiomelanocortin peptide (*Pomc*), a regulator of appetite, from Pomc neurons in the hypothalamus due to disruption of STAT3-Scr-1 binding and subsequent failure to induce *Pomc* expression (Yang et al., 2019). Thus, nuclear receptor coactivators are important controlling hubs for transcriptional regulation, suggesting Ncoa7 could have similar functions in development and maintenance of neural tissue and kidney, liver or lungs, where it is highly expressed, and its disruption could lead to significant phenotypic changes (Finelli et al., 2016). To date, however, no specific data regarding the transcriptional targets of NCOA7 in cells or tissue have been generated. Indeed, attempts to generate chromatin immunoprecipitation sequencing (ChIP-seq) data from cortical neurons have been hampered by the lack of reliable Ncoa7 antibodies for these particular methods (Oliver group, unpublished data).

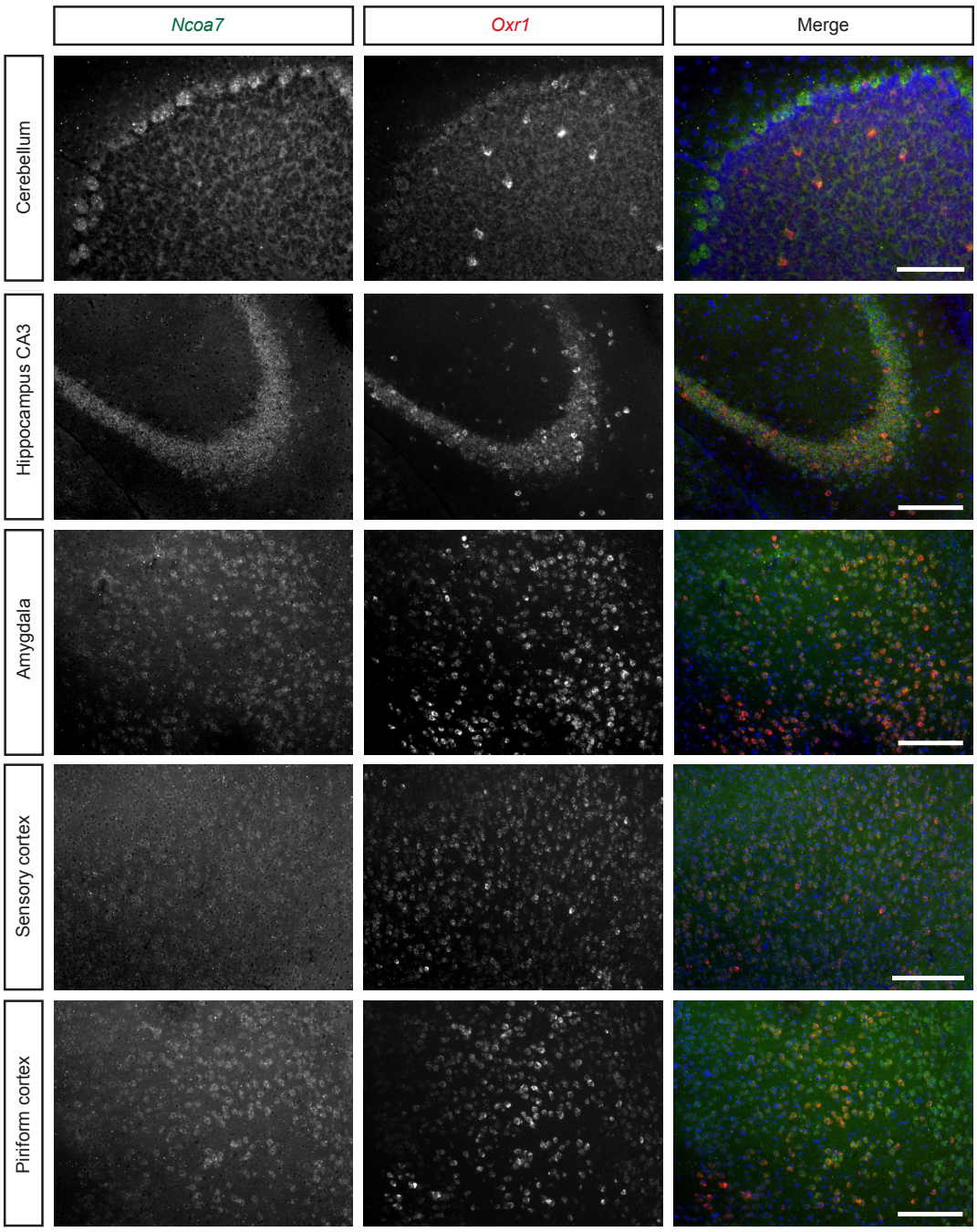


Figure 5.1 *Oxr1* and *Ncoa7* are co-expressed in the brain.
Expression of *Ncoa7* (green) and *Oxr1* (red) in P22 brain regions visualised using dual-colour fluorescent *in situ* hybridisation (Joery den Hoed). Cerebellum – sagittal section, scale bar 100μm; hippocampus, amygdala, sensory cortex, piriform cortex – coronal sections, scale bar 200μm. Sections were stained with DAPI to visualise cell nuclei.

The originally described *Oxr1* knockout mouse model (*bella*) was a spontaneous loss of a chromosomal locus spanning *Oxr1* and *Abra* genes resulting in cerebellar granule neuron loss and early death at P24-26 (Oliver et al., 2011). It was later confirmed in our laboratory that the phenotype is due to loss of *Oxr1* as the phenotype could be rescued using a ubiquitously-expressed Oxr1 transgene to restore normal levels of Oxr1 FL (Oliver et al., 2011). It was later shown that disruption of the TLDc domain of Oxr1 is sufficient to recapitulate the phenotype of the original knockout mouse, suggesting this domain is the key part of the molecule and further confirming the specific role of Oxr1 in driving the *bella* phenotype (Finelli et al., 2016, Finelli et al., 2018b). Interestingly, gene-trap mice with insertion specifically disrupting Oxr1-FL transcription and almost completely abolishing its expression do not display any neurological phenotype up to 12 months of age, suggesting Oxr1-C expression might be sufficient to prevent neurodegeneration (Oliver et al., 2011). Overall, these mouse models demonstrated the necessity for an intact TLDc domain of Oxr1 for brain function, thus it might be hypothesized that loss of Ncoa7 would also lead to an overt neurological phenotype.

As part of the Knockout Mouse Project KOMP2-DTCC, a non-conditional disrupted *Ncoa7* construct was generated. The insertion was designed at the 5' end of the gene, deleting two coding exons and inserting a LacZ cassette (*Ncoa7*^{tm1}) and subsequent removal of the Neo selection cassette by crossing to a ubiquitous Cre-driver (*Ncoa7*$^{tm1.1}$). Importantly, this mouse model is expected to expresses the short isoform (Ncoa7-B) of the protein (Fig. 5.2A, see Materials and Methods for details) (Merkulova et al., 2018). Phenotyping by the International Mouse Phenotype Consortium (on a C57BL/6N background) did not find any overt CNS phenotype, to the exception of an abnormal acoustic startle reflex, a symptom often seen in neurological disorders such as autism and schizophrenia (Kohl et al., 2014, Takahashi and Kamio, 2018). Importantly, consistent

with this observation, Doan et al. have recently reported a patient with autism spectrum disorder that harbours homozygous loss of NCOA7-FL due to premature stop codon (Doan et al., 2019). Highlighting the important role of Ncoa7-FL outside of the CNS, *Ncoa7*$^{tm1.1/tm1.1}$ animals have lower blood pressure, more acidic urine, enlarged intercalated cells in kidneys and reduced levels of B1, B2, A4 and A subunits of the V-ATPase (Merkulova et al., 2018). Therefore, these data demonstrate that Ncoa7-FL plays a role in the nervous system as well as outside of the CNS, and is possibly involved in vesicular organelles functioning as suggested by previously reported interaction with V-ATPase (Merkulova et al., 2015).

As no neurological or CNS-related phenotypes were observed in the *Ncoa7*$^{tm1.1/tm1.1}$ mouse, our laboratory performed a transcriptomic analysis to detect any potentially disrupted pathways that may also represent deregulation of *Ncoa7-FL* target genes. Surprisingly, microarray analysis of the frontal cortex of 12-week old mice revealed significant 2-fold down-regulation of only one gene, a chemokine *Ccl21c* (unpublished data). *Ccl21c* is expressed in lymphatic endothelium and plays role in transmigration of dendritic cells (Johnson and Jackson, 2010, Tal et al., 2011, Vaahtomeri et al., 2017). In the CNS, *Ccl21* has been shown to be expressed in damaged neurons to activate and attract microglia cells to the site of injury (de Jong et al., 2005). Therefore, these data may point to a role for Ncoa7 in attraction of immune cells, both resident and peripheral, to the site of neural tissue damage, or its role in peripheral cells transmigration though the endothelium.

As the total ablation of *Ncoa7-FL* in mice did not provide many insights into Ncoa7 function, another mouse model harboring a CRISPR-Cas9-mediated deletion of the whole *Ncoa7* locus was generated (*Ncoa7*^{del}) (Fig. 5.2B). The hypothesis was that the Ncoa7-B isoform, like Oxr1-C, is potentially masking a more overt neurological phenotype, thus

deleting both isoforms might be required. The characterization of the *Ncoa7*$^{del/del}$ mouse is currently ongoing; however, so far, no obvious phenotype has been observed in homozygous animals. The only observed difference is a slight reduction in the number of cortical interneurons, a type of inhibitory neurons that modulate neural circuits, in 18-month old *Ncoa7*$^{del/del}$ animals as compared to wild-type controls (Dr Peter Oliver, personal communication). Interestingly, interneuronal alterations, such as reduced cell numbers or decrease in interneuron marker expression, have been observed in animal models and patients with autism and schizophrenia, linking it back to abnormal acoustic startle effect seen in *Ncoa7*$^{tm1.1/tm1.1}$ mice (Gao and Penzes, 2015, Hashemi et al., 2017, Rapanelli et al., 2017). These data suggest potential involvement of *Ncoa7* in development of neuropsychiatric disorders. Microarray-based transcriptomics was also performed from frontal cortex of 12-week old *Ncoa7*$^{del/del}$ mice and littermate controls and no significantly deregulated genes were identified (data not shown). Together, these data suggest that *Ncoa7* disruption is not as detrimental as the genetic disruption of the TLDc domain of Oxr1, possibly due to functional compensation by other proteins.

Together, the findings to-date suggest that Oxr1 and Ncoa7 may have some overlapping functions in certain cell-types, such as cortical neurons where they are both co-expressed, yet any functional redundancy between these genes has not been explored. It is unclear whether TLDc genes are involved in similar cellular and organismal processes, apart from a general OS-associated protective function when over-expressed *in vitro*, and whether they can genetically and functionally compensate for disruption of another family member. Therefore, in this chapter, I will investigate the potential compensatory role of TLDc family members in the *Ncoa7*^{del} and *Ncoa7*$^{tm1.1}$ mouse models by gene expression studies and analyse potentially common functional roles by *in silico* analysis of TLDc gene transcriptional profiles and their regulation by transcription

factors. In addition, given the mild phenotype in *Ncoa7* knockout models, a genetic approach will be used to study the modulation of the *Oxr1*$^{d/d}$ phenotype *in vivo* by manipulation of the *Ncoa7* isoforms.

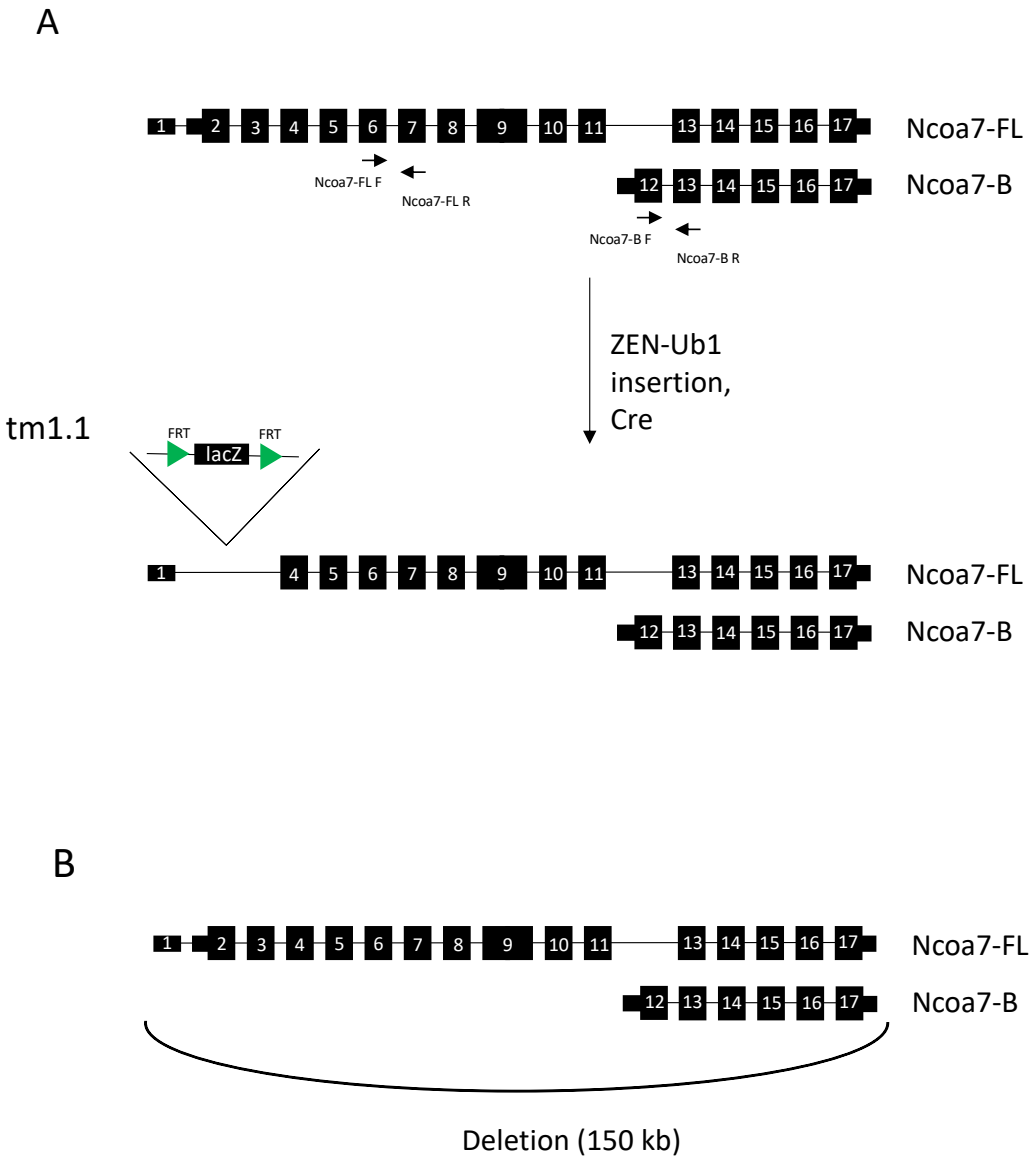


Figure 5.2 Schematic overview of Ncoa7 knockout mouse lines used in the work.
(A) *Ncoa7*$^{tm1.1}$ mouse line with disrupted *Ncoa7-FL* and preserved *Ncoa7-B* expression was generated by removal of the region spanning exons 2 and 3 and insertion of ZEN-Ub1 cassette, followed by crossing the line to ubiquitously Cre-recombinase expressing mouse line to remove neomycin-resistance gene and generate tm1.1 allele. (B) *Ncoa7*^{del} mouse was generated using CRISPR-Cas9 technology; whole *Ncoa7* locus was removed disrupting expression of all the isoforms. Arrows indicate the locations of RT-qPCR primers used in experiments in the chapter.

5.2 Results

5.2.1 Oxr1 and Ncoa7 are potentially involved in similar pathways during development

Common evolutionary origin of TLDc genes suggests potential functional redundancy; this in-turn is likely to rely on the presence of the gene products in the same place at the same time. Thus, I utilized an *in silico* approach to study possible roles of TLDc genes by analyzing the pattern of their promoters' activity and transcription factors (TFs) that likely regulate their expression. A putative promoter is a region of the DNA located upstream of the TSS, usually 100-1000 base pairs (bp) long, containing core promoter region and binding sites recognized by regulatory DNA-binding proteins (Haberle and Stark, 2018). As promoters do not have strict canonical sequence, they can be predicted by presence of certain markers – for example, trimethylation of histone H3 at lysine 4 (H3K4me3), epigenetic marker of active promoter, and cap analysis gene expression (CAGE) signal that shows regions corresponding to capped 5' ends of mRNA (Shiraki et al., 2003, Tserel et al., 2010). Thus, to predict the location and tissue-specific activity of TLDc genes' promoters, I analysed the distribution of these markers in all TLDc family members using a dataset containing histone modifications in the whole embryonic day (E) 14.5 mouse brain and various adult brain regions as well as other organs in Genome Browser (NCBI37/mm9 mouse genome assembly) (Kent et al., 2002, Rosenbloom et al., 2013). I also corroborate my findings with a different dataset, Eukaryotic Promoter Database (EPD) predicted promoters (Dreos et al., 2015).

Based on the location of H3K4me3 and CAGE signals and EPD predicted promoters, I identified three promoter regions within the *Oxr1* gene. One of them corresponded to the Oxr1-C isoform of the protein, whereas two others marked the 5'-ends of six longer

transcripts (Fig. 5.4A). In the rest of this chapter the 5'-most promoter will be referred to as *Oxr1-FL*-P1 and the second full-length promoter will be termed *Oxr1-FL*-P2. As the intensity of H3K4me3 signal reflects transcription levels, this dataset also shows the ratios of expression of different isoforms in selected organs (Karlic et al., 2010). In developing brain, all three *Oxr1* promoters are active, with the two regulating the full-length isoforms being active at similar levels. In the adult brain, on the other hand, transcriptional activity shifts to the *Oxr1-FL-P1* promoter, whereas shorter full-length and *Oxr1-C* isoforms are expressed at different ratios – for example, very low *Oxr1-C* promoter signal is seen in olfactory bulb, and in the cerebellum H3K4me3 signal intensities in these two promoters are similar, but significantly lower than that of the longest isoform (Fig. 5.4A). In the rest of the organism, *Oxr1-C* promoter signal was also absent from placenta and almost undetectable in testes, and the highest levels of its activity were found in brown adipose tissue, bone marrow derived macrophages, heart and spleen (Fig. 5.4A). Interestingly, *Oxr1-C* promoter activity was higher in adult heart sample as compared to embryonic tissue, suggesting its particular role in adult heart function (Fig. 5.4A). Both *Oxr1-FL*-P1 and *Oxr1-FL*-P2 promoters were active in all tissues and organs outside of the CNS, and while the 5'-most promoter signal was significantly lower in bone marrow, embryonic liver, spleen and testes samples as compared to other organs, *Oxr1-FL*-P2 was active at similar levels in all samples (Fig. 5.4A).

The transcripts under the control of the three *Oxr1* promoters identified encode six different full-length protein molecules in addition to two transcripts of the shortest isoform (Fig. 5.3). All of the full-length transcripts of Oxr1 include exons encoding GRAM, LysM and TLDc domains, and some of them included alternatively spliced exon 14, encoding 27 amino acid residues with putative casein kinase II (CK2) phosphorylation site (Fig. 5.3) (predicted with ScanProsite (de Castro et al., 2006)). Longer transcripts

encode proteins with additional 88 or 81 N-terminal amino acid residues. These extra residues contain a set of potential PTM sites, which differ between isoforms – the longest transcript contains N-glycosylation, cAMP and PKC phosphorylation sites, whereas the shorter one has PKC phosphorylation and N-myristoylation motifs (predicted with ScanProsite (de Castro et al., 2006)). This suggests that these isoforms, although containing the same set of domains, can be regulated individually at the protein level and might possess slightly different tertiary structure.

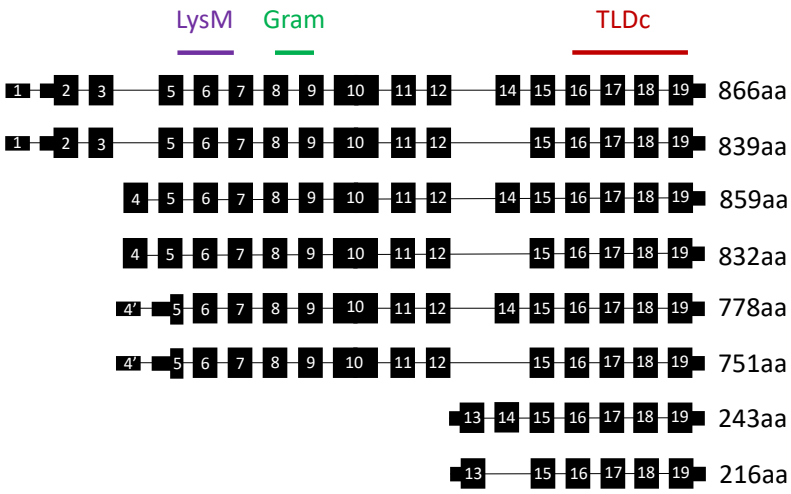


Figure 5.3 Exon and domain composition of Oxr1 transcript variants and proteins.
Oxr1 gene in mice contains 19 exons, and RefSeq database indicates expression of seven *Oxr1* transcripts and isoforms. Exons 5-7 encode LysM domain, exons 8-9 contain Gram domain sequence and TLDc domain is encoded by exons 16-19. aa, amino acids; (O'Leary et al., 2016)

Next, using a similar approach, I analysed the distribution of promoter markers in the *Ncoa7* gene. I identified two promoters located at 5'-ends of both full-length and short isoform-coding regions, as reported previously (Fig. 5.4B) (Yu et al., 2015). H3K4me3 signal in the short isoform promoter was very low in the embryonic brain and adult brain regions, as well as in testes, placenta and bone marrow derived macrophages (Fig. 5.4B). In other organs, activity of the promoter varied, but was always lower than that of the full-length promoter. The highest relative activity of the short isoform promoter was observed

in thymus, the site of maturation of T-cells (Fig. 5.4B) (Kurd and Robey, 2016, Seo and Taniuchi, 2016). In the heart and liver, its activities increased in adult samples as compared to embryonic organs at E14.5 (Fig. 5.4B). Full-length isoform promoter, on the other hand, was active in all analysed tissues at similar levels (Fig. 5.4B). Interestingly, I observed an additional H3K4me3 signal peak in the kidney corresponding to exon 2, suggesting expression of alternative full-length transcript lacking 5'-untranslated exon (Fig. 5.4B).

In the *Tbc1d24* gene, I identified one promoter suggesting expression of a single transcript. Based on H3K4me3 signal, *Tbc1d24* is expressed in all analysed adult CNS regions, as well as embryonic brain (Fig. 5.4C). Tbc1d24 promoter was also active at similar levels in all other tissues and organs, suggesting organism-wide expression of the gene (Fig. 5.4C).

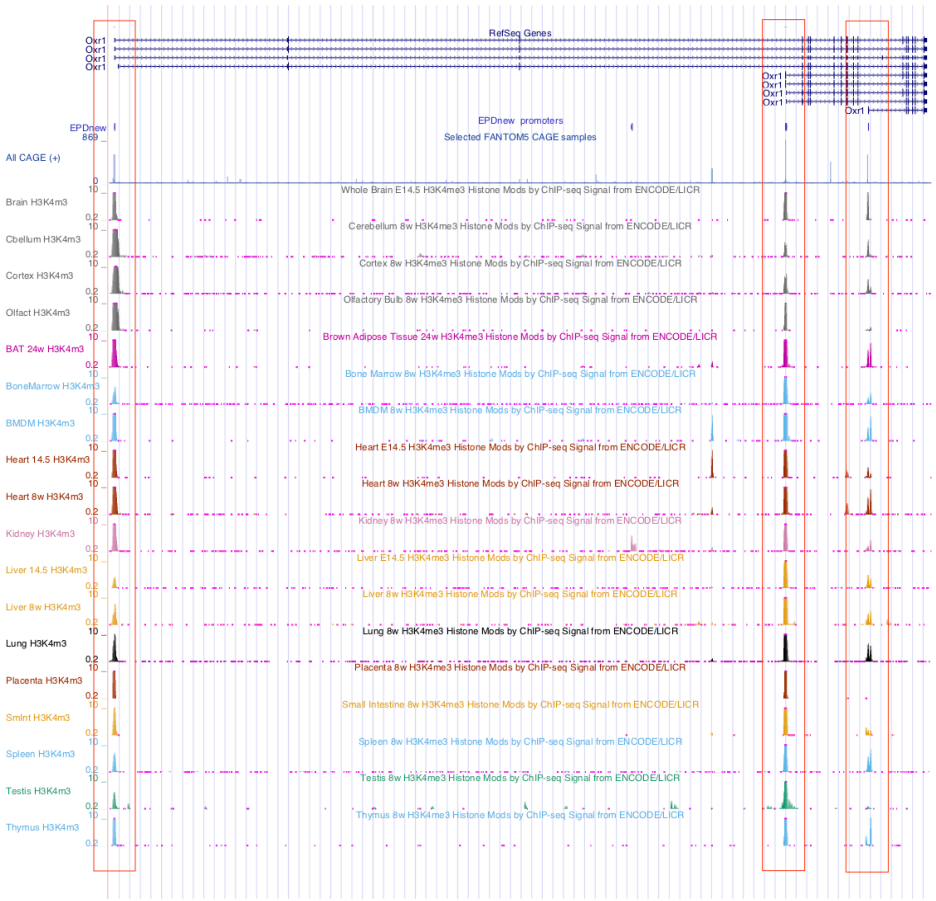
Expression of *mEAK7* (*Kiaa1609* or *TLDc1*) is also regulated by a single promoter located at the beginning of the gene. It is active in the embryonic brain and cerebellum, cortex and olfactory bulb of the adult animal, as well as all other analysed samples (Fig. 5.4D). The lowest level of promoter activity based on H3K4me3 signal was observed in placental tissue, while in other organs, including various brain regions, signal intensities were similar (Fig. 5.4D).

I also identified a single promoter within *C20Orf118* (*TLDc2*) gene. Interestingly, H3K4me3 signal was only detected in small intestine sample and its intensity is very low, suggesting limited expression of this gene in the organism (Fig. 5.4E).

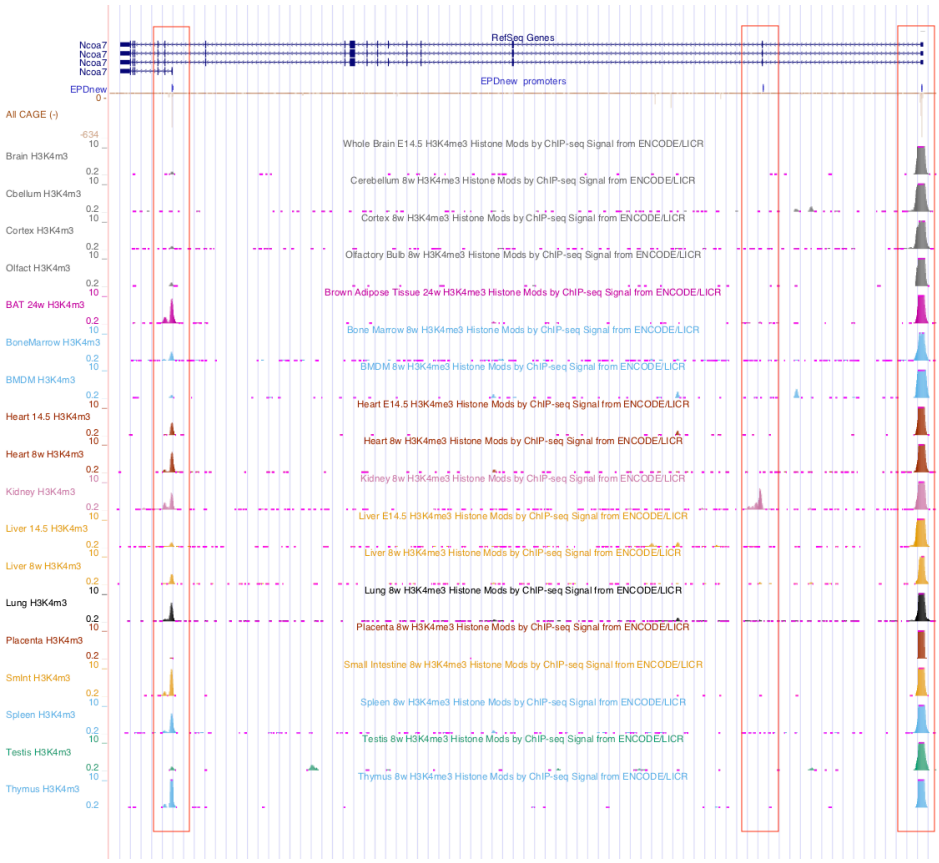
Together, these data show that TLDc genes are expressed, with *C20Orf118* as an exception, throughout the organism, and *Oxr1* and *Ncoa7* isoforms are expressed in

tissue- and time point-specific manner, suggesting their diverse functions in various organs.

A


RefSeq Genes
Oxr1
EPDnew promoters
Selected FANTOM5 CAGE samples
All CAGE (+)
Whole Brain E14.5 H3K4me3 Histone Mods by ChIP-seq Signal from ENCODE/LICR
Brain H3K4m3
Cerebellum 8w H3K4me3 Histone Mods by ChIP-seq Signal from ENCODE/LICR
Cbellum H3K4m3
Cortex 8w H3K4me3 Histone Mods by ChIP-seq Signal from ENCODE/LICR
Cortex H3K4m3
Olfactory Bulb 8w H3K4me3 Histone Mods by ChIP-seq Signal from ENCODE/LICR
Olfact H3K4m3
Brown Adipose Tissue 24w H3K4me3 Histone Mods by ChIP-seq Signal from ENCODE/LICR
BAT 24w H3K4m3
Bone Marrow 8w H3K4me3 Histone Mods by ChIP-seq Signal from ENCODE/LICR
BoneMarrow H3K4m3
BMDM 8w H3K4me3 Histone Mods by ChIP-seq Signal from ENCODE/LICR
BMDM H3K4m3
Heart E14.5 H3K4me3 Histone Mods by ChIP-seq Signal from ENCODE/LICR
Heart 14.5 H3K4m3
Heart 8w H3K4me3 Histone Mods by ChIP-seq Signal from ENCODE/LICR
Heart 8w H3K4m3
Kidney 8w H3K4me3 Histone Mods by ChIP-seq Signal from ENCODE/LICR
Kidney H3K4m3
Liver E14.5 H3K4me3 Histone Mods by ChIP-seq Signal from ENCODE/LICR
Liver 14.5 H3K4m3
Liver 8w H3K4me3 Histone Mods by ChIP-seq Signal from ENCODE/LICR
Liver 8w H3K4m3
Lung 8w H3K4me3 Histone Mods by ChIP-seq Signal from ENCODE/LICR
Lung H3K4m3
Placenta 8w H3K4me3 Histone Mods by ChIP-seq Signal from ENCODE/LICR
Placenta H3K4m3
Small Intestine 8w H3K4me3 Histone Mods by ChIP-seq Signal from ENCODE/LICR
SmInt H3K4m3
Spleen 8w H3K4me3 Histone Mods by ChIP-seq Signal from ENCODE/LICR
Spleen H3K4m3
Testis 8w H3K4me3 Histone Mods by ChIP-seq Signal from ENCODE/LICR
Testis H3K4m3
Thymus 8w H3K4me3 Histone Mods by ChIP-seq Signal from ENCODE/LICR
Thymus H3K4m3

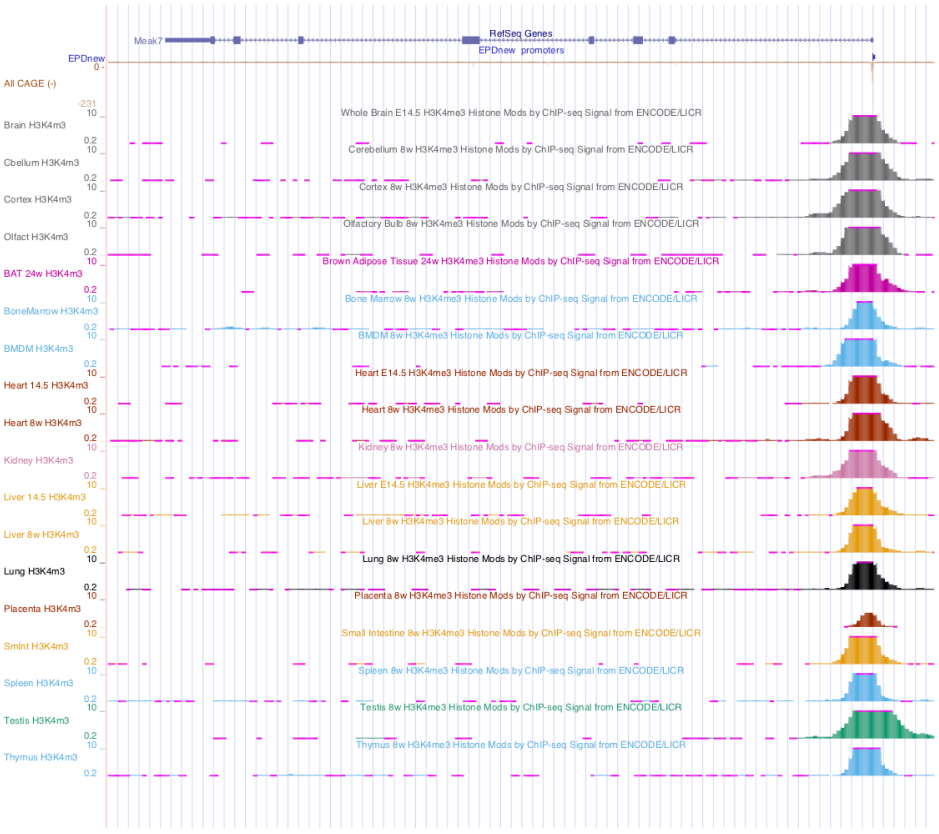
B


RefSeq Genes
Ncoa7
EPDnew promoters
All CAGE (-)
Whole Brain E14.5 H3K4me3 Histone Mods by ChIP-seq Signal from ENCODE/LICR
Brain H3K4m3
Cerebellum 8w H3K4me3 Histone Mods by ChIP-seq Signal from ENCODE/LICR
Cbellum H3K4m3
Cortex 8w H3K4me3 Histone Mods by ChIP-seq Signal from ENCODE/LICR
Cortex H3K4m3
Olfactory Bulb 8w H3K4me3 Histone Mods by ChIP-seq Signal from ENCODE/LICR
Olfact H3K4m3
Brown Adipose Tissue 24w H3K4me3 Histone Mods by ChIP-seq Signal from ENCODE/LICR
BAT 24w H3K4m3
Bone Marrow 8w H3K4me3 Histone Mods by ChIP-seq Signal from ENCODE/LICR
BoneMarrow H3K4m3
BMDM 8w H3K4me3 Histone Mods by ChIP-seq Signal from ENCODE/LICR
BMDM H3K4m3
Heart E14.5 H3K4me3 Histone Mods by ChIP-seq Signal from ENCODE/LICR
Heart 14.5 H3K4m3
Heart 8w H3K4me3 Histone Mods by ChIP-seq Signal from ENCODE/LICR
Heart 8w H3K4m3
Kidney 8w H3K4me3 Histone Mods by ChIP-seq Signal from ENCODE/LICR
Kidney H3K4m3
Liver E14.5 H3K4me3 Histone Mods by ChIP-seq Signal from ENCODE/LICR
Liver 14.5 H3K4m3
Liver 8w H3K4me3 Histone Mods by ChIP-seq Signal from ENCODE/LICR
Liver 8w H3K4m3
Lung 8w H3K4me3 Histone Mods by ChIP-seq Signal from ENCODE/LICR
Lung H3K4m3
Placenta 8w H3K4me3 Histone Mods by ChIP-seq Signal from ENCODE/LICR
Placenta H3K4m3
Small Intestine 8w H3K4me3 Histone Mods by ChIP-seq Signal from ENCODE/LICR
SmInt H3K4m3
Spleen 8w H3K4me3 Histone Mods by ChIP-seq Signal from ENCODE/LICR
Spleen H3K4m3
Testis 8w H3K4me3 Histone Mods by ChIP-seq Signal from ENCODE/LICR
Testis H3K4m3
Thymus 8w H3K4me3 Histone Mods by ChIP-seq Signal from ENCODE/LICR
Thymus H3K4m3

C


RefSeq Genes
Tbc1d24
Ntn3
EPDnew promoters
EPDnew
All CAGE (-)
Brain H3K4m3
Whole Brain E14.5 H3K4me3 Histone Mods by ChIP-seq Signal from ENCODE/LICR
Cbellum H3K4m3
Cerebellum 8w H3K4me3 Histone Mods by ChIP-seq Signal from ENCODE/LICR
Cortex H3K4m3
Cortex 8w H3K4me3 Histone Mods by ChIP-seq Signal from ENCODE/LICR
Olfact H3K4m3
Olfactory Bulb 8w H3K4me3 Histone Mods by ChIP-seq Signal from ENCODE/LICR
BAT 24w H3K4m3
Brown Adipose Tissue 24w H3K4me3 Histone Mods by ChIP-seq Signal from ENCODE/LICR
BoneMarrow H3K4m3
Bone Marrow 8w H3K4me3 Histone Mods by ChIP-seq Signal from ENCODE/LICR
BMDM H3K4m3
BMDM 8w H3K4me3 Histone Mods by ChIP-seq Signal from ENCODE/LICR
Heart 14.5 H3K4m3
Heart E14.5 H3K4me3 Histone Mods by ChIP-seq Signal from ENCODE/LICR
Heart 8w H3K4m3
Heart 8w H3K4me3 Histone Mods by ChIP-seq Signal from ENCODE/LICR
Kidney H3K4m3
Kidney 8w H3K4me3 Histone Mods by ChIP-seq Signal from ENCODE/LICR
Liver 14.5 H3K4m3
Liver E14.5 H3K4me3 Histone Mods by ChIP-seq Signal from ENCODE/LICR
Liver 8w H3K4m3
Liver 8w H3K4me3 Histone Mods by ChIP-seq Signal from ENCODE/LICR
Lung H3K4m3
Lung 8w H3K4me3 Histone Mods by ChIP-seq Signal from ENCODE/LICR
Placenta H3K4m3
Placenta 8w H3K4me3 Histone Mods by ChIP-seq Signal from ENCODE/LICR
SmInt H3K4m3
Small Intestine 8w H3K4me3 Histone Mods by ChIP-seq Signal from ENCODE/LICR
Spleen H3K4m3
Spleen 8w H3K4me3 Histone Mods by ChIP-seq Signal from ENCODE/LICR
Testis H3K4m3
Testis 8w H3K4me3 Histone Mods by ChIP-seq Signal from ENCODE/LICR
Thymus H3K4m3
Thymus 8w H3K4me3 Histone Mods by ChIP-seq Signal from ENCODE/LICR

D


RefSeq Genes
Meak7
EPDnew promoters
EPDnew
All CAGE (-)
Brain H3K4m3
Whole Brain E14.5 H3K4me3 Histone Mods by ChIP-seq Signal from ENCODE/LICR
Cbellum H3K4m3
Cerebellum 8w H3K4me3 Histone Mods by ChIP-seq Signal from ENCODE/LICR
Cortex H3K4m3
Cortex 8w H3K4me3 Histone Mods by ChIP-seq Signal from ENCODE/LICR
Olfact H3K4m3
Olfactory Bulb 8w H3K4me3 Histone Mods by ChIP-seq Signal from ENCODE/LICR
BAT 24w H3K4m3
Brown Adipose Tissue 24w H3K4me3 Histone Mods by ChIP-seq Signal from ENCODE/LICR
BoneMarrow H3K4m3
Bone Marrow 8w H3K4me3 Histone Mods by ChIP-seq Signal from ENCODE/LICR
BMDM H3K4m3
BMDM 8w H3K4me3 Histone Mods by ChIP-seq Signal from ENCODE/LICR
Heart 14.5 H3K4m3
Heart E14.5 H3K4me3 Histone Mods by ChIP-seq Signal from ENCODE/LICR
Heart 8w H3K4m3
Heart 8w H3K4me3 Histone Mods by ChIP-seq Signal from ENCODE/LICR
Kidney H3K4m3
Kidney 8w H3K4me3 Histone Mods by ChIP-seq Signal from ENCODE/LICR
Liver 14.5 H3K4m3
Liver E14.5 H3K4me3 Histone Mods by ChIP-seq Signal from ENCODE/LICR
Liver 8w H3K4m3
Liver 8w H3K4me3 Histone Mods by ChIP-seq Signal from ENCODE/LICR
Lung H3K4m3
Lung 8w H3K4me3 Histone Mods by ChIP-seq Signal from ENCODE/LICR
Placenta H3K4m3
Placenta 8w H3K4me3 Histone Mods by ChIP-seq Signal from ENCODE/LICR
SmInt H3K4m3
Small Intestine 8w H3K4me3 Histone Mods by ChIP-seq Signal from ENCODE/LICR
Spleen H3K4m3
Spleen 8w H3K4me3 Histone Mods by ChIP-seq Signal from ENCODE/LICR
Testis H3K4m3
Testis 8w H3K4me3 Histone Mods by ChIP-seq Signal from ENCODE/LICR
Thymus H3K4m3
Thymus 8w H3K4me3 Histone Mods by ChIP-seq Signal from ENCODE/LICR

E

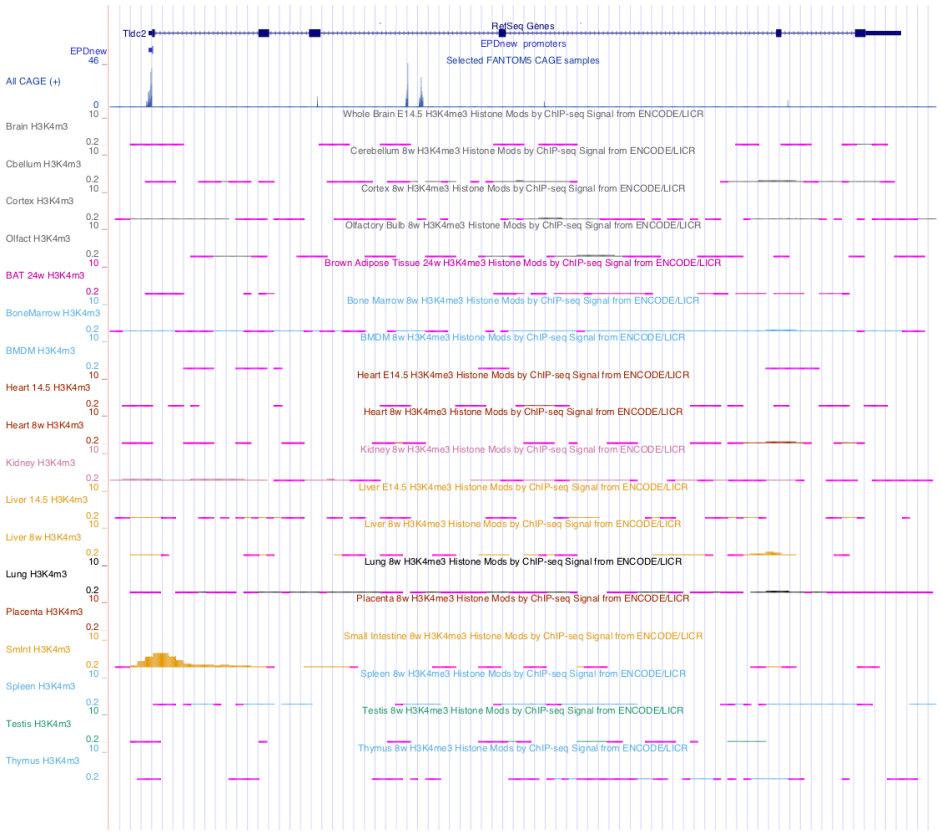


Figure 5.4 TLDc genes transcripts and promoter activities in mouse genome.
(A) Oxr1, (B) Ncoa7, (C) Tbc1d24, (D) mEAK7, (E) C20Orf118. Genome Browser was used to analyse location and activity of promoters of TLDc genes in the mouse genome (mm9 assembly) based on distribution of epigenetic marker and predicted promoters. EPD database contains information on experimentally validated eukaryotic promoters. CAGE signal location refers to mapped 5'-Caps H3K4me3 epigenetic mark indicates location of active promoter regions. CAGE, Cap analysis of gene expression; BAT, brown adipose tissue; BMDM, bone marrow derived macrophages; SmInt, small intestine.

Next, to study the possible functional roles of TLDc genes and their isoforms, I used publicly available ChIP-Seq data to analyse TFs and other regulatory proteins, such as histone modification enzymes, that have been shown to bind their promoters. TFs are regulatory proteins that bind promoter regions of target genes and suppress or activate mRNA synthesis in response to various stimuli in a tissue- and cell type-specific manner (Lambert et al., 2018). TFs orchestrate cellular response to OS, hormones, growth factors, small molecules and adjust cellular transcriptome to changing conditions (Licausi et al., 2011, Mendez and Janmey, 2012, Rossler and Thiel, 2017, Shi et al., 2015). The data were accessed via ChIP-Atlas and visualized using Integrated Genome Viewer (Oki et al., 2018, Thorvaldsdottir et al., 2013). The region 1000bp upstream and 250bp downstream from the TSS was used for the analysis of TFs as it has the highest density of TF binding sites in eukaryotic genes (Koudritsky and Domany, 2008, Messeguer et al., 2002, Yu et al., 2016). The data contains information on the cell type or organ where ChIP-Seq of TFs or other chromatin-binding proteins was performed; thus, TFs that regulate transcription of TLDc genes and their isoforms were analysed separately in all available tissues and organs. Importantly, as binding of TFs to promoter region is indicative of the regulation of corresponding gene expression, this data will not only provide information on tissue-specific regulation of TLDc gene expression, but also show an organism-wide pattern of expression. I did not include data obtained from experiments with cell lines as regulation of their transcriptome may differ from *in vivo* conditions.

Consistent with H3K4me3 data, all three Oxr1 promoters were bound by multiple TFs in all analysed organs and groups of tissues – adipose tissues, blood, immune, kidney and reproductive systems, gastrointestinal tract, heart, liver, lung, neural tube derivatives and embryonic stem cells (ESCs) (Appendix 1, Table S1). In contrast, *Ncoa7* isoforms displayed significant difference in TFs identified at their promoter regions – while *Ncoa7*-

FL was found to be transcriptionally regulated in all analysed organs, *Ncoa7-B* promoter was not found to interact with any TFs in neural tissues and gastrointestinal tract (Appendix 1, Table S1). *Tbc1d24* promoter was bound by regulatory proteins in all organs, with lungs being the only exception due to limited data available for this tissue (Appendix 1, Table S1). *mEAK7* promoter region was also occupied by an array of TFs in all organs, whereas *C20Orf118*, consistent with H3K4me3 data, was only found to be transcriptionally regulated in gastrointestinal tract regions; three TFs were also reported to bind its promoter region in ESCs (Appendix 1, Table S1).

Interestingly, many TFs bind to more than one TLDc promoter in a given tissue, suggesting shared regulatory mechanisms between these genes. For example, in the embryonic brain, neurogenic differentiation factor 2 (Neurod2), an important regulator of neural tissue development, was interacting with *Oxr1-FL*-P1, *Oxr1-FL*-P2, *Ncoa7-FL*, *Tbc1d24* and *mEAK7* promoters (Appendix 1, Table S1) (Bormuth et al., 2013, Pieper et al., 2019, Wilke et al., 2012). All *Oxr1* and *Ncoa7* isoforms, *Tbc1d24* and *mEAK7* were also regulated by TF B-cell lymphoma/leukemia 11B (Bcl11b), a key player in T-cell development, in thymus, thymocytes and CD4 CD8 double negative cells, and *Oxr1-FL*-P2 and *Ncoa7-FL* in CD4+ T-lymphocytes (Appendix 1, Table S1) (Famili et al., 2017). Together, these data show that TLDc genes are possibly involved in similar processes in the tissues where they are co-expressed. Thus, to get an insight into functional roles of the TLDc genes in the developing and adult mouse tissues and organs, I performed a GO pathway prediction analysis of identified TFs in an organ-specific manner.

As TLDc genes are highly expressed in the brain and their disruptions and mutations are associated with neurological phenotype, I used GO to predict the pathways and processes in which TLDc genes could potentially be involved in the CNS. Among the TLDc genes and their isoforms, only *Oxr1* and *Tbc1d24*, but not *Ncoa7-FL*, were predicted to be

involved in neurodevelopmental processes – neurogenesis, neuroblast proliferation, forebrain, diencephalon and telencephalon development; GO analysis also predicted involvement of all Oxr1 isoforms and Tbc1d24 in pituitary gland development. Oxr1-C was also predicted to play role in glial cell differentiation. Transcripts under regulation of *Ncoa7-FL*, *Oxr1-FL*-P1 and *Tbc1d24* promoters were predicted to play role in sensory perception of sound, although all promoters, except for mEAK7, were bound by TFs in multipotent otic progenitor sample, suggesting they all may be involved in hearing-related processes (Appendix 1, Table S2). For mEAK7, no relevant biological processes could be predicted by GO. Together, these data suggest a significant involvement of TLDc genes in the development and function of the CNS.

These data suggest that TLDc genes are potentially involved in multiple organismal and cellular processes, and these processes are shared between family members, giving a possibility they could potentially compensate for the disruption of each other's function.

5.2.2 Disruption of *Ncoa7-FL* expression results in deregulation of TLDc genes

Based on the evidence that other TLDc genes are regulated by similar TFs as the ones predicted to regulate *Ncoa7* expression and are involved in similar processes, I went on to investigate if they can genetically compensate for *Ncoa7* knockout through up-regulation of their transcripts, as this could explain the lack of severe phenotypic changes observed in $Ncoa7^{del/del}$ and $Ncoa7^{tm1.1/tm1.1}$ mice. Importantly, a microarray transcriptomic analysis of $Ncoa7^{tm1.1/tm1.1}$ mouse cortex previously performed in our laboratory has revealed down-regulation of a single gene *Ccl21c*, and no changes in the expression of the other TLDc genes were detected. Similarly, microarray analysis of pre-symptomatic $Oxr1^{d/d}$ cerebellum did not reveal any deregulation of TLDc family members

(Chapter 4, Table 4.1). Although microarray is an informative method of gene expression profile analysis, the platform we used for this study did not provide data on expression of gene's isoforms. Moreover, microarray transcriptional analysis from *Ncoa7*$^{tm1.1/tm1.1}$ cortex sample was performed with older Agilent array that did not even include *mEAK7* probes. Thus, to investigate if distinct isoforms of TLDc genes are differentially expressed following *Ncoa7-FL* knockout, I performed RT-qPCR analysis from cortices of 11-week old *Ncoa7*$^{tm1.1}$ heterozygous and homozygous knockout and control animals. The cortex was selected as all TLDc genes, with the exception of *C20Orf118*, are widely expressed in this region (Finelli et al., 2016).

First, as a key control, I analysed the levels of *Ncoa7-FL* and *Ncoa7-B* transcripts in *Ncoa7*$^{tm1.1/+}$ and *Ncoa7*$^{tm1.1/tm1.1}$ mice. Interestingly, *Ncoa7-FL* transcript levels were almost unchanged in heterozygous *Ncoa7*$^{tm1.1/+}$ animals, possibly due to compensatory up-regulation of transcription from the remaining wild-type gene copy, and significantly lower in *Ncoa7*$^{tm1.1/tm1.1}$ cortex compared to wild-type, although some signal was still detected (Fig. 5.5). As absence of the full-length protein and mRNA including exon 3 has been previously confirmed for this mouse model, the observed signal could be due to amplification from aberrant mRNA that is transcribed, but not translated (Merkulova et al., 2018). Importantly, I have detected expression of *Ncoa7-B*, although H3K4me3 and previously published RNA-Seq data report minimal levels of promoter activity and transcription (Pervouchine et al., 2015). It is of note that Ct values for this isoform were high, suggestive of low expression levels. Levels of *Ncoa7-B* were unchanged in *Ncoa7*$^{tm1.1/+}$ and *Ncoa7*$^{tm1.1/tm1.1}$ samples, consistent with the fact that the tm1.1 allele does not modify the *Ncoa7-B* first unique coding exon (Fig. 5.5).

Next, I evaluated the transcription levels of other TLDc genes in heterozygous and homozygous *Ncoa7*$^{tm1.1}$ 11-week old mice as compared to control littermates.

Interestingly, *Oxr1-FL* was significantly up-regulated in heterozygous *Ncoa7*$^{tm1.1/+}$ cortex by 30%, whereas its levels were non-significantly elevated in *Ncoa7*$^{tm1.1/tm1.1}$ tissue (Fig. 5.5). *Oxr1-C*, on the other hand, was significantly down-regulated in both heterozygous and homozygous samples by approximately 25%. Levels of *Tbc1d24* were reduced by approximately 20% in both *Ncoa7*$^{tm1.1/+}$ and *Ncoa7*$^{tm1.1/tm1.1}$ samples compared to wild-type controls, although only reaching significance in *Ncoa7*$^{tm1.1/+}$ samples due to some variation in control group (Fig. 5.5). Expression of *mEAK7* was significantly down-regulated in both heterozygous and homozygous knockout animals by 25% and 40%, respectively (Fig. 5.5). Together, these data indicate that disruption of *Ncoa7-FL* leads to some detectable deregulation of expression of other TLDc family members.

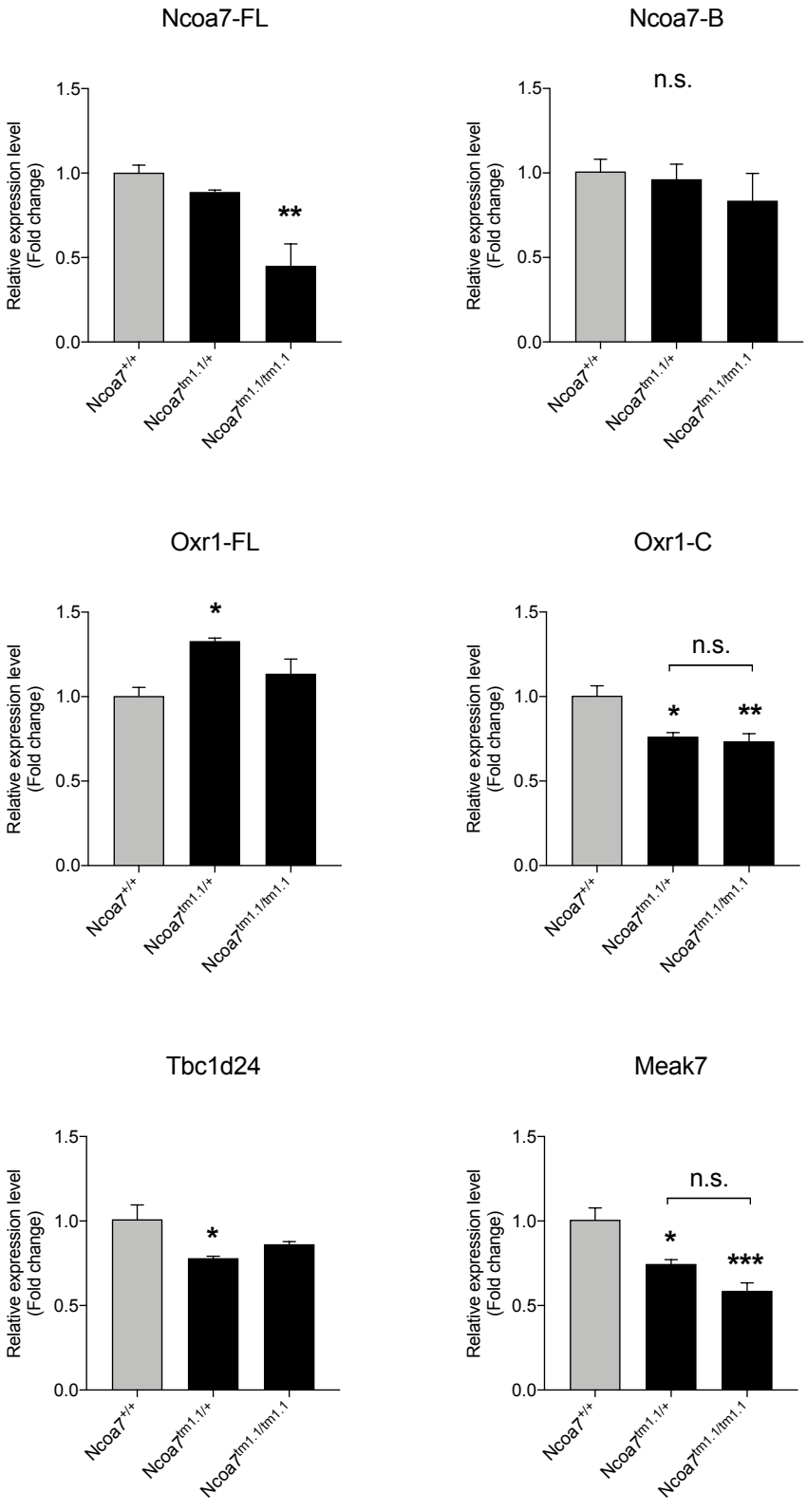


Figure 5.5 Ncoa7-FL knockout leads to deregulation of other TLDc family members' expression.

Expression of TLDc family members was analysed in cortices of 11 weeks old wild-type, Ncoa7$^{tm1.1/+}$ and Ncoa7$^{tm1.1/tm1.1}$ mice by RT-qPCR. N=4 animals per group. Data presented as mean ± SEM, one-way ANOVA with Bonferroni correction, *p<0.05, **p<0.01, ***p<0.001 as compared to wild-type.

5.2.3 *Ncoa7* locus deletion leads to deregulated expression of other TLDc genes

Next, I performed similar analysis in the *Ncoa7*^{del} mouse that lacks all *Ncoa7* isoforms. Of note, mice homozygous for this allele will not allow expression of the Ncoa7-B isoform, unlike homozygous *Ncoa7*$^{tm1.1/tm1.1}$ mice. Analysis was also performed in cortex tissues from 11-week old animals. Unexpectedly, *Oxr1-FL* expression was significantly down-regulated by 25% in *Ncoa7*$^{del/del}$ mice, whereas *Oxr1-C* levels were unchanged (Fig 5.6). Levels of both *Tbc1d24* and *mEAK7* transcripts were significantly up-regulated by approximately 35% in *Ncoa7*$^{del/del}$ animals as compared to wild-type controls (Fig. 5.6). These data suggest that there may be some co-regulatory mechanisms between TLDc genes at the RNA level, potentially involving a positive-feedback mechanism, as knockdown of *Ncoa7-FL* alone or both *Ncoa7* isoforms results in down-regulation of other TLDc genes. Together, these data suggest very subtle changes in TLDc genes expression upon deletion of *Ncoa7* locus. Interestingly, trend of expression changes of TLDc genes in *Ncoa7*$^{del/del}$ mouse cortex is opposite to that in *Ncoa7*$^{tm1.1/tm1.1}$ cortex, suggesting the presence of the *Ncoa7-B* transcript, even at low levels, can influence their expression.

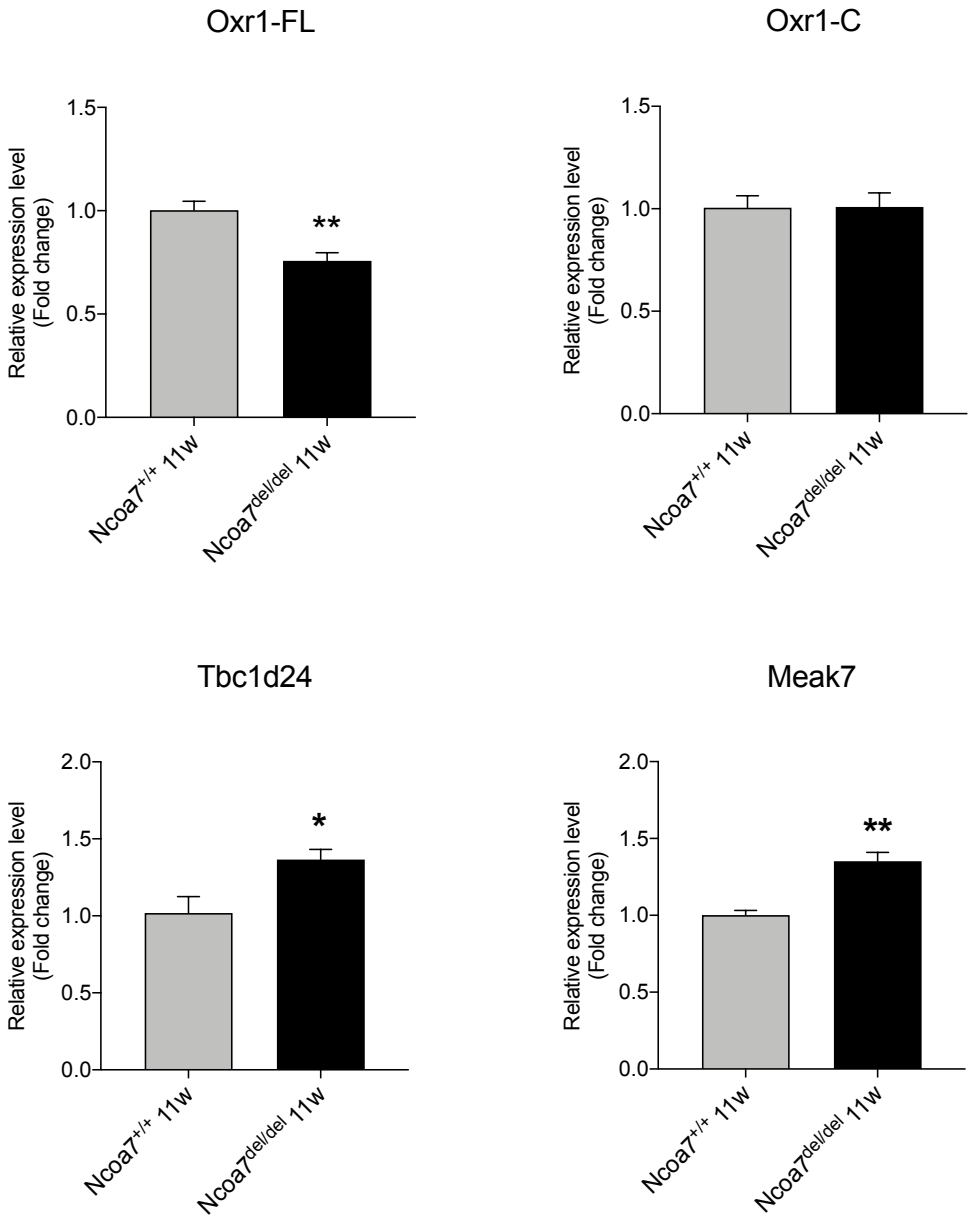


Figure 5.6 *Ncoa7* locus deletion leads to deregulated expression of other TLDc genes.
Expression of TLDc family members was analysed in cortices of 11 weeks old wild-type and *Ncoa7*$^{del/del}$ mice by RT-qPCR. N=4 samples per group. Data presented as mean ± SEM, t-test: *p<0.05, **p<0.01 as compared to wild-type.

5.2.4 *Ncoa7* locus deletion does not lead to aberrant glia activation

Initial histopathology did not reveal any cell death in any brain region in adult (12-week old) *Ncoa7*$^{del/del}$ mice (unpublished); however, given the increase in inflammation markers in *Oxr1* knockout tissue, I decided to assess the levels of neuroinflammatory markers in the cortex of adult and aged *Ncoa7*$^{del/del}$ animals. Importantly, given that the *Ncoa7-B* isoform is significantly up-regulated in response to interferon (Goujon et al., 2013, Yu et al., 2015), and that this specific isoform has been shown to be induced in the hippocampus upon peritoneal LPS injection (Joery den Hoed, unpublished data), absence of *Ncoa7-B* in the *Ncoa7*$^{del/del}$ could disrupt endogenous inflammatory pathways in the brain. The natural ageing of neural tissue leads to microglia priming, accumulation of ROS and aggregated proteins (Wyss-Coray, 2016), therefore I hypothesised that the ageing process might exacerbate an inflammatory phenotype in *Ncoa7*$^{del/del}$ mice. Therefore, I next investigated whether there was any indication that inflammatory pathways were disrupted in *Ncoa7*$^{del/del}$ mouse line. I assessed the levels of *Cd68*, a marker of microglia activation and glial fibrillary acidic protein (Gfap), an intermediate filament protein, a marker of astrocyte activation (Boisvert et al., 2018, Clarke et al., 2018, Liddelow and Barres, 2017).

At 11 weeks of age, no increase in levels of *Cd68* and *Gfap* was observed in *Ncoa7*$^{del/del}$ as compared to wild-type, confirming absence of inflammatory response in young adult animals. A small cohort of *Ncoa7*$^{del/del}$ animals aged to 18m was maintained, and cortical RNA was prepared as before. Interestingly, I observed small but significant increase in *Cd68* expression in wild-type and *Ncoa7*$^{del/del}$ cortex tissues of aged mice as compared to corresponding young adult animals, consistent with known *Cd68* elevation with ageing due to microglia priming (Fig. 5.7) (Norden and Godbout, 2013). No increase in *Cd68* was detected in aged *Ncoa7*$^{del/del}$ cortex tissue as compared to aged wild-type control,

suggesting normal age-associated microglia priming in these animals (Fig. 5.7). Similarly to *Cd68*, *Gfap* was slightly increased in 18 months old mice, although these transcriptional changes did not reach significance in both wild-type and *Ncoa7*$^{del/del}$ group due to some variation between samples (Fig. 5.7). Together, these data suggest that total *Ncoa7* locus deletion does not cause overt aberrant glia activation in mice.

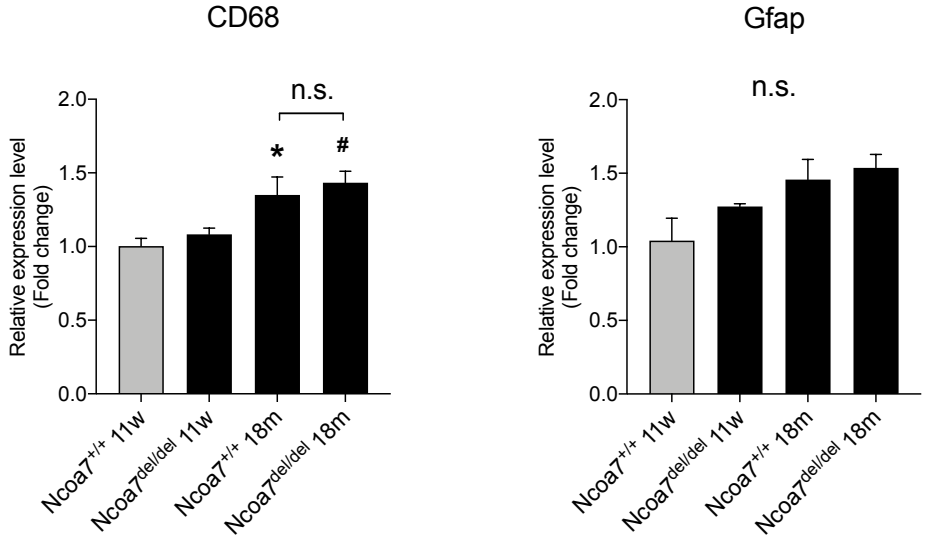


Figure 5.7 *Ncoa7* deletion does not cause aberrant neuroinflammatory response.
Expression levels of microglia activation marker *Cd68* and astrocytes activation marker *Gfap* were analysed by RT-qPCR in cortices of 11 week and 18 months old wild-type and *Ncoa7*$^{del/del}$ mice. N=4 animals per group. Data presented as mean ± SEM, one-way ANOVA with Bonferroni correction, *p<0.05 as compared to 11 weeks old wild-type, $^{\#}$p<0.05 as compared to 11 weeks old *Ncoa7*$^{del/del}$.

5.2.5 *Oxr1* and *Ncoa7* are both required for successful early embryonic development

As *Ncoa7* and *Oxr1* are the most closely-related members of the TLDc family, and considering the strikingly different phenotypes in the various knockout lines, it was decided to investigate their potential genetic interactions by intercrossing the mutant lines together.

Firstly, the *Oxr1*$^{d/+}$ *and Ncoa7*$^{del/+}$ lines were intercrossed over two generations in the attempt to generate all possible allelic combinations. All mice that were born were monitored carefully as it was predicted that *Oxr1*$^{d/d}$ amimals also lacking one or both alleles of *Ncoa7* may show a more severe neurodegenerative or neurodevelopmental phenotype. A small number (4) of pups were found dead at P0-P5 and these were also genotyped, alongside the others (132) that were culled at P22 for tissue collection. Analysis of the genotypic data (Table 5.1) shows that, surprisingly, no double knockout mice were found from this cross. The ratio of the other genotypes was close to expected ratios, suggesting that mice lacking both genes are not viable (Table 5.1). It is noteworthy that mice lacking either *Oxr1* or *Ncoa7* were viable with only one functional allele of the other gene, demonstrating that only a single copy of either *Oxr1* or *Ncoa7* is required for embryonic viability in mice. To investigate whether double-knockouts might be severly developmentally impaired, an initial examination at E15.5 was carried out by crossing *Oxr1*$^{d/+}$*/Ncoa7*$^{del/del}$ males with *Oxr1*$^{d/+}$*/Ncoa7*$^{del/del}$ females. From three litters and 18 embryos, all looked generally normal, and the genotyping data showed once again that no double knockouts were present (Joery Den Hoed, unpublished data, Table 5.2).

In an attempt to ascertain whether *Ncoa7-B* was sufficient for viability in the absence of *Oxr1*, the *Oxr1*^{d} line was next intercrossed to *Ncoa7*$^{tm1.1}$ mutants over two generations.

In the interests of time and funding availablilty, the F2 breeding was set-up from *Oxr1*$^{d/+}$/*Ncoa7*$^{tm1.1/+}$ and *Oxr1*$^{d/+}$/*Ncoa7*$^{tm1.1/tm1.1}$ animals as opposed to double heterozygous mice. As above, mice were taken to P22 for tissue collection and genotyping; however, no double knockouts were identified once again.

As the genotyping in search for *Oxr1*$^{d/d}$/*Ncoa7*$^{del/del}$ embryos was performed at E15.5, double knockouts could have been missed if they had died or had been resorbed at earlier stages of development. Thus, I decided to analyse the genotype of embryos at E6.5-E10.5 from the *Oxr1*^{d}/*Ncoa7*$^{tm1.1}$ cross (*Oxr1*$^{d/+}$/*Ncoa7*$^{tm1.1/+}$ and *Oxr1*$^{d/+}$/*Ncoa7*$^{tm1.1/tm1.1}$ animals). Each conceptus was dissected from the uterus and decidua and embryonic membranes were removed to avoid the amplification of contaminating maternal DNA. In total, 60 embryos were successfully genotyped and no *Oxr1*$^{d/d}$/*Ncoa7*$^{tm1.1/tm1.1}$ animals were found (Table 5.3), suggesting that one allele of *Ncoa7-B* is not sufficient to support the embryonic development in the absence of *Oxr1* and *Ncoa7-FL* from E6.5. Interestingly, I also observed a few deciduas with resorbing embryos that fused with decidual tissue and could not be biopsied for the genotyping. Therefore, I cannot exclude that some *Oxr1*$^{d/d}$/*Ncoa7*$^{tm1.1/tm1.1}$ embryos are formed, but they cannot be carried further through development. Based on these results, it appears that simultaneous homozygous knockout of *Oxr1* and *Ncoa7-FL* leads to early developmental abnormalities and potentially resorption of the embryo (Papaioannou and Behringer, 2012). Surprisingly, no *Oxr1*$^{d/d}$/*Ncoa7*$^{tm1.1/+}$ embryos were identified amongst these embryos, although animals with this genotype are found among adult mice (Table 5.3).

Table 5.1. Generation of *Oxr1$^{d/d}$/Ncoa7$^{del/del}$* mouse.
Number of P22 animals of each genotype observed and expected following *Oxr1$^{d/+}$/ Ncoa7$^{del/+}$* and *Oxr1$^{d/+}$/ Ncoa7$^{del/+}$* intercross (Joery den Hoed).

	Oxr1$^{+/+}$/Nco a7$^{+/+}$	*Oxr1$^{+/+}$/Nco a7$^{del/+}$*	*Oxr1$^{+/+}$/Nco a7$^{del/del}$*	*Oxr1$^{d/+}$/Nco a7$^{+/+}$*	*Oxr1$^{d/+}$/Nco a7$^{del/+}$*	*Oxr1$^{d/+}$/Nco a7$^{del/del}$*	*Oxr1$^{d/d}$/Nco a7$^{+/+}$*	*Oxr1$^{d/d}$/Nco a7$^{del/+}$*	*Oxr1$^{d/d}$/Nco a7$^{del/del}$*	Total
Observed	17	23	8	25	26	19	8	10	0	136
Expected	8.50	17.00	8.50	17.00	34.00	17.00	8.50	17.00	8.50	136
Binomial probability	0.0029	0.0301	0.1416	0.0129	0.0229	0.0862	0.1416	0.0195	0.0002	

Table 5.2. Generation of *Oxr1$^{d/d}$/Ncoa7$^{del/del}$* mouse.
Number of E15.5 embryos of each genotype observed and expected following *Oxr1$^{d/+}$/Ncoa7$^{del/del}$* and *Oxr1$^{d/+}$/Ncoa7$^{del/del}$* intercross (Joery den Hoed).

	Oxr1$^{+/+}$/Ncoa7$^{del/del}$	*Oxr1$^{+/d}$/Ncoa7$^{del/del}$*	*Oxr1$^{d/d}$/Ncoa7$^{del/del}$*	Total
Observed	5	13	0	18
Expected	4.5	9	4.5	18
Binomial probability	0.1988	0.1855	0.0056	

Table 5.3. Generation of *Oxr1$^{d/d}$/Ncoa7$^{tm1.1/tm1.1}$* mouse.
Number of embryos of each genotype observed and expected following *Oxr1$^{d/+}$/Ncoa7$^{tm1.1/+}$* and *Oxr1$^{d/+}$/Ncoa7$^{tm1.1/tm1.1}$* intercross.

	Oxr1$^{+/+}$/Ncoa7$^{tm1.1/+}$	*Oxr1$^{+/+}$/Ncoa7$^{tm1.1/tm 1.1}$*	*Oxr1$^{d/+}$/Ncoa7$^{tm1.1/+}$*	*Oxr1$^{d/+}$/Ncoa7$^{tm1.1/tm 1.1}$*	*Oxr1$^{d/d}$/Ncoa7$^{tm1.1/+}$*	*Oxr1$^{d/d}$/Ncoa7$^{tm1.1/tm 1.1}$*	Total
Observed	18	13	21	8	0	0	60
Expected	7.5	7.5	15	15	7.5	7.5	60
Binomial probability	0.00018	0.018	0.024	0.012	0.0003	0.0003	

5.2.6 *Ncoa7* deletion exacerbates neuroinflammation in *Oxr1*$^{d/d}$ mouse cerebellum

The transcriptomics data suggest that loss of *Ncoa7*, either full-length transcripts only or entire locus altogether, is well-tolerated in mice, unlike loss of *Oxr1*. Yet, despite the fact that mice lacking two alleles of both full-length genes are not viable, *Oxr1*$^{d/d}$ mice with heterozygous loss of *Ncoa7* survive. Visual inspection of the animals prior to tissue collection at P22 suggest these mice display the same ataxic phenotype as *Oxr1*$^{d/d}$ animals. However, considering the significant homology and partial overlapping expression of *Oxr1* and *Ncoa7* in glial cells, it is possible that heterozygosity for *Ncoa7* may influence the inflammatory pathways affected by *Oxr1* knockout. Thus, I next investigated the effect of heterozygous *Ncoa7* deletion on the expression of neuroinflammatory markers identified by microarray analysis of *Oxr1*$^{d/d}$ cerebella (Chapter 4). RT-qPCR analysis was performed on P22 cerebellar samples from control, *Oxr1*$^{d/d}$ and *Oxr1*$^{d/d}$*/Ncoa7*$^{del/+}$ animals. This time point was selected as gene deregulation at this stage is more marked than P18 (Fig. 4.2 Chapter 4) and the same animals were required to reach P22 to assess their general health as well as any gait defects.

First, I confirmed the absence of *Oxr1* transcripts and down-regulation of *Ncoa7* in *Oxr1*$^{d/d}$ and *Oxr1*$^{d/d}$*/Ncoa7*$^{del/+}$ mice (Fig. 5.8A). Analysis of *Ncoa7* isoforms expression revealed a non-significant 2-fold down-regulation of *Ncoa7-FL* levels in *Oxr1*$^{d/d}$*/Ncoa7*$^{del/+}$ samples due to some variation between samples, while, interestingly, *Ncoa7-B* transcript abundance was slightly elevated in *Oxr1*$^{d/d}$ cerebellum and significantly up-regulated in *Oxr1*$^{d/d}$*/Ncoa7*$^{del/+}$ animals, possibly due to induction of this short isoform as a result of the infammation in the cerebellum (Fig. 5.8A).

Next, I assessed the levels of expression of *C1qb*, *Cd68*, *Ctss*, *FcrlS*, *HexB* and *Ly86* neuroinflammatory markers identified in Chapter 4. In all cases, the significant up-

regulation was observed in *Oxr1*$^{d/d}$ samples as compared to *Oxr1*$^{+/+}$, consistent with previous findings (Chapter 4, Fig. 4.2). When comparing *Oxr1*$^{d/d}$/*Ncoa7*$^{+/+}$ and *Oxr1*$^{d/d}$/*Ncoa7*$^{del/+}$ tissues, a small but non-significant increase in expression were observed for *C1qb*, *Ctss*, *FcrlS* and *HexB* between these genotypes, yet *Cd68* and *Ly86* were significantly up-regulated in *Oxr1*$^{d/d}$/*Ncoa7*$^{del/+}$ as compared to *Oxr1*$^{d/d}$/*Ncoa7*$^{+/+}$ cerebellum (Fig 5.8B). Together, these data suggest that heterozygous deletion of *Ncoa7* exacerbates neuroinflammatory response observed in *Oxr1*$^{d/d}$ mouse cerebellum, possibly due to further deregulation of regulatory pathways in glial cells.

Overall, these genetic and expression data reveal that Oxr1 and Ncoa7 share some key functions during early embryonic development, and are possibly involved in similar cellular processes based on data on TFs that bind their promoters in various tissues and organs, as well as exacerbation of *Oxr1*$^{d/d}$ phenotype in presence of heterozygous *Ncoa7-FL* knockout. These data has also shown that disruptions in *Ncoa7* gene expression lead to subtle deregulation of other TLDc genes, suggesting they could be functionally linked in the tissue analysed.

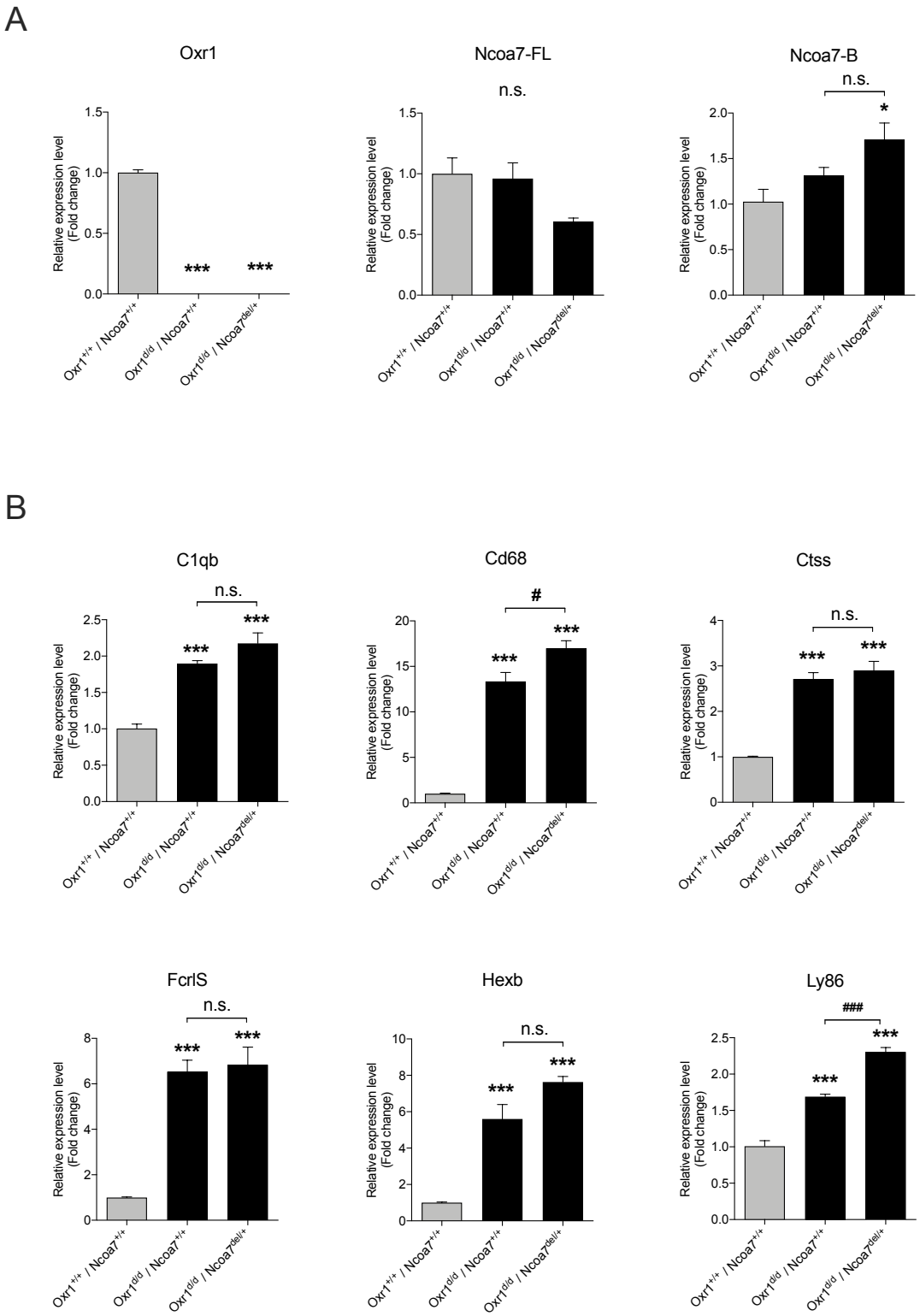


Figure 5.8 Heterozygous deletion of *Ncoa7* in *Oxr1* knockout mouse exacerbates neuroinflammatory phenotype in the cerebellum at P22.

(A) Expression levels of *Oxr1*, *Ncoa7-FL* and *Ncoa7-B* were analysed in wild-type, $Oxr1^{d/d}/Ncoa7^{+/+}$ and $Oxr1^{d/d}/Ncoa7^{del/+}$ cerebellar samples by RT-qPCR. (B) Expression of neuroinlfammatory markers identified in $Oxr1^{d/d}$ P18 cerebellum was analysed in wild-type, $Oxr1^{d/d}/Ncoa7^{+/+}$ and $Oxr1^{d/d}/Ncoa7^{del/+}$ cerebellar samples. N=4 animals per group. Data presented as mean ± SEMone-way ANOVA with Bonferroni correction, *p<0.05, **p<0.01, ***p<0.001 as compared to wild-type, $^{\#}$p<0.05, $^{\#\#\#}$p<0.001 as compared to $Oxr1^{d/d}/Ncoa7^{+/+}$.

5.3 Discussion

In this chapter, I have focused on comparative analysis of mouse TLDc gene expression patterns and possible common biological processes based on experimental ChIP-Seq data and the identity of TFs that bind their promoters in various cells, tissues and organs. As TLDc genes have common evolutionary origin and based on the Gene Ontology enrichment analysis are involved in similar pathways, I hypothesized that they could functionally compensate for the disruption of one another. Thus, I analysed if expression of other TLDc family members is potentially affected in the cortex in response to *Ncoa7* disruption, explaining absence of any CNS-related phenotype in *Ncoa7*^{del} and *Ncoa7*$^{tm1.1}$ mouse models and showed that *Ncoa7-FL* knockout or complete *Ncoa7* locus deletion led to deregulation in expression of *Oxr1* isoforms, *Tbc1d24* and *mEAK7*, suggesting all family members are functionally or transcriptionally linked. I have also shown that presence of at least one allele of *Oxr1* in the absence of Ncoa7 is required for successful early embryonic development, suggesting they share some functions during embryogenesis.

5.3.1 Evolutionary conservation of TLDc genes functions and regulation mechanisms

The computational analysis has predicted the presence of potential additional promoter in *Ncoa7* gene – a third H3K4me3 signal peak, referring to exon 2, was observed in kidney sample (Fig. 5.4B). Importantly, exon 1 is untranslated, meaning the proteins expressed from the putative novel and from the ubiquitously used full-length promoters will be identical. 5’ untranslated regions (5’UTR) of mRNA are known to play role in translation regulation by forming secondary and tertiary structures, thus regulating

ribosome entry (Leppek et al., 2017). Translation levels can also be modulated by binding of RNA binding proteins that can promote or inhibit ribosome entry in presence or absence of particular stimuli (Araujo et al., 2012). *Ncoa7* 5'UTR, encoded by exon 1, exhibits high GC content – 75%, which suggests complex secondary structure of this mRNA region that may interfere with or decrease levels of its translation. Thus, presence of alternative promoter may ensure constant levels of Ncoa-FL translation, independent of external factors, such as presence of specific helicases that unwind these structures (Leppek et al., 2018). Presence of an alternative promoter regulating expression of a transcript with shorter 5'UTR has also been reported for *SHOX* gene; importantly, longer 5'UTR attenuated translation via seven upstream AUG codons that interfere with ribosomal scanning, while shorter 5'UTR provided stable translation levels (Blaschke et al., 2003). It is possible that an alternative promoter is used in situations when there is an immediate need for a protein, while a transcript with longer 5'UTR is expressed to allow fine-tuning of translation levels. Potential existence of similar system in the *Ncoa7* gene suggests importance of its stable expression levels in the kidney. Indeed, Ncoa7-FL expression disruption leads to higher urine pH and larger kidney intercalated cells as observed in *Ncoa7*$^{tm1.1}$ mouse model, suggesting an important Ncoa7-FL role in regulating kidney function (Merkulova et al., 2018).

TFs and promoter activity analyses suggest broad expression of TLDc genes throughout the organism, including the CNS, gastrointestinal tract, lungs, liver, testes and other organs, as well as ESCs. Interestingly, these data also demonstrated transcriptional activity of TLDc genes in various types of mature and immature lymphocytes, thymus, leukocytes and bone marrow cells (Appendix 1, Table S1). Moreover, in the embryonic liver *Oxr1-FL*-P1, *Oxr1-FL*-P2, *Ncoa7-FL*, *Ncoa7-B* and *Tbc1d24* promoters interact with the Core-binding subunit beta (Cbfb) TF – a part of the regulatory complex that controls

the emergence of hematopoietic stem cells from endothelial cells (Link et al., 2010). Endothelial cells of mouse fetal liver are known to be a site of hematopoiesis, and these data suggest that TLDc genes may be involved in this process (Khan et al., 2016). This suggests strong involvement of TLDc genes in processes related to hematopoiesis, lymphocyte maturation and bone marrow functioning, and potentially immunity. There is emerging evidence that TLDc family members are interferon-regulated genes and play role in immune response and defense mechanisms (Doyle et al., 2018, Goujon et al., 2013, Rusinova et al., 2013, Wang et al., 2012, Yu et al., 2015). Short isoform of Ncoa7, Ncoa7-B, has initially been identified as INFβ-inducible gene in peripheral blood mononuclear cells and cell lines (Yu et al., 2015). It has later been shown to be up-regulated in response to INFα treatment in primary T-cells and monocytes and multiple cell lines, and to prevent endosome-mediated viral entry via cytoplasmic vesicle acidification (Doyle et al., 2018, Goujon et al., 2013). Analysis of available gene expression data has revealed that other TLDc genes also display interferon-responsive expression changes. *TBC1D24* has been reported to be down-regulated in blood cells following INFα and INFγ treatment and in monocyte derived macrophages upon INFβ and INFγ treatment (Rusinova et al., 2013). *MEAK7* is up-regulated in skin melanoma, fetal microglia and umbilical cord endothelial cells after INFγ treatment and down-regulated in blood in response to short INFα and INFγ treatment; interestingly, prolonged INFγ treatment led to slight up-regulation of *MEAK7*, suggesting a complex mechanism of its involvement in immune response (Rusinova et al., 2013). Human and mouse *Oxr1-C* have been reported to be 1.5-2-fold down-regulated following INFγ treatment in bone marrow derived macrophages and blood cells, as well as upon IFNα treatment in natural killer (NK) cells (Rusinova et al., 2013). Importantly, responsiveness to INF treatment has only been observed for *Oxr1-C*, whereas *Oxr1-FL* is not reported to be differentially expressed following cytokine

treatment. Similarly, only *Ncoa7-B*, but not *Ncoa7-FL*, is induced upon interferon treatment. This suggests a specific role of short isoforms in the immune response processes. Interestingly, the nuclear short isoform of *Drosophila* Oxr1 ortholog Mustard (Mtd) has been shown to be involved in innate immune response – overexpression of this specific isoform resulted in increased tolerance to oral *Vibrio cholerae* infection, differential expression of antimicrobial peptides *diptericin* and *drosomycin*, as well as other genes, and higher intestinal stem cell division rate (Wang et al., 2012, Wang et al., 2013). Together, these preliminary data suggest strong involvement of TLDc genes in immune response mechanisms and highlights the importance of further investigation of their role in the innate and adaptive immune cells, in particular microglia.

My analysis has revealed that TLDc genes are regulated by overlapping sets of TFs within each studied tissue, suggesting they are involved in similar pathways. If TLDc genes evolved following gene duplication event, they are likely to retain the regulatory elements of the ancestor gene, while acquiring novel domains or structural elements to diversify their functions. Based on promoter activity data, most of the family members are expressed in all major organs, suggesting either gene redundancy or specialisation of each gene or expression in a defined group of cells within an organ, as in case with *Oxr1* and *Ncoa7* that are expressed specifically in CGCs and Purkinje cells, respectively, in the cerebellum. Thus, it is possible that TLDc genes have evolved to carry out similar functions in a cell compartment-specific manner and their additional activities, such as nuclear receptor binding of Ncoa7, have co-evolved during evolution via addition or loss of extra domains.

The analysis of TFs that have been shown to bind TLDc promoters has revealed involvement of the family members in multiple processes in various organs. Importantly, the approach I used to analyse TFs bears some limitations – although the database is said

to include all publicly available ChIP-Seq experiments, it may not include TF binding data from smaller studies. For example, *Oxr1-FL*-P1 promoter is known to be regulated by Otx2 in postnatal mouse cortex, but it is not reflected in ChIP-Atlas data (Sakai et al., 2017). On the other hand, the same study has also found Otx2 binding at *Oxr1-C* promoter in neural retina, consistent with ChIP-Atlas (Sakai et al., 2017). A study previously performed in our laboratory has predicted several putative TFs to regulate human and mouse *Oxr1-C* expression (Dr Matthew Williamson, unpublished data). Among twelve factors, three were also identified in this study; importantly, mutating binding sites of two of these – Pbx1 and Nkx2.5 – led to significant changes in reporter gene expression from altered *Oxr1-C* promoter, suggesting they play important role in the regulation of *Oxr1-C* transcription activity (Dr Matthew Williamson, unpublished data). Thus, the list of TFs binding the promoters of the TLDc genes I obtained from the database used in this study may not be exhaustive, but it still provides valuable data on expression and possible roles of TLDc genes throughout the organism, suggesting the direction for future studies.

5.3.2 Disruption of *Ncoa7* expression leads to deregulation of other TLDc genes

Based on common evolutionary origin and similarity in TFs and predicted functions, I hypothesised that TLDc genes could genetically compensate for the knockout of other family members. As *Ncoa7*^{del} and *Ncoa7*$^{tm1.1}$ mouse lines do not possess any overt neurological phenotype, it is possible that disrupted *Ncoa7* is compensated by one or more TLDc proteins in the CNS. In *Ncoa*$^{tm1.1/tm1.1}$ mouse cortex I observed significant down-regulation of *Oxr1-C* and *mEAK7*, and in *Ncoa7*$^{del/del}$ mouse I detected statistically significant down-regulation of *Oxr1-FL* and increase in *Tbc1d24* and *mEAK7* expression levels, with no changes in *Oxr1-C*. Together, these data suggest that although *Ncoa7-FL*

knockout and *Ncoa7* locus deletion lead to deregulation of TLDc genes expression, they do not cause marked up-regulation of any of the family members. Mechanism of genetic compensation is based on NMD of mutant mRNA that possesses premature termination codon. Resulting RNA fragments are transported into the nucleus and bind to homologous sequence in a closely related gene in an RNA-protein complex, promoting epigenetic changes at the promoter of the corresponding gene and transcription induction (El-Brolosy et al., 2019, Ma et al., 2019). Thus, complete deletion of the gene cannot promote genetic compensation, as it does not produce mRNA that can undergo NMD. *Ncoa7*^{del} mouse harbours complete deletion of the *Ncoa7* locus, suggesting it cannot up-regulate closely related TLDc gene via such mechanism. On the other hand, *Ncoa7*$^{tm1.1}$ mouse expresses *Ncoa7-FL* transcript that possesses premature stop codon, meaning it could induce compensatory up-regulation of other genes. Consistent with this hypothesis, I observed slight but significant up-regulation if *Oxr1-FL* in *Ncoa7*$^{tm1.1/+}$ and non-significant up-regulation in *Ncoa7*$^{tm1.1/tm1.1}$. Importantly, compensatory up-regulation of paralogous genes may also occur on translational, not transcriptional levels. Such mechanism of compensatory translation induction has been observed in mouse models of *Hdac1* and *Hdac2* knockout, where deletion of one of the genes led to increased protein levels of another one, without increase in its mRNA abundance (Winter et al., 2013). Thus, combination of transcriptomic and proteomic approaches could be more informative in search for genetic compensation or analysis of knockout phenotypes.

Ncoa7-B is known to be induced *in vivo* in human blood cells and *in vitro* in response to anti-inflammatory interferon β-1b administration (Yu et al., 2015), in multiple cell lines and primary T-cells and monocytes upon IFNα treatment (Goujon et al., 2013), and upon LPS treatment *in vitro* in macrophages differentiated from induced pluripotent stem cells and monocyte-derived macrophages and *in vivo* in mouse hippocampus (Alasoo et al.,

2015, Doyle et al., 2018) (Joery den Hoed, unpublished data). Response to both these factors is primarily mediated by lymphocytes and microglia cells in the CNS (D'Angelo et al., 2017, Ngkelo et al., 2012). Based on my analysis of ChIP-Seq data, *Ncoa7-B* promoter has not been shown to be regulated by any TFs in the brain, suggesting it is only expressed at very low levels under normal conditions, but it is bound by multiple TFs in blood and immune cells, which is in agreement with its possible expression in microglia. Indeed, previously published RNA-Seq data report very low expression of this isoform in the brain, with some expression detected only in pericytes, endothelial cells and microglia (Consortium, 2015, Pervouchine et al., 2015, Zhang et al., 2014b). Thus, loss of *Ncoa7-B* expression in *Ncoa7*^{del} mouse would mostly affect myeloid cells of the CNS. In *Ncoa7*$^{del/del}$ cortex samples I observed slight but statistically significant increase in *Tbc1d24* and *mEAK7* transcripts abundance. Based on cell type-specific RNA-Seq data, both genes are expressed in all brain cell types, including microglia (Zhang et al., 2014b). Therefore, *mEAK7* up-regulation could potentially be a compensatory induction; alternatively, *mEAK7* transcription may be induced in response to unidentified changes caused by *Ncoa7-B* knockout. Tbc1d24 is known to function at synapses, where it regulates synaptic vesicle recycling and endocytosis (Finelli et al., 2018a, Fischer et al., 2016), and microglia has been shown to regulate functioning, formation and pruning of synapses throughout the life (Ji et al., 2013, Miyamoto et al., 2016, Siskova and Tremblay, 2013). Thus, *Ncoa7* deletion could lead to alteration of synapse-related microglia activities, such as reduced synapse pruning, and small, but functionally critical, induction of *Tbc1d24* expression.

Interestingly, previously performed microarray analysis of transcriptional changes in cortical tissues of *Ncoa7*$^{tm1.1/tm1.1}$ mouse model did not identify any alterations of TLDc genes expression. All fold-changes of TLDc genes levels obtained by RT-qPCR analysis are below 1.5-fold, which is in the range of low correlation between qPCR and microarray

analysis (Morey et al., 2006). Moreover, in this chapter I analysed transcription levels of individual isoforms, while the microarray platform used did not provide such information. For example, data on *Ncoa7*$^{tm1.1/tm1.1}$ cerebellum suggest slight induction of *Oxr1-FL* and decrease in *Oxr1-C* levels, which would potentially 'balance' each other out across the microarray probes. Thus, the use of RNA-Seq, a method that allows quantifying expression levels of individual splice variants, could be used to study in more detail the effect of *Ncoa7* knockout on the transcriptional profile of the brain.

5.3.3 Possible roles of *Ncoa7* in the organism

Microarray analysis was performed from a cortex tissue of 12-week old animals, but nothing is known about transcriptional changes that occur in other brain regions or organs upon knockout of *Ncoa7-FL* or complete *Ncoa7* locus deletion. Based on previously published qPCR and RNA-Seq data and my computational promoter activity analysis, *Ncoa7-FL* is expressed throughout the organism, while *Ncoa7-B* is transcribed in adipose tissue, bone marrow, heart, kidney, lung, small and large intestine, colon, mammary gland, ovary, spleen and thymus and is absent or expressed at minimal levels in the CNS, adult liver, testes, stomach, duodenum, adrenal gland and placenta (Finelli et al., 2016, Pervouchine et al., 2015). Thus, these proteins may play important roles outside of the CNS. For example, it has been shown that *Ncoa7-FL* knockout leads to high urine pH and enlarged intercalated cells in kidney (Merkulova et al., 2015, Merkulova et al., 2018). It is also possible that transcriptional changes occur in specific cell-types and analysis of the whole cortical tissue masks these alterations. Although *Ncoa7* is widely expressed in cortex, potential transcriptional changes could depend on other cellular factors, such as neuron type, its connectivity or activation state of glial cells. For instance, *Ncoa7-B* has been shown to be strongly induced upon IFN-β treatment, while very low expression is

observed in its absence (Yu et al., 2015). Thus, it is possible that pathways associated with *Ncoa7-B* function could only be detected in the CNS or blood cells after immune challenge in wild-type and *Ncoa7-B* deficient mice.

Ncoa7-FL has been initially identified as a nuclear receptor co-activator, a class of proteins that interact with nuclear receptors and modulate their transcription regulation activity. Thus, one would expect *Ncoa7-FL* knockout to lead to deregulation of expression of its target genes. Indeed, knockouts of other Ncoa proteins have been reported to lead to deregulation of their target genes. For example, alkaline phosphatase (ALPL) was identified as one of the SRC-1 target genes in human osteosarcoma cell line by ChIP-Seq, and SCR-1 silencing led to its down-regulation in these cells; bone marrow cells from SCR-1 knockout mice displayed decreased ALPL protein signal and strong but non-significant decrease in ALPL mRNA levels (Watters et al., 2017). Down-regulation of SRC-1 also led to decrease in tumor necrosis factor receptor superfamily 11b (*TNFRSF11B*), leukemia inhibitory factor (*LIF*) and *HO-1*, all identified as SRC-1 targets by ChIP-Seq (Watters et al., 2017). Overall, this study identified 6007 SRC-1 targets across human genome (Watters et al., 2017). *Ncoa3* knockout is associated with decreased platelet counts in mice and has been shown to be involved in megakaryocyte development via regulation of induction of *GATA1* factor expression in response to estrogen treatment by interaction with ERβ; *Ncoa3* depletion leads to inability of cells to induce *GATA1* (Du et al., 2017). Another study has shown that Ncoa2 and Bmal1 co-occupy promoter regions of more than 1,500 genes in the liver, and Ncoa2 ablation alters circadian locomotor behaviour, cyclic liver metabolism and leads to aberrant circadian clock gene expression (Stashi et al., 2014). The fact that there were so few gene alterations following *Ncoa7-FL* knockout may also reflect the fact that in the adult mouse brain transcriptional co-factor function of Ncoa7 is not critical. Ncoa7-FL is known to interact with estrogen, thyroid hormone, aryl

hydrocarbon, peroxisome proliferator-activated and retinoic acid receptors - regulators of transcription that play role in many organs and cells outside of the CNS (Halachmi et al., 1994, Lazennec et al., 1997, Nguyen et al., 1999, Shao et al., 2002). For example, Pparγ is involved in glucose metabolism regulation, adipocyte differentiation and lipid accumulation, and is highly expressed in fat cells (Lasar et al., 2018, Wafer et al., 2017), while estrogen receptors α, β1 and β2 are expressed throughout the organism and play role in very diverse processes, ranging from development of reproductive organs and pregnancy to regulation of osteoclasts and osteoblasts, lipid metabolism regulation and growth and differentiation of neurites (Lee et al., 2012). Importantly, estrogen levels in mice are tightly regulated and depend on various factors – such as the animal's age, the tissue under study and the estrous cycle stage in females (Konkle and McCarthy, 2011, Nilsson et al., 2015). Moreover, estrogen possesses sex-specific roles in male and female brains, regulating behaviour, synaptic plasticity, reproductive system control, brain-bone signaling axis and body weight (Gillies and McArthur, 2010, Herber et al., 2019, Wang et al., 2018, Wu and Tollkuhn, 2017, Xu et al., 2015). In the cortex and the hippocampus, estrogen levels are the highest during embryonic development and drop significantly and reach plateau by ~P30 in rats (Konkle and McCarthy, 2011). In this study, we used female 11-week old mice; but taking into account all these evidence, transcriptomic analysis of brain tissue from young females could be more informative and reveal deregulation of Ncoa7-FL target genes, and use of male mice tissues could reveal possible sex-specific functions of the gene.

Importantly, although Ncoa7-FL has been shown to interact with these receptors *in vitro*, there is no evidence to support the interactions *in vivo*, including the brain. The only study performed in brain tissue utilized beads-immobilised ER to pull down the binding partner and did not provide any data on interaction of endogenously expressed proteins

(Paramanik and Thakur, 2010). Thus, binding of Ncoa7-FL to these receptors may not take place in the brain *in vivo*, or could be limited to particular group of cells – for example, Purkinje cells in the cerebellum, where it is expressed. Cerebellar ERα and ERβ expression reaches peak levels around P7, a period of dendritic growth of Purkinje cells, and ERα is mainly expressed in these neurons (Hedges et al., 2012). Estrogen and thyroid hormones signaling play important role in Purkinje cells development and maturation – mutations in TRα affected cell body alignment and arborisation in a cell-autonomous manner (Fauquier et al., 2014), and estrogen was shown to facilitate Purkinje cell-parallel fiber synaptic transmission, promote cerebellar memory and synapse formation (Andreescu et al., 2007, Hedges et al., 2018, Sasahara et al., 2007). These data suggest that deletion of Ncoa7-FL may specifically affect the transcription profile of Purkinje cells and laser capture microdissection and subsequent microarray or RNA-Seq analysis may reveal more details about the pathways regulated by this TLDc protein.

5.3.4 *Ncoa7* deletion exacerbates neuroinflammation in *Oxr1*$^{d/d}$ mouse cerebellum

In search for functional overlaps between *Oxr1* and *Ncoa7* genes, I focused on the neuroinflammation because I have shown in Chapter 4 that *Oxr1* knockout leads to up-regulation of neuroinflammatory markers in the cerebellum. Loss of both *Ncoa7* and *Oxr1* has a more dramatic effect on inflammation than loss of either one on its own. Such exacerbation of a phenotype following disruption of a more than one evolutionary related gene has previously been reported. For example, mutations in ceroid-lipofuscinosis neuronal protein 1 and 5 (CLN1 and CLN5) genes are known to cause classic infantile NCL and late infantile variant NCL, respectively. Mouse models of both conditions display disease phenotype, and animals with double knockout are presented with more severe

pathology, including earlier seizures and motor deficit, accumulation of lipopigments and enhanced astrogliosis and microglia activation (Blom et al., 2013). CLN1 and CLN5 have been shown to interact with each other and share common binding partners – ER transmembrane protein CLN8 and F1 domain of mitochondrial ATPase, suggesting they are involved in similar molecular processes (Lyly et al., 2008, Lyly et al., 2009, Mukherjee et al., 2019). Similarly, Oxr1 and Ncoa7 share unique domain architecture and both have been shown to interact with Atp6v1b1, Prdx2 and Gpi1, suggesting they could be carrying out similar or overlapping functions (Finelli et al., 2018b, Merkulova et al., 2015, Svistunova et al., 2018). Importantly, Prdx2 is known to play a role in the inflammation. Glutathionylated Prdx2 has been shown to be secreted from macrophage cell line, primary human macrophages and peripheral blood mononuclear cells in response to LPS treatment and to induce tumor necrosis factor alpha (TNF-α) production in primary macrophages, suggesting it can act as a danger signal and immune response modulator (Salzano et al., 2014). Extracellular Prdx2 was later shown to promote microglia activation *in vitro* through TLR4 signaling pathway and induce secretion of pro-inflammatory interleukins IL-1β and IL-6 (Lu et al., 2018). As both proteins have been shown to interact with Prdx2 and to modulate its PTMs *in vitro* and/or *in vivo* (Chapter 3, Svistunova et al. (2018)), they could also play role in its glutathionylation and secretion and knockout of either *Oxr1* or *Ncoa7* would lead to deregulation in these mechanisms leading to neuroinflammation.

In *Oxr1*$^{d/d}$*/Ncoa7*$^{del/+}$ P22 cerebellum samples, I also observed slight but significant increase in *Ncoa7-B* levels, suggestive of inflammatory response. Interestingly, *Ncoa7-B* was not induced in *Oxr1*$^{d/d}$*/Ncoa7*$^{+/+}$ tissues, suggesting this transcriptional deregulation is not due to overall neuroinflammatory picture seen in the *Oxr1*$^{d/d}$ cerebellum, but rather specifically due to heterozygous *Ncoa7* locus deletion. Importantly, very little is known

about *Ncoa7-B* expression in the brain – RNA-Seq analysis has revealed its transcription in microglia, perycites and endothelial cells, but no data on its distribution in each brain region is available (Zhang et al., 2014b). Moreover, *Ncoa7-B* tissue- and cell type-specific expression analyses were performed in untreated cells, but nothing is known about cell types and brain structures where *Ncoa7-B* is induced upon inflammatory stimuli; attempts to generate a Ncoa7-B-specific antibody were unsuccessful. Therefore, we can only hypothesise the origin of *Ncoa7-B* increased mRNA signal; it is possible that *Ncoa7-B* is induced to compensate for heterozygous loss of *Ncoa7-B* coding region via auto-regulatory mechanism or due to deregulation of additional genes or pathways, not affected in $Oxr1^{d/d}/Ncoa7^{+/+}$.

5.3.5 Expression of both *Oxr1* and *Ncoa7-FL* is required for mouse embryo development

Oxr1 and *Ncoa7* are the most closely related genes in the TLDc family, and I have shown here that at least one copy of *Oxr1* is required for mouse embryo development and survival and my data suggest that expression of only one allele of Ncoa7-B on a Oxr1 knockout background is not sufficient for embryonic development. Indeed, based on my ChIP-Seq data analysis and GO processes prediction, Ncoa7-B is not functionally close to the full-length isoform or any of Oxr1 isoforms, suggesting it would not be able to functionally compensate for the absence of other transcripts. As no viable embryos are already observed at E7.5, the disruption in the developmental process is likely to occur at earlier stages. The implantation takes place at E4.5, and at E7.0 embryo already has formed three germinal layers. Thus, disruptions in blastocyst formation, implantation, placenta development or gastrulation could potentially lead to early embryo death.

Based on TFs that have been shown to bind their promoters, I have predicted that both Oxr1-FL and Ncoa7-FL, but not their short isoforms, are involved in blastocyst formation and growth processes. Moreover, Oxr1-FL, Ncoa7-FL and Ncoa7-B were predicted to play role in endoderm and mesoderm cell fate commitment, a later stage of embryo development. Based on H3K4me3 signal, both *Oxr1* and *Ncoa7* full-length isoforms, but not *Oxr1-C* or *Ncoa7-B*, are expressed in placental tissue, suggesting they might also be expressed in it at early stages. Importantly, as these two proteins are the only proteins in mouse proteome that possess a unique set of LysM, Gram and TLDc domains, disruption of both of them may potentially disrupt some aspects of blastulation, gastrulation or result in inability of the placenta to form properly. Other TLDc genes – *Tbc1d24* and *mEAK7* – are also expressed in placenta and have been predicted to be involved in endoderm and mesoderm development, but they may not be able to functionally compensate for *Oxr1* and *Ncoa7* knockout as they do not possess the same set of domains.

Interestingly, both Oxr1 and Ncoa7 have been shown to interact with v-ATPase kidney-specific subunit Atp6v1b1 in a recent study (Merkulova et al., 2015). The v-ATPase is a proton pump located in the membranes of vesicular organelles, such as endosomes and lysosomes, that maintains acidic luminal pH by pumping cytosolic H^+ inside the organelle (Maxson and Grinstein, 2014). Interestingly, mutations in v-ATPase subunits and accessory proteins are linked to neurodegeneration, cognitive impairment, cerebellar atrophy, parkinsonism and spasticity, linking v-ATPase complex function to neurological disorders (Colacurcio and Nixon, 2016, Dubos et al., 2015, Gupta et al., 2015, Korvatska et al., 2013). Functional v-ATPase has also been shown to be required for successful early embryonic development, with mutant embryos failing in development shortly after implantation due to defects in embryonic and extraembryonic tissues

development (Sun-Wada et al., 2000). V-ATPase complex stability and function is regulated by other proteins, and identification of Oxr1 and Ncoa7 as interactors of its subunit suggest they may also be implicated in these processes. Thus, it is possible that deletion of both genes results in deregulation of V-ATPase function and, subsequently, embryonic lethality.

Conclusion

Here, I have investigated the evolutionary conservation of TLDc genes' functions and regulation and have shown that family members are potentially regulated by similar sets of TFs and may be involved in closely related pathways and processes. I have also shown that loss of *Ncoa7* (all isoforms or *Ncoa7-FL* only) lead to subtle changes in *Oxr1*, *Tbc1d24* and *mEAK7* expression levels, and *Ncoa7* deletion does not cause aberrant glia activation. I also demonstrated the crucial role of both *Oxr1* and *Ncoa7* together for early embryonic development.

6. Final discussion

The aim of this work was to dissect the mechanisms of action of TLDc proteins, focusing in particular on the role of Oxr1 in protection against OS and maintenance of neuronal tissue homeostasis. Using an *Oxr1* knockout mouse model I analysed the effect of Oxr1 depletion on the transcriptional profile of the cerebellum *in vivo* and identified microglia activation and neuroinflammatory response as the major deregulated processes that occur prior to neurodegeneration. At a functional level, I have also shown that Oxr1 interacts with a key antioxidant enzyme Prdx2 and regulates its oligomeric state via the modulation of PTMs. Furthermore, I have also contributed to our understanding of the molecular function of TLDc proteins by identifying Oxr1 as a putative chaperone. Finally, I initiated the investigation of the functional overlap and genetic interactions between the TLDc proteins, demonstrating that mice lacking both *Oxr1* and *Ncoa7* are not viable and likely fail in the very early embryonic stages.

Since its discovery as OS protective gene, Oxr1 has been repeatedly shown to influence the expression of key antioxidant enzymes, such as Gpx1, Gpx2, HO-1, catalase, SOD1, SOD2, SOD3, PRDX4, possibly via p53 and JNK signaling pathways (Jaramillo-Gutierrez et al., 2010, Oliver et al., 2011, Yang et al., 2014, Yang et al., 2015), yet mechanistically, nothing is known regarding its direct involvement in the regulation of the OS response. In Chapter 3, I have shown that Oxr1 interacts with the multifunctional enzyme Prdx2 and regulates its PTMs in a brain region-specific manner. *Oxr1* disruption *in vivo* leads to deregulation of Prdx2 hyperoxidation and S-nitrosation, two inhibitory modifications that are known to disable its antioxidant activity and modulate chaperone assembly (Svistunova et al., 2018). Aberrant protein PTMs are observed in various NDDs; for example, tau hyper-phosphorylation is considered to precede its aggregation and neurofibrillary tangle formation, an increase in phospho-α-synuclein levels is observed in

PD and incorrect prion protein glycosylation patterns have been reported in prion diseases (Didonna and Benetti, 2015, Grimm et al., 2011, Simic et al., 2016). Interestingly, while a general increase in oxidative protein modifications, including that of PRDX2, is observed under OS conditions and in NDDs (Butterfield and Boyd-Kimball, 2018, Cesaratto et al., 2005, Collins et al., 2016, Grimm et al., 2011, Lee et al., 2008, Liu and O'Flaherty, 2017, van der Reest et al., 2018), in the OS-associated *Oxr1* knockout model, a specific increase in S-nitrosation and decrease in hyperoxidation of Prdx2 was observed (Finelli et al., 2016, Oliver et al., 2011, Svistunova et al., 2018). Moreover, Oxr1 overexpression led to opposite situation of an increase in hyperoxidised Prdx2 and a decrease in S-nitrosated Prdx2 levels; together, these data suggest that Prdx2 PTMs are regulated by Oxr1 directly and specifically, not as a consequence of cellular redox state (Svistunova et al., 2018). Thus, my data has revealed a novel link between Oxr1 and cellular antioxidant system, showing it is not only a potential upstream regulator of OS response, but also a fine regulator of a potent antioxidant enzyme and chaperone Prdx2. Thus, this may be an additional feature of Oxr1 protective properties in tandem with as-yet undiscovered mechanisms that directly or indirectly regulate the transcription of other antioxidants. Interestingly, other members of the OS response system have been identified among Oxr1 and TLDc binding partners in pull-down assays from the brain, thus in the future it would be interesting to investigate whether similar modulatory mechanisms occur.

In this thesis, I have also discovered that Oxr1-FL and Oxr1-C possess a potential holdase chaperone activity *in vitro* – a novel molecular function of the protein. This new finding potentially places Oxr1 as part of the well-established protein folding and proteostasis pathways (Balchin et al., 2016, Hipp et al., 2019). Proteostasis plays a crucial role in the maintenance of the CNS, with mutations in chaperones, co-chaperones and

autophagy pathway members being implicated in many disorders including adult neuronal ceroid lipofuscinosis, PD, ALS, cerebellar ataxia, spinocerebellar ataxia, Charcot Marie Tooth disease and autosomal recessive spastic ataxia of Charlevoix-Saguenay; furthermore, protein aggregates are core pathological features observed in AD, PD, ALS, prion diseases, HD and FTLD (Fujikake et al., 2018, Gorenberg and Chandra, 2017, Kumar et al., 2016, Levine and Kroemer, 2019, Zarouchlioti et al., 2018). Discovery of Oxr1 holdase activity could potentially explain previous data in which Oxr1 was shown to reduce the aggregation of FUS and TDP-43 *in vitro* (Finelli et al., 2015). In these *in vitro* experiments, Oxr1-C overexpression in cells was shown to reduce the mislocalisation and aggregation of ALS-associated mutant FUS and TDP-43 through an unknown mechanism, independent of proteasome degradation or autophagy (Finelli et al., 2015). Importantly, it was shown that preservation of Oxr1:FUS or Oxr1:TDP-43 interaction is essential for this apparent anti-aggregation activity, as some of the studied disease-causing mutations disrupted the interaction with Oxr1-C (e.g. A321G) alongside an inability to rescue the aggregation, whereas for other mutations (e.g. M337V), the binding and subsequent prevention of aggregation was preserved (Finelli et al., 2015). The ability of Oxr1 to prevent mutant TDP-43 aggregate formation was recently confirmed in mice expressing a single copy of a human TDP-43^{M337V} bacterial artificial chromosome construct in addition to an Oxr1-FL transgene under control of a neuronal (Prnp) promoter (Gordon et al., 2019, Williamson et al., 2019). Cultured motor neurons from TDP-43$^{M337V/-}$ animals displayed aberrant cytoplasmic localisation of the mutant TDP-43 protein, while cells from double transgenic TDP-43$^{M337V/-}$/Oxr1$^{Prnp/-}$ mice had significantly reduced proportion of cytoplasmic TDP-43 (Williamson et al., 2019). The molecular mechanisms involved are currently under investigation.

Although chaperones are often non-specific in their mode of action, in certain cases a lack of binding to a specific target protein leads to misfolding and aggregation (Bose and Chakrabarti, 2017, Choudhury and Bhattacharyya, 2015, Koide et al., 2002). For example, mutations in HSP47 have been identified in patients with osteogenesis imperfecta type X that is caused by aggregation and misfolding of collagen molecules (Ito and Nagata, 2017, Marini et al., 2014). Significantly, HSP47 is a collagen-specific chaperone, and mutations in an HSP47-binding site significantly weaken this interaction, resulting in pathogenic aggregates of collagen (Widmer et al., 2012). Thus, the inability of Oxr1-C to reduce the aggregation of these specific TDP-43 and FUS mutants could be due to disruption of a related chaperone recognition mechanism. Similarly, ALS-associated mutation in FUS have been shown to severely weaken the binding with chaperone protein transportin (TNPO1), thus leading to stress granule accumulation of mutant FUS (Hofweber et al., 2018). Interestingly, Fus was identified as a binding partner of both Oxr1 isoforms, while Tdp-43 only interacted with Oxr1-C (Finelli et al., 2015), suggesting different interactors between two isoforms or presence of another Fus-related function in Oxr1-FL (Finelli et al., 2015). These data suggest that Oxr1 may act as TDP-43- and FUS-specific chaperone, making it an attractive therapeutic target for TDP-43 and FUS proteinopathies.

In this thesis I focused on holdase activity of Oxr1, however, further work is required to investigate whether it also acts as a foldase and actively folds client proteins, or possesses disaggregase activity, facilitating the disassembly of preformed aggregates. Foldase chaperone activity can be tested both *in vitro* using recombinant proteins and in cells utilising luciferase-based assay (Walther and Maddalo, 2012). The remaining time in the laboratory did not allow completion of such assay, however I began to set-up a cell-based chaperone activity assay that allows assessing both foldase and holdase activities of the protein of interest *in vitro*. Briefly, the assay is based on the ability of exogenously

expressed chaperones to prevent heat-induced denaturation and promote refolding of the luciferase following the treatment. The activity of putative chaperones can be monitored as a decrease and subsequent increase in luciferase activity after treatment and recovery, respectively; to prevent the protection of luciferase by endogenous chaperones expressed following the heat-shock, cells are treated with cycloheximide, a protein synthesis inhibitor. Disaggregase activity of the protein can be assayed by incubating pre-aggregated substrates, such as GFP or luciferase, with a protein of interest and monitored by measuring fluorescence or luminescence of recovered proteins, respectively. Moreover, my experiments have also shown absence of holdase activity in TBC1D24; analysis of remaining family members, especially the closely related Ncoa7, would aid our understanding of functional conservation of the TLDc protein family and their role in cellular homeostasis.

The ability to regulate protein aggregation and to modulate activity of a potent antioxidant enzyme suggests that Oxr1 is a potentially important player of the neurodegeneration process. Interestingly, the *Oxr1*$^{d/d}$ mouse displays selective loss of CGCs, a type of neurons that has been shown to be especially sensitive to oxidative insults (Oliver et al., 2011, Wang et al., 2009, Wang and Michaelis, 2010). It has been proposed that such selective vulnerability is due to elevated endogenous ROS levels, deficient DNA damage repair, Ca^{2+} signaling dysfunction and lower level of ATP as compared to less-vulnerable neuronal sub-types such as cerebral cortical neurons or A10 dopaminergic neurons (Michaelis, 2012, Narciso et al., 2016, Wang et al., 2009, Wang and Michaelis, 2010). Thus, deletion of *Oxr1* in CGCs could lead to detrimental increase in ROS levels, while in less-sensitive neurons, OS will still be within the range that can be tolerated. It is particularly interesting that the CA3 sub-field of the hippocampus displays the highest level of *Oxr1* expression in the mouse brain (Chapter 1, Fig. 1.3) given that this region is

known to be more resistant to degeneration in conditions such as AD and in cerebral ischemia as compared to the CA1 sub-field (Michaelis, 2012, Oliver et al., 2011, Yin et al., 2017). As such, endogenous Oxr1 levels may confer some specific OS-associated protection in specific regions of the hippocampus. Moreover, as discussed in Chapter 5, functional compensation by Ncoa7 or other TLDc proteins may play an important role in the *Oxr1*$^{d/d}$ model. Future work to investigate this vulnerability using conditional deletion of *Oxr1* in motor neurons (ChAT-cre driven) and in substantia nigra pars compacta neurons (DAT-cre driven) is underway.

I demonstrated that loss of *Oxr1* results in a selective increase in inactivated SNO-Prdx2 levels in the cerebellum, suggesting cells in this region are likely exposed to even higher levels of ROS as compared to wild-type as a result of enzyme inactivation. Interestingly, we do not observe cell death of other neurons in the *Oxr1*$^{d/d}$ mouse brain at the end stage of the disease, suggesting CGCs are particularly dependent on Oxr1 function. Interestingly, a protein binding partner screen has also identified ER membrane protein complex subunit 3 (Emc3) as an interactor of Oxr1-FL (unpublished data). Emc3 is a subunit of the Emc transmembrane protein complex that has been shown to tether the ER to the mitochondrial outer membrane (Chitwood et al., 2018, Guna et al., 2018, Lahiri et al., 2014, Shurtleff et al., 2018). Emc3 itself has been shown to interact with ER-associated degradation (ERAD) pathway members, a mechanism for clearance of misfolded proteins in the ER (Christianson et al., 2011). Stress conditions and disturbance of cellular homeostasis can promote accumulation of unfolded and misfolded proteins within ER lumen, leading to activation of the UPR - upon accumulation of misfolded proteins, an ER chaperone HSPA5 dissociates from regulatory proteins that translocate from the ER membrane and induce transcription of stress response genes while suppressing global protein synthesis (Cai et al., 2016). In yeast, loss of Emc has been reported to result in

accumulation of misfolded membrane proteins and induction of UPR (Jonikas et al., 2009). Signs of UPR have been observed in AD, PD, ALS, HD and prion disease, suggesting it is a common feature of NDDs (Hetz and Saxena, 2017). Importantly, depending on severity of ER stress and levels of protein aggregation, UPR may either lead to clearance of misfolded protein species and restoration of cellular homeostasis, or to apoptosis (Iurlaro and Munoz-Pinedo, 2016).

Interestingly, CGCs are especially vulnerable to ER stress as they display insufficient induction of the UPR pathway members as compared to less vulnerable cortical neurons (Sun et al., 2013). Moreover, mutation in chloride channel CLIC-like 1 (Clcc1), an ER-localised transmembrane ion channel, leads to ER stress and loss of exclusively CGCs without affecting other neurons in mice, and results in induction of UPR *in vitro* (Jia et al., 2015). A putative Oxr1:Emc3 interaction may be important for its ERAD-related function, and loss of *Oxr1* could disrupt already diminished response to accumulation of misfolded proteins within ER lumen, leading to CGCs death. ER stress is also linked to autophagy induction – as well as regulating expression of chaperones and decreasing overall protein production levels, UPR also leads to increased expression of autophagy-related genes, including Beclin-1 and autophagy related (ATG) genes, and inhibition of mTORC1 (Cai et al., 2016, Rashid et al., 2015). Autophagy stimulation promotes clearance of misfolded proteins via sequestration of ER portions into autophagosomes (Cai et al., 2016, Smith and Wilkinson, 2017). In agreement with the idea that Oxr1 is involved in UPR, I have shown in Chapter 4 that the loss of *Oxr1* leads to a pre-symptomatic increase in LC3-II levels in both the cerebrum and cerebellum, suggestive of autophagy induction. Immunostaining of pre-symptomatic *Oxr1*$^{d/d}$ brain sections for markers of UPR and ER stress, such as Hsp60, Hsp90, inositol-requiring enzyme 1 (Ire1), phosphorylated eIF2, alternatively spliced X-box-binding protein 1 (Xbp1), phosphorylated JNK and PKR-like

ER kinase (PERK)-dissociated glucose-regulated protein 78 (Grp78), would reveal if *Oxr1* knockout indeed disrupts cellular response to ER stress. Analysis of levels of these markers and cell death in cells lacking or overexpressing *Oxr1* treated with ER stress inducer, such as tunicamycin or thapsigargin, could confirm the role of Oxr1 in UPR and ER stress pathways. Interestingly, the microarray analysis of pre-symptomatic *Oxr1*$^{d/d}$ cerebellum did not reveal differential expression of these markers, suggesting Oxr1 depletion could lead to a failure in ER stress and UPR pathways, further diminishing insufficient induction of these networks in CGCs. Importantly, ER stress and UPR are flagged by specific PTMs, such as eIF2 and LAMP2A phosphorylation or by re-localisation of proteins from ER to the nucleus or the cytoplasm, therefore, an alternative strategy would be required to detect these changes.

Transcriptomic analysis of *Oxr1*$^{d/d}$ mouse cerebellum has revealed aberrant expression of microglia activation-related genes, in-line with an induction of the neuroinflammatory response. Importantly, RNA from whole cerebellar tissue was used for the microarray analysis, although Oxr1 expression levels are known to vary significantly between cell types and only approximately 25% of microglia cells have been shown to express Oxr1 (Chapter 4, Table 4.3). The range of differentially expressed genes identified in *Oxr1*$^{d/d}$ cerebellum somewhat surprisingly significantly overlaps with the genes deregulated in mouse models of LSDs, such as NPC, nGD and MPS VII (Dasgupta et al., 2015, Liao et al., 2010, Lopez et al., 2012, Parente et al., 2012). These include lysosomal enzymes *Ctss*, *Ctsd*, *Ctsz*, *HexB*, complement pathway members *C1qa*, *b* and *c*, microglia marker *Cd68* amongst others. Importantly, in these LSD model transcriptomic experiments, the mutants are generally characterized by a significantly greater number of differential gene expression profile changes than the *Oxr1*$^{d/d}$ microarray data, and include additional lysosomal-specific DE genes such as transmembrane glycoprotein

NMB, lysozyme 1 and 2 and membrane-spanning 4-domain subfamily A members 4 and 6D (Dasgupta et al., 2015, Liao et al., 2010, Lopez et al., 2012, Parente et al., 2012). This suggests that neuroinflammation in *Oxr1*$^{d/d}$ pre-symptomatic mouse brain potentially differs from the cause of the neuroinflammatory response observed in other NDD models and conditions. Interestingly, computational analysis of TFs regulating expression of TLDc genes and isoforms performed in Chapter 5 revealed binding of INF-response regulating factors from Stat (Signal transducer and activator of transcription) and Irf (Interferon regulatory factor) families to promoter regions of all TLDc family members in various types of immune cells, suggesting their role in inflammatory response process (Supplementary Table 1). Indeed, previously published studies report INF- and LPS-induced up-regulation of *Ncoa7-B in vitro* and *in vivo* and its involvement in the inhibition of endosome-mediated viral entry (Doyle et al., 2018, Goujon et al., 2013, Yu et al., 2015). Consistent with these data, Interferome database reports highly significant Ncoa7-B induction upon INF stimuli as well as differential expression of *Tbc1d24* and *mEAK7* in INF-treated conditions and approximately 2-fold down-regulation of Oxr1-C in response to INFγ treatment *in vitro* (Rusinova et al., 2013). In addition to its well-known roles in inflammatory response to pathogens and antiviral response, the cytokine INFγ is known to be involved in neuronal differentiation and in cerebellar external granule neuron layer development, and to induce microglia and astroglia activation, leading to neurodegeneration (Barcia et al., 2011, Kak et al., 2018, Kang et al., 2018, Monteiro et al., 2017, Rock et al., 2005, Wang et al., 2004). Oxr1-C is normally expressed in the mouse brain at high levels (Oliver et al., 2011), and its down-regulation following INFγ induction could be a step in the immune response mechanism, possibly an upstream regulator of other molecules or processes – lowering Oxr1 levels could, for example, enable aberrant translocation or PTMs of its downstream targets. Thus, loss of *Oxr1* in resident immune

cells in the brain may trigger its downstream targets, leading to reactive microglia phenotype and cell death. Similar mechanism is observed in cancer cells, where epigenetic silencing of negative signaling regulators results in constitutive activation of downstream signaling (Ying and Tao, 2009). Similarly, in yeast, transposon insertion in a negative regulator of amino acid sensing-induced transcription results in constitutive signaling and target gene expression (Eckert-Boulet et al., 2006). Thus, based on my results and possible links between Oxr1 and ER stress, together with known sensitivity and vulnerability of CGCs, I propose a mechanism of neurodegeneration in *Oxr1*$^{d/d}$ mouse brain whereby microglia activation and CGCs death are partially independent from one another. To begin to investigate this further, it would be interesting to generate a microglial-specific conditional deletion of *Oxr1* (e.g. using *Cx3cr1*^{Cre}) to determine whether losing even the small proportion of *Oxr1* that is present in these cells would be detrimental to neuronal survival.

Although the exact role of Oxr1 in the organism is not well understood, it is now emerging as a multifunctional protein involved in a variety of aspects of cellular homeostasis, including glucose metabolism via an interaction with Gpi1 and OS protection and proteostasis through binding to Prdx2. Moreover, a previous work from our group has shown that neuronal Oxr1 overexpression is protective in two mouse models of ALS, and a recent publication reported that Oxr1 overexpression is protective in a mouse model of PD (Jiang et al., 2019, Liu et al., 2015, Williamson et al., 2019). Together, these properties of Oxr1 make it an attractive therapeutic target for a spectrum of NDDs. Pharmacological regulation of antioxidant system activity and expression has been previously investigated as potential therapies of various neurodegenerative conditions. For example, induction of antioxidant gene expression via Nrf2 signaling modulation was tested in cell and mouse models of PD and AD, providing promising data suggestive of OS

suppression, increased HO-1 and NQO1 expression and reduction in Aβ levels (Lee et al., 2018, Tian et al., 2019, Yu et al., 2019). Recently, oral administration of antioxidants N-acetylcysteine amide and vitamin E was reported to reduce seizure-like activity in *Drosophila* expressing ROS-hypersensitive mutant TBC1D24^{G501R} (Lüthy et al., 2019). Furthermore, pharmacological modulation of the proteostasis system has also been studied as a possible therapeutic approach to AD and PD treatment. A number of molecules have been shown to induce the cellular chaperome *in vitro* and *in vivo* via inhibition of Hsp90, a protein that binds and blocks activity of HSF1 TF, thus promoting Hsp genes expression, or via direct induction of specific chaperone expression or activity (Campanella et al., 2018, Dimant et al., 2012, Friesen et al., 2017). Involvement of Oxr1 in both proteostasis and the OS response pathways makes it an ideal candidate for pharmacological targeting as it would allow acting on distinct protective pathways simultaneously.

An unpublished study from our group has established an experimental set-up for high-throughput screening of small molecules capable of regulating Oxr1-C promoter activity; one promising compound that up-regulated the reporter gene expression has already been identified (Dr Matthew Williamson, unpublished data). As a note of caution, the unknown functions of OXR1, in particular outside of the CNS, suggest a mechanism to deliver the pharmacological compound to the organ of interest may be required, avoiding off-target effects in the other parts of the organism. Yet, driving Oxr1 expression in the mouse using a ubiquitous promoter (as a rescue experiment in the original *bella Oxr1* knockout study) does not lead to any documented adverse effects, suggesting that exogenous Oxr1 is tolerated and safe *in vivo*.

Although extensive research is ongoing to unravel the functions of TLDc proteins, very little is known regarding their normal role in biology. The computational analysis I

performed in Chapter 5 has predicted their involvement in processes in various organs and some degree of functional conservation between family members, suggesting they are widely involved in similar or overlapping processes throughout the organism. ChIP-Seq data analysis and prediction of relevant cellular processes suggest strong involvement of TLDc genes in the CNS development. In agreement with this, patients with mutations in TLDc genes are presented with related neurodevelopmental disorders - heterozygous disruption of the OXR1-C isoform was reported in a family with specific language impairment, while homozygous loss of NCOA7-FL was very recently identified in a family with autism spectrum disorder (Chen et al., 2017, Doan et al., 2019, Leyfer et al., 2008). Moreover, disruption of Tbc1d24 expression by *in utero* electroporation led to aberrant neuronal migration and dendritic arborisation in rats (Falace et al., 2014). In agreement with this, mutations in *TBC1D24* are associated with a spectrum of neurological conditions, including mental retardation, deafness and various types of epilepsy – conditions considered to be of a neurodevelopmental nature in some cases (Balestrini et al., 2016, Bozzi et al., 2012, Fernandes et al., 2014, Finelli et al., 2018a, Fischer et al., 2016, Mucha et al., 2017). This confirms that the computational prediction of gene functions can be used as a guidance for the direction of future investigations.

For example, in this work, expression of *Oxr1*, *Tbc1d24* and *Kiaa1609* genes was predicted to be regulated by Circadian locomotor output cycles kaput (Clock) TF, a core circadian cycle regulator, in brown preadipocytes and liver, suggesting it may also regulate their expression outside of these organs (van den Berg et al., 2018, Tahara and Shibata, 2016). Importantly, circadian oscillations in redox status of peroxiredoxins are now believed to be central component of non-transcriptional circadian clock in distant kingdoms of life (Edgar et al., 2012), and the discovered role of Oxr1 in the regulation of Prdx2-$SO_{2/3}$ levels and its possible circadian rhythm-dependent expression suggest it

might be involved as an up- or downstream player of Prdx circadian signaling. It is therefore interesting that the expression of Oxr1 in the suprachiasmatic nucleus of the hypothalamus is cyclic in mice, peaking at the boundary of light and dark under a 12-hour light-dark cycle (Pembroke et al., 2015). Analysis of *Oxr1* expression oscillations in various organs and possible perturbations in Prdx2-$SO_{2/3}$ circadian rhythms in *Oxr1*$^{d/d}$ tissues could reveal if TLDc genes are involved in this fundamental biological mechanism. Another future research direction suggested by computational analysis is investigation of the role of TLDc genes in hematopoiesis and immune cell maturation. All genes were found to be regulated by hematopoiesis-specific TFs in both lymphoid and myeloid branches, and in the embryonic liver *Oxr1*, *Ncoa7* and *Tbc1d24* promoters interact with the Core-binding subunit beta (Cbfb) TF – a part of the regulatory complex that controls the emergence of hematopoietic stem cells from endothelial cells (Link et al., 2010). Endothelial cells of mouse fetal liver are known to be a site of hematopoiesis, and these data suggest that TLDc genes may be involved in this process (Khan et al., 2016).

Despite the presence of a shared protein domain, TLDc mutations lead to a wide range of phenotypes in human clinical studies and experimental systems, suggesting many as-yet undiscovered differences in cell type-specific expression, intracellular localisation, protein binding partners or PTMs that define specific functional roles in each brain region. Of note, more detail regarding the sub-cellular localization of each TLDc protein is needed; these studies have been hampered by a lack of reliable reagents for immunocyto- and immunohistochemistry. Indeed, genetic disruption of either *Oxr1* or *Ncoa7*, the two most closely-related TLDc family members, leads to contrasting phenotypes in mice, and it has been reported that mice lacking *Tbc1d24* are not viable after birth yet develop to E18.5 (Tona et al., 2019). Computational transcriptional analysis carried out in this thesis provided us with preliminary data on possible functions of the TLDc family members as

well as suggested future research directions – not only to investigate the significance of their expression outside of the CNS, but also possibility to utilise these potent OS protective genes in treatment of non-neurological disorders, such as autoimmune diseases or infections.

In conclusion, the work in this thesis has provided a several novel contributions to TLDc protein biology; the results provide novel links between TLDc proteins and OS protection machinery, thus advancing our understanding of the mechanisms of TLDc protective activity. Identification of the first molecular function of Oxr1 as a putative chaperone shed light on its possible role in NDD and protective function in ALS models, and analysis of TLDc family functional conservation opened promising lines of future research in this field.

Appendix 1

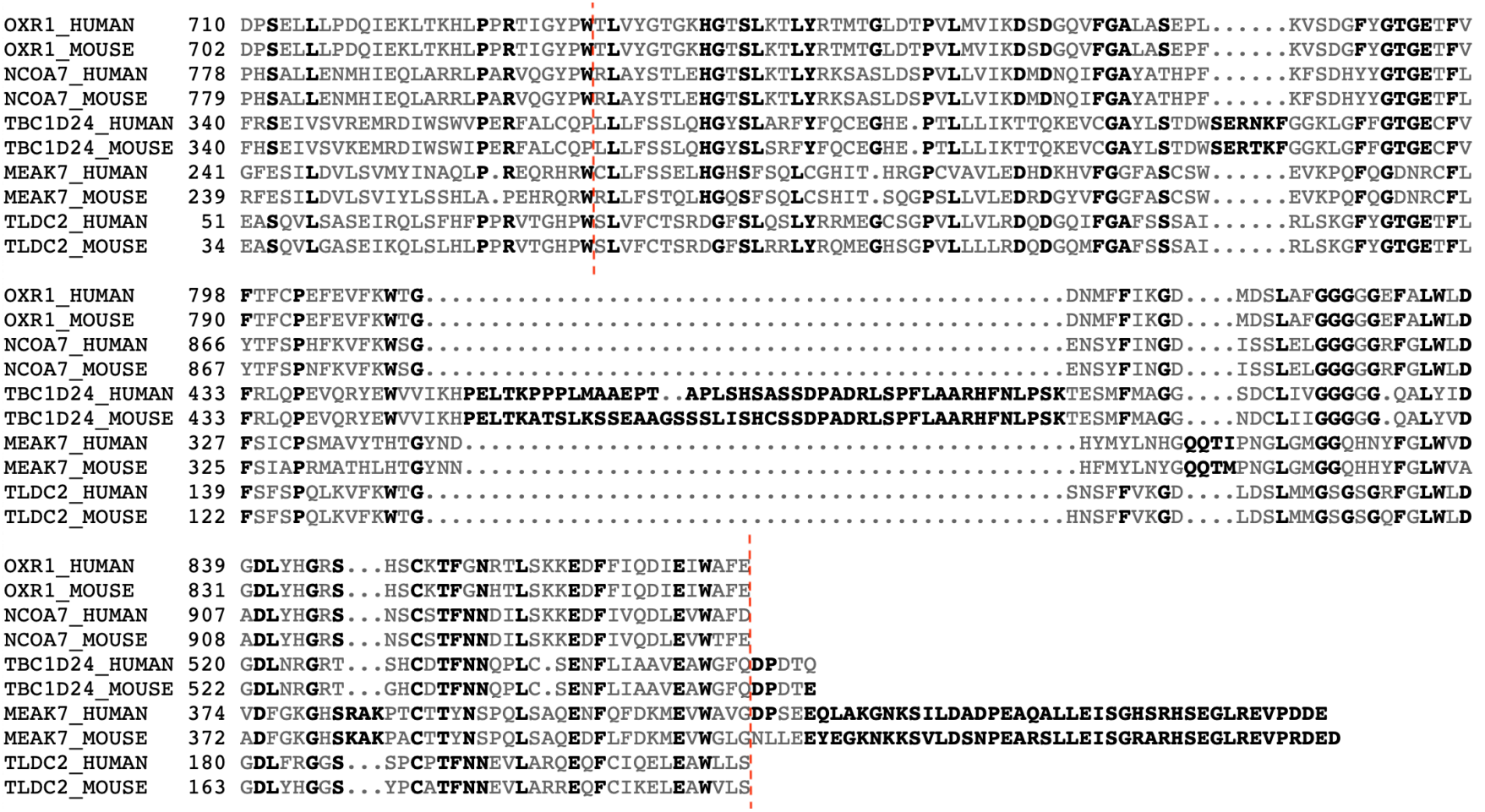


Figure S1. Alignment of protein sequences of TLDc domains of family members from mouse and human. Borders of the TLDc domain are marked by vertical red lines. Sequences were aligned using Clustal Omega program and visualized using Aligment Annotator (www.bioinformatics.org/strap/aa/)

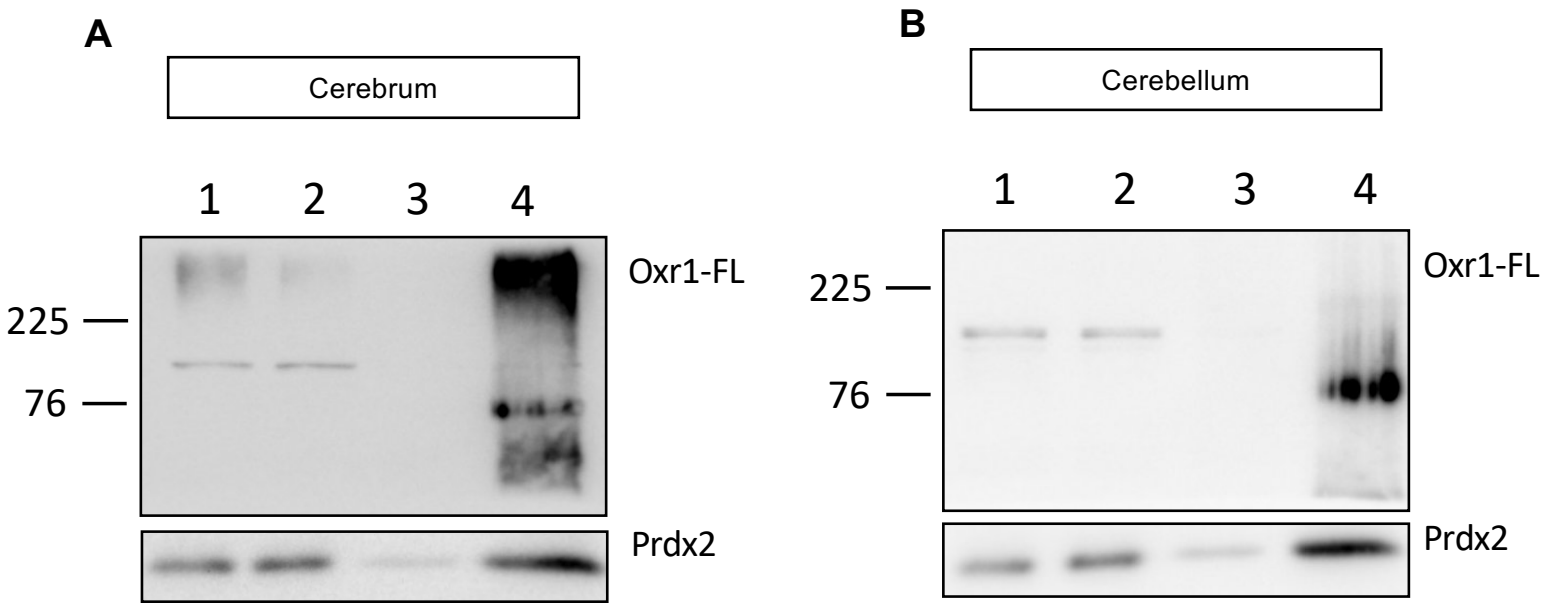


Figure S2. Oxr1:Prdx2 co-immunoprecipitation from cerebrum and cerebellum tissues. (A) Uncropped western blot of co-immunoprecipitation of Oxr1 and Prdx2 from cerebrum. Lanes 1,2 – input, lane 3 – IgG control, lane 4 – anti-Prdx2 IP. (B) Uncropped western blot of co-immunoprecipitation of Oxr1 and Prdx2 from cerebellum. Lanes 1,2 – input, lane 3 – IgG control, lane 4 – anti-Prdx2 IP.

Appendix 2

Table S1. Transcription factors and other DNA-binding proteins known to bind TLDc promoter regions.
ChIP-Seq data was accessed at ChIP-Atlas and TFs that were found at TLDc promoter regions (-750 and +250 from TSS) were included.

Oxr1-FL-P1	Oxr1-FL-P2	Oxr1-C	Ncoa7-FL	Ncoa7-B	Tbc1d24	mEAK7	C20Orf118
Adipose tissue							
Brown adipocytes: Hdac3, Nr1d1, Pparg, Prdm16 **Brown preadipocytes:** Brd4, Clock, Creb1, Ep300, Kmt2d **White adipocytes:** Nr3c1	**Brown adipocytes:** Cebpb, Pparg, **Brown preadipocytes:** Brd4, Creb1, Crebbp, Ebf2, Ep300, Kmt2d **Preadipocytes:** Brd4	**Brown adipocytes:** Hdac3, Nr1d1, Pparg, Prdm16 **Brown preadipocytes:** Brd4, Cebpa, Clock, Creb1, Crebbp, Kmt2d **White adipocytes:** Nr3c1, Pparg	**Brown adipocytes:** Cebpb, Nfia, Prdm16 **Brown preadipocytes:** Brd4, Cebpb, Creb1, Ep300, Kmt2d **Preadipocytes:** Brd4 **White adipocytes:** Nr3c1	**Brown adipocytes:** Hdac3 **White adipocytes:** Nr3c1	**Brown adipocytes:** Prdm16 **Brown preadipocytes:** Brd4, Creb1, Crebbp, Ebf2, Ep300, Kmt2d **White adipocytes:** Nr3c1	**Brown adipocytes:** Ebf2, Esrra, Hdac2, Hdac3, Nr1d1, Prdm16 **Brown preadipocytes:** Brd4, Cebpa, Clock, Creb1, Crebbp, Ebf2, Kmt2d. Ncor1 **White adipocytes:** Nr1d1, Nr3c1	
Blood and immune system							
Bone marrow cells: Asxl1, Ctcf, Gfi1, Spi1 **Bone marrow stromal cells:** Ctcf, Runx2 **Hematopoietic stem cells:** Cbx8, Spi1	**Plasmablast:** Irf4 **Pro-B cells:** Ebf1, Ets1, Irf4, Med1, Phf6, Tcf3 **B-lymphocytes:** Chd4, Ets1, Hdac1, Hdac2, Irf4, Kmt2a, Myc, Nipbl, Rad21, Rag2,	**Bone marrow cells:** Spi1 **Hematopoietic stem cells:** Spi1 **Myeloid cells:** Spi1 **Macrophages:** Cebpb, Creb1, Elf1, Elf4, Jun, Jund, Rela, Smarca4,	**Bone marrow cells:** Asxl1, Gfi1, Spi1 **Bone marrow stromal cells:** Ctcf, Runx2 **Hematopoietic stem cells:** Cbx8, Spi1 **Myeloid cells:** Spi1	**Bone marrow cells:** Gfi1 **Hematopoietic stem cells:** Spi1 **Myeloid cells:** Spi1 **Macrophages:** Brd4, Creb1, Elf4, Fli1, Irf1, Irf8, Junb, Rad21, Rela,	**Bone marrow stromal cells:** Runx2 **Hematopoietic stem cells:** Cbx8 **Macrophages:** Cebpb, Creb1, Elf4, Hes1, Jun, Jund, Myc, Nelfe, Rela,	**Bone marrow cells:** Asxl1, Ctcf **Bone marrow stromal cells:** Ctcf, Runx2 **Hematopoietic stem cells:** Cbx7, Spi1 **Myeloid cells:** Irf7, Spi1	

Macrophages: Atf3, Cebpb, Elf1, Elf4, Fli1, Fos, Gabpa, Hes1, Irf1, Jun, Mafb, Myc, Nr1h3, Rela, Runx1, Smarca4, Spi1, Srebf1, Stat1, Stat6, Usf2 **Pro-B cells:** Bach2, Ctcf, Irf4, Lmo2, Med1, Tcf3 **B-lymphocytes:** Chd4, Ctcf, Hdac1, Hdac2, Kmt2a, Nipbl, Rad21, Rag2, Smarca4 **Mast cells:** Erg, Fli1, Fos, Gata2, Lmo2, Mitf, Runx1, Spi1 **Megakaryocytes:** Fli1 **Thymus:** Bcl11b, Ctcf, Satb1 **Thymocytes:** Bcl11b, Cbfb, Rag2, Satb1 **T-lymphocytes:** Nipbl, Stat5a **CD4+ T-lymphocytes:** Men1, Stat1, Stat3, Tbx21	Smarca4, Supt5, Tcf3, Wdr5 **Mast cells:** Erg, Fli1, Lmo2, Runx1, Spi1 **Dendritic cells:** Irf1 **Erythroid cells:** Rad21 **Thymus:** Bcl11b, Ctcf **Thymocytes:** Bcl11b, Cbfb, Rag1, Rag2 **T-lymphocytes:** Brd2, Rela **CD4+ T-lymphocytes:** Bcl11b, Egr2, Ezh2, Men1, Pou2f1, Stat1, Stat2, Stat3, Tbx21 **Th1:** Ep300, Stat3, Tbx21 **Th17:** Irf4, Jund, Stat1 **CD4- CD8- cells:** Bcl11b, Ikzf1, Mta2, Runx1 **CD4+ CD8+ cells:** Nipbl **NK T-cells:** Runx1 **Germinal center:** Tfap4	Spi1, Srebf1, Stat1, Usf2 **Pro-B cells:** Irf4, Spi1, Tead1 **B-lymphocytes:** Ctcf, Hdac1, Hdac2, Ikzf1, Kat2a, Kmt2a, Myc, Nipbl, Paxip1, Rad21, Rag2, Runx1, Wdr5 **Mast cells:** Runx1 **Dendritic cells:** Cebpb **Megakaryocytes:** Fli1 **Thymus:** Bcl11b, Ikzf1, Satb1 **Thymocytes:** Bcl11b, Cbfb, Rag1, Rag2, Satb1 **CD4+ T-lymphocytes:** Bach2, Men1, Pou2f1 **Th1:** Ep300, Stat5a **Th17:** Jund **CD4- CD8- cells:** Bcl11b, Chd4, Ikzf1, Mta2, Runx1 **CD4+ CD8+ cells:** Gtf2b, Tcf3 **CD25+ cells:** Spi1 **NK T-cells:** Runx1	**Macrophages:** Atf3, Cebpa, Cebpb, Creb1, Elf1, Elf4, Fli1, Hes1, Jun, Jund, Nelfe, Rela, Rxra, Spi1, Srebf1, Stat1, Usf2 **Plasmablast:** Irf4, Spi1 **Pro-B cells:** Ets1, Ikzf1, Irf4, Phf6, Tcf3 **B-lymphocytes:** Chd4, Ets1, Hdac1, Hdac2, Ikzf1, Kmt2a, Myc, Nipbl, Rad21, Rag2, Smarca4, Supt5, Tcf3, Wdr5 **Mast cells:** Erg, Fli1, Gata2, Lmo2, Runx1, Spi1, Tal1 **Dendritic cells:** Cebpb, Spi1 **Erythroid cells:** Rad21 **Granulocytes:** Kdm1a **Erythroblasts:** Brd2 **Thymus:** Bcl11b **Thymocytes:** Bcl11b, Cbfb, Rag1, Rag2 **T-lymphocytes:** Brd2, Nipbl, Rela, Smc3 **CD4+ T-lymphocytes:**	Smarca4, Spi1, Srebf1, Srf, Stat1, Stat2, Usf2 **Plasmablast:** Prdm1 **Pro-B cells:** Irf4, Tcf3 **B-lymphocytes:** Hdac2, Kmt2a, Nipbl, Rad21, Smarca4 **Dendritic cells:** Batf3, Irf8, Spi1 **Megakaryocytes:** Fli1 **Mast cells:** Runx1 **Thymus:** Bcl11b, Ikzf1 **Thymocytes:** Bcl11b, Cbfb, Rag2, Satb1 **CD4+ T-lymphocytes:** Pou2f1, Stat1, Stat2, Stat3 **Th1:** Ep300, Stat3, Stat5a, Tbx21 **Th17:** Batf, Irf4, Jund **CD8+ T-lymphocytes:** Ep300 **CD4- CD8- cells:** Bcl11b, Chd4, Ikzf1, Mta2, Runx1, Spi1, Suz12	Runx1, Spi1, Srebf1, Usf2 **Pro-B cells:** Bach2, Ctcf, Ebf1, Irf4 **B-lymphocytes:** Bhlhe41, Chd4, Ctcf, Hdac1, Hdac2, Ikzf1, Myc, Nipbl, Rad21, Rag2, Smarca4, Supt5 **Mast cells:** Ctcf, Erg, Fli1, Gata2, Runx1 **Erythroblasts:** Gata1 **Erythroid cells:** Rad21 **Ter119 erythrocytes:** Ctcf **Thymus:** Bcl11b **Thymocytes:** Bcl11b, Cbfb, Rag2, **T-lymphocytes:** Brd2 **CD4+ T-lymphocytes:** Bhlhe40, Egr2, Gata3, Men1, Pou2af1, Pou2f1, Stat2 **Th1:** Ctcf, Stat6 **Th17:** Ctcf **CD8+ T-lymphocytes:** Tfap4	**Macrophages:** Cebpb, Creb1, Elf4, Fli1, Gabpa, Jund, Nelfe, Nr1h3, Rad21, Rela, Runx1, Rxra, Smarca4, Spi1, Srebf1, Stat1, Usf2 **Plasmablast:** Ctcf, Irf4, Spi1 **Pro-B cells:** Chd4, Ctcf, Ebf1, Ikzf1, Irf4, Smarca4, Spi1, Tcf3, Tead1 **B-lymphocytes:** Chd4, Ctcf, Ets1, Hdac1, Hdac2, Ikzf1, Kat2a, Kmt2a, Myc, Nipbl, Paxip1, Rad21, Rag2, Smarca4, Smc1a, Smc3, Supt5, Wdr5 **Mast cells:** Ctcf, Erg, Fli1, Lmo2, Runx1, Spi1 **Megakaryocytes:** Fli1 **Dendritic cells:** Ctcf, Spi1 **Erythroblasts:** Brd2 **Erythroid cells:** Rad21 **Granulocytes:** Kdm1a **Thymus:** Bcl11b, Satb1	

Th0: Ctcf **Th1:** Brd4, Ctcf, Ep300, Rela, Smarca4, Stat3, Stat4, Stat5a, Tbx21 **Th17:** Ctcf, Ep300, Irf4, Jund, Stat1, Stat3, Suz12, Trim33 **CD4- CD8- cells:** Bcl11b, Ctcf, Ikzf1, Mta2, Runx1, Spi1, Suz12 **CD4+ CD8+ cells:** Ctcf, Nipbl, Smc1a **NK T-cells:** Ep300, Runx1, Runx3, Stat1, Stat5a **Spleen:** Bach2			Bcl11b, Egr2, Men1, Stat1, Stat2, Stat3, Stat5b **Th0:** Irf4 **Th1:** Ep300, Stat3, Stat5a, Tbx21 **Th2:** Batf3, Irf4, Men1 **Th9:** Stat6 **Th17:** Brd2, Ep300, Jund, Trim33 **CD8+ T-lymphocytes:** Tfap4 **CD25+ cells:** Spi1 **CD4+ CD8+ cells:** Nipbl, Smc1a **CD4- CD8- cells:** Bcl11b, Mta2, Runx1, Spi1 **NK T-cells:** Runx1, Runx3, Stat1, Stat5a **Germinal center:** Tfap4 **Spleen:** Bach2	**CD4+ CD8+ cells:** Ikzf1 **CD25+ cells:** Spi1	**NK T-cells:** Runx1, Runx3 **CD4- CD8- cells:** Bcl11b, Chd4, Ikzf1, Mta2, Runx1, Suz12 **CD4+ CD8+ cells:** Nipbl	**Thymocytes:** Bcl11b, Cbfb, Rag2, Satb1 **T-lymphocytes:** Brd2, Ctcf, Smc3 **CD4+ T-lymphocytes:** Egr2, Elf1, Men1, Pou2af1, Pou2f1, Runx1, Stat2, Stat3 **Th0:** Ctcf **Th1:** Ctcf, Ep300, Smarca4, Stat1, Stat3, Stat5a, Stat6, Tbx21 **Th2:** Smarca4 **Th17:** Brd2, Irf4, Jmjd6, Jund, Smarca4, Stat1 **CD25+ cells:** Spi1 **CD4- CD8- cells:** Bcl11b, Ctcf, Runx1, Smc3 **CD4+ CD8+ cells:** Ctcf, Smc1a **NK T-cells:** Ep300, Stat1, Stat4, Stat5a **Spleen:** Ctcf	
Bones and muscles							
Chondrocytes: Ep300, Jun **Myoblasts:** Hdac1, Runx1, Tcf3 **Quadriceps muscle:** Hdac3	**Chondrocytes:** Ep300, Jun, Sox9 **Myoblasts:** Jun, Runx1, Spin1, Tcf3 **Skeletal muscle:** Brd4	**Chondrocytes:** Sox9 **Skeletal muscle:** Brd4	**Chondrocytes:** Jun **Myoblasts:** Hdac1, Runx1, Spin1 **Skeletal muscle:** Brd4	**Satellite cells skeletal muscle:** Sirt1	**Myoblasts:** Runx1 **Skeletal muscle:** Brd4	**Chondrocytes:** Sox9 **Myoblasts:** Spin1, Tcf3 **Skeletal muscle:** Brd4	

						Quadriceps muscle: Hdac3	
Embryonic stem cells							
Aebp2, Atrx, Brd2, Brd4, Btaf1, Cbx7, Cdk8, Chd4, Ctcf, Dppa2, Dr1, Ep300, Epop, Ezh2, Gabbr1, Gtf3c1, Hcfc1, Hdac1, Hdac2, Htatsf1, Ino80, Jarid2, Kdm1a, Kdm2b, Kdm4c, Kmt2b, Mcrs1, Med1, Med12, Men1, Mettl3, Nanog, Ncaph2, Nelfa, Otx2, Pou5f1, Rad21, Rad23b, Rbbp5, Rnf2, Supt5, Suz12, Taf3, Tbp, Tcf12, Tcf3, Tet1, tet3, Tgif1, Utf1, Zbtb2, Zfp217, Zfp281, Zfp42, Zfp57	Aebp2, Aff3, Atrx, Brd4, Btaf1, Dppa2, Dpy30, Dr1, Ep300, Epop, Ezh2, Fam60a, Fgfr1, Gabbr1, Gtf3c1, Htatsf1, Ino80, Kdm1a, Kdm2a, Kdm2b, Kdm4c, Klf4, Klf5, Kmt2b, Mcrs1, Med1, Med12, Men1, Mettl3, Msl2, Nanog, Ncaph2, Nelfa, Nipbl, Nr4a1, Otx2, Pou5f1, Rad21, Rad23b, Rara, Rbbp5, Rnf2, Rxra, Smad2, Smarca4, Supt5, Suz12, Taf3, Tbp, Tcf12, Tcf3, Tet1, Tet3, Tgif1, Utf1, Zbtb2, Zfp217, Zfp281, Zfp57	Gabbr1, Nanog, Nfyb, Nfyc, Nrf1, Pknox1, Yy1	Aebp2, Atrx, Brd2, Brd4, Btaf1, Dppa2, Dpy30, Dr1, Ep300, Epop, Ezh2, Fam60a, fgfr1, Gabbr1, Gata4, Gtf2b, Gtf3c1, Hcfc1, Htatsf1, ino80, kdm2b, Kdm4c, Klf4, Klf5, Kmt2b, Mcrs1, Med12, Men1, Mettl3, Nanog, Ncaph2, Nrf1, Otx2, Pou5f1, Rad21, rad23b, Rara, Rbbp5, Rnf2, Rxra, Smarca4, Supt5, Suz12, Taf3, Tbp, Tcf12, Tdg, Tet1, Tet3, Utf1, Yy1, Zbtb2, Zfp217, Zfp281, Zfp42, Zfp57, Zic3	Ep300, Gabbr1, Med1, Nanog, Nrf1, Otx2, Rad23b, Sox2, Tbp, Tcf12, Tcf3, Tdg, Utf1, Zfp384	Aebp2, Brd4, Btaf1, Cbx7, Ctcf, Dr1, Ezh2, Fam60a, Fgfr1, Gabbr1, Gtf3c1, Ino80, Kdm1a, Kdm4c, Klf4, Klf5, Kdm2b, Kmt2b, Max, Med1, Med12, Nanog, Ncapd3, Nelfa, Nipbl, Nrf1, Otx2, Pou5f1, Rad23b, Rnf2, Stag1, Stag2, Supt5, Suz12, Tcf12, Tfe3, Utf1, Yy1, Zfp217, Zfp281, Zfp57	Brd2, Cdk7, Ctcf, Dr1, Ep300, Epop, Fgfr1, Gabbr1, Hcfc1, Jarid2, Kat5, Kdm1a, Kdm4c, Kmt2b, Med1, Men1, Mettl3, Nanog, Ncapd3, Ncaph2, Nelfa, Nfya, Nfyb, Nrf1, Otx2, Pknox1, Pou5f1, Rad21, Rad23b, Smad2, Smc1a, Smc3, Stag1, Stag2, Sumo2, Supt5, Tcf12, Tdg, Tet1, Tet3, Utf1, Yy1, Zc3h11a, Zfp217, Zfp281, Zfp384	Mettl3, Nanog, Zfp57
Gastrointestinal tract							
Embryonic pancreas: Foxa2, Rbpjl	**Embryonic pancreas:** Foxa2 **Intestinal stem cells:** Tcf4	**Embryonic pancreas:** Foxa2 **Intestinal crypt:** E2f3, Myc	**Embryonic pancreas:** Foxa2 **Islet of Langerhans:** Nkx6-1		**Embryonic pancreas:** Foxa2 **Islet of Langerhans:** Nkx6-1	**Embryonic pancreas:** Foxa2 **Pancreas:** Ptf1a	**Colon:** Hnf4a **Intestinal crypt:** Myc **Intestinal villus:** Hnf4a

Pancreatic B cells: Insm1, Neurod1	**Jejunum:** Hnf4a, Hnf4g **Pancreatic B cells:** Insm1, Neurod1 **Small intestine:** Irf1	**Islet of Langerhans:** Nkx6-1 **Jejunum:** Hnf4a, Hnf4g **Pancreatic B cells:** Foxa2 **Small intestine:** Vdr	**Pancreatic B cells:** Insm1, Neurod1		**Pancreatic B cells:** Insm1, Foxa2	**Pancreatic B cells:** Insm1, Neurod1 **Small intestine:** Vdr	**Jejunum:** Hnf4a, Hnf4g **Small intestine:** Vdr
Heart							
Heart: Ep300, Gtf2b, Nkx2-5, Rbfox2, Tbx3 **Heart ventricles:** Ctcf **Embryonic heart:** Sap130	**Heart:** Ep300, Gtf2b, Rbfox2, Tbx3 **Heart ventricles:** Hdac2 **Embryonic heart:** Sap130	**Heart:** Gata4, Gtf2b, Nkx2-5	**Heart:** Gtf2b, Rbfox2, Tbx3 **Embryonic heart:** Sap130		**Heart:** Gata4, Gtf2b, Nkx2-5, Rbfox2, Tbx3 **Embryonic heart:** Sap130	**Heart:** Ep300, Gtf2b, Nkx2-5, Rbfox2 **Heart ventricles:** Ctcf **Embryonic heart:** Sap130	
Kidney and reproductive system							
Epididymis: Tfap2a **Kidney:** Ctcf, Hnf4a **Kidney cortex:** Wt1 **Prostate:** Erg **Spermatids:** Ctcf **Spermatogonia:** Zbtb16, Zfp384 **Testis:** Ctcf	**Epididymis:** Tfap2a **Kidney:** Tfap2a **Kidney cortex:** Wt1 **Prostate:** Foxa1, Tfap2a **Sperm:** Smc1a **Spermatogonia:** Sall4, Zbtb16, Zfp384 **Testis:** Dmc1, Taf7l **Uterus:** Esr1	**Embryonic kidney:** Six2 **Prostate:** Ncoa2, Nkx3-1 **Spermatogonia:** Zfp384 **Testis:** Dmc1 **Uterus:** Gata2, Esr1, Pgr	**Kidney:** Tfap2a **Kidney cortex:** Wt1 **Sperm:** Smc1a **Spermatogonia:** Sall4, Zfp384 **Testis:** Dmc1, Mybl1, Taf7l, Tbpl1 **Uterus:** Esr1	**Prostate:** Erg **Spermatogonia:** Zbtb16, Zfp384	**Spermatogonia:** Zfp384 **Testis:** Taf7l, Tbpl1 **Uterus:** Esr1, Gata2	**Kidney:** Ar, Ctcf **Prostate:** Erg **Sperm:** Smc1a **Spermatids:** Ctcf **Spermatogonia:** Zfp384 **Testis:** Ctcf, Rfx2, Taf7l, Tbp, Tbpl1 **Uterus:** Esr1	
Liver							

Embryonic liver: Cbfb **Hepatocytes:** Ctcf **Liver:** Brd4, Ctcf, Gata4, Rxra, Taf3	**Embryonic liver:** Cbfb **Hepatocytes:** Ep300, Tcf4 **Liver:** Brd4, Clock, Ctcf, Hnf4a, Nr1d1, Nr1h4, Nr3c1, Rad21, Rara, Rora, Taf3, Tbp	**Hepatocytes:** Cebpa **Liver:** Brd4, Cebpa, Cebpb, Esr1, Gata4, Gtf2b, Hdac3, Hnf4a, Med1, Myc, Ncoa2, Nr1d1, Nr1d2, Nr3c1, Prox1, Rorc, Rxra, Tead4, Xbp1	**Embryonic liver:** Cbfb **Liver:** Brd4, Med1, Nr1h4, Rad21, Rxra, Taf3	**Embryonic liver:** Cbfb	**Embryonic liver:** Cbfb **Hepatocytes:** Ctcf **Liver:** Arntl, Brd4, Cebpb, Clock, Gata4, Gtf2b, Gtf2e2, Med1, Myc, Ncoa2, Nr1d1, Nr1h4, Nr3c1, Rad21, Rara, Taf3, Xbp1	**Hepatocyte:** Tcf4 **Liver:** Brd4, Cebpb, Clock, Esr1, Gtf2b, Gtf2e2, Hdac3, Hnf4a, Med1, Myc, Ncoa2, Ncor2, Nr1d1, Nr3c1, Onecut1, Rad21, Rara, Rxra, Taf3, Tbp, Tead4, Xbp1	
Lung							
Lung: Foxf1, Smad4	**Alveolar type II cells:** Etv5 **Lung:** Foxf1	**Lung:** Foxf1, Smad4	**Alveolar type II cells:** Etv5 **Lung:** Foxf1	**Lung:** Foxf1		**Lung:** Ctcf, Foxf1, Smad4 **Alveolar type II cells:** Etv5	
Mammary gland							
Ctcf	Stat3	Elf5, Nfib, Nr3c1, Pgr, Stat3, Stat5a	Nfib, Pgr	Elf5, Nfib, Nr3c1, Stat3, Stat5a	Kdm6a	Ctcf, Elf5, Kdm6a, Nr3c1, Pgr, Smc1a, Stat3, Stat5a	
Neural tube and its derivatives							
Brain: Cxxc1; **Cerebellum:** Chd4, Ctcf, Zic1; **Cortex:** Ctcf; **Cortical neuron:** Kdm1a; **Cortical oligodendrocyte progenitor:** Stat3;	**Brain:** Rnf2; **Cerebellum:** Zic1; **Embryonic brain:** Kdm6b, Neurod2; **Frontal cortex:** Esrra; **Hippocampus:** Ctcf; **Neural stem cells:** Kdm1a, Smad4;	**Basal ganglia:** Nkx2-1: **Brain:** Cxxc1; **Cortex:** Sox2; **Cortical neuron:** Fos; **Cortical oligodendrocyte progenitor:** Stat3;	**Brain:** Cxxc1, Rnf2; **Cerebellum:** Chd4, Zic1; **Cortex:** Rai1; **Embryonic brain:** Kdm6b, Neurod2, Smad3; **Frontal cortex:** Esrra; **Hippocampus:** Ctcf, Hdac3;		**Brain:** Auts2; **Cerebellum:** Zic1; Cortex: Rai1; **Embryonic brain:** Kdm6b, Neurod2, Smad3; **Hippocampus:** Ctcf, Hdac3; **Neural progenitor cells:** Ascl1; **Neural**	**Brain:** Cxxc1; **Cerebellum:** Ctcf, Zic1; **Cortex:** Ctcf; **Cortical neurons:** Fos; **Embryonic brain:** Chd8, Kdm6b, Neurod2, Pbx1, Smad3, Smc1a;	

Embryonic brain: Ctcf, Kdm6b, Neurod2, Smad3; **Frontal cortex:** Esrra; **Hippocampus:** Ctcf; **Neural stem cells:** Ascl1, Kdm1a, Npas3, Smad4; **Olfactory nerve:** Ctcf, Rad21; **Retina:** Brd4, Ctcf, Mef2d; **Retinal rod photoreceptor cell:** Ctcf	**Neural tube:** Prdm13; **Retina:** Brd4, Ctcf;	**Embryonic brain:** Jund, Otx2, Pbx1, Sox2, Tbr1; **Neural stem cells:** Kdm1a; **Neural tube:** Rbpj; **Retina:** Brd4, Crx, Ctcf, Otx2;	**Neural stem cells:** Tcf3; **Olfactory nerve:** Ebf4; **Retina:** Brd4, Ctcf;		**stem cells:** Kdm1a, Npas3; **Olfactory nerve:** Ebf4; **Retina:** Brd4, Ctcf;	**Hippocampus:** Ctcf; **Neural stem cells:** Ctcf, Rad21; **Neural tube:** Prdm13; **Neurons:** Mapk8, Nfya;	

Table S2. Biological processes represented by TFs as predicted by Gene Ontology.
Gene Ontology service was used to predict tissue- and organ-relevant biological processes and pathways, where TLDc proteins might be involved, based on TFs that have been shown to bind their promoter regions. FDR, false discovery rate.

TLDc promoter	GO biological process	p-value	FDR
Adipose tissue			
Oxr1-FL-P1			
	regulation of glucocorticoid receptor signaling pathway	1.41E-05	2.14E-03
	positive regulation of intracellular steroid hormone receptor signaling pathway	4.16E-05	5.26E-03
	regulation of gluconeogenesis	1.34E-06	3.27E-04
	brown fat cell differentiation	1.19E-04	1.24E-02
	positive regulation of fat cell differentiation	2.66E-06	5.97E-04
	circadian regulation of gene expression	2.93E-06	6.28E-04
	response to estrogen	2.37E-04	2.16E-02
	regulation of circadian rhythm	1.44E-05	2.17E-03
	regulation of steroid biosynthetic process	5.06E-04	3.97E-02
	response to retinoic acid	6.04E-04	4.53E-02
	intracellular receptor signaling pathway	6.04E-04	4.51E-02
	regulation of cold-induced thermogenesis	3.12E-05	4.15E-03
	positive regulation of lipid metabolic process	3.96E-05	5.09E-03
	regulation of peptide hormone secretion	1.17E-04	1.22E-02
Oxr1-FL-P2			
	brown fat cell differentiation	2.54E-07	1.73E-04
	positive regulation of transforming growth factor beta receptor signaling pathway	4.87E-05	9.67E-03
	positive regulation of fat cell differentiation	1.25E-06	5.15E-04
	response to estrogen	1.48E-04	2.27E-02

	positive regulation of NIK/NF-kappaB signaling	2.92E-04	4.02E-02
	regulation of intracellular steroid hormone receptor signaling pathway	3.51E-04	4.47E-02
	response to retinoic acid	3.78E-04	4.74E-02
	rhythmic process	9.45E-07	4.36E-04
	cellular response to hepatocyte growth factor stimulus	1.72E-05	4.14E-03
Oxr1-C			
	brown fat cell differentiation	5.43E-07	1.70E-04
	positive regulation of fat cell differentiation	1.36E-08	5.47E-06
	circadian regulation of gene expression	2.93E-06	8.05E-04
	regulation of circadian rhythm	1.44E-05	3.18E-03
	regulation of cold-induced thermogenesis	3.12E-05	5.83E-03
	positive regulation of lipid metabolic process	3.96E-05	6.90E-03
	regulation of peptide hormone secretion	1.17E-04	1.81E-02
	cellular response to hepatocyte growth factor stimulus	2.76E-05	5.27E-03
Ncoa7-FL			
	brown fat cell differentiation	5.59E-05	1.54E-02
	positive regulation of fat cell differentiation	7.82E-07	4.91E-04
	response to estrogen	1.11E-04	2.60E-02
Tbc1d24			
	cellular response to hepatocyte growth factor stimulus	1.29E-05	4.59E-03
	positive regulation of transforming growth factor beta receptor signaling pathway	3.66E-05	9.40E-03
	brown fat cell differentiation	5.59E-05	1.27E-02
	response to estrogen	1.11E-04	2.18E-02
	positive regulation of fat cell differentiation	1.63E-04	3.02E-02
	positive regulation of NIK/NF-kappaB signaling	2.20E-04	3.78E-02
	regulation of intracellular steroid hormone receptor signaling pathway	2.64E-04	4.31E-02
	rhythmic process	4.33E-05	1.01E-02
mEAK7			
	cellular response to hepatocyte growth factor stimulus	4.77E-05	8.50E-03

	brown fat cell differentiation	1.29E-06	3.37E-04
	circadian regulation of gene expression	2.86E-10	1.18E-07
	negative regulation of JNK cascade	2.06E-04	2.84E-02
	negative regulation of intracellular steroid hormone receptor signaling pathway	2.29E-04	3.13E-02
	positive regulation of fat cell differentiation	6.31E-06	1.48E-03
	positive regulation of cold-induced thermogenesis	2.35E-05	4.91E-03
	lipid homeostasis	6.75E-05	1.08E-02
Brain			
Oxr1-FL-P1			
	anterior/posterior pattern specification	8.81E-04	4.94E-02
	cell population proliferation	5.64E-06	1.02E-03
	detection of mechanical stimulus involved in sensory perception of sound	1.43E-04	1.31E-02
	embryonic organ morphogenesis	1.29E-04	1.22E-02
	ERK1 and ERK2 cascade	3.15E-04	2.25E-02
	eye development	2.15E-04	1.76E-02
	in utero embryonic development	4.17E-05	4.60E-03
	interleukin-6-mediated signaling pathway	6.21E-05	6.41E-03
	negative regulation of neurogenesis	1.62E-04	1.43E-02
	neuron development	5.04E-04	3.20E-02
	neuron fate commitment	4.61E-05	5.02E-03
	nose development	9.27E-05	8.97E-03
	pallium development	9.76E-06	1.47E-03
	pituitary gland development	5.52E-04	3.44E-02
	positive regulation of ATP biosynthetic process	6.21E-05	6.45E-03
	positive regulation of endopeptidase activity	2.67E-04	2.05E-02
	positive regulation of neuroblast proliferation	2.75E-04	2.08E-02
	positive regulation of neuron differentiation	3.20E-05	3.58E-03
	positive regulation of Notch signaling pathway	6.32E-06	1.10E-03

	regulation of glycolytic process	6.07E-04	3.68E-02
	regulation of transforming growth factor beta2 production	3.08E-05	3.52E-03
	response to hypoxia	5.49E-04	3.44E-02
	SMAD protein complex assembly	2.46E-05	3.02E-03
	stem cell differentiation	1.10E-05	1.53E-03
Oxr1-FL-P2			
	positive regulation of neuroblast proliferation	8.91E-05	2.03E-02
	pituitary gland development	1.79E-04	3.56E-02
	cell fate commitment	2.36E-04	4.56E-02
Oxr1-C			
	anterior/posterior pattern specification	3.44E-04	3.62E-02
	diencephalon morphogenesis	1.02E-05	2.08E-03
	eye photoreceptor cell differentiation	4.95E-04	4.85E-02
	forebrain neuron fate commitment	3.82E-05	6.05E-03
	forebrain regionalization	1.47E-04	1.94E-02
	glial cell differentiation	1.59E-04	2.05E-02
	inner ear development	2.62E-04	3.00E-02
	negative regulation of neurogenesis	1.35E-06	4.14E-04
	pituitary gland development	1.18E-08	5.14E-06
	positive regulation of neuroblast proliferation	1.47E-04	1.95E-02
	positive regulation of Notch signaling pathway	2.39E-06	6.36E-04
	regulation of neuron differentiation	7.19E-05	1.04E-02
	telencephalon development	4.25E-04	4.36E-02
Ncoa7-FL			
	detection of mechanical stimulus involved in sensory perception of sound	1.00E-04	2.07E-02
	cell cycle arrest	3.90E-05	8.99E-03
	regulation of mitotic cell cycle	2.07E-05	5.23E-03
	negative regulation of cell differentiation	1.38E-04	2.68E-02
Tbc1d24			

	cell cycle arrest	3.18E-05	6.92E-03
	detection of mechanical stimulus involved in sensory perception of sound	8.79E-05	1.44E-02
	developmental growth	1.73E-04	2.38E-02
	forebrain neuron differentiation	1.05E-05	3.10E-03
	negative regulation of cell differentiation	5.63E-06	1.80E-03
	negative regulation of nervous system development	7.65E-05	1.28E-02
	nose development	5.70E-05	1.01E-02
	pallium development	1.60E-04	2.27E-02
	pituitary gland development	3.41E-04	3.90E-02
	positive regulation of neuroblast proliferation	1.70E-04	2.37E-02
	positive regulation of neuron differentiation	1.95E-04	2.55E-02
	positive regulation of Notch signaling pathway	3.58E-04	4.04E-02
	regulation of cysteine-type endopeptidase activity involved in apoptotic process	2.85E-04	3.39E-02
	regulation of mitotic cell cycle	1.45E-05	3.79E-03
Embryonic stem cells			
Oxr1-FL-P1			
	blastocyst formation	4.14E-04	2.33E-02
	cellular response to leukemia inhibitory factor	2.92E-04	1.75E-02
	circadian rhythm	3.19E-04	1.84E-02
	DNA methylation involved in embryo development	2.55E-04	1.55E-02
	endodermal cell fate specification	1.59E-04	1.05E-02
	mesodermal cell fate commitment	5.12E-04	2.83E-02
	negative regulation of retinoic acid receptor signaling pathway	2.04E-04	1.30E-02
	negative regulation of telomerase activity	5.90E-04	3.12E-02
	positive regulation of stem cell proliferation	3.03E-04	1.79E-02
	regulation of gastrulation	1.65E-04	1.07E-02
	regulation of intracellular steroid hormone receptor signaling pathway	9.96E-04	4.69E-02
	regulation of stem cell population maintenance	8.26E-05	6.05E-03

	stem cell differentiation	5.46E-05	4.33E-03
	stem cell population maintenance	1.14E-06	1.40E-04
Oxr1-FL-P2			
	blastocyst formation	5.11E-04	2.22E-02
	blastocyst growth	8.56E-05	4.88E-03
	cell fate determination	2.32E-04	1.20E-02
	cellular response to growth factor stimulus	5.54E-04	2.37E-02
	cellular response to leukemia inhibitory factor	3.85E-04	1.77E-02
	embryonic pattern specification	7.06E-04	2.80E-02
	endodermal cell fate specification	1.83E-04	9.75E-03
	mesodermal cell fate commitment	5.90E-04	2.45E-02
	negative regulation of retinoic acid receptor signaling pathway	2.35E-04	1.20E-02
	nodal signaling pathway	5.90E-04	2.44E-02
	peroxisome proliferator activated receptor signaling pathway	2.35E-04	1.19E-02
	positive regulation of stem cell proliferation	3.74E-04	1.74E-02
	regulation of cell fate specification	1.83E-05	1.22E-03
	regulation of gastrulation	1.25E-07	1.37E-05
	regulation of intracellular steroid hormone receptor signaling pathway	1.23E-03	4.40E-02
	regulation of mesoderm development	1.10E-03	4.02E-02
	regulation of stem cell population maintenance	1.02E-04	5.71E-03
	response to estrogen	3.54E-04	1.67E-02
	response to retinoic acid	2.92E-06	2.28E-04
	retinoic acid receptor signaling pathway	1.10E-03	4.01E-02
	stem cell differentiation	9.52E-04	3.60E-02
	stem cell population maintenance	3.85E-12	8.63E-10
Ncoa7-FL			
	blastocyst formation	4.61E-04	2.34E-02
	blastocyst growth	7.70E-05	5.14E-03
	cell fate determination	2.09E-04	1.22E-02

	cellular response to leukemia inhibitory factor	2.07E-05	1.70E-03
	endodermal cell fate specification	1.71E-04	1.04E-02
	gastrulation with mouth forming second	1.28E-04	8.04E-03
	mesodermal cell fate commitment	5.50E-04	2.70E-02
	positive regulation of cell population proliferation	2.90E-05	2.28E-03
	positive regulation of transmembrane receptor protein serine/threonine kinase signaling pathway	1.86E-04	1.10E-02
	regulation of cell fate specification	1.65E-05	1.37E-03
	regulation of cellular response to growth factor stimulus	6.02E-04	2.89E-02
	regulation of gastrulation	4.88E-06	4.66E-04
	regulation of protein kinase B signaling	6.17E-04	2.93E-02
	regulation of stem cell population maintenance	9.21E-05	5.97E-03
	response to estrogen	1.02E-05	9.02E-04
	response to retinoic acid	8.11E-08	1.14E-05
	retinoic acid receptor signaling pathway	1.03E-03	4.43E-02
	stem cell differentiation	8.34E-04	3.74E-02
	stem cell population maintenance	8.70E-11	2.13E-08
Ncoa7-B			
	endodermal cell fate specification	8.76E-06	3.52E-03
	regulation of gastrulation	2.79E-04	4.76E-02
	response to lipid	7.18E-07	3.75E-04
Tbc1d24			
	cellular response to leukemia inhibitory factor	9.03E-05	9.97E-03
	endodermal cell fate specification	8.70E-05	9.88E-03
	in utero embryonic development	2.04E-04	1.81E-02
	mesodermal cell fate commitment	2.81E-04	2.32E-02
	regulation of cell fate specification	5.94E-06	9.41E-04
	regulation of gastrulation	1.25E-06	2.33E-04
	regulation of stem cell population maintenance	3.35E-05	4.30E-03
	regulation of stem cell proliferation	4.75E-04	3.45E-02

	response to retinoic acid	4.58E-04	3.36E-02
	stem cell population maintenance	5.66E-09	1.58E-06
mEAK7			
	blastocyst formation	2.41E-04	1.84E-02
	cellular response to leukemia inhibitory factor	1.44E-04	1.16E-02
	embryonic pattern specification	3.34E-04	2.46E-02
	endodermal cell fate specification	1.10E-04	9.40E-03
	mesodermal cell fate commitment	3.55E-04	2.57E-02
	negative regulation of cell differentiation	7.25E-04	4.72E-02
	positive regulation of developmental process	7.21E-04	4.71E-02
	positive regulation of stem cell proliferation	1.76E-04	1.40E-02
	positive regulation of transmembrane receptor protein serine/threonine kinase signaling pathway	7.88E-05	6.98E-03
	regulation of cell fate specification	8.50E-06	1.07E-03
	regulation of cellular response to growth factor stimulus	2.15E-04	1.67E-02
	regulation of gastrulation	9.55E-05	8.32E-03
	regulation of mesoderm development	6.64E-04	4.41E-02
	regulation of stem cell population maintenance	4.78E-05	4.74E-03
	stem cell differentiation	2.23E-05	2.47E-03
	stem cell population maintenance	4.08E-10	1.12E-07
Heart			
Oxr1-FL-P1			
	bundle of His development	1.27E-06	1.17E-03
	cardiac muscle cell fate commitment	2.36E-06	1.48E-03
	cardiac pacemaker cell development	1.77E-06	1.32E-03
	heart looping	1.43E-04	3.26E-02
	His-Purkinje system cell differentiation	5.06E-07	6.11E-04
	outflow tract morphogenesis	2.64E-04	4.92E-02
	positive regulation of cardiocyte differentiation	6.22E-05	1.74E-02

	regulation of cardiac muscle tissue growth	2.38E-04	4.67E-02
	ventricular septum morphogenesis	8.68E-05	2.20E-02
Oxr1-FL-P2			
	regulation of sarcomere organization	3.98E-06	6.93E-03
	cardiac muscle cell development	1.53E-04	4.61E-02
	regulation of cardiac muscle tissue growth	1.70E-04	4.69E-02
Oxr1-C			
	atrial septum morphogenesis	2.06E-06	8.09E-03
	BMP signaling pathway	4.00E-05	1.57E-02
	canonical Wnt signaling pathway	4.61E-05	1.72E-02
	cardiac muscle cell development	3.08E-05	1.56E-02
	cardiac muscle tissue growth	7.59E-06	9.16E-03
	cardiac right ventricle morphogenesis	2.53E-06	7.94E-03
	heart looping	2.06E-05	1.41E-02
	muscle organ morphogenesis	5.49E-05	1.87E-02
	negative regulation of cardiac muscle cell apoptotic process	6.37E-06	9.08E-03
	outflow tract morphogenesis	3.80E-05	1.75E-02
	positive regulation of cardioblast differentiation	3.38E-07	2.65E-03
	regulation of cardiac muscle cell proliferation	1.42E-05	1.17E-02
	regulation of cardiac muscle contraction	2.91E-05	1.52E-02
	septum secundum development	1.21E-07	1.89E-03
	vasculogenesis	4.61E-05	1.68E-02
	ventricular cardiac muscle tissue development	2.43E-05	1.46E-02
	ventricular septum development	3.90E-05	1.65E-02
Tbc1d24			
	atrial septum morphogenesis	1.03E-05	3.94E-03
	BMP signaling pathway	1.98E-04	3.11E-02
	bundle of His development	9.04E-07	1.58E-03
	canonical Wnt signaling pathway	2.29E-04	3.45E-02

	cardiac muscle cell fate commitment	1.69E-06	1.56E-03
	cardiac muscle tissue growth	3.78E-05	9.89E-03
	cardiac pacemaker cell development	1.27E-06	1.42E-03
	cardiac right ventricle morphogenesis	1.26E-05	4.50E-03
	heart looping	3.68E-07	2.89E-03
	His-Purkinje system cell differentiation	3.62E-07	5.67E-03
	muscle organ morphogenesis	2.72E-04	3.88E-02
	negative regulation of cardiac muscle cell apoptotic process	3.17E-05	8.73E-03
	outflow tract morphogenesis	9.16E-07	1.44E-03
	positive regulation of cardioblast differentiation	1.69E-06	1.65E-03
	regulation of cardiac muscle cell proliferation	7.05E-05	1.58E-02
	regulation of cardiac muscle contraction	1.44E-04	2.58E-02
	septum secundum development	6.03E-07	1.58E-03
	vasculogenesis	2.29E-04	3.41E-02
	ventricular septum morphogenesis	6.21E-05	1.43E-02
mEAK7			
	positive regulation of cardiocyte differentiation	4.45E-05	2.11E-02
Kidney and reproductive system			
Oxr1-FL-P2			
	metanephric nephron development	2.00E-06	3.13E-02
Oxr1-C			
	intracellular steroid hormone receptor signaling pathway	9.40E-06	2.11E-02
	ovulation cycle process	1.14E-05	1.99E-02
	regulation of epithelial cell proliferation	4.07E-06	3.19E-02
	negative regulation of epithelial cell apoptotic process	1.42E-05	1.85E-02
Ncoa7-FL			
	male meiosis I	7.23E-06	8.10E-03
	spermatid development	3.56E-06	5.07E-03

mEAK7			
	acrosome assembly	5.46E-06	1.07E-02
Liver			
Oxr1-FL-P2			
	cholesterol homeostasis	2.98E-07	7.43E-05
	circadian regulation of gene expression	1.10E-05	2.02E-03
	glandular epithelial cell development	7.96E-05	1.04E-02
	hormone-mediated signaling pathway	2.98E-05	4.67E-03
	intracellular receptor signaling pathway	2.59E-07	6.67E-05
	negative regulation of I-kappaB kinase/NF-kappaB signaling	4.11E-04	3.93E-02
	negative regulation of interferon-gamma production	2.34E-04	2.55E-02
	positive regulation of circadian rhythm	1.70E-04	1.98E-02
	positive regulation of lipid biosynthetic process	3.28E-05	5.04E-03
	regulation of bile acid biosynthetic process	2.77E-05	4.39E-03
	regulation of glucocorticoid receptor signaling pathway	3.28E-05	5.09E-03
	regulation of gluconeogenesis	3.51E-08	1.04E-05
	response to dexamethasone	1.82E-04	2.06E-02
	response to estrogen	5.49E-04	4.75E-02
	triglyceride homeostasis	1.88E-06	4.28E-04
Oxr1-C			
	androgen metabolic process	1.29E-04	6.85E-03
	animal organ regeneration	2.56E-04	1.23E-02
	cellular response to fluid shear stress	1.04E-04	5.68E-03
	cellular response to growth factor stimulus	3.01E-04	1.42E-02
	cellular response to lipopolysaccharide	6.27E-04	2.67E-02
	cellular response to xenobiotic stimulus	2.56E-04	1.22E-02
	cholesterol homeostasis	5.30E-05	3.25E-03
	circadian regulation of gene expression	2.78E-07	3.63E-05

	ERK1 and ERK2 cascade	3.15E-04	1.45E-02
	glandular epithelial cell differentiation	7.76E-06	6.76E-04
	glucose homeostasis	5.32E-04	2.28E-02
	hepatocyte differentiation	4.51E-05	2.83E-03
	hepatocyte proliferation	1.92E-05	1.41E-03
	intracellular steroid hormone receptor signaling pathway	5.47E-06	5.13E-04
	intrinsic apoptotic signaling pathway in response to endoplasmic reticulum stress	4.99E-04	2.18E-02
	negative regulation of glucose import	1.72E-04	8.70E-03
	peroxisome proliferator activated receptor signaling pathway	2.46E-05	1.70E-03
	positive regulation of circadian rhythm	2.75E-04	1.30E-02
	positive regulation of glucocorticoid receptor signaling pathway	1.44E-05	1.11E-03
	positive regulation of hepatocyte proliferation	3.08E-05	2.04E-03
	positive regulation of TOR signaling	4.99E-04	2.19E-02
	regulation of bile acid biosynthetic process	4.51E-05	2.84E-03
	regulation of gluconeogenesis	1.06E-05	8.72E-04
	regulation of inflammatory response	1.51E-04	7.84E-03
	response to drug	3.38E-04	1.54E-02
	response to estrogen	8.88E-04	3.56E-02
	secretion	8.19E-04	3.33E-02
	triglyceride homeostasis	4.25E-04	1.89E-02
Tbc1d24			
	animal organ regeneration	2.56E-04	1.57E-02
	cellular response to growth factor stimulus	3.01E-04	1.79E-02
	cellular response to lipopolysaccharide	6.22E-07	1.05E-04
	cellular response to nutrient	4.49E-04	2.39E-02
	cellular triglyceride homeostasis	2.46E-05	2.45E-03
	cholesterol homeostasis	5.30E-05	4.49E-03
	circadian regulation of gene expression	2.78E-07	5.52E-05
	developmental growth	4.61E-04	2.43E-02

	embryonic organ development	4.09E-05	3.66E-03
	ERK1 and ERK2 cascade	3.15E-04	1.82E-02
	fatty acid homeostasis	9.27E-05	6.96E-03
	in utero embryonic development	6.39E-04	3.18E-02
	intracellular steroid hormone receptor signaling pathway	5.25E-04	2.70E-02
	intrinsic apoptotic signaling pathway in response to endoplasmic reticulum stress	4.99E-04	2.59E-02
	liver development	1.70E-06	2.47E-04
	negative regulation of glucocorticoid receptor signaling pathway	1.92E-05	2.03E-03
	positive regulation of circadian rhythm	2.75E-04	1.66E-02
	positive regulation of defense response	1.32E-04	9.32E-03
	positive regulation of glucocorticoid receptor signaling pathway	1.44E-05	1.59E-03
	positive regulation of hepatocyte proliferation	3.08E-05	2.89E-03
	regulation of bile acid biosynthetic process	4.51E-05	3.95E-03
	regulation of gluconeogenesis	8.21E-04	3.95E-02
	response to drug	2.71E-05	2.60E-03
	response to estrogen	8.88E-04	4.18E-02
	response to redox state	4.51E-05	3.97E-03
	secretion	8.19E-04	3.95E-02
	steroid metabolic process	8.48E-04	4.02E-02
mEAK7			
	androgen metabolic process	1.91E-04	1.22E-02
	animal organ regeneration	3.78E-04	2.09E-02
	cellular response to estrogen stimulus	1.37E-04	9.41E-03
	cellular response to fluid shear stress	1.54E-04	1.04E-02
	cellular response to lipopolysaccharide	5.04E-05	4.12E-03
	cholesterol homeostasis	9.58E-05	6.89E-03
	circadian regulation of gene expression	6.29E-07	9.13E-05
	ERK1 and ERK2 cascade	4.64E-04	2.45E-02
	glandular epithelial cell development	1.91E-04	1.23E-02

	glucose homeostasis	9.49E-04	4.38E-02
	in utero embryonic development	7.35E-06	8.18E-04
	intracellular steroid hormone receptor signaling pathway	9.93E-06	1.06E-03
	intrinsic apoptotic signaling pathway in response to endoplasmic reticulum stress	7.35E-04	3.55E-02
	liver development	9.95E-10	2.56E-07
	negative regulation of glucose import	2.54E-04	1.54E-02
	negative regulation of intracellular steroid hormone receptor signaling pathway	7.35E-04	3.57E-02
	organ growth	2.19E-04	1.37E-02
	peroxisome proliferator activated receptor signaling pathway	3.64E-05	3.10E-03
	positive regulation of glucocorticoid receptor signaling pathway	2.13E-05	2.01E-03
	positive regulation of hepatocyte proliferation	4.55E-05	3.77E-03
	positive regulation of TOR signaling	7.35E-04	3.56E-02
	regulation of cellular ketone metabolic process	2.73E-04	1.64E-02
	regulation of defense response	3.25E-04	1.84E-02
	regulation of gluconeogenesis	1.93E-05	1.83E-03
	regulation of lipid biosynthetic process	6.99E-04	3.41E-02
	response to drug	8.75E-04	4.10E-02
	retinoic acid receptor signaling pathway	1.72E-04	1.14E-02
	triglyceride homeostasis	6.26E-04	3.17E-02

Appendix 3

Free Radical Biology and Medicine 130 (2019) 151–162

Contents lists available at ScienceDirect

Free Radical Biology and Medicine

journal homepage: www.elsevier.com/locate/freeradbiomed

Original article

Oxidation resistance 1 regulates post-translational modifications of peroxiredoxin 2 in the cerebellum

Daria M. Svistunova[a], Jillian N. Simon[b], Elzbieta Rembeza[c], Mark Crabtree[b], Wyatt W. Yue[c], Peter L. Oliver[a,d,*], Mattéa J. Finelli[a,*]

[a] Department of Physiology, Anatomy and Genetics, University of Oxford, Oxford OX1 3PT, UK
[b] Division of Cardiovascular Medicine, Radcliffe Department of Medicine, John Radcliffe Hospital, University of Oxford, Oxford OX3 9DU, UK
[c] Structural Genomics Consortium, Nuffield Department of Clinical Medicine, University of Oxford, OX3 7DQ, UK
[d] MRC Harwell Institute, Harwell Campus, Oxfordshire OX11 0RD, UK

ARTICLE INFO

Keywords:
Oxidative stress
Chaperone
Antioxidant
Peroxiredoxin
Neurodegeneration
Mouse

ABSTRACT

Protein aggregation, oxidative and nitrosative stress are etiological factors common to all major neurodegenerative disorders. Therefore, identifying proteins that function at the crossroads of these essential pathways may provide novel targets for therapy. Oxidation resistance 1 (Oxr1) is a protein proven to be neuroprotective against oxidative stress, although the molecular mechanisms involved remain unclear. Here, we demonstrate that Oxr1 interacts with the multifunctional protein, peroxiredoxin 2 (Prdx2), a potent antioxidant enzyme highly expressed in the brain that can also act as a molecular chaperone. Using a combination of *in vitro* assays and two animal models, we discovered that expression levels of Oxr1 regulate the degree of oligomerization of Prdx2 and also its post-translational modifications (PTMs), specifically suggesting that Oxr1 acts as a functional switch between the antioxidant and chaperone functions of Prdx2. Furthermore, we showed in the Oxr1 knockout mouse that Prdx2 is aberrantly modified by overoxidation and S-nitrosylation in the cerebellum at the pre-symptomatic stage; this in-turn affected the oligomerization of Prdx2, potentially impeding its normal functions and contributing to the specific cerebellar neurodegeneration in this mouse model.

1. Introduction

Neurodegenerative disorders are becoming more prevalent with increased global life expectancy and a better understanding of the underlying disease mechanisms will be essential for designing new therapeutic approaches to tackle this growing health burden [1–3]. Aberrant proteostasis and increased oxidative and nitrosative (O/N) stress have been strongly linked with the neurodegenerative process, irrespective of the etiology [4,5]. O/N stress arises from an excessive accumulation of reactive oxygen species (ROS) and reactive nitrogen species (RNS) resulting from an imbalance between free radical production and detoxification by antioxidant proteins [6]. Elevated levels of O/N stress markers such as oxidised lipids and nitrated proteins have been reported in *post mortem* tissue of individuals affected by major neurodegenerative disorders such as Alzheimer's disease (AD), Parkinson's disease (PD), and amyotrophic lateral sclerosis (ALS) [7–9]. Importantly, these markers are not only observed at the end-stage of the disease but are also detected in peripheral blood of patients during the course of the disease and pre-symptomatically in animal models of these conditions [10–14]. For example, mouse models of ALS show elevated levels of carbonylated proteins, a marker of ROS-induced protein damage, before any motor neuron pathology or clinical features are observed, suggesting that O/N stress is an early event of the neurodegenerative process [15].

Protein aggregation is another important feature consistently observed in neurodegenerative disease. Indeed, the formation of

Abbreviations: Oxr1, Oxidation resistance 1; Prdx2, peroxiredoxin 2; PTMs, post-translational modifications; O/N, oxidative and nitrosative; ROS, reactive oxygen species; RNS, reactive nitrogen species; AD, Alzheimer's disease; PD, Parkinson's disease; ALS, amyotrophic lateral sclerosis; PDI, protein disulfide-isomerase; TBC1D24, TBC1 Domain Family Member 24; DOORS, deafness, onychodystrophy, osteodystrophy and mental retardation with seizures; Ncoa7, nuclear receptor coactivator 7; HMW, high molecular weight; GPI/Gpi1, glucose-6-phosphate isomerase; Oxr1-FL, full-length Oxr1; CS, citrate synthase; SNOC, S-nitrosocysteine; SNO-protein, S-nitrosylated protein; ORC, organomercury resin capture; BCA, bicinchoninic acid; IPTG, isopropyl β-D-1-thiogalactopyranoside; FOX, ferrous oxidation-xylenol orange; veh, vehicle; DTT, dithiothreitol

* Corresponding authors. Department of Physiology, Anatomy and Genetics, University of Oxford, Oxford OX1 3PT, UK.
E-mail addresses: p.oliver@har.mrc.ac.uk (P.L. Oliver), mattea.finelli@ndcn.ox.ac.uk (M.J. Finelli).

https://doi.org/10.1016/j.freeradbiomed.2018.10.447
Received 24 July 2018; Received in revised form 28 October 2018; Accepted 29 October 2018
Available online 31 October 2018
0891-5849/ Crown Copyright © 2018 Published by Elsevier Inc. This is an open access article under the CC BY-NC-ND license (http://creativecommons.org/licenses/BY-NC-ND/4.0/).

neurotoxic protein aggregates has been reported in brain and spinal cord regions affected by AD, PD, and ALS [16]. In normal conditions, chaperone proteins are employed to fold misfolded proteins and disassemble protein aggregates, and thus play a key role in the global cellular proteostasis [17]. In neurodegenerative disease, however, the chaperone activity in cells is disrupted. For instance, mutations in the gene encoding for the mitochondrial chaperone mtHsp70 have been identified in patients with PD, and have been shown to disrupt mtHsp70 activity and to lead to apoptosis [18,19]. In addition, PTMs, such as S-nitrosylation and sulfonylation, have been associated with dysregulation of protein function. For instance, aberrant S-nitrosylation of the chaperone protein disulfide-isomerase (PDI) inhibits its activity, leading to neurodegeneration [20,21]. Therefore, identifying proteins that function in both the O/N stress and proteostasis pathways may produce valuable insights into the underlying pathogenic mechanisms of neurodegenerative conditions.

Oxidation resistance 1 (OXR1) was originally identified as a gene capable of rescuing bacterial oxidative DNA damage [22]. Subsequently, Oxr1 has been shown to act as a potent regulator of oxidative stress in mammalian neurons that can also delay neurodegeneration *in vivo*. Oxr1 possesses a highly conserved C-terminal TLDc domain shared with four other proteins in mammals, several of which have been proven to be important for brain function [23]. Mutations in the TLDc domain of TBC1 domain family member 24 (TBC1D24) influence its role in neuronal cell development and function and are associated with a range of familial neurological disorders, including epilepsy and deafness, onychodystrophy, osteodystrophy and mental retardation with seizures (DOORS) syndrome [23–25]. Moreover, mice lacking all Oxr1 isoforms present a progressive ataxic phenotype concomitant with degeneration of granule neurons in the cerebellum from postnatal day 19 (P19) [26–28]. Conversely, over-expression of Oxr1 *in vivo* is able to delay motor neuron degeneration and motor dysfunction in a mouse model of ALS [29]. *In vitro* studies in mammalian cells also demonstrated that levels of Oxr1 can modulate the sensitivity of neurons to oxidative stress [26,28]: knock-down of Oxr1 leads to oxidative stress-induced cell death while over-expression of Oxr1 reduces ROS levels and apoptosis of cells subjected to oxidative stress [26,28]. Furthermore, studies in a range of experimental systems have demonstrated a dysregulation of the expression of a number of antioxidant genes when Oxr1 is disrupted. For example, glutathione peroxidase 2 (GPX2), heme oxygenase-1 (HO-1), catalase (CAT) and peroxiredoxin 4 are reportedly down-regulated in OXR1-depleted mammalian cell lines [30–32], whereas in mosquitos, gene knock-down of OXR1 regulates the basal levels of CAT and Gpx expression [33].

As well as Oxr1, the TLDc-containing protein nuclear receptor coactivator 7 (Ncoa7) can reduce the levels of the O/N stress-induced PTM, S-nitrosylation, in neurons [26]; thus taken together, these data suggest that the TLDc proteins have the ability to reduce O/N stress. However, no superoxide dismutase or catalase-like catalytic activity has been detected for Oxr1, and the three-dimensional structure of the TLDc domain provides no clues regarding the molecular function of this important group of proteins [28,34,35]. In addition, Oxr1 has been shown to reduce the aggregation and mislocalisation of the ALS-associated proteins FUS and TDP-43 via protein interaction, although the precise mechanism involved is currently unclear [36].

Here, we demonstrate that Oxr1 interacts with peroxiredoxin 2 (Prdx2), a highly abundant and potent antioxidant enzyme that also possesses a chaperone function. Our results suggest that Oxr1 acts as a functional switch for Prdx2 activity, from an H_2O_2 scavenger to a high molecular weight (HMW) chaperone complex, through the modulation of its overoxidation and S-nitrosylation. We also report an unexpected and novel function for Oxr1 as a potential holdase.

2. Materials and methods

2.1. Reagents

Reagents used were as follows: Insulin (I0516, Sigma), citrate synthase (C3260, Sigma), protease inhibitor (5871S, Cell Signaling), protease/phosphatase inhibitor (5872S, Cell Signaling), protease inhibitor (11836170001, Roche). Antibodies used were: Prdx2 (10545–2-AP, Proteintech), Prdx-$SO_{2/3}$ (ab16830, Abcam), β-actin (ab8226, Abcam), HA (H6908, Sigma), α-tubulin (Sigma), MYC (Sigma), Oxr1 [28].

2.2. Animals

Constitutive Oxr1 knockout ($Oxr1^{d/d}$) mice maintained on a C57BL6/J background have been previously described [27]. Oxr1 Tg mice, where a full-length cDNA transgene of Oxr1-FL is expressed from a ubiquitous actin-derived promoter, were also maintained on a C57BL6/J background and have been previously described [28]. All experiments were conducted in adherence with the guidelines set forth by the UK Home Office regulations, and with the approval of the University of Oxford Ethical Review Panel.

2.3. Expression constructs

Mouse Prdx2 cDNA (NM_001317385.1) was cloned from total brain cDNA extract into pET-22b vector with or without introducing thrombin cleavage site (Thr) in frame with a His_6 tag: F – 5′-GAGACA TATGGCCTCCGGCAACGCGCAAATC-3′, R – 5′-GAGACTCGAGGCTGCC ACGCGGCACCAGGTTGTGTTTGGAGAAGTATTCC-3′; or F – 5′-GAGAC ATATGGCCTCCGGCAACGCGCAAATC-3′, R – 5′-GAGACTCGAGGTTGT GTTTGGAGAAGTATTCC-3′, respectively. Mouse Oxr1-C (NM_001130164) was cloned from total brain cDNA into pET-22b backbone in frame with His_6 tag (F – 5′-GAGACATATGTCCCGTCTCTG GTATGGGAAAAAAG-3′, R – 5′- GAGACTCGAGTTCAAAAGCCCAGATT TCAATG-3′). For expression in mammalian cells, mouse Prdx2 was cloned into pcDNA3.1 with a C-terminal MYC tag. All other constructs used have been previously described [26,28].

2.4. Cell culture, transfection, and treatment

Neuro2a (N2a) and SH-SY5Y cells were cultured in DMEM with GlutaMAX (Gibco) and Ham's F12:DMEM (Gibco) respectively, supplemented with 10% fetal bovine serum (Gibco) and 1% penicillin-streptomycin solution (Gibco) in an incubator at 37 °C in 5% CO_2 atmosphere. Cells were seeded 24 h prior to transfection. Cells were transfected using Fugene 6 (Promega) diluted in Opti-MEM (Gibco) according to manufacturer's protocol. 24 h after transfection culture media was changed to media supplemented with desired concentrations of H_2O_2. For cell death assay, cells were treated with 500 μM H_2O_2 for 5 h, and for Prdx2 overoxidation experiments, cells were treated with 300 μM H_2O_2 for 1 h. Fluorescent microscope Axioplan2 Imaging (Carl Zeiss) was used for cell death assay to visualise the pyknotic nuclei. For S-nitrosocysteine (SNOC) treatment of SH-SY5Y cells, a fresh stock solution of SNOC was prepared immediately before each use by mixing 200 mM cysteine (Sigma) with 200 mM $NaNO_2$ (Sigma) supplemented with HCl (0.5 N). Cells were treated with 200 μM SNOC for 30 min. Control cells were treated with a vehicle solution (HCl diluted in water).

2.5. Immunoprecipitation and western blotting

SDS-PAGE- Tissue samples or cells were lysed in cold RIPA buffer supplemented with protease inhibitor (Cell signaling) and 1% Triton X-100 or 1% CHAPS in a tissue Precellys homogenizer (Bertin Corp.) (for tissue) or by trituration with a syringe (for cells). Protein concentration was assessed by bicinchoninic acid (BCA) assay (Novagen). For co-

immunoprecipitation, protein extracts were incubated overnight at 4 °C with either Prdx2 antibody, EZview MYC beads (Sigma) or G protein sepharose beads (Sigma) only, as a control. Protein-antibody complexes were pulled down using G protein sepharose beads (Sigma) and washed with cold RIPA buffer. Immunoprecipitated proteins were incubated with Laemmli loading buffer (Bio-Rad) or NuPAGE loading buffer (Life Technologies) supplemented with 5% β-mercaptoethanol (Sigma) at 100 °C for 5 min.

Blue Native-PAGE (BN-PAGE)- Brain and cerebella tissue samples and cells were homogenised in cold PBS buffer supplemented with protease/phosphatase inhibitors (New England Biolabs) using Precellys homogenizer (only for tissue samples) and lysed by repeated freezing and thawing (for tissue and cells). After measuring protein concentration using BCA assay (Novagen), samples were mixed with 5x loading buffer (62.5 mM Tris-HCl pH 6.8, 40% glycerol, 0.01% bromophenol blue) and were resolved on 10% Bis-Tris native gel.

After samples were run on either SDS-PAGE or BN-PAGE, proteins were transferred to PVDF membrane (Amersham). The membrane was then blocked with 5% skim milk in PBST for 1 h at room temperature and incubated overnight with primary antibodies at 4 °C. The membranes were washed with PBST and incubated with secondary HRP-conjugated antibodies and signal was detected using ECL or ECL Prime Western Blotting detection kit (both Amersham) using an ImageQuant LAS 4000 (GE Healthcare). Western blot signal was quantified using ImageJ.

2.6. Protein expression and purification

Prdx2-His_6 and Prdx2-Thr-His_6 proteins were produced in *E.coli* strain BL21(DE3) (Invitrogen) and purified according to protocol published by Yan et al. [37]. Briefly, protein expression was induced at OD_{600} ~0.7–0.8 by addition of isopropyl β-D-1-thiogalactopyranoside (IPTG) (Sigma) to final concentration of 0.8 mM. After incubation on a shaker for 5 h at 25 °C, bacterial cells were collected by centrifugation and resuspended in 500 mM NaCl PBS supplemented with protease inhibitors. After sonication of the bacterial cultures and centrifugation for 30 min at 4 °C, recombinant His_6-tagged protein was incubated with 1 ml TALON metal affinity resin (Clontech) for 1 h at 4 °C. Proteins were washed using increasing concentration of imidazole, and eluted with 500 mM imidazole. Eluted samples were dialysed overnight against PBS buffer at 4 °C using Slide-A-Lyzer dialysis cassette (Thermo Fisher). The His_6 tag was cleaved from Prdx2-Thr-His_6 using the Thrombin Clean-Cleave Kit (Sigma Aldrich) at 17 °C for 4 h, as per the manufacturer's protocol and dialysed against PBS buffer following cleavage. Oxr1-C was produced as described before [28]. Briefly, protein expression was induced at OD_{600} ~ 0.8 by addition of IPTG to a final concentration of 0.8 mM. Bacterial cultures were incubated on a shaker for 16 h at 18 °C and bacterial cells were collected by centrifugation. Protein was purified as described above. Full-length human OXR1 recombinant protein expressed in *E.Coli* was purchased from Origene (TP760961). Purified proteins were analysed by western blotting with anti-Prdx2 and anti-Oxr1 antibodies. Protein concentrations were measured using NanoDrop spectrophotometer with extinction coefficients of 21,555 M^{-1} cm^{-1} for Prdx2 and 38,055 M^{-1} cm^{-1} for Oxr1-C and. DNA fragments encoding TB1D24 full-length (aa 1–553) and TLDc domain (aa 336–553) were subcloned into the pFB-Lic-Bse for insect Sf9 cell expression and pNIC28-Bsa4 for *E. coli* expression, respectively. Recombinant full-length TBC1D24 was expressed in Sf9 cells, while the TBC1D24 TLDc-domain was expressed in *E.Coli* and purified as above, followed by size exclusion chromatography. The purity of the recombinant protein preparation was ascertained by coomassie staining (Supplementary Fig. 1).

2.7. Peroxiredoxin activity assay

Prdx2 activity was assessed using ferrous oxidation-xylenol orange (FOX) assay [38]. The assay solution contained 100 μM dithiothreitol (DTT, Sigma Aldrich), 50 μM H_2O_2 (Sigma Aldrich), 2.2 μg recombinant uncleaved purified Prdx2, with 0 or 0.95 μg Oxr1-C or 4.5 μg OXR1-FL. The reaction was initiated by addition of H_2O_2 and quenched at appropriate time points by addition of 200 μl of FOX reagent (1 part of FOX A reagent (25 mM ammonium ferrous sulfate (Sigma) in 2.5 M H_2SO_4 (Sigma)) and 100 parts of FOX B reagent (100 mM sorbitol (Sigma) with 125 μM xylenol orange (Sigma) in water)). Samples were incubated at room temperature for at least 30 min before reading absorbance at 560 nm with Fluostar Omega plate reader.

2.8. Chaperone activity assay

In vitro holdase activity of cleaved Prdx2 and Oxr1-C was assessed in chemically- and thermally-induced aggregation assays. The ability of Prdx2 and Oxr1-C to protect insulin from DTT-induced aggregation was measured as change of absorbance at 650 nm at 25 °C. The reaction solution contained 30 μg insulin (Sigma Aldrich) with or without 20 μg Prdx2, with 22 μg (6 μM final concentration), 33 μg (9 μM) Oxr1-C, 22 μg Tbc1d24, 22 μg Tbc1d24 TLDc domain or 85 μg (6 μM) OXR1-FL and was initiated by addition of DTT to a final concentration of 6.66 mM. Ability of Prdx2 and Oxr1-C to protect citrate synthase (CS) from aggregating was monitored by changes in absorbance at 360 nm during incubation at 44 °C. Reaction solution contained 10 μg of CS and 10 μg of Prdx2, Oxr1-C or both in 50 mM HEPES pH 8.0.

2.9. Biotin switch assay

The biotin switch assay was performed as previously described using the reagents from the S-nitrosylated protein detection kit (Cayman) [39]. For tissue, snap-frozen brains or cerebella were homogenised in buffer A supplemented with protease inhibitors (Cell Signaling) using a tissue Precellys homogenizer (Bertin Corp.). After centrifugation at maximum speed for 30 min at 4 °C, protein concentration was quantified using a BCA assay (Thermo Scientific) and an equal amount of protein was used per sample. All subsequent steps were performed protected from direct light and in amber tubes. Blocking reagent provided in the kit was added, and samples were incubated for 30 min at 50 °C with regular vortexing. Proteins were subsequently precipitated using cold acetone to remove any trace of blocking reagent, and incubated at −20 °C for at least 30 min, followed by centrifugation at 3000*g* for 10 min at 4 °C. Protein pellets were resuspended in the labelling/reducing reagent provided and prepared as per the manufacturer's instructions. A combined protein sample was incubated with diluted dimethylformamide only as a negative control. Samples were incubated for 1 h at room temperature on a shaker. Proteins were acetone precipitated as above. Protein pellets were resuspended in wash buffer provided; a fraction of the protein extracts was kept aside as input to determine total Prdx2 levels. To pull down S-nitrosylated proteins, protein extracts were incubated overnight at 4 °C on a shaker with 50 μl EZview streptavidin beads (Sigma). Beads were washed three times with wash buffer and resuspended in NuPAGE loading buffer supplemented with β-mercaptoethanol, and boiled for 5 min. Total protein (input) and S-nitrosylated proteins were run on pre-cast NuPAGE gels as per standard procedures. Results were expressed as intensity of signal for SNO-Prdx2 over total level of Prdx2 per sample.

For cells, cells transfected for 48 h and treated with either vehicle or SNOC were washed with PBS and scraped from the dish. After centrifugation at 1000 rpm for 5 min, cell pellets were resuspended directly in blocking reagent diluted in buffer A and incubated at 50 °C for 30 min. After centrifugation and subsequent acetone precipitation, protein pellets were resuspended in labelling/reducing reagent and incubated at room temperature for 1 h. After acetone precipitation, proteins were resuspended in wash buffer and quantified by BCA assay (Thermo Scientific). The subsequent steps are identical as for tissue above.

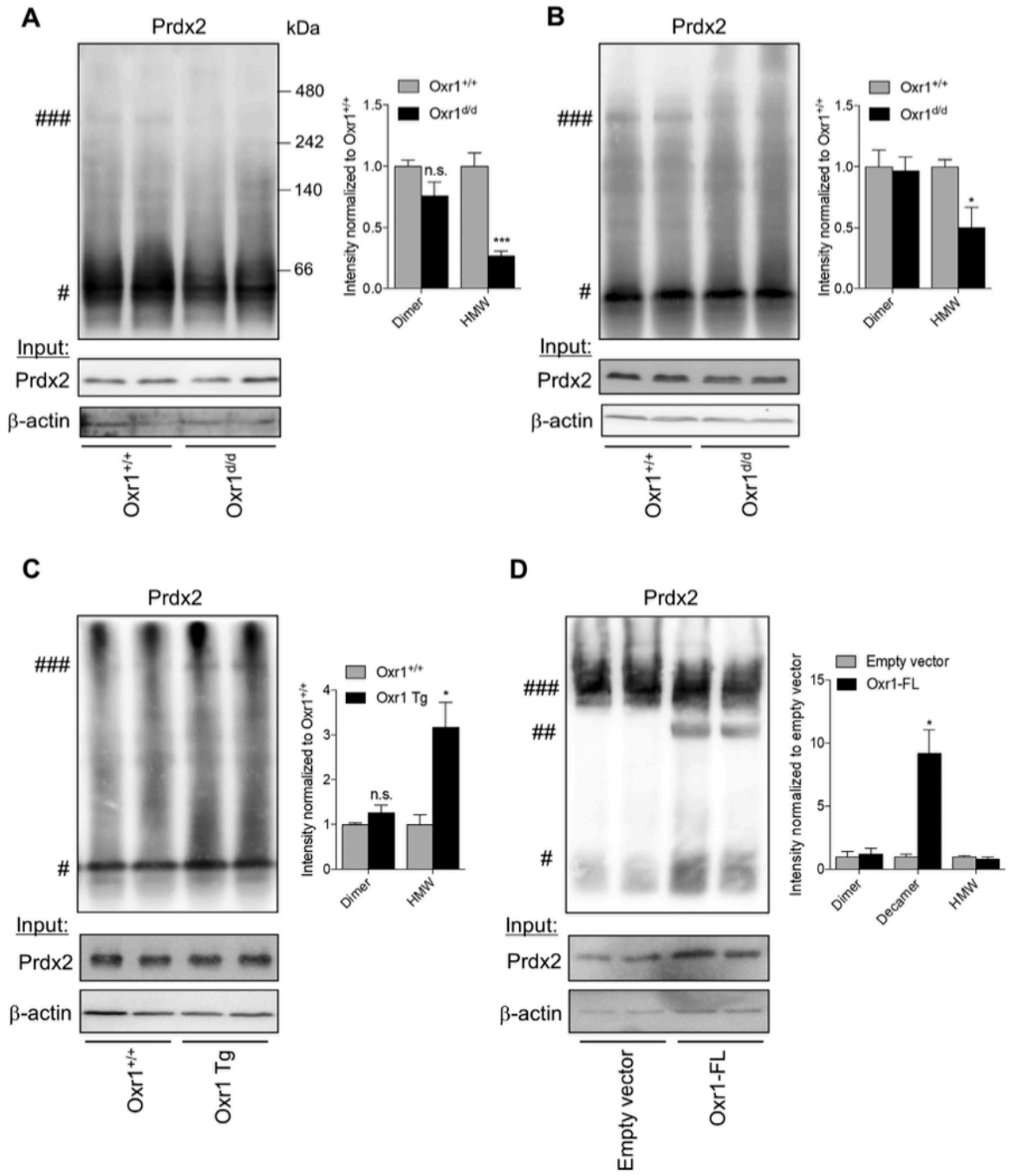


Fig. 1. Oxr1 plays a role in the regulation of the oligomerization status of Prdx2 *in vitro* and *in vivo*. (A-B) Representative western blot of Prdx2 from protein extracts of P18 wild-type control ($Oxr1^{+/+}$) and $Oxr1^{d/d}$ brain tissue with the cerebellum removed (A) and the cerebellum alone (B). Quantification of the HMW Prdx2 complexes (###) and the Prdx2 dimer (#) is shown (N = 8 animals per group (A) and N = 3 (B)). (C) Western blot of Prdx2 from protein extracts of adult wild-type and Oxr1 Tg mouse brains without the cerebellum. Quantification of the HMW Prdx2 complexes and the dimer is shown (N = 3 animals per group). (D) Western blot of Prdx2 from protein extracts of N2A cells transfected with either an empty vector or Oxr1-FL and treated with 300 μM H_2O_2 for 1 h. Quantification of the HMW Prdx2 complexes, the Prdx2 dimer (#) and the decamer (##) is shown (N = 3 independent repeats). For all panels, extracts were run on 10% BN-PAGE (native) gels and levels of Prdx2 and β-actin (input) were determined for the same samples, but run in reducing conditions on separate gels. β-actin was used as a loading control. Data are represented as mean ± SEM. Panels A-D: *t*-test; *p < 0.05, ***p < 0.001.

2.10. Organomercury resin capture (ORC)

ORC from brain and cerebellum tissue was performed as previously described [40]. Briefly, samples were homogenised in homogenization buffer (250 mM HEPES free acid, 1 mM DTPA, 0.1 mM neocuproine, 1% Triton X-100, pH 7.7) using a tissue Precellys homogenizer (Bertin Corp.). Samples were clarified by centrifugation at full speed for 10 min at 4 °C and protein concentration was quantified by BCA assay (Thermo Scientific). An equal amount of protein was used per sample. As a negative control a combined protein sample was incubated with the reducing agent DTT (10 mM) for 15 min at room temperature. Proteins were acetone precipitated and resuspended in blocking buffer (250 mM HEPES acid free, 1 mM DTPA, 0.1 mM neocuproine, 2.5% SDS, pH 7.7) supplemented with 50 mM blocking agent MMTS. Protein extracts were incubated for 30 min at 50 °C, with frequent vortexing, followed by acetone precipitation. Protein pellets were resuspended in loading

buffer (250 mM MES, 1 mM DTPA, 1% SDS, pH 6.0) and ready to be loaded on to the activated resin in glass columns; a fraction was kept aside as input. Organomercury resin (produced by the laboratory of Professor Harry Ischiropoulos University of Pennsylvania, USA and provided by Dr Mark Crabtree, University of Oxford) was washed and activated by consecutive washes with isopropanol, water, 0.1 M sodium bicarbonate pH 8.8, and equilibration buffer (50 mM NaCl, 50 mM MES, 1 mM DTPA, pH 6.0). After the resin was drained, samples were added and capped with 0.5 ml loading buffer and incubated at room temperature for 1 h protected from light to allow the reaction between S-nitrosylated proteins and the organomercury resin. The S-nitrosylated proteins cross-linked to the resin were then washed with consecutive 50 bed volumes of buffer A (50 mM Tris-HCl, 0.3 mM NaCl, 0.5% SDS, pH 7.5), buffer B (50 mM Tris-HCl, 0.3 mM NaCl, 0.05% SDS, pH 7.5), buffer C (50 mM Tris-HCl, 0.3 mM NaCl, 1% Triton X-100, 1 M urea, pH 7.5), and buffer D (50 mM Tris-HCl, 0.3 mM NaCl, 0.1% Triton X-100, 0.1 M urea, pH 7.5), followed by three washes of 200 bed volumes of water. Bound S-nitrosylated protein were then eluted by incubating the resin with 5% performic acid for 45 min at room temperature. The eluted proteins were precipitated by adding one volume of 100% TCA to four volumes of protein sample and incubated overnight at 4 °C. After centrifugation at full speed for 30 min at 4 °C, protein pellets were washed in cold acetone and resuspended in NuPAGE loading buffer supplemented with β-mercaptoethanol, and boiled for 5 min. Total protein (input) and S-nitrosylated proteins were run on pre-cast NuPAGE gels as per standard procedures. Results were expressed as intensity of signal for SNO-Prdx2 over total level of Prdx2 per sample.

2.11. Statistical analyses

Statistical analysis was performed using Prism software using one-way ANOVA or unpaired *t*-test. Data are presented as mean ± SEM.

3. Results

3.1. Oxr1 modulates the oligomerization state of the antioxidant enzyme Prdx2

It has been shown recently that Oxr1 regulates the activity and degree of oligomerization of the multifunctional enzyme glucose-6-phosphate isomerase (GPI/Gpi1) via protein-protein interaction [27]. Therefore, seeing that Oxr1 can influence ROS levels as well as protein multimer formation and aggregation, we tested the hypothesis that Oxr1 is neuroprotective against O/N stress by regulating the function of essential proteins within these two pathways [26,28,36,41]. As a promising candidate interactor for Oxr1, we selected peroxiredoxin 2 (Prdx2) because it acts both as a chaperone and an antioxidant as well as being highly expressed in neurons [42–44]. Indeed, the expression patterns of Prdx2 and Oxr1 overlap in the CNS, including the granule cell layer of the cerebellum [26,42,45]. Furthermore, similar to the knockout of *Oxr1*, loss of *Prdx2* in mice leads to accumulation of ROS and oxidative DNA damage, although this occurs in the CA1 region of the hippocampus as opposed to the cerebellum of *Oxr1* knockout mutants [46].

Given that the multiple functions of Prdx2 are regulated by its degree of oligomerization, we first tested whether Oxr1 levels would affect Prdx2 oligomerization in the brain [47,48]. Using non-reducing native PAGE to preserve protein complexes, we assessed Prdx2 oligomerization in tissues from a constitutive *Oxr1* knockout mouse in which all isoforms of the protein are disrupted ($Oxr1^{d/d}$) [26–28]. Tissue samples were collected at a pre-symptomatic timepoint (P18), prior to the onset of neurodegeneration in this model. In wild-type ($Oxr1^{+/+}$) brain tissue, we observed a dimeric form of Prdx2 in addition to HMW complexes with an apparent molecular weight of approximately 400 kDa, as previously described (Fig. 1A) [48–50]. Interestingly, there was a significant decrease in these HMW Prdx2 complexes in the brain of $Oxr1^{d/d}$ mice compared to wild-type controls, both in the brain without the cerebellum (Fig. 1A) and in the cerebellum alone (Fig. 1B). To confirm that Oxr1 levels regulate Prdx2 oligomerization, we next assessed the levels of Prdx2 multimers in brains from adult mice overexpressing an HA-tagged full-length Oxr1 (Oxr1-FL) cDNA transgene (Oxr1 Tg) [28]. Conversely to the observations from $Oxr1^{d/d}$ knockout mice, levels of the HMW Prdx2 complexes were significantly increased in Oxr1 Tg tissue compared to wild-type controls (Fig. 1C). Together, these data suggest that the levels of Oxr1 modulate Prdx2 oligomerization *in vivo*. To validate that higher levels of Oxr1 indeed favour higher-order Prdx2 complexes, we next analysed the degree of oligomerization of Prdx2 in cells over-expressing Oxr1 and upon treatment with H_2O_2 to promote assembly of HMW Prdx2 complexes via Prdx2 overoxidation [48,50,51]. Interestingly, in cells over-expressing Oxr1-FL, specific HMW Prdx2 complexes were detected - namely its decameric species at the molecular weight of approximately 220 kDa - while this was not present in control vector-transfected cells (Fig. 1D). Overall, our data suggest that Oxr1 is able to modulate Prdx2 oligomerization.

3.2. Oxr1 interacts with the antioxidant enzyme Prdx2

To understand the mechanism by which Oxr1 regulates the oligomerization of Prdx2, we next tested whether Oxr1 and Prdx2 could interact. To assess binding between Prdx2 and Oxr1, we performed co-immunoprecipitation experiments in neuronal N2A cells co-expressing Prdx2 and either Oxr1-FL or the shortest Oxr1 isoform (Oxr1-C). The latter isoform primarily consists of the TLDc domain, but is highly expressed in the brain and has a proven function as a neuroprotective protein [26,28]. Both Oxr1 isoforms were found to co-immunoprecipitate with Prdx2 (Fig. 2A). The TLDc domain is common between both Oxr1 isoforms, thus we went on to investigate whether this interaction would be maintained with other TLDc-containing proteins. We discovered that Prdx2 also interacts with full-length nuclear receptor coactivator 7 (Ncoa7-FL), and to a lesser extent with the shorter TLDc domain-containing isoform (Ncoa7-B) (Fig. 2A). We also observed binding to Tbc1d24, suggesting that Prdx2 is a common binding partner for most of the TLDc proteins (Fig. 2A). To investigate whether the Oxr1 interaction occurs *in vivo*, we performed co-immunoprecipitation from wild-type mouse brain tissue and detected an interaction between endogenous Oxr1 and Prdx2, confirming our *in vitro* data (Fig. 2B).

3.3. Oxr1 and Prdx2 do not synergistically regulate H_2O_2–induced cell death

To investigate the significance of the Oxr1:Prdx2 interaction, we next tested systematically how Oxr1 and Prdx2 might influence each other's functional roles. Both Oxr1 and Prdx2 have been shown to be neuroprotective under oxidative stress; therefore, we quantified H_2O_2-induced cell death in a neuronal cell line expressing either Oxr1, Prdx2 or both proteins [26,52]. Consistent with previous reports, over-expression of Oxr1-FL, Oxr1-C or Prdx2 significantly reduced cell death under oxidative stress conditions; however, Prdx2 was significantly less protective than Oxr1 in this assay (Fig. 2C) [26,28,53]. Co-expression of Prdx2 together with Oxr1 did not alter significantly the neuroprotective properties of Oxr1.

Considering that Prdx2 can reduce H_2O_2 at a high kinetic rate, we next investigated whether the neuroprotection against oxidative stress that is conferred by Oxr1 could be via regulation of Prdx2 activity [54,55]. To test this, we carried out a peroxide activity assay that measures reduction of H_2O_2 using purified recombinant proteins, and as expected, recombinant Prdx2 was able to dramatically reduce H_2O_2 levels (Fig. 2D) [37]. Recombinant Oxr1-C and OXR1-FL were not, however, able to reduce H_2O_2 levels in this assay, similar to what has been observed previously (Fig. 2D) [28]. When Prdx2 and Oxr1-C were

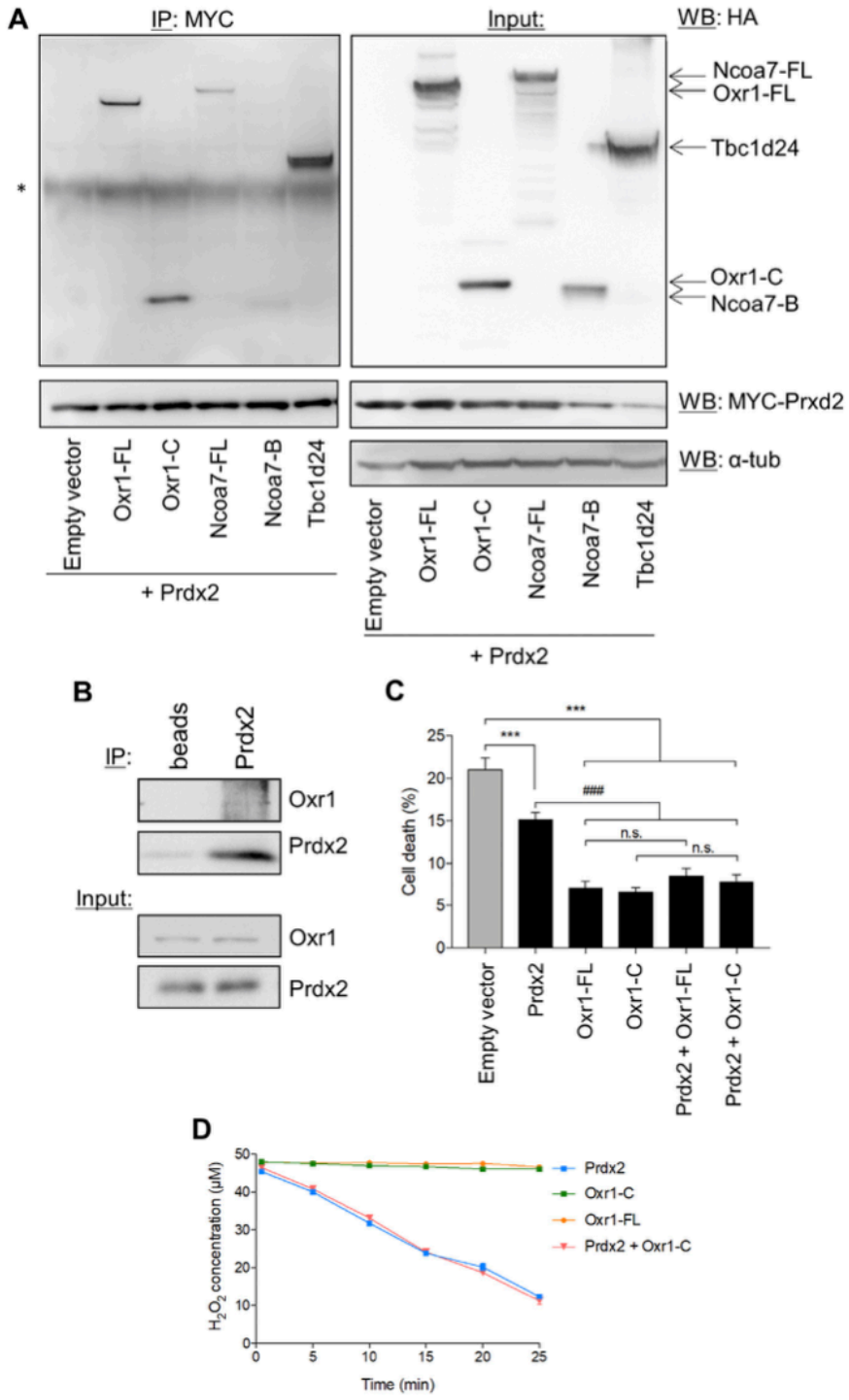


Fig. 2. Prdx2 binds to TLDc proteins, but does not interact functionally with Oxr1 to regulate H_2O_2-induced cell death. (A) N2A cells were co-transfected with Prdx2-MYC and HA-tagged TLDc constructs as indicated and data from co-immunoprecipitations (IP) of the TLDc proteins using an anti-MYC antibody are shown by immunoblotting for HA (left panel). α-tubulin was used as a loading control for the input samples (right panel). The asterisk (*) represents non-specific IgG heavy chains. (B) Co-immunoprecipitation of Oxr1-FL with Prdx2 from adult wild-type mouse brain tissue (excluding the cerebellum). (C) N2A cells transfected with the indicated constructs were treated with 500 μM H_2O_2 for 5 h and cell death was quantified as the number of pyknotic nuclei. 10 fields of view per condition were quantified (N = 100–150 cells per field of view). (D) Changes in H_2O_2 concentration were monitored using a colorimetric ferrous oxidation-xylenol orange (FOX) assay over 25 min with either recombinant purified Prdx2, Oxr1-C, OXR1-FL or Prdx2 with Oxr1-C proteins with 50 μM H_2O_2. (N = 3 independent repeats). Data are represented as mean ± SEM. Panel C: 1-way ANOVA; $^{***}p < 0.001$ compared to empty vectors, $^{###}p < 0.001$ compared to transfection with Prdx2.

incubated together, no enhancement in the rate of H_2O_2 decay was observed as compared to the rate observed for Prdx2 alone (Fig. 2D), suggesting that Prdx2 and Oxr1 do not interact synergistically to regulate cell death under oxidative stress or to reduce H_2O_2 levels.

3.4. Oxr1 and Prdx2 both modulate protein aggregation in vitro

As well as being an antioxidant enzyme, Prdx2 also possesses holdase activity [48,56]. Holdases are a class of chaperones that bind unfolded or misfolded molecules and prevent them from aggregating in an ATP-independent manner [17]. To investigate any functional interactions between Oxr1 and Prdx2 that may modulate Prdx2 chaperone activity, we used a well-established *in vitro* aggregation assay with recombinant proteins. Insulin was induced to form large aggregates by incubation with DTT; its aggregation correlates with an increased turbidity of the reaction solution, which can be quantified by spectrophotometry [57]. Using this system, we observed a reduction in the aggregation of insulin in the presence of recombinant Prdx2, as expected, while lysozyme, a non-chaperone control, did not affect aggregation (Fig. 3A-C). Importantly, when Prdx2 was incubated with recombinant Oxr1-C, this led to a further significant reduction in insulin aggregation rate and in the aggregation at endpoint as compared to Prdx2 alone; this suggests that Oxr1-C may enhance the chaperone activity of Prdx2 (Fig. 3A-C). We confirmed these data by using a

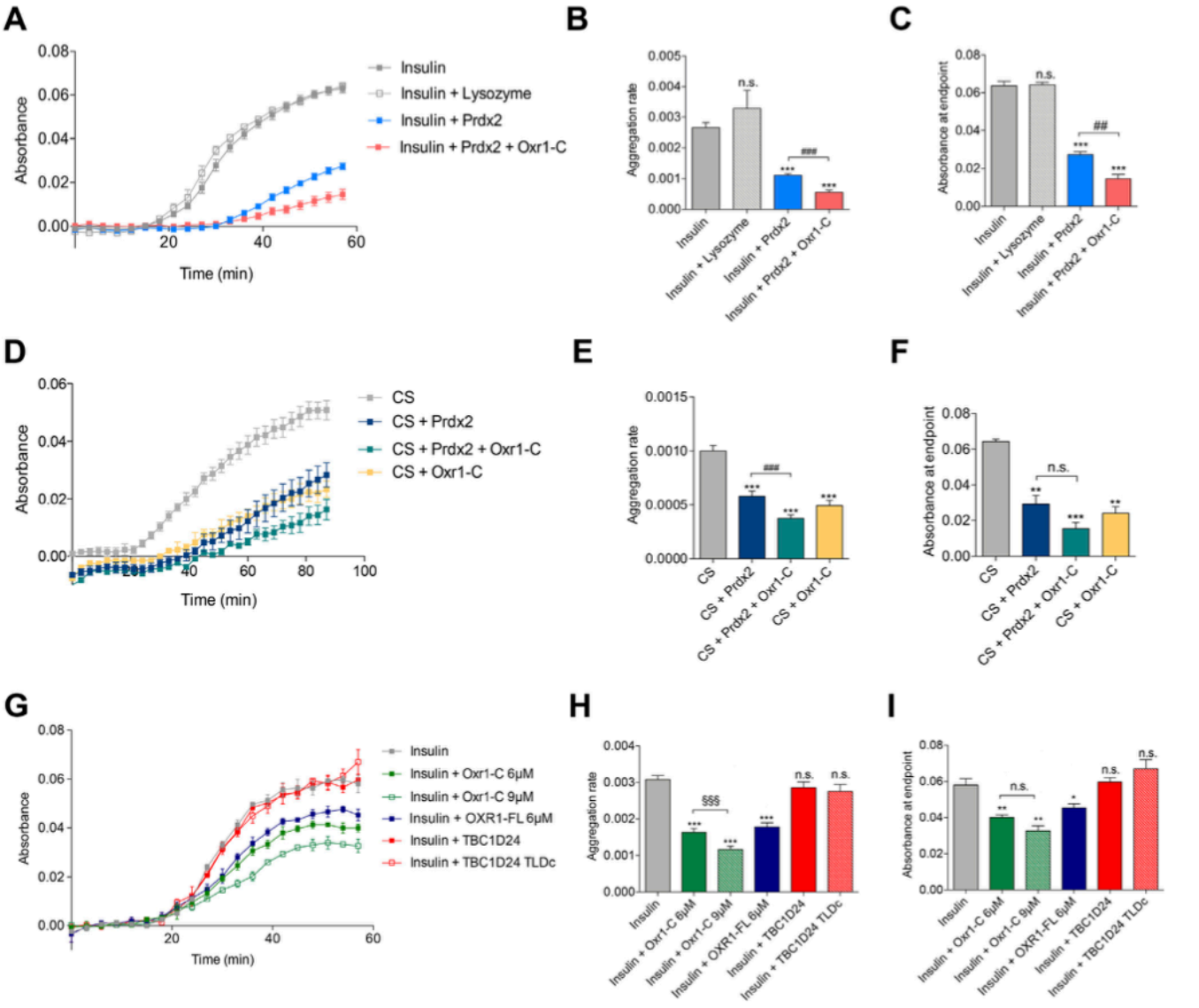


Fig. 3. Prdx2 and Oxr1 possess holdase activity. (A-C) DTT-induced insulin aggregation assay using recombinant Prdx2 and Oxr1-C with lysozyme as a negative control. Absorbance readings at 650 nm were taken every 3 min (A). Quantification of the aggregation rate (B) and absorbance at endpoint (C) are shown. (D-F) Thermally-induced citrate synthase (CS) aggregation assay using recombinant Prdx2 and Oxr1-C. Absorbance readings at 360 nm were taken every 3 min (D). Aggregation rate (E) and absorbance at end point (F) are shown. (G-I) DTT-induced insulin aggregation assay using two concentrations (6 μM and 9 μM) of recombinant Oxr1-C or human OXR1-FL (6 μM), in parallel with human TBC1D24 and the TLDc domain of TBC1D24 (TBC1D24 TLDc). Absorbance readings at 650 nm were taken every 3 min (G). Quantification of the aggregation rate (H) and absorbance at endpoint (I) are presented. (A-I) All values are shown as normalized to the background signal. Data are represented as mean ± SEM. B, C, H, I, E, F: *t*-test, $^{*}p < 0.05$, $^{**}p < 0.01$, $^{***}p < 0.001$ as compared to insulin (B, C, H, I) or CS (E, F), $^{\#\#}p < 0.01$, $^{\#\#\#}p < 0.001$ as compared to insulin + Prdx2 (B, C, H, I) or CS + Prdx2 (E, F), $^{\S\S\S}p < 0.001$ as compared to insulin + Oxr1-C 6 μM (H, I).

second aggregation assay that utilises thermally-induced aggregation of citrate synthase (CS). In agreement with the insulin aggregation data, the presence of Prdx2 reduced the thermally-induced aggregation of CS, and the rate of aggregation was significantly reduced further when Prdx2 was co-incubated with Oxr1-C (Fig. 3D-F).

Surprisingly, when these assays were performed with Oxr1-C only, we detected a significant reduction of approximately 50% in both the chemically- and thermally-induced aggregation rate of insulin and CS (Fig. 3D-I). Given that these assays are cell-free, these data are not reliant on other proteins, thus suggesting that Oxr1-C possesses a potential holdase activity. To confirm this observation, we tested whether increasing Oxr1-C concentration would lead to an increase in protective activity against chemically-induced protein aggregation. We did observe a significant decrease in substrate aggregation rate as well as a slight reduction in the aggregation at end point with an increased concentration of Oxr1-C, further supporting a chaperone activity for Oxr1-C (Fig. 3G-I).

As the Oxr1-C isoform is mainly comprised of the TLDc domain, our data indicate that the chaperone activity we observe may be conserved in other TLDc-containing proteins. To test this hypothesis, we quantified the chaperone activity of full-length OXR1 (OXR-FL) and TBC1D24 using the chemically-induced protein aggregation assay. Using a recombinant OXR1-FL, we detected a significant reduction in both the aggregation rate and aggregation at end point compared to the control, suggesting that OXR1-FL also possesses holdase activity (Fig. 3G-I). Interestingly, we did not detect any reduction in the formation of insulin aggregates when incubated with full-length TBC1D24, suggesting that TBC1D24 does not possess holdase activity (Fig. 3G-I). We performed a similar experiment using a recombinant protein constituted of only the C-terminal TLDc domain of TBC1D24. Similar to full-length TBC1D24, the TLDc domain alone did not show any chaperone activity (Fig. 3G-I). Therefore, we have identified a novel activity for Oxr1 as a

potential holdase that is likely not conserved with the related TLDc protein TBC1D24.

3.5. Oxr1 modulates Prdx2 post-translational modifications (PTMs)

Prdx2 function is regulated by its level of oligomerization and through PTMs such as overoxidation and S-nitrosylation, in addition to conformational changes [48,58–60]. In particular, reversible oxidation of catalytic cysteine residues occurs during the catalytic cycle of Prdx2: in the presence of low levels of H_2O_2, Prdx2 is oxidised and reactivated, while under high levels of H_2O_2, its cysteine residues are overoxidized, forming sulfinic and sulfonic acid (Prdx-$SO_{2/3}$), which inactivates its antioxidant activity but stabilizes the HMW complexes which drive its chaperone activity [48,51,61]. Given our findings that Oxr1 levels modulate Prdx2 oligomerization, we next investigated whether Oxr1 could affect Prdx2 overoxidation. We first assessed overoxidation of endogenous Prdx2 *in vitro* by quantifying the levels of Prdx2-$SO_{2/3}$ over the total level of Prdx2 from H_2O_2-treated cells. Using an antibody that recognises overoxidized Prdx1, Prdx2, Prdx3 and Prdx4, we confirmed previously reported overoxidation of the aforementioned Prdxs induced by H_2O_2 treatment [62]. Interestingly, under these conditions, levels of Prdx2 overoxidation were significantly higher in cells overexpressing Oxr1-FL (Fig. 4A) and a similar effect was observed in cells over-expressing Oxr1-C (Fig. 4B). This suggests that Oxr1 modulates, directly or indirectly, Prdx2 overoxidation. We next tested if levels of Oxr1 would similarly affect overoxidation of Prdx2 *in vivo* by using the cerebellum and the remaining brain tissue from Oxr1 Tg mice or control littermates. Similar to what we observed *in vitro* in Oxr1 over-expressing cells, a significant increase in Prdx2 overoxidation levels in brain of transgenic animals were detectable as compared to wild-type mice (Fig. 4C). There was also a significant increase in Prdx2-$SO_{2/3}$ levels in cerebellar tissue from Oxr1 Tg mice (Fig. 4D). To further investigate the role of Oxr1 in regulating Prdx2 overoxidation, we analysed the levels of Prdx-$SO_{2/3}$ in brains from *Oxr1*$^{d/d}$ mice as compared to controls at the presymptomatic P18 timepoint. We did not observe any significant changes in Prdx2 overoxidation in the brain (Fig. 4E); however, levels of Prdx2-$SO_{2/3}$ were significantly reduced in cerebella from *Oxr1*$^{d/d}$ animals as compared to controls (Fig. 4F). These data suggest that Oxr1 regulates levels of Prdx2 overoxidation; interestingly, this occurs differentially in the cerebellum – the site of neurodegeneration in the *Oxr1*$^{d/d}$ mutant – as compared to the rest of the brain.

S-nitrosylation is another essential PTM regulating Prdx2 function. Indeed, addition of an NO group at its cysteine residues has been shown to reduce the antioxidant activity of Prdx2 [58]. To test whether Oxr1 would have an effect on Prdx2 S-nitrosylation *in vitro*, we used a neuronal cell line SH-SY5Y treated with the physiological cell-permeable NO-donor, S-nitrosocysteine (SNOC), to induce S-nitrosylation of proteins. Using a biotin switch assay, we quantified levels of S-nitrosylated endogenous PRDX2 (SNO-PRDX2) and found that cells treated with SNOC show a significant increase in levels of SNO-PRDX2, as previously described (Fig. 5A) [58]. However, both in vehicle- and SNOC-treated conditions, the levels of SNO-PRDX2 were significantly reduced when cells were over-expressing Oxr1-FL or Oxr1-C as compared to control cells suggesting that Oxr1 reduces SNO-Prdx2 levels (Fig. 5A). To test whether similar observations could be made *in vivo*, we quantified the levels of SNO-Prdx2 in brain and cerebellum extracts from Oxr1 Tg mice and wild-type controls. While levels of SNO-Prdx2 in the brain were slightly decreased without reaching significance (Fig. 5B), we showed a significant reduction in the levels of SNO-Prdx2 in the cerebella of Oxr1 Tg mice as compared to controls (Fig. 5C). To investigate further whether levels of Oxr1 modulate SNO-Prdx2, we next quantified the levels of SNO-Prdx2 in *Oxr1*$^{d/d}$ mice using two different approaches: first, the originally described biotin switch method to detect SNO-proteins, that converts S-nitrosylated residues to biotinylated cysteines which are then immunoprecipitated by streptavidin beads, and second, a newly developed approach, organomercury resin capture (ORC) that relies on the selective and semi-stable reaction of S-nitrosylated residues with phenylmercury compounds of an organomercury resin [40,63]. We showed that SNO-Prdx2 levels were similar in the brain of *Oxr1*$^{d/d}$ and control animals, using either the biotin switch or ORC approach (Fig. 5D and 5F). In contrast, a significant increase in the levels of SNO-Prdx2 was seen with both approaches in cerebella of *Oxr1*$^{d/d}$ mice as compared to controls (Fig. 5E and 5G) suggesting that Oxr1 participates in the modulation of Prdx2 S-nitrosylation in the cerebellum. Together, we have shown that Oxr1 modulates two essential Prdx2 PTMs, overoxidation and S-nitrosylation.

4. Discussion

Our current study sheds new light on the molecular mode of action of Oxr1 as a functional switch for the essential antioxidant and chaperone Prdx2. Indeed, we show that Oxr1 modulates oligomerization of HMW Prdx2 chaperone complexes and key PTMs regulating the dual functions of Prdx2.

Our study is in accordance with our previous observations that Oxr1 reduces aggregation of the mutated ALS-associated TDP-43 and FUS proteins in cellular models of ALS; this process relies on the interaction between Oxr1 and TDP-43 or FUS, but is independent of the proteasome or autophagy [36]. Based on our current findings, we hypothesise that Oxr1 may reduce protein aggregation first through its chaperone activity and second by favoring the formation of HMW Prdx2 chaperone complexes. Another key function described for Oxr1 is its ability to reduce levels of ROS and oxidative stress markers in oxidative stress-treated neurons as well as in SOD1^{G93A} ALS mouse model [26,29]. However, Oxr1 has no direct catalytic activity, thus it has remained unclear how Oxr1 could carry out this role. Here, we showed that Oxr1 regulates the activity of the antioxidant protein Prdx2, in particular, by modulating two key PTMs of Prdx2, its overoxidation and S-nitrosylation: loss of Oxr1 increases SNO-Prdx2 and reduces its overoxidation, while increasing Oxr1 levels leads to the opposite effect. This is significant because these PTMs regulate Prdx2 antioxidant activity and are intertwined: S-nitrosylation of Prdx2 reduces its H_2O_2-induced overoxidation and inhibits its antioxidant activity [58]. By affecting both the degree of oligomerization and the PTMs of Prdx2, Oxr1 could potentially fine-tune the amount of peroxidases versus chaperones in cells. A slight shift in this proportion could have a major impact on the global cell function given that Prdxs represent 0.2–0.8% of the total soluble protein fraction in cells and tissues, and that Prdx2 is highly expressed in neurons [42–44,64]. Therefore, Oxr1 may indirectly regulate the levels of oxidative stress in cells by modulating the PTMs of Prdx2 and subsequently fine-tuning its antioxidant activity. This newly described function is likely to run in concert with the proposed role for Oxr1 as a regulator of antioxidant gene expression, this latter regulatory hypothesis being supported by a number of studies that have combined OXR1 knock-down with genome-wide or targeted transcriptomics [30,33]. Further work is required to understand the molecular mechanisms involved, although there is evidence that gene modulation via p53-associated pathways is more plausible than Oxr1 acting upstream of the antioxidant Nrf2 signaling cascade [30,31].

The current study also provides an insight into the link between loss of Oxr1 and cellular degeneration in the cerebellum of the *Oxr1*$^{d/d}$ mouse [28]. We observed higher levels of SNO-Prdx2 and reduced levels of Prdx2-$SO_{2/3}$ in the neurodegenerative *Oxr1* knockout mouse at a presymptomatic stage, specifically in the cerebellum - the only brain region affected in this mutant - suggesting that aberrant PTM of Prdx2 may participate in the neurodegeneration observed in this mouse. Importantly, SNO-Prdx2 breaks the normal redox cycle that regenerates Prdx2, inhibiting Prdx2 antioxidant activity and leading to high levels of oxidative stress in cells [58]. Increased levels of SNO-Prdx2 have been observed in the brain of the PQ/MB-exposed PD mouse model, as well as in dopaminergic neurons differentiated from induced pluripotent stem cells from PD patients and in *post mortem* brains of PD

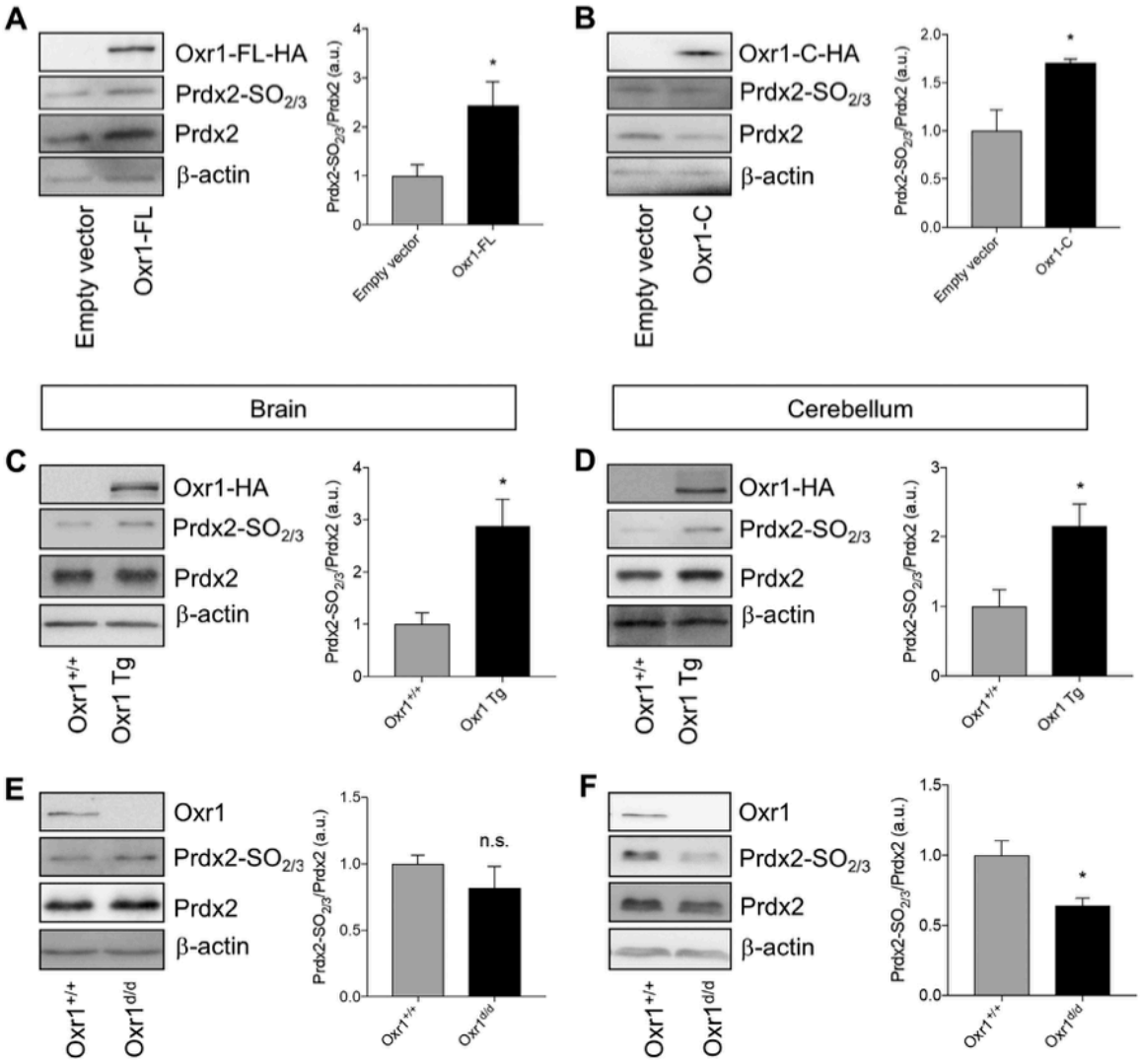


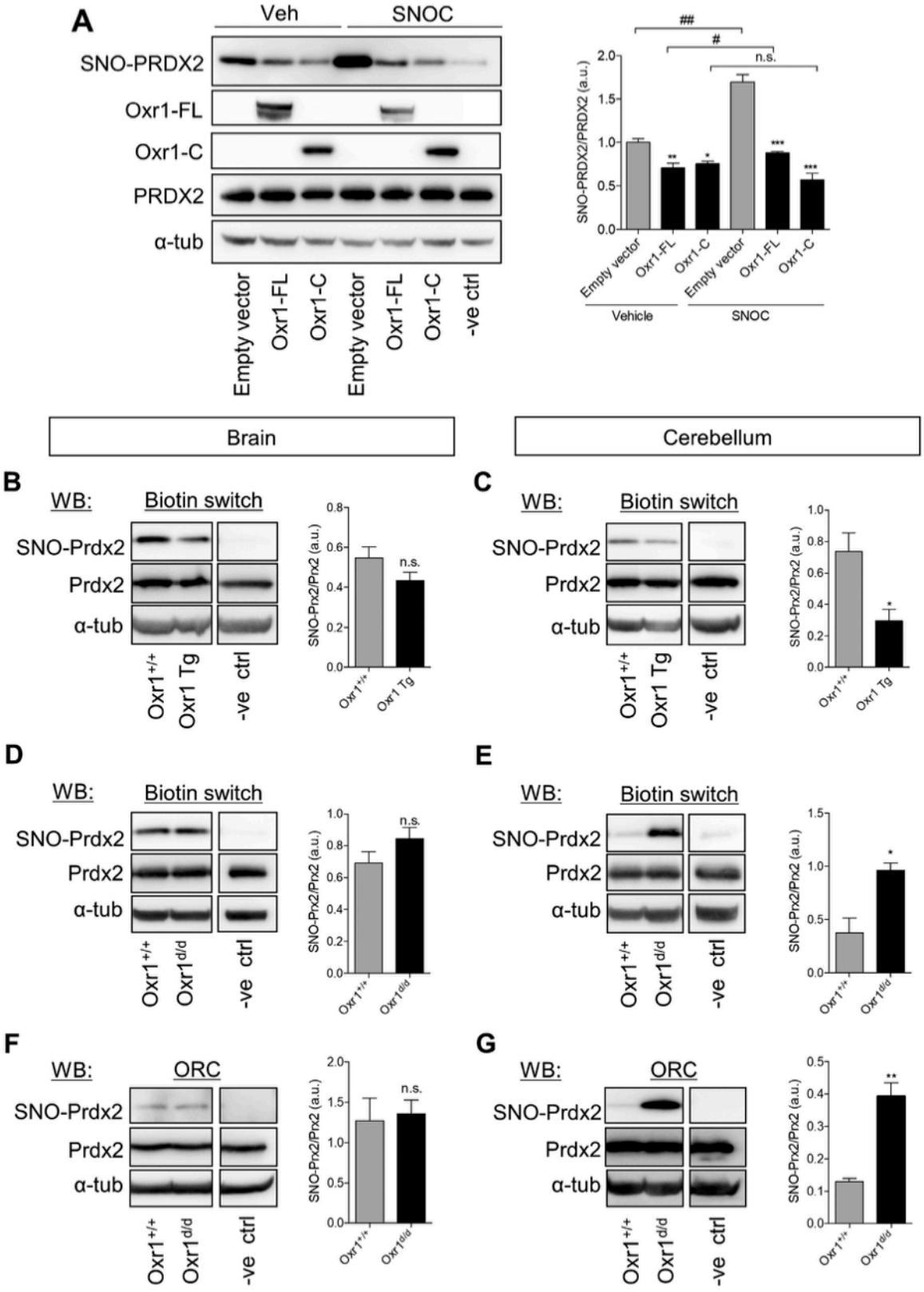
Fig. 4. Oxr1 modulates overoxidation of Prdx2 catalytic residues *in vitro* and *in vivo*. (A-B) N2A cells were transfected with either Oxr1-FL (A) or Oxr1-C (B) and treated with 300 μM H_2O_2 for 1 h. Representative image of western blots and quantification of Prdx2 overoxidation is shown as the ratio of Prdx2-$SO_{2/3}$ to total Prdx2 (N = 6 independent repeats for Oxr1-FL and N = 3 independent repeats for Oxr1-C). (C-F) Representative westerns blots of protein extracts from an adult Oxr1 overexpressing mouse (Oxr1 Tg) (C-D) and a P18 Oxr1 knockout ($Oxr1^{d/d}$) mouse (E-F) from both the brain lacking the cerebellum and cerebellar tissues, with quantification of Prdx2 overoxidation compared to wild-type controls (N = 3–4 animals per group). β-actin was used as a loading control. Data presented as mean ± SEM. Panels A-F: *t*-test; $^*p < 0.05$.

patients, suggesting that SNO-Prdx2 participates in the neurodegenerative process [58,65]. It was also shown *in vitro* that S-nitrosylation of Prdx2 led to a reduction of Prdx2-$SO_{2/3}$ and of its neuroprotective function against H_2O_2 –induced apoptosis [58]. Therefore, our current model is that loss of *Oxr1* in the knockout mouse model impairs Prdx2 chaperone activity through reduction of HMW Prdx2 chaperone complexes and reduction of the complexes-stabilising PTM, Prdx2-$SO_{2/3}$. In addition, Prdx2 antioxidant activity is also inactivated by the increase in S-nitrosylation of Prdx2. These changes in PTMs being cerebellum-specific, this may lead to a detrimental increase in protein aggregation and oxidative stress in the cerebellum, precipitating the degeneration of the cerebellar granule cells in *Oxr1* knockout animals. Of note, we focused here on overoxidation and S-nitrosylation of Prdx2; however, Prdx2 function can be affected by other PTMs, such as phosphorylation and nitration, which have also been involved in neurodegeneration [66].

Using two *in vitro* assay systems, we have discovered that Oxr1-C and OXR1-FL possess a potential holdase activity. Because Oxr1-C is almost exclusively constituted of the TLDc domain, we tested whether this function was shared with another TLDc-containing protein. Surprisingly, however, TBC1D24 did not possess any holdase activity; neither the full-length protein nor the TLDc domain alone. This interesting finding indicates that, although all TLDc-containing proteins are neuroprotective, they may also carry out their own specific functions [23]. This may be driven in part by key residues in the TLDc domain that are yet to be identified. Importantly, we also showed that Tbc1d24 interacts with Prdx2, suggesting that the holdase activity is independent of the ability to bind Prdx2. Here, we have focused on the interplay between Oxr1 and Prdx2; yet the fact that Prdx2 has the ability to bind to other TLDc-containing proteins suggests that functional compensation and competition with other TLDc proteins may play a part, and would require further investigation.

5. Conclusions

In summary, our study not only discovered a new function for Oxr1 as a potential holdase, it also identified a novel mode of action for Oxr1, acting on the oxidative stress response and protein aggregation by modulating the oligomerization and PTMs of the fundamental antioxidant enzyme Prdx2. Our study also places Oxr1 at the intersection



(caption on next page)

between two key pathways involved in the neurodegenerative process.

Acknowledgments

The research leading to these results has received funding from the European Research Council under the European Union's Seventh Framework Programme (FP7/2007–2013)/ERC grant agreement number 311394/'PAROSIN' to PLO and supporting PLO, MJF and DMS, and from the John Fell Oxford University Press (OUP) Research Fund (to MF - PLO, JS, and MC co-PI). We thank Professor Harry

Fig. 5. Oxr1 regulates S-nitrosylation of Prdx2 *in vitro* and *in vivo* in the cerebellum. (A) SH-SY5Y cells were treated for 30 min with 200 μM SNOC or vehicle (veh) and processed for the biotin switch assay to quantify the levels of S-nitrosylated endogenous PRDX2 (SNO-PRDX2) by western blot in the presence of the constructs as indicated. (N = 3 independent repeats). (B-C) Representative western blots of SNO-Prdx2 levels in brain (B) or cerebellum (C) as determined by biotin switch from mice over-expressing Oxr1 (Oxr1 Tg) compared to wild-type controls ($Oxr1^{+/+}$) (N = 3 animals per group). (D-E) SNO-Prdx2 levels in brain (D-F) or cerebellum (E-G) determined by biotin switch (D-E) or organomercury resin capture (ORC, F-G) from Oxr1 knockout ($Oxr1^{d/d}$) mice compared to wild-type controls (N = 3 animals per group). In all panels, quantification is shown as the ratio of SNO-Prdx2 to total Prdx2 with α-tubulin used as a loading control. Data presented as mean ± SEM. Negative controls (-ve Ctrl) were combined proteins diluted in dimethylformamide without labelling/reducing reagent (for biotin switch) or proteins incubated with 10 mM DTT for 15 min (for ORC). Panel A: 1-way ANOVA (comparison of constructs to empty vector in either vehicle or SNOC-treated condition) and *t*-test (comparison of each construct between vehicle and SNOC-treated conditions), Panels B-G: *t*-test; $^{*}p < 0.05$, $^{**}p < 0.01$, $^{***}p < 0.001$ as compared to empty vector-transfected cells or to control mice, $^{\#}p < 0.05$, $^{\#\#}p < 0.01$ as compared to vehicle treated cells.

Ischiropoulos and Dr Paschalis-Thomas Doulias, University of Pennsylvania, USA for producing the organomercury resin.

Appendix A. Supplementary material

Supplementary data associated with this article can be found in the online version at doi:10.1016/j.freeradbiomed.2018.10.447.

References

[1] L.G. Apostolova, Alzheimer's disease, Continuum 22 (2) (2016) 419–434.
[2] A. Chio, G. Logroscino, B.J. Traynor, J. Collins, J.C. Simeone, L.A. Goldstein, L.A. White, Global epidemiology of amyotrophic lateral sclerosis: a systematic review of the published literature, Neuroepidemiology 41 (2) (2013) 118–130.
[3] S.J. Evans, I. Douglas, M.D. Rawlins, N.S. Wexler, S.J. Tabrizi, L. Smeeth, Prevalence of adult Huntington's disease in the UK based on diagnoses recorded in general practice records, J. Neurol. Neurosurg. Psychiatry 84 (10) (2013) 1156–1160.
[4] J.K. Andersen, Oxidative stress in neurodegeneration: cause or consequence? Nat. Med. 10 Suppl. (2004) S18–S25.
[5] K.K. Chung, K.K. David, Emerging roles of nitric oxide in neurodegeneration, Nitric Oxide 22 (4) (2010) 290–295.
[6] D.P. Jones, Radical-free biology of oxidative stress, Am. J. Physiol. Cell Physiol. 295 (4) (2008) C849–C868.
[7] J. Navarro-Yepes, L. Zavala-Flores, A. Anandhan, F. Wang, M. Skotak, N. Chandra, M. Li, A. Pappa, D. Martinez-Fong, L.M. Del Razo, B. Quintanilla-Vega, R. Franco, Antioxidant gene therapy against neuronal cell death, Pharmacol. Ther. 142 (2) (2014) 206–230.
[8] T.T. Reed, W.M. Pierce Jr., D.M. Turner, W.R. Markesbery, D.A. Butterfield, Proteomic identification of nitrated brain proteins in early Alzheimer's disease inferior parietal lobule, J. Cell. Mol. Med. 13 (8B) (2009) 2019–2029.
[9] T.T. Reed, Lipid peroxidation and neurodegenerative disease, Free Radic. Biol. Med. 51 (7) (2011) 1302–1319.
[10] Y. Chang, Q. Kong, X. Shan, G. Tian, H. Ilieva, D.W. Cleveland, J.D. Rothstein, D.R. Borchelt, P.C. Wong, C.L. Lin, Messenger, RNA oxidation occurs early in disease pathogenesis and promotes motor neuron degeneration in ALS, PLOS One 3 (8) (2008) e2849.
[11] B. Halter, J.L. Gonzalez de Aguilar, F. Rene, S. Petri, B. Fricker, A. Echaniz-Laguna, L. Dupuis, Y. Larmet, J.P. Loeffler, Oxidative stress in skeletal muscle stimulates early expression of Rad in a mouse model of amyotrophic lateral sclerosis, Free Radic. Biol. Med. 48 (7) (2010) 915–923.
[12] D. Hartl, V. Schuldt, S. Forler, C. Zabel, J. Klose, M. Rohe, Presymptomatic alterations in energy metabolism and oxidative stress in the APP23 mouse model of Alzheimer disease, J. Proteome Res. 11 (6) (2012) 3295–3304.
[13] M.S. Medeiros, A. Schumacher-Schuh, A.M. Cardoso, G.V. Bochi, J. Baldissarelli, A. Kegler, D. Santana, C.M. Chaves, M.R. Schetinger, R.N. Moresco, C.R. Rieder, M.R. Fighera, Iron and oxidative stress in Parkinson's disease: an observational study of injury biomarkers, PLOS One 11 (1) (2016) e0146129.
[14] A. Skoumalova, J. Hort, Blood markers of oxidative stress in Alzheimer's disease, J. Cell. Mol. Med. 16 (10) (2012) 2291–2300.
[15] P.K. Andrus, T.J. Fleck, M.E. Gurney, E.D. Hall, Protein oxidative damage in a transgenic mouse model of familial amyotrophic lateral sclerosis, J. Neurochem. 71 (5) (1998) 2041–2048.
[16] I. Lindberg, J. Shorter, R.L. Wiseman, F. Chiti, C.A. Dickey, P.J. McLean, Chaperones in neurodegeneration, J. Neurosci. 35 (41) (2015) 13853–13859.
[17] R.U. Mattoo, P. Goloubinoff, Molecular chaperones are nanomachines that catalytically unfold misfolded and alternatively folded proteins, Cell. Mol. Life Sci. 71 (17) (2014) 3311–3325.
[18] L. De Mena, E. Coto, E. Sanchez-Ferrero, R. Ribacoba, L.M. Guisasola, C. Salvador, M. Blazquez, V. Alvarez, Mutational screening of the mortalin gene (HSPA9) in Parkinson's disease, J. Neural Transm. 116 (10) (2009) 1289–1293.
[19] R. Wadhwa, J. Ryu, H.M. Ahn, N. Saxena, A. Chaudhary, C.O. Yun, S.C. Kaul, Functional significance of point mutations in stress chaperone mortalin and their relevance to Parkinson disease, J. Biol. Chem. 290 (13) (2015) 8447–8456.
[20] M.E. Conway, M. Harris, S-nitrosylation of the thioredoxin-like domains of protein disulfide isomerase and its role in neurodegenerative conditions, Front. Chem. 3 (2015) 27.
[21] G.S. Jeon, T. Nakamura, J.S. Lee, W.J. Choi, S.W. Ahn, K.W. Lee, J.J. Sung, S.A. Lipton, Potential effect of S-nitrosylated protein disulfide isomerase on mutant SOD1 aggregation and neuronal cell death in amyotrophic lateral sclerosis, Mol. Neurobiol. 49 (2) (2014) 796–807.
[22] M.R. Volkert, N.A. Elliott, D.E. Housman, Functional genomics reveals a family of eukaryotic oxidation protection genes, Proc. Natl. Acad. Sci. USA 97 (26) (2000) 14530–14535.
[23] M.J. Finelli, P.L. Oliver, TLDc proteins: new players in the oxidative stress response and neurological disease, Mamm. Genome: Off. J. Int. Mamm. Genome Soc. 28 (9–10) (2017) 395–406.
[24] S. Balestrini, M. Milh, C. Castiglioni, K. Luthy, M.J. Finelli, P. Verstreken, A. Cardon, B.G. Strazisar, J.L. Holder Jr., G. Lesca, M.M. Mancardi, A.L. Poulat, G.M. Repetto, S. Banka, L. Bilo, L.E. Birkeland, F. Bosch, K. Brockmann, J.H. Cross, D. Doummar, T.M. Felix, F. Giuliano, M. Hori, I. Huning, H. Kayserili, U. Kini, M.M. Lees, G. Meenakshi, L. Mewasingh, A.T. Pagnamenta, S. Peluso, A. Mey, G.M. Rice, J.A. Rosenfeld, J.C. Taylor, M.M. Troester, C.M. Stanley, D. Ville, M. Walkiewicz, A. Falace, A. Fassio, J.R. Lemke, S. Biskup, J. Tardif, N.F. Ajeawung, A. Tolun, M. Corbett, J. Gecz, Z. Afawi, K.B. Howell, K.L. Oliver, S.F. Berkovic, I.E. Scheffer, F.A. de Falco, P.L. Oliver, P. Striano, F. Zara, P.M. Campeau, S.M. Sisodiya, TBC1D24 genotype-phenotype correlation: epilepsies and other neurologic features, Neurology 87 (1) (2016) 77–85.
[25] M.J. Finelli, D. Aprile, E. Castroflorio, A. Jeans, M. Moschetta, L. Chessum, M.T. Degiacomi, J. Grasegger, A. Lupien-Meilleur, A. Bassett, E. Rossignol, P.M. Campeau, M.R. Bowl, F. Benfenati, A. Fassio, P.L. Oliver, The epilepsy-associated protein TBC1D24 is required for normal development, survival and vesicle trafficking in mammalian neurons, Hum. Mol. Genet. (2018) (ddy370-ddy370).
[26] M.J. Finelli, L. Sanchez-Pulido, K.X. Liu, K.E. Davies, P.L. Oliver, The evolutionarily conserved Tre2/Bub2/Cdc16 (TBC), Lysin Motif (LysM), Domain Catalytic (TLDc) domain is neuroprotective against oxidative stress, J. Biol. Chem. 291 (6) (2016) 2751–2763.
[27] M.J. Finelli, T. Paramo, E. Pires, B.J. Ryan, R. Wade-Martins, P.C. Biggin, J. McCullagh, P.L. Oliver, Oxidation resistance 1 modulates glycolytic pathways in the cerebellum via an interaction with glucose-6-phosphate isomerase, Mol. Neurobiol. (2018), https://doi.org/10.1007/s12035-018-1174-x.
[28] P.L. Oliver, M.J. Finelli, B. Edwards, E. Bitoun, D.L. Butts, E.B. Becker, M.T. Cheeseman, B. Davies, K.E. Davies, Oxr1 is essential for protection against oxidative stress-induced neurodegeneration, PLOS Genet. 7 (10) (2011) e1002338.
[29] K.X. Liu, B. Edwards, S. Lee, M.J. Finelli, B. Davies, K.E. Davies, P.L. Oliver, Neuron-specific antioxidant OXR1 extends survival of a mouse model of amyotrophic lateral sclerosis, Brain 138 (Pt 5) (2015) 1167–1181.
[30] M. Yang, X. Lin, A. Rowe, T. Rognes, L. Eide, M. Bjørås, Transcriptome analysis of human OXR1 depleted cells reveals its role in regulating the p53 signaling pathway, Sci. Rep. 30 (5) (2015).
[31] M. Yang, L. Luna, J.G. Sørbø, I. Alseth, R.F. Johansen, P.H. Backe, N.C. Danbolt, L. Eide, M. Bjørås, Human OXR1 maintains mitochondrial DNA integrity and counteracts hydrogen peroxide-induced oxidative stress by regulating antioxidant pathways involvingp21, Free Radic. Biol. Med. 77 (0) (2014) 41–48.
[32] X. Zhang, S. Zhang, X. Liu, Y. Wang, J. Chang, X. Zhang, S.G. Mackintosh, A.J. Tackett, Y. He, D. Lv, R.-M. Laberge, J. Campisi, J. Wang, G. Zheng, D. Zhou, Oxidation resistance 1 is a novel senolytic target, Aging Cell 17 (4) (2018) (e12780-e12780).
[33] G. Jaramillo-Gutierrez, A. Molina-Cruz, S. Kumar, C. Barillas-Mury, The Anopheles gambiae oxidation resistance 1 (OXR1) gene regulates expression of enzymes that detoxify reactive oxygen species, PLOS One 5 (6) (2010) e11168.
[34] M. Blaise, H.M. Alsarraf, J.E. Wong, S.R. Midtgaard, F. Laroche, L. Schack, H. Spaink, J. Stougaard, S. Thirup, Crystal structure of the TLDc domain of oxidation resistance protein 2 from zebrafish, Proteins 80 (6) (2012) 1694–1698.
[35] Y. Sanada, S. Asai, A. Ikemoto, T. Moriwaki, N. Nakamura, M. Miyaji, Q.M. Zhang-Akiyama, Oxidation resistance 1 is essential for protection against oxidative stress and participates in the regulation of aging in Caenorhabditis elegans, Free Radic. Res. 48 (8) (2014) 919–928.
[36] M.J. Finelli, K.X. Liu, Y. Wu, P.L. Oliver, K.E. Davies, Oxr1 improves pathogenic cellular features of ALS-associated FUS and TDP-43 mutations, Hum. Mol. Genet. 24 (12) (2015) 3529–3544.
[37] S. Yan, S. Chen, Z. Li, H. Wang, T. Huang, X. Wang, J. Wang, Biochemical characterization of human peroxiredoxin 2, an antioxidative protein, Acta Biochim. Biophys. Sin. 44 (9) (2012) 759–764.
[38] K.J. Nelson, D. Parsonage, Measurement of peroxiredoxin activity, Curr. Protoc. Toxicol. (2011) (Chapter 7: Unit7.10).
[39] S.R. Jaffrey, H. Erdjument-Bromage, C.D. Ferris, P. Tempst, S.H. Snyder, Protein S-nitrosylation: a physiological signal for neuronal nitric oxide, Nat. Cell Biol. 3 (2) (2001) 193–197.
[40] P.T. Doulias, K. Raju, J.L. Greene, M. Tenopoulou, H. Ischiropoulos, Mass

spectrometry-based identification of S-nitrosocysteine in vivo using organic mercury assisted enrichment, Methods 62 (2) (2013) 165–170.
[41] M. Yang, L. Luna, J.G. Sorbo, I. Alseth, R.F. Johansen, P.H. Backe, N.C. Danbolt, L. Eide, M. Bjoras, Human OXR1 maintains mitochondrial DNA integrity and counteracts hydrogen peroxide-induced oxidative stress by regulating antioxidant pathways involvingp21, Free Radic. Biol. Med. 77 (2014) 41–48.
[42] J. Goemaere, B. Knoops, Peroxiredoxin distribution in the mouse brain with emphasis on neuronal populations affected in neurodegenerative disorders, J. Comp. Neurol. 520 (2) (2012) 258–280.
[43] F. Hattori, S. Oikawa, Peroxiredoxins in the central nervous system, Subcell. Biochem. 44 (2007) 357–374.
[44] T.A. Sarafian, M.A. Verity, H.V. Vinters, C.C. Shih, L. Shi, X.D. Ji, L. Dong, H. Shau, Differential expression of peroxiredoxin subtypes in human brain cell types, J. Neurosci. Res. 56 (2) (1999) 206–212.
[45] E.S. Lein, M.J. Hawrylycz, N. Ao, M. Ayres, A. Bensinger, A. Bernard, A.F. Boe, M.S. Boguski, K.S. Brockway, E.J. Byrnes, L. Chen, L. Chen, T.M. Chen, M.C. Chin, J. Chong, B.E. Crook, A. Czaplinska, C.N. Dang, S. Datta, N.R. Dee, A.L. Desaki, T. Desta, E. Diep, T.A. Dolbeare, M.J. Donelan, H.W. Dong, J.G. Dougherty, B.J. Duncan, A.J. Ebbert, G. Eichele, L.K. Estin, C. Faber, B.A. Facer, R. Fields, S.R. Fischer, T.P. Fliss, C. Frensley, S.N. Gates, K.J. Glattfelder, K.R. Halverson, M.R. Hart, J.G. Hohmann, M.P. Howell, D.P. Jeung, R.A. Johnson, P.T. Karr, R. Kawal, J.M. Kidney, R.H. Knapik, C.L. Kuan, J.H. Lake, A.R. Laramee, K.D. Larsen, C. Lau, T.A. Lemon, A.J. Liang, Y. Liu, L.T. Luong, J. Michaels, J.J. Morgan, R.J. Morgan, M.T. Mortrud, N.F. Mosqueda, L.L. Ng, R. Ng, G.J. Orta, C.C. Overly, T.H. Pak, S.E. Parry, S.D. Pathak, O.C. Pearson, R.B. Puchalski, Z.L. Riley, H.R. Rockett, S.A. Rowland, J.J. Royall, M.J. Ruiz, N.R. Sarno, K. Schaffnit, N.V. Shapovalova, T. Sivisay, C.R. Slaughterbeck, S.C. Smith, K.A. Smith, B.I. Smith, A.J. Sodt, N.N. Stewart, K.R. Stumpf, S.M. Sunkin, M. Sutram, A. Tam, C.D. Teemer, C. Thaller, C.L. Thompson, L.R. Varnam, A. Visel, R.M. Whitlock, P.E. Wohnoutka, C.K. Wolkey, V.Y. Wong, M. Wood, M.B. Yaylaoglu, R.C. Young, B.L. Youngstrom, X.F. Yuan, B. Zhang, T.A. Zwingman, A.R. Jones, Genome-wide atlas of gene expression in the adult mouse brain, Nature 445 (7124) (2007) 168–176.
[46] S.U. Kim, M.H. Jin, Y.S. Kim, S.H. Lee, Y.S. Cho, K.J. Cho, K.S. Lee, Y.I. Kim, G.W. Kim, J.M. Kim, T.H. Lee, Y.H. Lee, M. Shong, H.C. Kim, K.T. Chang, D.Y. Yu, D.S. Lee, Peroxiredoxin II preserves cognitive function against age-linked hippocampal oxidative damage, Neurobiol. Aging 32 (6) (2011) 1054–1068.
[47] H.H. Jang, K.O. Lee, Y.H. Chi, B.G. Jung, S.K. Park, J.H. Park, J.R. Lee, S.S. Lee, J.C. Moon, J.W. Yun, Y.O. Choi, W.Y. Kim, J.S. Kang, G.W. Cheong, D.J. Yun, S.G. Rhee, M.J. Cho, S.Y. Lee, Two enzymes in one; two yeast peroxiredoxins display oxidative stress-dependent switching from a peroxidase to a molecular chaperone function, Cell 117 (5) (2004) 625–635.
[48] J.C. Moon, Y.S. Hah, W.Y. Kim, B.G. Jung, H.H. Jang, J.R. Lee, S.Y. Kim, Y.M. Lee, M.G. Jeon, C.W. Kim, M.J. Cho, S.Y. Lee, Oxidative stress-dependent structural and functional switching of a human 2-Cys peroxiredoxin isotype II that enhances HeLa cell resistance to H2O2-induced cell death, J. Biol. Chem. 280 (31) (2005) 28775–28784.
[49] H.H. Jang, S.Y. Kim, S.K. Park, H.S. Jeon, Y.M. Lee, J.H. Jung, S.Y. Lee, H.B. Chae, Y.J. Jung, K.O. Lee, C.O. Lim, W.S. Chung, J.D. Bahk, D.J. Yun, M.J. Cho, S.Y. Lee, Phosphorylation and concomitant structural changes in human 2-Cys peroxiredoxin isotype I differentially regulate its peroxidase and molecular chaperone functions, FEBS Lett. 580 (1) (2006) 351–355.
[50] T.J. Phalen, K. Weirather, P.B. Deming, V. Anathy, A.K. Howe, A. van der Vliet, T.J. Jonsson, L.B. Poole, N.H. Heintz, Oxidation state governs structural transitions in peroxiredoxin II that correlate with cell cycle arrest and recovery, J. Cell Biol. 175 (5) (2006) 779–789.
[51] E.A. Veal, Z.E. Underwood, L.E. Tomalin, B.A. Morgan, C.S. Pillay, Hyperoxidation of peroxiredoxins: gain or loss of function? Antioxid. Redox Signal. 28 (7) (2018) 574–590.
[52] Y. Gan, X. Ji, X. Hu, Y. Luo, L. Zhang, P. Li, X. Liu, F. Yan, P. Vosler, Y. Gao, R.A. Stetler, J. Chen, Transgenic overexpression of peroxiredoxin-2 attenuates ischemic neuronal injury via suppression of a redox-sensitive pro-death signaling pathway, Antioxid. Redox Signal. 17 (5) (2012) 719–732.
[53] S. Zhou, Q. Han, R. Wang, X. Li, Q. Wang, H. Wang, J. Wang, Y. Ma, PRDX2 protects hepatocellular carcinoma SMMC-7721 cells from oxidative stress, Oncol. Lett. 12 (3) (2016) 2217–2221.
[54] B. Manta, M. Hugo, C. Ortiz, G. Ferrer-Sueta, M. Trujillo, A. Denicola, The peroxidase and peroxynitrite reductase activity of human erythrocyte peroxiredoxin 2, Arch. Biochem. Biophys. 484 (2) (2009) 146–154.
[55] A.V. Peskin, N. Dickerhof, R.A. Poynton, L.N. Paton, P.E. Pace, M.B. Hampton, C.C. Winterbourn, Hyperoxidation of peroxiredoxins 2 and 3: rate constants for the reactions of the sulfenic acid of the peroxidatic cysteine, J. Biol. Chem. 288 (20) (2013) 14170–14177.
[56] E.M. Lee, S.S. Lee, B.N. Tripathi, H.S. Jung, G.P. Cao, Y. Lee, S. Singh, S.H. Hong, K.W. Lee, S.Y. Lee, J.Y. Cho, B.Y. Chung, Site-directed mutagenesis substituting cysteine for serine in 2-Cys peroxiredoxin (2-Cys Prx A) of Arabidopsis thaliana effectively improves its peroxidase and chaperone functions, Ann. Bot. 116 (4) (2015) 713–725.
[57] Z.T. Farahbakhsh, Q.L. Huang, L.L. Ding, C. Altenbach, H.J. Steinhoff, J. Horwitz, W.L. Hubbell, Interaction of alpha-crystallin with spin-labeled peptides, Biochemistry 34 (2) (1995) 509–516.
[58] J. Fang, T. Nakamura, D.H. Cho, Z. Gu, S.A. Lipton, S-nitrosylation of peroxiredoxin 2 promotes oxidative stress-induced neuronal cell death in Parkinson's disease, Proc. Natl. Acad. Sci. USA 104 (47) (2007) 18742–18747.
[59] Y. Ogasawara, T. Ohminato, Y. Nakamura, K. Ishii, Structural and functional analysis of native peroxiredoxin 2 in human red blood cells, Int. J. Biochem. Cell Biol. 44 (7) (2012) 1072–1077.
[60] A.V. Peskin, P.E. Pace, J.B. Behring, L.N. Paton, M. Soethoudt, M.M. Bachschmid, C.C. Winterbourn, Glutathionylation of the active site cysteines of peroxiredoxin 2 and recycling by glutaredoxin, J. Biol. Chem. 291 (6) (2016) 3053–3062.
[61] P.A. Karplus, A primer on peroxiredoxin biochemistry, Free Radic. Biol. Med. 80 (2015) 183–190.
[62] M.M. Stacey, M.C. Vissers, C.C. Winterbourn, Oxidation of 2-cys peroxiredoxins in human endothelial cells by hydrogen peroxide, hypochlorous acid, and chloramines, Antioxid. Redox Signal. 17 (3) (2012) 411–421.
[63] S.R. Jaffrey, S.H. Snyder, The biotin switch method for the detection of S-nitrosylated proteins, Sci. STKE 2001 (86) (2001) 11.
[64] H.Z. Chae, H.J. Kim, S.W. Kang, S.G. Rhee, Characterization of three isoforms of mammalian peroxiredoxin that reduce peroxides in the presence of thioredoxin, Diabetes Res. Clin. Pract. 45 (2–3) (1999) 101–112.
[65] C.R. Sunico, A. Sultan, T. Nakamura, N. Dolatabadi, J. Parker, B. Shan, X. Han, J.R. Yates 3rd, E. Masliah, R. Ambasudhan, N. Nakanishi, S.A. Lipton, Role of sulfiredoxin as a peroxiredoxin-2 denitrosylase in human iPSC-derived dopaminergic neurons, Proc. Natl. Acad. Sci. USA 113 (47) (2016) E7564–E7571.
[66] D. Qu, J. Rashidian, M.P. Mount, H. Aleyasin, M. Parsanejad, A. Lira, E. Haque, Y. Zhang, S. Callaghan, M. Daigle, M.W. Rousseaux, R.S. Slack, P.R. Albert, I. Vincent, J.M. Woulfe, D.S. Park, Role of Cdk5-mediated phosphorylation of Prx2 in MPTP toxicity and Parkinson's disease, Neuron 55 (1) (2007) 37–52.

References

Abel, O., Shatunov, A., Jones, A. R., Andersen, P. M., Powell, J. F. & Al-Chalabi, A. 2013. Development of a Smartphone App for a Genetics Website: The Amyotrophic Lateral Sclerosis Online Genetics Database (ALSoD). *JMIR Mhealth Uhealth,* 1**,** e18.

Afawi, Z., Mandelstam, S., Korczyn, A. D., Kivity, S., Walid, S., Shalata, A., Oliver, K. L., Corbett, M., Gecz, J., Berkovic, S. F. & Jackson, G. D. 2013. TBC1D24 mutation associated with focal epilepsy, cognitive impairment and a distinctive cerebro-cerebellar malformation. *Epilepsy Res,* 105**,** 240-4.

Ahn, S. G. & Thiele, D. J. 2003. Redox regulation of mammalian heat shock factor 1 is essential for Hsp gene activation and protection from stress. *Genes Dev,* 17**,** 516-28.

Akizu, N., Cantagrel, V., Zaki, M. S., Al-Gazali, L., Wang, X., Rosti, R. O., Dikoglu, E., Gelot, A. B., Rosti, B., Vaux, K. K., Scott, E. M., Silhavy, J. L., Schroth, J., Copeland, B., Schaffer, A. E., Gordts, P. L., Esko, J. D., Buschman, M. D., Field, S. J., Napolitano, G., Abdel-Salam, G. M., Ozgul, R. K., Sagiroglu, M. S., Azam, M., Ismail, S., Aglan, M., Selim, L., Mahmoud, I. G., Abdel-Hadi, S., Badawy, A. E., Sadek, A. A., Mojahedi, F., Kayserili, H., Masri, A., Bastaki, L., Temtamy, S., Muller, U., Desguerre, I., Casanova, J. L., Dursun, A., Gunel, M., Gabriel, S. B., De Lonlay, P. & Gleeson, J. G. 2015. Biallelic mutations in SNX14 cause a syndromic form of cerebellar atrophy and lysosome-autophagosome dysfunction. *Nat Genet,* 47**,** 528-34.

Alam, H., Williams, T. W., Dumas, K. J., Guo, C., Yoshina, S., Mitani, S. & Hu, P. J. 2010. EAK-7 controls development and life span by regulating nuclear DAF-16/FoxO activity. *Cell Metab,* 12**,** 30-41.

Alasoo, K., Martinez, F. O., Hale, C., Gordon, S., Powrie, F., Dougan, G., Mukhopadhyay, S. & Gaffney, D. J. 2015. Transcriptional profiling of macrophages derived from monocytes and iPS cells identifies a conserved response to LPS and novel alternative transcription. *Sci Rep,* 5**,** 12524.

Ali, Y. O., Allen, H. M., Yu, L., Li-Kroeger, D., Bakhshizadehmahmoudi, D., Hatcher, A., Mccabe, C., Xu, J., Bjorklund, N., Taglialatela, G., Bennett, D. A., De Jager, P. L., Shulman, J. M., Bellen, H. J. & Lu, H. C. 2016. NMNAT2:HSP90 Complex Mediates Proteostasis in Proteinopathies. *PLoS Biol,* 14**,** e1002472.

Aliaga, L., Lai, C., Yu, J., Chub, N., Shim, H., Sun, L., Xie, C., Yang, W. J., Lin, X., O'donovan, M. J. & Cai, H. 2013. Amyotrophic lateral sclerosis-related VAPB P56S mutation differentially affects the function and survival of corticospinal and spinal motor neurons. *Hum Mol Genet,* 22**,** 4293-305.

Alves, S., Cormier-Dequaire, F., Marinello, M., Marais, T., Muriel, M. P., Beaumatin, F., Charbonnier-Beaupel, F., Tahiri, K., Seilhean, D., El Hachimi, K., Ruberg, M., Stevanin, G., Barkats, M., Den Dunnen, W., Priault, M., Brice, A., Durr, A., Corvol, J. C. & Sittler, A. 2014. The autophagy/lysosome pathway is impaired in SCA7 patients and SCA7 knock-in mice. *Acta Neuropathol,* 128**,** 705-22.

Amick, J., Schlanger, S. E., Wachnowsky, C., Moseng, M. A., Emerson, C. C., Dare, M., Luo, W. I., Ithychanda, S. S., Nix, J. C., Cowan, J. A., Page, R. C. & Misra, S. 2014. Crystal structure of the nucleotide-binding domain of mortalin, the mitochondrial Hsp70 chaperone. *Protein Sci,* 23**,** 833-42.

An, B. C., Lee, S. S., Lee, E. M., Lee, J. T., Wi, S. G., Jung, H. S., Park, W., Lee, S. Y. & Chung, B. Y. 2011. Functional switching of a novel prokaryotic 2-Cys peroxiredoxin (PpPrx) under oxidative stress. *Cell Stress Chaperones,* 16**,** 317-28.

Andican, G., Konukoglu, D., Bozluolcay, M., Bayulkem, K., Firtiina, S. & Burcak, G. 2012. Plasma oxidative and inflammatory markers in patients with idiopathic Parkinson's disease. *Acta Neurol Belg,* 112**,** 155-9.

Andreescu, C. E., Milojkovic, B. A., Haasdijk, E. D., Kramer, P., De Jong, F. H., Krust, A., De Zeeuw, C. I. & De Jeu, M. T. 2007. Estradiol improves cerebellar memory formation by activating estrogen receptor beta. *J Neurosci,* 27**,** 10832-9.

Annese, A., Manzari, C., Lionetti, C., Picardi, E., Horner, D. S., Chiara, M., Caratozzolo, M. F., Tullo, A., Fosso, B., Pesole, G. & D'erchia, A. M. 2018. Whole transcriptome profiling of Late-Onset Alzheimer's Disease patients provides insights into the molecular changes involved in the disease. *Scientific Reports,* 8**,** 4282.

Antonucci, F., Corradini, I., Fossati, G., Tomasoni, R., Menna, E. & Matteoli, M. 2016. SNAP-25, a Known Presynaptic Protein with Emerging Postsynaptic Functions. *Front Synaptic Neurosci,* 8**,** 7.

Aprile, D., Fruscione, F., Baldassari, S., Fadda, M., Ferrante, D., Falace, A., Buhler, E., Sartorelli, J., Represa, A., Baldelli, P., Benfenati, F., Zara, F. & Fassio, A. 2019. TBC1D24 regulates axonal outgrowth and membrane trafficking at the growth cone in rodent and human neurons. *Cell Death Differ*.

Araujo, P. R., Yoon, K., Ko, D., Smith, A. D., Qiao, M., Suresh, U., Burns, S. C. & Penalva, L. O. 2012. Before It Gets Started: Regulating Translation at the 5' UTR. *Comp Funct Genomics,* 2012**,** 475731.

Ariga, H., Takahashi-Niki, K., Kato, I., Maita, H., Niki, T. & Iguchi-Ariga, S. M. 2013. Neuroprotective function of DJ-1 in Parkinson's disease. *Oxid Med Cell Longev,* 2013**,** 683920.

Azaiez, H., Booth, K. T., Bu, F., Huygen, P., Shibata, S. B., Shearer, A. E., Kolbe, D., Meyer, N., Black-Ziegelbein, E. A. & Smith, R. J. 2014. TBC1D24 mutation causes autosomal-dominant nonsyndromic hearing loss. *Hum Mutat,* 35**,** 819-23.

Bakhchane, A., Charif, M., Salime, S., Boulouiz, R., Nahili, H., Roky, R., Lenaers, G. & Barakat, A. 2015. Recessive TBC1D24 Mutations Are Frequent in Moroccan Non-Syndromic Hearing Loss Pedigrees. *PLoS One,* 10**,** e0138072.

Balchin, D., Hayer-Hartl, M. & Hartl, F. U. 2016. In vivo aspects of protein folding and quality control. *Science,* 353**,** aac4354.

Balestrini, S., Milh, M., Castiglioni, C., Luthy, K., Finelli, M. J., Verstreken, P., Cardon, A., Strazisar, B. G., Holder, J. L., Jr., Lesca, G., Mancardi, M. M., Poulat, A. L., Repetto, G. M., Banka, S., Bilo, L., Birkeland, L. E., Bosch, F., Brockmann, K., Cross, J. H., Doummar, D., Felix, T. M., Giuliano, F., Hori, M., Huning, I., Kayserili, H., Kini, U., Lees, M. M., Meenakshi, G., Mewasingh, L., Pagnamenta, A. T., Peluso, S., Mey, A., Rice, G. M., Rosenfeld, J. A., Taylor, J. C., Troester, M. M., Stanley, C. M., Ville, D., Walkiewicz, M., Falace, A., Fassio, A., Lemke, J. R., Biskup, S., Tardif, J., Ajeawung, N. F., Tolun, A., Corbett, M., Gecz, J., Afawi, Z., Howell, K. B., Oliver, K. L., Berkovic, S. F., Scheffer, I. E., De Falco, F. A., Oliver, P. L., Striano, P., Zara, F., Campeau, P. M. & Sisodiya, S. M. 2016. TBC1D24 genotype-phenotype correlation: Epilepsies and other neurologic features. *Neurology,* 87**,** 77-85.

Banuelos, E., Ramsey, K., Belnap, N., Krishnan, M., Balak, C., Szelinger, S., Siniard, A. L., Russell, M., Richholt, R., De Both, M., Piras, I., Naymik, M., Claasen, A. M., Rangasamy, S., Huentelman, M. J., Craig, D. W., Campeau, P. M., Narayanan, V. & Schrauwen, I. 2017. Case Report: Novel mutations in TBC1D24 are associated with autosomal dominant tonic-clonic and myoclonic epilepsy and recessive Parkinsonism, psychosis, and intellectual disability. *F1000Res,* 6**,** 553.

Barcia, C., Ros, C. M., Annese, V., Gomez, A., Ros-Bernal, F., Aguado-Yera, D., Martinez-Pagan, M. E., De Pablos, V., Fernandez-Villalba, E. & Herrero, M. T. 2011. IFN-gamma signaling, with the synergistic contribution of TNF-alpha, mediates cell specific microglial and astroglial activation in experimental models of Parkinson's disease. *Cell Death Dis,* 2**,** e142.

Barrientos, R. M., Kitt, M. M., Watkins, L. R. & Maier, S. F. 2015. Neuroinflammation in the normal aging hippocampus. *Neuroscience,* 309**,** 84-99.
Bayes, A., Collins, M. O., Croning, M. D., Van De Lagemaat, L. N., Choudhary, J. S. & Grant, S. G. 2012. Comparative study of human and mouse postsynaptic proteomes finds high compositional conservation and abundance differences for key synaptic proteins. *PLoS One,* 7**,** e46683.
Bayes, A., Collins, M. O., Reig-Viader, R., Gou, G., Goulding, D., Izquierdo, A., Choudhary, J. S., Emes, R. D. & Grant, S. G. 2017. Evolution of complexity in the zebrafish synapse proteome. *Nat Commun,* 8**,** 14613.
Bayés, A., Van De Lagemaat, L. N., Collins, M. O., Croning, M. D. R., Whittle, I. R., Choudhary, J. S. & Grant, S. G. N. 2011. Characterization of the proteome, diseases and evolution of the human postsynaptic density. *Nature neuroscience,* 14**,** 19-21.
Beck, M. 2016. The Link Between Lysosomal Storage Disorders and More Common Diseases. *Journal of Inborn Errors of Metabolism and Screening,* 4**,** 2326409816682767.
Beckhauser, T. F., Francis-Oliveira, J. & De Pasquale, R. 2016. Reactive Oxygen Species: Physiological and Physiopathological Effects on Synaptic Plasticity. *J Exp Neurosci,* 10**,** 23-48.
Bennett, M. L., Bennett, F. C., Liddelow, S. A., Ajami, B., Zamanian, J. L., Fernhoff, N. B., Mulinyawe, S. B., Bohlen, C. J., Adil, A., Tucker, A., Weissman, I. L., Chang, E. F., Li, G., Grant, G. A., Hayden Gephart, M. G. & Barres, B. A. 2016. New tools for studying microglia in the mouse and human CNS. *Proc Natl Acad Sci U S A,* 113**,** E1738-46.
Benoit, M. E., Hernandez, M. X., Dinh, M. L., Benavente, F., Vasquez, O. & Tenner, A. J. 2013. C1q-induced LRP1B and GPR6 proteins expressed early in Alzheimer disease mouse models, are essential for the C1q-mediated protection against amyloid-beta neurotoxicity. *J Biol Chem,* 288**,** 654-65.
Bertoldi, M. 2016. Human Peroxiredoxins 1 and 2 and Their Interacting Protein Partners; Through Structure Toward Functions of Biological Complexes. *Protein Pept Lett,* 23**,** 69-77.
Bertram, L. & Tanzi, R. E. 2005. The genetic epidemiology of neurodegenerative disease. *J Clin Invest,* 115**,** 1449-57.
Bian, C., Huang, Y., Zhu, H., Zhao, Y., Zhao, J. & Zhang, J. 2018. Steroid Receptor Coactivator-1 Knockdown Decreases Synaptic Plasticity and Impairs Spatial Memory in the Hippocampus of Mice. *Neuroscience,* 377**,** 114-125.
Bilan, D. S. & Belousov, V. V. 2016. HyPer Family Probes: State of the Art. *Antioxid Redox Signal,* 24**,** 731-51.
Birben, E., Sahiner, U. M., Sackesen, C., Erzurum, S. & Kalayci, O. 2012. Oxidative stress and antioxidant defense. *World Allergy Organ J,* 5**,** 9-19.
Birdsall, V. & Waites, C. L. 2018. Autophagy at the synapse. *Neurosci Lett*.
Blaise, M., Alsarraf, H. M., Wong, J. E., Midtgaard, S. R., Laroche, F., Schack, L., Spaink, H., Stougaard, J. & Thirup, S. 2012. Crystal structure of the TLDc domain of oxidation resistance protein 2 from zebrafish. *Proteins,* 80**,** 1694-8.
Blaschke, R. J., Topfer, C., Marchini, A., Steinbeisser, H., Janssen, J. W. & Rappold, G. A. 2003. Transcriptional and translational regulation of the Leri-Weill and Turner syndrome homeobox gene SHOX. *J Biol Chem,* 278**,** 47820-6.
Blokhuis, A. M., Groen, E. J., Koppers, M., Van Den Berg, L. H. & Pasterkamp, R. J. 2013. Protein aggregation in amyotrophic lateral sclerosis. *Acta Neuropathol,* 125**,** 777-94.
Blom, T., Schmiedt, M. L., Wong, A. M., Kyttala, A., Soronen, J., Jauhiainen, M., Tyynela, J., Cooper, J. D. & Jalanko, A. 2013. Exacerbated neuronal ceroid lipofuscinosis phenotype in Cln1/5 double-knockout mice. *Dis Model Mech,* 6**,** 342-57.

Boisvert, M. M., Erikson, G. A., Shokhirev, M. N. & Allen, N. J. 2018. The Aging Astrocyte Transcriptome from Multiple Regions of the Mouse Brain. *Cell Rep,* 22**,** 269-285.
Bormuth, I., Yan, K., Yonemasu, T., Gummert, M., Zhang, M., Wichert, S., Grishina, O., Pieper, A., Zhang, W., Goebbels, S., Tarabykin, V., Nave, K. A. & Schwab, M. H. 2013. Neuronal basic helix-loop-helix proteins Neurod2/6 regulate cortical commissure formation before midline interactions. *J Neurosci,* 33**,** 641-51.
Bosch, M. E. & Kielian, T. 2015. Neuroinflammatory paradigms in lysosomal storage diseases. *Front Neurosci,* 9**,** 417.
Bose, D. & Chakrabarti, A. 2017. Substrate specificity in the context of molecular chaperones. *IUBMB Life,* 69**,** 647-659.
Bouayed, J. & Bohn, T. 2010. Exogenous antioxidants--Double-edged swords in cellular redox state: Health beneficial effects at physiologic doses versus deleterious effects at high doses. *Oxidative medicine and cellular longevity,* 3**,** 228-237.
Bozzi, Y., Casarosa, S. & Caleo, M. 2012. Epilepsy as a neurodevelopmental disorder. *Front Psychiatry,* 3**,** 19.
Brazill, J. M., Li, C., Zhu, Y. & Zhai, R. G. 2017. NMNAT: It's an NAD(+) synthase... It's a chaperone... It's a neuroprotector. *Curr Opin Genet Dev,* 44**,** 156-162.
Brehme, M., Voisine, C., Rolland, T., Wachi, S., Soper, J. H., Zhu, Y., Orton, K., Villella, A., Garza, D., Vidal, M., Ge, H. & Morimoto, R. I. 2014. A chaperome subnetwork safeguards proteostasis in aging and neurodegenerative disease. *Cell Rep,* 9**,** 1135-50.
Brieger, K., Schiavone, S., Miller, F. J., Jr. & Krause, K. H. 2012. Reactive oxygen species: from health to disease. *Swiss Med Wkly,* 142**,** w13659.
Brigelius-Flohe, R. & Maiorino, M. 2013. Glutathione peroxidases. *Biochim Biophys Acta,* 1830**,** 3289-303.
Brodehl, A., Gaertner-Rommel, A., Klauke, B., Grewe, S. A., Schirmer, I., Peterschroder, A., Faber, L., Vorgerd, M., Gummert, J., Anselmetti, D., Schulz, U., Paluszkiewicz, L. & Milting, H. 2017. The novel alphaB-crystallin (CRYAB) mutation p.D109G causes restrictive cardiomyopathy. *Hum Mutat,* 38**,** 947-952.
Bross, P. & Fernandez-Guerra, P. 2016. Disease-Associated Mutations in the HSPD1 Gene Encoding the Large Subunit of the Mitochondrial HSP60/HSP10 Chaperonin Complex. *Front Mol Biosci,* 3**,** 49.
Brownjohn, P. W., Smith, J., Solanki, R., Lohmann, E., Houlden, H., Hardy, J., Dietmann, S. & Livesey, F. J. 2018. Functional Studies of Missense TREM2 Mutations in Human Stem Cell-Derived Microglia. *Stem Cell Reports,* 10**,** 1294-1307.
Bumgarner, R. 2013. Overview of DNA microarrays: types, applications, and their future. *Current protocols in molecular biology,* Chapter 22**,** Unit-22.1.
Buonocore, G., Perrone, S. & Tataranno, M. L. 2010. Oxygen toxicity: chemistry and biology of reactive oxygen species. *Semin Fetal Neonatal Med,* 15**,** 186-90.
Burbulla, L. F., Schelling, C., Kato, H., Rapaport, D., Woitalla, D., Schiesling, C., Schulte, C., Sharma, M., Illig, T., Bauer, P., Jung, S., Nordheim, A., Schols, L., Riess, O. & Kruger, R. 2010. Dissecting the role of the mitochondrial chaperone mortalin in Parkinson's disease: functional impact of disease-related variants on mitochondrial homeostasis. *Hum Mol Genet,* 19**,** 4437-52.
Burré, J. 2015. The Synaptic Function of α-Synuclein. *J Parkinsons Dis,* 5**,** 699-713.
Butterfield, D. A. & Boyd-Kimball, D. 2018. Redox proteomics and amyloid beta-peptide: insights into Alzheimer disease. *J Neurochem*.
Cai, Y., Arikkath, J., Yang, L., Guo, M. L., Periyasamy, P. & Buch, S. 2016. Interplay of endoplasmic reticulum stress and autophagy in neurodegenerative disorders. *Autophagy,* 12**,** 225-44.

Calderwood, S. K., Murshid, A. & Prince, T. 2009. The shock of aging: molecular chaperones and the heat shock response in longevity and aging--a mini-review. *Gerontology,* 55**,** 550-8.

Campanella, C., Pace, A., Caruso Bavisotto, C., Marzullo, P., Marino Gammazza, A., Buscemi, S. & Palumbo Piccionello, A. 2018. Heat Shock Proteins in Alzheimer's Disease: Role and Targeting. *Int J Mol Sci,* 19.

Campeau, P. M., Kasperaviciute, D., Lu, J. T., Burrage, L. C., Kim, C., Hori, M., Powell, B. R., Stewart, F., Felix, T. M., Van Den Ende, J., Wisniewska, M., Kayserili, H., Rump, P., Nampoothiri, S., Aftimos, S., Mey, A., Nair, L. D., Begleiter, M. L., De Bie, I., Meenakshi, G., Murray, M. L., Repetto, G. M., Golabi, M., Blair, E., Male, A., Giuliano, F., Kariminejad, A., Newman, W. G., Bhaskar, S. S., Dickerson, J. E., Kerr, B., Banka, S., Giltay, J. C., Wieczorek, D., Tostevin, A., Wiszniewska, J., Cheung, S. W., Hennekam, R. C., Gibbs, R. A., Lee, B. H. & Sisodiya, S. M. 2014. The genetic basis of DOORS syndrome: an exome-sequencing study. *Lancet Neurol,* 13**,** 44-58.

Can, M., Guven, B., Bektas, S. & Arikan, I. 2014. Oxidative stress and apoptosis in preeclampsia. *Tissue Cell,* 46**,** 477-81.

Casillas-Espinosa, P. M., Powell, K. L. & O'brien, T. J. 2012. Regulators of synaptic transmission: roles in the pathogenesis and treatment of epilepsy. *Epilepsia,* 53 Suppl 9**,** 41-58.

Cekanaviciute, E. & Buckwalter, M. S. 2016. Astrocytes: Integrative Regulators of Neuroinflammation in Stroke and Other Neurological Diseases. *Neurotherapeutics,* 13**,** 685-701.

Cenini, G., Lloret, A. & Cascella, R. 2019. Oxidative Stress in Neurodegenerative Diseases: From a Mitochondrial Point of View. *Oxid Med Cell Longev,* 2019**,** 2105607.

Cesaratto, L., Vascotto, C., D'ambrosio, C., Scaloni, A., Baccarani, U., Paron, I., Damante, G., Calligaris, S., Quadrifoglio, F., Tiribelli, C. & Tell, G. 2005. Overoxidation of peroxiredoxins as an immediate and sensitive marker of oxidative stress in HepG2 cells and its application to the redox effects induced by ischemia/reperfusion in human liver. *Free Radic Res,* 39**,** 255-68.

Chae, H. Z., Kim, H. J., Kang, S. W. & Rhee, S. G. 1999. Characterization of three isoforms of mammalian peroxiredoxin that reduce peroxides in the presence of thioredoxin. *Diabetes Res Clin Pract,* 45**,** 101-12.

Chae, H. Z., Oubrahim, H., Park, J. W., Rhee, S. G. & Chock, P. B. 2012. Protein glutathionylation in the regulation of peroxiredoxins: a family of thiol-specific peroxidases that function as antioxidants, molecular chaperones, and signal modulators. *Antioxid Redox Signal,* 16**,** 506-23.

Chai, Y. L., Chong, J. R., Weng, J., Howlett, D., Halsey, A., Lee, J. H., Attems, J., Aarsland, D., Francis, P. T., Chen, C. P. & Lai, M. K. P. 2018. Lysosomal cathepsin D is upregulated in Alzheimer's disease neocortex and may be a marker for neurofibrillary degeneration. *Brain Pathol*.

Chakraborthy, A., Ramani, P., Sherlin, H. J., Premkumar, P. & Natesan, A. 2014. Antioxidant and pro-oxidant activity of Vitamin C in oral environment. *Indian J Dent Res,* 25**,** 499-504.

Chang, Y., Kong, Q., Shan, X., Tian, G., Ilieva, H., Cleveland, D. W., Rothstein, J. D., Borchelt, D. R., Wong, P. C. & Lin, C. L. 2008. Messenger RNA oxidation occurs early in disease pathogenesis and promotes motor neuron degeneration in ALS. *PLoS One,* 3**,** e2849.

Chen, H. J., Anagnostou, G., Chai, A., Withers, J., Morris, A., Adhikaree, J., Pennetta, G. & De Belleroche, J. S. 2010. Characterization of the properties of a novel mutation in VAPB in familial amyotrophic lateral sclerosis. *J Biol Chem,* 285**,** 40266-81.

Chen, X. & Pan, W. 2014. The Treatment Strategies for Neurodegenerative Diseases by Integrative Medicine. *Integrative Medicine International*, 223-225.
Chen, X. S., Reader, R. H., Hoischen, A., Veltman, J. A., Simpson, N. H., Francks, C., Newbury, D. F. & Fisher, S. E. 2017. Next-generation DNA sequencing identifies novel gene variants and pathways involved in specific language impairment. *Sci Rep,* 7, 46105.
Cheng-Hathaway, P. J., Reed-Geaghan, E. G., Jay, T. R., Casali, B. T., Bemiller, S. M., Puntambekar, S. S., Von Saucken, V. E., Williams, R. Y., Karlo, J. C., Moutinho, M., Xu, G., Ransohoff, R. M., Lamb, B. T. & Landreth, G. E. 2018. The Trem2 R47H variant confers loss-of-function-like phenotypes in Alzheimer's disease. *Mol Neurodegener,* 13, 29.
Chitwood, P. J., Juszkiewicz, S., Guna, A., Shao, S. & Hegde, R. S. 2018. EMC Is Required to Initiate Accurate Membrane Protein Topogenesis. *Cell,* 175, 1507-1519 e16.
Choudhury, K. R. & Bhattacharyya, N. P. 2015. Chaperone protein HYPK interacts with the first 17 amino acid region of Huntingtin and modulates mutant HTT-mediated aggregation and cytotoxicity. *Biochem Biophys Res Commun,* 456, 66-73.
Christianson, J. C., Olzmann, J. A., Shaler, T. A., Sowa, M. E., Bennett, E. J., Richter, C. M., Tyler, R. E., Greenblatt, E. J., Harper, J. W. & Kopito, R. R. 2011. Defining human ERAD networks through an integrative mapping strategy. *Nat Cell Biol,* 14, 93-105.
Chu, C. L., Yu, Y. L., Shen, K. Y., Lowell, C. A., Lanier, L. L. & Hamerman, J. A. 2008. Increased TLR responses in dendritic cells lacking the ITAM-containing adapters DAP12 and FcRgamma. *Eur J Immunol,* 38, 166-73.
Chu, K. L., Lew, Q. J., Rajasegaran, V., Kung, J. T., Zheng, L., Yang, Q., Shaw, R., Cheong, N., Liou, Y. C. & Chao, S. H. 2013. Regulation of PRDX1 peroxidase activity by Pin1. *Cell Cycle,* 12, 944-52.
Chung, C. G., Lee, H. & Lee, S. B. 2018. Mechanisms of protein toxicity in neurodegenerative diseases. *Cell Mol Life Sci,* 75, 3159-3180.
Chung, M. C., Alem, F., Hamer, S. G., Narayanan, A., Shatalin, K., Bailey, C., Nudler, E. & Hakami, R. M. 2017. S-nitrosylation of peroxiredoxin 1 contributes to viability of lung epithelial cells during Bacillus anthracis infection. *Biochim Biophys Acta,* 1861, 3019-3029.
Clark, A. K., Yip, P. K. & Malcangio, M. 2009. The liberation of fractalkine in the dorsal horn requires microglial cathepsin S. *J Neurosci,* 29, 6945-54.
Clarke, D. D. & Sokoloff, L. 1999. Chapter 31. Circulation and energy metabolism of the brain. *Basic neurochemis- try: molecular, cellular and medical aspects.* Philadelphia: Lippincott-Raven.
Clarke, L. E., Liddelow, S. A., Chakraborty, C., Munch, A. E., Heiman, M. & Barres, B. A. 2018. Normal aging induces A1-like astrocyte reactivity. *Proc Natl Acad Sci U S A,* 115, E1896-E1905.
Climer, L. K., Hendrix, R. D. & Lupashin, V. V. 2018. Conserved Oligomeric Golgi and Neuronal Vesicular Trafficking. *Handb Exp Pharmacol,* 245, 227-247.
Cohen, T. J., Guo, J. L., Hurtado, D. E., Kwong, L. K., Mills, I. P., Trojanowski, J. Q. & Lee, V. M. 2011. The acetylation of tau inhibits its function and promotes pathological tau aggregation. *Nat Commun,* 2, 252.
Colacurcio, D. J. & Nixon, R. A. 2016. Disorders of lysosomal acidification-The emerging role of v-ATPase in aging and neurodegenerative disease. *Ageing Res Rev,* 32, 75-88.
Collin, F. 2019. Chemical Basis of Reactive Oxygen Species Reactivity and Involvement in Neurodegenerative Diseases. *Int J Mol Sci,* 20.
Collins, J. A., Wood, S. T., Nelson, K. J., Rowe, M. A., Carlson, C. S., Chubinskaya, S., Poole, L. B., Furdui, C. M. & Loeser, R. F. 2016. Oxidative Stress Promotes Peroxiredoxin

Hyperoxidation and Attenuates Pro-survival Signaling in Aging Chondrocytes. *J Biol Chem,* 291**,** 6641-54.
Consortium, G. 2015. Human genomics. The Genotype-Tissue Expression (GTEx) pilot analysis: multitissue gene regulation in humans. *Science,* 348**,** 648-60.
Cooke, S. F. & Bliss, T. V. 2006. Plasticity in the human central nervous system. *Brain,* 129**,** 1659-73.
Corbett, M. A., Bahlo, M., Jolly, L., Afawi, Z., Gardner, A. E., Oliver, K. L., Tan, S., Coffey, A., Mulley, J. C., Dibbens, L. M., Simri, W., Shalata, A., Kivity, S., Jackson, G. D., Berkovic, S. F. & Gecz, J. 2010. A focal epilepsy and intellectual disability syndrome is due to a mutation in TBC1D24. *Am J Hum Genet,* 87**,** 371-5.
D'angelo, B., Astarita, C., Boffo, S., Massaro-Giordano, M., Antonella Ianuzzi, C., Caporaso, A., Macaluso, M. & Giordano, A. 2017. LPS-induced inflammatory response triggers cell cycle reactivation in murine neuronal cells through retinoblastoma proteins induction. *Cell Cycle,* 16**,** 2330-2336.
Dagdelen, M., Temur, M., Yilmaz, O., Altindag, T., Uslu, T. & Ozbay, P. O. 2016. Placental bed apoptosis is increased in pregnant women with pre-eclampsia versus normotensive pregnant women. *J Obstet Gynaecol,* 36**,** 974-979.
Daneman, R. & Prat, A. 2015. The blood-brain barrier. *Cold Spring Harb Perspect Biol,* 7**,** a020412.
Dardiotis, E., Siokas, V., Pantazi, E., Dardioti, M., Rikos, D., Xiromerisiou, G., Markou, A., Papadimitriou, D., Speletas, M. & Hadjigeorgiou, G. M. 2017. A novel mutation in TREM2 gene causing Nasu-Hakola disease and review of the literature. *Neurobiol Aging,* 53**,** 194 e13-194 e22.
Dasgupta, N., Xu, Y. H., Li, R., Peng, Y., Pandey, M. K., Tinch, S. L., Liou, B., Inskeep, V., Zhang, W., Setchell, K. D., Keddache, M., Grabowski, G. A. & Sun, Y. 2015. Neuronopathic Gaucher disease: dysregulated mRNAs and miRNAs in brain pathogenesis and effects of pharmacologic chaperone treatment in a mouse model. *Hum Mol Genet,* 24**,** 7031-48.
Davis, R. S., Stephan, R. P., Chen, C.-C., Dennis, G. & Cooper, M. D. 2004. Differential B cell expression of mouse Fc receptor homologs. *International Immunology,* 16**,** 1343-1353.
De Castro, E., Sigrist, C. J., Gattiker, A., Bulliard, V., Langendijk-Genevaux, P. S., Gasteiger, E., Bairoch, A. & Hulo, N. 2006. ScanProsite: detection of PROSITE signature matches and ProRule-associated functional and structural residues in proteins. *Nucleic Acids Res,* 34**,** W362-5.
De Jong, E. K., Dijkstra, I. M., Hensens, M., Brouwer, N., Van Amerongen, M., Liem, R. S., Boddeke, H. W. & Biber, K. 2005. Vesicle-mediated transport and release of CCL21 in endangered neurons: a possible explanation for microglia activation remote from a primary lesion. *J Neurosci,* 25**,** 7548-57.
De Mena, L., Coto, E., Sanchez-Ferrero, E., Ribacoba, R., Guisasola, L. M., Salvador, C., Blazquez, M. & Alvarez, V. 2009. Mutational screening of the mortalin gene (HSPA9) in Parkinson's disease. *J Neural Transm (Vienna),* 116**,** 1289-93.
Dell'orco, M., Milani, P., Arrigoni, L., Pansarasa, O., Sardone, V., Maffioli, E., Polveraccio, F., Bordoni, M., Diamanti, L., Ceroni, M., Peverali, F. A., Tedeschi, G. & Cereda, C. 2016. Hydrogen peroxide-mediated induction of SOD1 gene transcription is independent from Nrf2 in a cellular model of neurodegeneration. *Biochim Biophys Acta,* 1859**,** 315-23.
Dheen, S. T., Kaur, C. & Ling, E. A. 2007. Microglial activation and its implications in the brain diseases. *Curr Med Chem,* 14**,** 1189-97.
Didonna, A. & Benetti, F. 2015. Post-translational modifications in neurodegeneration.

Dimant, H., Ebrahimi-Fakhari, D. & Mclean, P. J. 2012. Molecular chaperones and co-chaperones in Parkinson disease. *Neuroscientist,* 18**,** 589-601.

Doan, R. N., Lim, E. T., De Rubeis, S., Betancur, C., Cutler, D. J., Chiocchetti, A. G., Overman, L. M., Soucy, A., Goetze, S., Autism Sequencing, C., Freitag, C. M., Daly, M. J., Walsh, C. A., Buxbaum, J. D. & Yu, T. W. 2019. Recessive gene disruptions in autism spectrum disorder. *Nat Genet,* 51**,** 1092-1098.

Doerks, T., Copley, R. R., Schultz, J., Ponting, C. P. & Bork, P. 2002. Systematic identification of novel protein domain families associated with nuclear functions. *Genome Res,* 12**,** 47-56.

Doummar, D., Mignot, C., Apartis, E., Villard, L., Rodriguez, D., Chantot-Bastauraud, S. & Burglen, L. 2015. A Novel Homozygous TBC1D24 Mutation Causing Multifocal Myoclonus With Cerebellar Involvement. *Mov Disord,* 30**,** 1431-2.

Doyle, T., Moncorge, O., Bonaventure, B., Pollpeter, D., Lussignol, M., Tauziet, M., Apolonia, L., Catanese, M. T., Goujon, C. & Malim, M. H. 2018. The interferon-inducible isoform of NCOA7 inhibits endosome-mediated viral entry. *Nat Microbiol,* 3**,** 1369-1376.

Dreos, R., Ambrosini, G., Perier, R. C. & Bucher, P. 2015. The Eukaryotic Promoter Database: expansion of EPDnew and new promoter analysis tools. *Nucleic Acids Res,* 43**,** D92-6.

Du, C., Xu, Y., Yang, K., Chen, S., Wang, X., Wang, S., Wang, C., Shen, M., Chen, F., Chen, M., Zeng, D., Li, F., Wang, T., Wang, F., Zhao, J., Ai, G., Cheng, T., Su, Y. & Wang, J. 2017. Estrogen promotes megakaryocyte polyploidization via estrogen receptor beta-mediated transcription of GATA1. *Leukemia,* 31**,** 945-956.

Dubos, A., Castells-Nobau, A., Meziane, H., Oortveld, M. A., Houbaert, X., Iacono, G., Martin, C., Mittelhaeuser, C., Lalanne, V., Kramer, J. M., Bhukel, A., Quentin, C., Slabbert, J., Verstreken, P., Sigrist, S. J., Messaddeq, N., Birling, M. C., Selloum, M., Stunnenberg, H. G., Humeau, Y., Schenck, A. & Herault, Y. 2015. Conditional depletion of intellectual disability and Parkinsonism candidate gene ATP6AP2 in fly and mouse induces cognitive impairment and neurodegeneration. *Hum Mol Genet,* 24**,** 6736-55.

Durand, M., Kolpak, A., Farrell, T., Elliott, N. A., Shao, W., Brown, M. & Volkert, M. R. 2007. The OXR domain defines a conserved family of eukaryotic oxidation resistance proteins. *BMC Cell Biol,* 8**,** 13.

Eckert-Boulet, N., Larsson, K., Wu, B., Poulsen, P., Regenberg, B., Nielsen, J. & Kielland-Brandt, M. C. 2006. Deletion of RTS1, encoding a regulatory subunit of protein phosphatase 2A, results in constitutive amino acid signaling via increased Stp1p processing. *Eukaryot Cell,* 5**,** 174-9.

Edgar, R. S., Green, E. W., Zhao, Y., Van Ooijen, G., Olmedo, M., Qin, X., Xu, Y., Pan, M., Valekunja, U. K., Feeney, K. A., Maywood, E. S., Hastings, M. H., Baliga, N. S., Merrow, M., Millar, A. J., Johnson, C. H., Kyriacou, C. P., O'neill, J. S. & Reddy, A. B. 2012. Peroxiredoxins are conserved markers of circadian rhythms. *Nature,* 485**,** 459-64.

Edvardson, S., Cinnamon, Y., Ta-Shma, A., Shaag, A., Yim, Y. I., Zenvirt, S., Jalas, C., Lesage, S., Brice, A., Taraboulos, A., Kaestner, K. H., Greene, L. E. & Elpeleg, O. 2012. A deleterious mutation in DNAJC6 encoding the neuronal-specific clathrin-uncoating co-chaperone auxilin, is associated with juvenile parkinsonism. *PLoS One,* 7**,** e36458.

El-Brolosy, M. A., Kontarakis, Z., Rossi, A., Kuenne, C., Gunther, S., Fukuda, N., Kikhi, K., Boezio, G. L. M., Takacs, C. M., Lai, S. L., Fukuda, R., Gerri, C., Giraldez, A. J. & Stainier, D. Y. R. 2019. Genetic compensation triggered by mutant mRNA degradation. *Nature,* 568**,** 193-197.

Elali, A. & Rivest, S. 2016. Microglia in Alzheimer's disease: A multifaceted relationship. *Brain Behav Immun,* 55**,** 138-50.

Elliot, M. G. 2016. Oxidative stress and the evolutionary origins of preeclampsia. *J Reprod Immunol,* 114**,** 75-80.

Elliott, N. A. & Volkert, M. R. 2004. Stress induction and mitochondrial localization of Oxr1 proteins in yeast and humans. *Mol Cell Biol,* 24**,** 3180-7.
Elobeid, A., Libard, S., Leino, M., Popova, S. N. & Alafuzoff, I. 2016. Altered Proteins in the Aging Brain. *J Neuropathol Exp Neurol,* 75**,** 316-25.
Emperador-Melero, J., Huson, V., Van Weering, J., Bollmann, C., Fischer Von Mollard, G., Toonen, R. F. & Verhage, M. 2018. Vti1a/b regulate synaptic vesicle and dense core vesicle secretion via protein sorting at the Golgi. *Nature Communications,* 9**,** 3421.
Erkkinen, M. G., Kim, M. O. & Geschwind, M. D. 2018. Clinical Neurology and Epidemiology of the Major Neurodegenerative Diseases. *Cold Spring Harb Perspect Biol,* 10.
Falace, A., Buhler, E., Fadda, M., Watrin, F., Lippiello, P., Pallesi-Pocachard, E., Baldelli, P., Benfenati, F., Zara, F., Represa, A., Fassio, A. & Cardoso, C. 2014. TBC1D24 regulates neuronal migration and maturation through modulation of the ARF6-dependent pathway. *Proc Natl Acad Sci U S A,* 111**,** 2337-42.
Famili, F., Wiekmeijer, A. S. & Staal, F. J. 2017. The development of T cells from stem cells in mice and humans. *Future Sci OA,* 3**,** FSO186.
Fang, J., Nakamura, T., Cho, D. H., Gu, Z. & Lipton, S. A. 2007. S-nitrosylation of peroxiredoxin 2 promotes oxidative stress-induced neuronal cell death in Parkinson's disease. *Proc Natl Acad Sci U S A,* 104**,** 18742-7.
Fauquier, T., Chatonnet, F., Picou, F., Richard, S., Fossat, N., Aguilera, N., Lamonerie, T. & Flamant, F. 2014. Purkinje cells and Bergmann glia are primary targets of the TRalpha1 thyroid hormone receptor during mouse cerebellum postnatal development. *Development,* 141**,** 166-75.
Fernandes, A. C., Uytterhoeven, V., Kuenen, S., Wang, Y. C., Slabbaert, J. R., Swerts, J., Kasprowicz, J., Aerts, S. & Verstreken, P. 2014. Reduced synaptic vesicle protein degradation at lysosomes curbs TBC1D24/sky-induced neurodegeneration. *J Cell Biol,* 207**,** 453-62.
Ferreira, C. R. & Gahl, W. A. 2017. Lysosomal storage diseases. *Transl Sci Rare Dis,* 2**,** 1-71.
Finelli, M. J., Aprile, D., Castroflorio, E., Jeans, A., Moschetta, M., Chessum, L., Degiacomi, M. T., Grasegger, J., Lupien-Meilleur, A., Bassett, A., Rossignol, E., Campeau, P. M., Bowl, M. R., Benfenati, F., Fassio, A. & Oliver, P. L. 2018a. The epilepsy-associated protein TBC1D24 is required for normal development, survival and vesicle trafficking in mammalian neurons. *Hum Mol Genet*.
Finelli, M. J., Liu, K. X., Wu, Y., Oliver, P. L. & Davies, K. E. 2015. Oxr1 improves pathogenic cellular features of ALS-associated FUS and TDP-43 mutations. *Hum Mol Genet,* 24**,** 3529-44.
Finelli, M. J., Paramo, T., Pires, E., Ryan, B. J., Wade-Martins, R., Biggin, P. C., Mccullagh, J. & Oliver, P. L. 2018b. Oxidation Resistance 1 Modulates Glycolytic Pathways in the Cerebellum via an Interaction with Glucose-6-Phosphate Isomerase. *Mol Neurobiol*.
Finelli, M. J., Sanchez-Pulido, L., Liu, K. X., Davies, K. E. & Oliver, P. L. 2016. The Evolutionarily Conserved Tre2/Bub2/Cdc16 (TBC), Lysin Motif (LysM), Domain Catalytic (TLDc) Domain Is Neuroprotective against Oxidative Stress. *J Biol Chem,* 291**,** 2751-63.
Fischer, B., Luthy, K., Paesmans, J., De Koninck, C., Maes, I., Swerts, J., Kuenen, S., Uytterhoeven, V., Verstreken, P. & Versees, W. 2016. Skywalker-TBC1D24 has a lipid-binding pocket mutated in epilepsy and required for synaptic function. *Nat Struct Mol Biol,* 23**,** 965-973.
Fischer, D., Mukrasch, M. D., Von Bergen, M., Klos-Witkowska, A., Biernat, J., Griesinger, C., Mandelkow, E. & Zweckstetter, M. 2007. Structural and microtubule binding properties of tau mutants of frontotemporal dementias. *Biochemistry,* 46**,** 2574-82.

Fiskus, W., Coothankandaswamy, V., Chen, J., Ma, H., Ha, K., Saenz, D. T., Krieger, S. S., Mill, C. P., Sun, B., Huang, P., Mumm, J. S., Melnick, A. M. & Bhalla, K. N. 2016. SIRT2 Deacetylates and Inhibits the Peroxidase Activity of Peroxiredoxin-1 to Sensitize Breast Cancer Cells to Oxidant Stress-Inducing Agents. *Cancer Res,* 76**,** 5467-78.

Flagmeier, P., Meisl, G., Vendruscolo, M., Knowles, T. P., Dobson, C. M., Buell, A. K. & Galvagnion, C. 2016. Mutations associated with familial Parkinson's disease alter the initiation and amplification steps of alpha-synuclein aggregation. *Proc Natl Acad Sci U S A,* 113**,** 10328-33.

Fonseca, M. I., Chu, S. H., Hernandez, M. X., Fang, M. J., Modarresi, L., Selvan, P., Macgregor, G. R. & Tenner, A. J. 2017. Cell-specific deletion of C1qa identifies microglia as the dominant source of C1q in mouse brain. *J Neuroinflammation,* 14**,** 48.

Freimann, K., Zschiedrich, K., Bruggemann, N., Grunewald, A., Pawlack, H., Hagenah, J., Lohmann, K., Klein, C. & Westenberger, A. 2013. Mortalin mutations are not a frequent cause of early-onset Parkinson disease. *Neurobiol Aging,* 34**,** 2694 e19-20.

Friesen, E. L., De Snoo, M. L., Rajendran, L., Kalia, L. V. & Kalia, S. K. 2017. Chaperone-Based Therapies for Disease Modification in Parkinson's Disease. *Parkinsons Dis,* 2017**,** 5015307.

Fujikake, N., Shin, M. & Shimizu, S. 2018. Association Between Autophagy and Neurodegenerative Diseases. *Front Neurosci,* 12**,** 255.

Gan, P., Xia, Q., Hang, G., Zhou, Y., Qian, X., Wang, X. & Ding, L. 2018. Knockdown of cathepsin D protects dopaminergic neurons against neuroinflammation-mediated neurotoxicity through inhibition of NF-kappaB signalling pathway in Parkinson's disease model. *Clin Exp Pharmacol Physiol*.

Gan, Y., Ji, X., Hu, X., Luo, Y., Zhang, L., Li, P., Liu, X., Yan, F., Vosler, P., Gao, Y., Stetler, R. A. & Chen, J. 2012. Transgenic overexpression of peroxiredoxin-2 attenuates ischemic neuronal injury via suppression of a redox-sensitive pro-death signaling pathway. *Antioxid Redox Signal,* 17**,** 719-32.

Gandhi, S. & Abramov, A. Y. 2012. Mechanism of oxidative stress in neurodegeneration. *Oxid Med Cell Longev,* 2012**,** 428010.

Gao, R. & Penzes, P. 2015. Common mechanisms of excitatory and inhibitory imbalance in schizophrenia and autism spectrum disorders. *Curr Mol Med,* 15**,** 146-67.

Garrido, C., Paul, C., Seigneuric, R. & Kampinga, H. H. 2012. The small heat shock proteins family: the long forgotten chaperones. *Int J Biochem Cell Biol,* 44**,** 1588-92.

Geng, J. & Klionsky, D. J. 2010. The Golgi as a potential membrane source for autophagy. *Autophagy,* 6**,** 950-1.

Getahun, A. & Cambier, J. C. 2015. Of ITIMs, ITAMs, and ITAMis: revisiting immunoglobulin Fc receptor signaling. *Immunol Rev,* 268**,** 66-73.

Gilgun-Sherki, Y., Melamed, E. & Offen, D. 2001. Oxidative stress induced-neurodegenerative diseases: the need for antioxidants that penetrate the blood brain barrier. *Neuropharmacology,* 40**,** 959-75.

Gilley, J., Mayer, P. R., Yu, G. & Coleman, M. P. 2019. Low levels of NMNAT2 compromise axon development and survival. *Hum Mol Genet,* 28**,** 448-458.

Gillies, G. E. & Mcarthur, S. 2010. Estrogen actions in the brain and the basis for differential action in men and women: a case for sex-specific medicines. *Pharmacol Rev,* 62**,** 155-98.

Glorieux, C. & Calderon, P. B. 2017. Catalase, a remarkable enzyme: targeting the oldest antioxidant enzyme to find a new cancer treatment approach. *Biol Chem,* 398**,** 1095-1108.

Gmitterova, K., Gawinecka, J., Heinemann, U., Valkovic, P. & Zerr, I. 2018. DNA versus RNA oxidation in Parkinson's disease: Which is more important? *Neurosci Lett,* 662**,** 22-28.
Goedert, M. & Spillantini, M. G. 2000. Tau mutations in frontotemporal dementia FTDP-17 and their relevance for Alzheimer's disease. *Biochim Biophys Acta,* Jul 26;1502(1):110-21.
Goemaere, J. & Knoops, B. 2012. Peroxiredoxin distribution in the mouse brain with emphasis on neuronal populations affected in neurodegenerative disorders. *J Comp Neurol,* 520**,** 258-80.
Gonzalo, S., Greentree, W. K. & Linder, M. E. 1999. SNAP-25 is targeted to the plasma membrane through a novel membrane-binding domain. *J Biol Chem,* 274**,** 21313-8.
Gordon, D., Dafinca, R., Scaber, J., Alegre-Abarrategui, J., Farrimond, L., Scott, C., Biggs, D., Kent, L., Oliver, P. L., Davies, B., Ansorge, O., Wade-Martins, R. & Talbot, K. 2019. Single-copy expression of an amyotrophic lateral sclerosis-linked TDP-43 mutation (M337V) in BAC transgenic mice leads to altered stress granule dynamics and progressive motor dysfunction. *Neurobiol Dis,* 121**,** 148-162.
Gorenberg, E. L. & Chandra, S. S. 2017. The Role of Co-chaperones in Synaptic Proteostasis and Neurodegenerative Disease. *Front Neurosci,* 11**,** 248.
Goswami, A. V., Samaddar, M., Sinha, D., Purushotham, J. & D'silva, P. 2012. Enhanced J-protein interaction and compromised protein stability of mtHsp70 variants lead to mitochondrial dysfunction in Parkinson's disease. *Hum Mol Genet,* 21**,** 3317-32.
Goujon, C. & Malim, M. H. 2010. Characterization of the alpha interferon-induced postentry block to HIV-1 infection in primary human macrophages and T cells. *J Virol,* 84**,** 9254-66.
Goujon, C., Moncorge, O., Bauby, H., Doyle, T., Ward, C. C., Schaller, T., Hue, S., Barclay, W. S., Schulz, R. & Malim, M. H. 2013. Human MX2 is an interferon-induced post-entry inhibitor of HIV-1 infection. *Nature,* 502**,** 559-62.
Grabert, K., Michoel, T., Karavolos, M. H., Clohisey, S., Baillie, J. K., Stevens, M. P., Freeman, T. C., Summers, K. M. & Mccoll, B. W. 2016. Microglial brain region-dependent diversity and selective regional sensitivities to aging. *Nat Neurosci,* 19**,** 504-16.
Grimm, S., Hoehn, A., Davies, K. J. & Grune, T. 2011. Protein oxidative modifications in the ageing brain: consequence for the onset of neurodegenerative disease. *Free Radic Res,* 45**,** 73-88.
Guerrero, E. N., Wang, H., Mitra, J., Hegde, P. M., Stowell, S. E., Liachko, N. F., Kraemer, B. C., Garruto, R. M., Rao, K. S. & Hegde, M. L. 2016. TDP-43/FUS in motor neuron disease: Complexity and challenges. *Prog Neurobiol,* 145-146**,** 78-97.
Guna, A., Volkmar, N., Christianson, J. C. & Hegde, R. S. 2018. The ER membrane protein complex is a transmembrane domain insertase. *Science,* 359**,** 470-473.
Guo, C., Sun, L., Chen, X. & Zhang, D. 2013. Oxidative stress, mitochondrial damage and neurodegenerative diseases. *Neural Regen Res,* 8**,** 2003-14.
Gupta, H. V., Vengoechea, J., Sahaya, K. & Virmani, T. 2015. A splice site mutation in ATP6AP2 causes X-linked intellectual disability, epilepsy, and parkinsonism. *Parkinsonism Relat Disord,* 21**,** 1473-5.
Guven, A. & Tolun, A. 2013. TBC1D24 truncating mutation resulting in severe neurodegeneration. *J Med Genet,* 50**,** 199-202.
Gwon, Y., Kam, T. I., Kim, S. H., Song, S., Park, H., Lim, B., Lee, H., Lee, W., Jo, D. G. & Jung, Y. K. 2018. TOM1 Regulates Neuronal Accumulation of Amyloid-beta Oligomers by FcgammaRIIb2 Variant in Alzheimer's Disease. *J Neurosci,* 38**,** 9001-9018.
Haberle, V. & Stark, A. 2018. Eukaryotic core promoters and the functional basis of transcription initiation. *Nat Rev Mol Cell Biol,* 19**,** 621-637.

Halachmi, S., Marden, E., Martin, G., Mackay, H., Abbondanza, C. & Brown, M. 1994. Estrogen receptor-associated proteins: possible mediators of hormone-induced transcription. *Science,* 264**,** 1455-8.

Halter, B., Gonzalez De Aguilar, J. L., Rene, F., Petri, S., Fricker, B., Echaniz-Laguna, A., Dupuis, L., Larmet, Y. & Loeffler, J. P. 2010. Oxidative stress in skeletal muscle stimulates early expression of Rad in a mouse model of amyotrophic lateral sclerosis. *Free Radic Biol Med,* 48**,** 915-23.

Han, E. S., Muller, F. L., Perez, V. I., Qi, W., Liang, H., Xi, L., Fu, C., Doyle, E., Hickey, M., Cornell, J., Epstein, C. J., Roberts, L. J., Van Remmen, H. & Richardson, A. 2008. The in vivo gene expression signature of oxidative stress. *Physiol Genomics,* 34**,** 112-26.

Hartl, D., Schuldt, V., Forler, S., Zabel, C., Klose, J. & Rohe, M. 2012. Presymptomatic alterations in energy metabolism and oxidative stress in the APP23 mouse model of Alzheimer disease. *J Proteome Res,* 11**,** 3295-304.

Hashemi, E., Ariza, J., Rogers, H., Noctor, S. C. & Martinez-Cerdeno, V. 2017. The Number of Parvalbumin-Expressing Interneurons Is Decreased in the Prefrontal Cortex in Autism. *Cereb Cortex,* 27**,** 1931-1943.

Hedges, V. L., Chen, G., Yu, L., Krentzel, A. A., Starrett, J. R., Zhu, J. N., Suntharalingam, P., Remage-Healey, L., Wang, J. J., Ebner, T. J. & Mermelstein, P. G. 2018. Local Estrogen Synthesis Regulates Parallel Fiber-Purkinje Cell Neurotransmission Within the Cerebellar Cortex. *Endocrinology,* 159**,** 1328-1338.

Hedges, V. L., Ebner, T. J., Meisel, R. L. & Mermelstein, P. G. 2012. The cerebellum as a target for estrogen action. *Front Neuroendocrinol,* 33**,** 403-11.

Heneka, M. T., Carson, M. J., El Khoury, J., Landreth, G. E., Brosseron, F., Feinstein, D. L., Jacobs, A. H., Wyss-Coray, T., Vitorica, J., Ransohoff, R. M., Herrup, K., Frautschy, S. A., Finsen, B., Brown, G. C., Verkhratsky, A., Yamanaka, K., Koistinaho, J., Latz, E., Halle, A., Petzold, G. C., Town, T., Morgan, D., Shinohara, M. L., Perry, V. H., Holmes, C., Bazan, N. G., Brooks, D. J., Hunot, S., Joseph, B., Deigendesch, N., Garaschuk, O., Boddeke, E., Dinarello, C. A., Breitner, J. C., Cole, G. M., Golenbock, D. T. & Kummer, M. P. 2015. Neuroinflammation in Alzheimer's disease. *Lancet Neurol,* 14**,** 388-405.

Herber, C. B., Krause, W. C., Wang, L., Bayrer, J. R., Li, A., Schmitz, M., Fields, A., Ford, B., Zhang, Z., Reid, M. S., Nomura, D. K., Nissenson, R. A., Correa, S. M. & Ingraham, H. A. 2019. Estrogen signaling in arcuate Kiss1 neurons suppresses a sex-dependent female circuit promoting dense strong bones. *Nat Commun,* 10**,** 163.

Herculano-Houzel, S. 2010. Coordinated scaling of cortical and cerebellar numbers of neurons. *Front Neuroanat,* 4**,** 12.

Hetz, C. & Saxena, S. 2017. ER stress and the unfolded protein response in neurodegeneration. *Nat Rev Neurol,* 13**,** 477-491.

Hickman, S. E., Kingery, N. D., Ohsumi, T. K., Borowsky, M. L., Wang, L. C., Means, T. K. & El Khoury, J. 2013. The microglial sensome revealed by direct RNA sequencing. *Nat Neurosci,* 16**,** 1896-905.

Hipp, M. S., Kasturi, P. & Hartl, F. U. 2019. The proteostasis network and its decline in ageing. *Nat Rev Mol Cell Biol,* 20**,** 421-435.

Hishikawa, N., Takahashi, Y., Amakusa, Y., Tanno, Y., Tuji, Y., Niwa, H., Murakami, N. & Krishna, U. K. 2012. Effects of turmeric on Alzheimer's disease with behavioral and psychological symptoms of dementia. *Ayu,* 33**,** 499-504.

Hofweber, M., Hutten, S., Bourgeois, B., Spreitzer, E., Niedner-Boblenz, A., Schifferer, M., Ruepp, M. D., Simons, M., Niessing, D., Madl, T. & Dormann, D. 2018. Phase Separation of FUS Is Suppressed by Its Nuclear Import Receptor and Arginine Methylation. *Cell,* 173**,** 706-719 e13.

Holroyd, A. K. & Michie, A. M. 2018. The role of mTOR-mediated signaling in the regulation of cellular migration. *Immunol Lett,* 196**,** 74-79.
Holtman, I. R., Raj, D. D., Miller, J. A., Schaafsma, W., Yin, Z., Brouwer, N., Wes, P. D., Moller, T., Orre, M., Kamphuis, W., Hol, E. M., Boddeke, E. W. & Eggen, B. J. 2015. Induction of a common microglia gene expression signature by aging and neurodegenerative conditions: a co-expression meta-analysis. *Acta Neuropathol Commun,* 3**,** 31.
Hong, S., Beja-Glasser, V. F., Nfonoyim, B. M., Frouin, A., Li, S., Ramakrishnan, S., Merry, K. M., Shi, Q., Rosenthal, A., Barres, B. A., Lemere, C. A., Selkoe, D. J. & Stevens, B. 2016. Complement and microglia mediate early synapse loss in Alzheimer mouse models. *Science,* 352**,** 712-716.
Huang, D., Ou, B. & Prior, R. L. 2005. The chemistry behind antioxidant capacity assays. *J Agric Food Chem,* 53**,** 1841-56.
Huang, Q., Ding, L., Phan, K. B., Cheng, C., Xia, C. H., Gong, X. & Horwitz, J. 2009. Mechanism of cataract formation in alphaA-crystallin Y118D mutation. *Invest Ophthalmol Vis Sci,* 50**,** 2919-26.
Huang, W. J., Zhang, X. & Chen, W. W. 2015. Gaucher disease: a lysosomal neurodegenerative disorder. *Eur Rev Med Pharmacol Sci,* 19**,** 1219-26.
Ito, S. & Nagata, K. 2017. Biology of Hsp47 (Serpin H1), a collagen-specific molecular chaperone. *Semin Cell Dev Biol,* 62**,** 142-151.
Iurlaro, R. & Munoz-Pinedo, C. 2016. Cell death induced by endoplasmic reticulum stress. *FEBS J,* 283**,** 2640-52.
Janelidze, S., Mattsson, N., Stomrud, E., Lindberg, O., Palmqvist, S., Zetterberg, H., Blennow, K. & Hansson, O. 2018. CSF biomarkers of neuroinflammation and cerebrovascular dysfunction in early Alzheimer disease. *Neurology,* 91**,** e867-e877.
Jang, H. H., Kim, S. Y., Park, S. K., Jeon, H. S., Lee, Y. M., Jung, J. H., Lee, S. Y., Chae, H. B., Jung, Y. J., Lee, K. O., Lim, C. O., Chung, W. S., Bahk, J. D., Yun, D. J., Cho, M. J. & Lee, S. Y. 2006. Phosphorylation and concomitant structural changes in human 2-Cys peroxiredoxin isotype I differentially regulate its peroxidase and molecular chaperone functions. *FEBS Lett,* 580**,** 351-5.
Jang, H. H., Lee, K. O., Chi, Y. H., Jung, B. G., Park, S. K., Park, J. H., Lee, J. R., Lee, S. S., Moon, J. C., Yun, J. W., Choi, Y. O., Kim, W. Y., Kang, J. S., Cheong, G. W., Yun, D. J., Rhee, S. G., Cho, M. J. & Lee, S. Y. 2004. Two enzymes in one; two yeast peroxiredoxins display oxidative stress-dependent switching from a peroxidase to a molecular chaperone function. *Cell,* 117**,** 625-35.
Jaramillo-Gutierrez, G., Molina-Cruz, A., Kumar, S. & Barillas-Mury, C. 2010. The Anopheles gambiae oxidation resistance 1 (OXR1) gene regulates expression of enzymes that detoxify reactive oxygen species. *PLoS One,* 5**,** e11168.
Jay, T. R., Von Saucken, V. E. & Landreth, G. E. 2017. TREM2 in Neurodegenerative Diseases. *Mol Neurodegener,* 12**,** 56.
Ji, K., Akgul, G., Wollmuth, L. P. & Tsirka, S. E. 2013. Microglia actively regulate the number of functional synapses. *PLoS One,* 8**,** e56293.
Jia, J., Abudu, Y. P., Claude-Taupin, A., Gu, Y., Kumar, S., Choi, S. W., Peters, R., Mudd, M. H., Allers, L., Salemi, M., Phinney, B., Johansen, T. & Deretic, V. 2018. Galectins Control mTOR in Response to Endomembrane Damage. *Mol Cell,* 70**,** 120-135 e8.
Jia, Y., Jucius, T. J., Cook, S. A. & Ackerman, S. L. 2015. Loss of Clcc1 results in ER stress, misfolded protein accumulation, and neurodegeneration. *J Neurosci,* 35**,** 3001-9.
Jian, W., Wei, X., Chen, L., Wang, Z., Sun, Y., Zhu, S., Lou, H., Yan, S., Li, X., Zhou, J. & Zhang, B. 2017. Inhibition of HDAC6 increases acetylation of peroxiredoxin1/2 and ameliorates 6-OHDA induced dopaminergic injury. *Neurosci Lett,* 658**,** 114-120.

Jiang, Y., Liu, J., Chen, L., Jin, Y., Zhang, G., Lin, Z., Du, S., Fu, Z., Chen, T., Qin, Y. & Sun, X. 2019. Serum secreted miR-137-containing exosomes affects oxidative stress of neurons by regulating OXR1 in Parkinson's disease. *Brain Res*, 146331.

Joerger, A. C. & Fersht, A. R. 2016. The p53 Pathway: Origins, Inactivation in Cancer, and Emerging Therapeutic Approaches. *Annu Rev Biochem,* 85, 375-404.

Johnson, L. A. & Jackson, D. G. 2010. Inflammation-induced secretion of CCL21 in lymphatic endothelium is a key regulator of integrin-mediated dendritic cell transmigration. *Int Immunol,* 22, 839-49.

Jonikas, M. C., Collins, S. R., Denic, V., Oh, E., Quan, E. M., Schmid, V., Weibezahn, J., Schwappach, B., Walter, P., Weissman, J. S. & Schuldiner, M. 2009. Comprehensive characterization of genes required for protein folding in the endoplasmic reticulum. *Science,* 323, 1693-7.

Kak, G., Raza, M. & Tiwari, B. K. 2018. Interferon-gamma (IFN-gamma): Exploring its implications in infectious diseases. *Biomol Concepts,* 9, 64-79.

Kam, T. I., Song, S., Gwon, Y., Park, H., Yan, J. J., Im, I., Choi, J. W., Choi, T. Y., Kim, J., Song, D. K., Takai, T., Kim, Y. C., Kim, K. S., Choi, S. Y., Choi, S., Klein, W. L., Yuan, J. & Jung, Y. K. 2013. FcgammaRIIb mediates amyloid-beta neurotoxicity and memory impairment in Alzheimer's disease. *J Clin Invest,* 123, 2791-802.

Kamhi, A. G. & Clark, M. K. 2013. Specific language impairment. *Handb Clin Neurol,* 111, 219-27.

Kanekura, K., Nishimoto, I., Aiso, S. & Matsuoka, M. 2006. Characterization of amyotrophic lateral sclerosis-linked P56S mutation of vesicle-associated membrane protein-associated protein B (VAPB/ALS8). *J Biol Chem,* 281, 30223-33.

Kang, S., Brown, H. M. & Hwang, S. 2018. Direct Antiviral Mechanisms of Interferon-Gamma. *Immune Netw,* 18, e33.

Kapeli, K., Martinez, F. J. & Yeo, G. W. 2017. Genetic mutations in RNA-binding proteins and their roles in ALS. *Human genetics,* 136, 1193-1214.

Karlic, R., Chung, H. R., Lasserre, J., Vlahovicek, K. & Vingron, M. 2010. Histone modification levels are predictive for gene expression. *Proc Natl Acad Sci U S A,* 107, 2926-31.

Karplus, P. A. 2015. A primer on peroxiredoxin biochemistry. *Free Radic Biol Med,* 80, 183-90.

Kato, S., Kato, M., Abe, Y., Matsumura, T., Nishino, T., Aoki, M., Itoyama, Y., Asayama, K., Awaya, A., Hirano, A. & Ohama, E. 2005. Redox system expression in the motor neurons in amyotrophic lateral sclerosis (ALS): immunohistochemical studies on sporadic ALS, superoxide dismutase 1 (SOD1)-mutated familial ALS, and SOD1-mutated ALS animal models. *Acta Neuropathologica,* 110, 101-112.

Kempuraj, D., Thangavel, R., Natteru, P. A., Selvakumar, G. P., Saeed, D., Zahoor, H., Zaheer, S., Iyer, S. S. & Zaheer, A. 2016. Neuroinflammation Induces Neurodegeneration. *J Neurol Neurosurg Spine,* 1.

Kent, W. J., Sugnet, C. W., Furey, T. S., Roskin, K. M., Pringle, T. H., Zahler, A. M. & Haussler, D. 2002. The human genome browser at UCSC. *Genome Res,* 12, 996-1006.

Ketterer, S., Gomez-Auli, A., Hillebrand, L. E., Petrera, A., Ketscher, A. & Reinheckel, T. 2017. Inherited diseases caused by mutations in cathepsin protease genes. *FEBS J,* 284, 1437-1454.

Khan, J. A., Mendelson, A., Kunisaki, Y., Birbrair, A., Kou, Y., Arnal-Estape, A., Pinho, S., Ciero, P., Nakahara, F., Ma'ayan, A., Bergman, A., Merad, M. & Frenette, P. S. 2016. Fetal liver hematopoietic stem cell niches associate with portal vessels. *Science,* 351, 176-80.

Kiernan, M. C., Vucic, S., Cheah, B. C., Turner, M. R., Eisen, A., Hardiman, O., Burrell, J. R. & Zoing, M. C. 2011. Amyotrophic lateral sclerosis. *Lancet,* 377, 942-55.

Kim, G. H., Kim, J. E., Rhie, S. J. & Yoon, S. 2015. The Role of Oxidative Stress in Neurodegenerative Diseases. *Exp Neurobiol,* 24**,** 325-40.
Kim, S. H., Fountoulakis, M., Cairns, N. & Lubec, G. 2001. Protein levels of human peroxiredoxin subtypes in brains of patients with Alzheimer's disease and Down syndrome. *J Neural Transm Suppl***,** 223-35.
Kim, S. U., Jin, M. H., Kim, Y. S., Lee, S. H., Cho, Y. S., Cho, K. J., Lee, K. S., Kim, Y. I., Kim, G. W., Kim, J. M., Lee, T. H., Lee, Y. H., Shong, M., Kim, H. C., Chang, K. T., Yu, D. Y. & Lee, D. S. 2011. Peroxiredoxin II preserves cognitive function against age-linked hippocampal oxidative damage. *Neurobiol Aging,* 32**,** 1054-68.
Kim, S. Y., Jang, H. H., Lee, J. R., Sung, N. R., Lee, H. B., Lee, D. H., Park, D.-J., Kang, C. H., Chung, W. S., Lim, C. O., Yun, D.-J., Kim, W. Y., Lee, K. O. & Lee, S. Y. 2009. Oligomerization and chaperone activity of a plant 2-Cys peroxiredoxin in response to oxidative stress. *Plant Science,* 177**,** 227-232.
Kim, Y. C. & Guan, K. L. 2015. mTOR: a pharmacologic target for autophagy regulation. *J Clin Invest,* 125**,** 25-32.
Klucken, J., Shin, Y., Masliah, E., Hyman, B. T. & Mclean, P. J. 2004. Hsp70 Reduces alpha-Synuclein Aggregation and Toxicity. *J Biol Chem,* 279**,** 25497-502.
Koga, H., Kaushik, S. & Cuervo, A. M. 2011. Protein homeostasis and aging: The importance of exquisite quality control. *Ageing Res Rev,* 10**,** 205-15.
Kohl, S., Wolters, C., Gruendler, T. O., Vogeley, K., Klosterkotter, J. & Kuhn, J. 2014. Prepulse inhibition of the acoustic startle reflex in high functioning autism. *PLoS One,* 9**,** e92372.
Koide, T., Takahara, Y., Asada, S. & Nagata, K. 2002. Xaa-Arg-Gly triplets in the collagen triple helix are dominant binding sites for the molecular chaperone HSP47. *J Biol Chem,* 277**,** 6178-82.
Kollmann, K., Damme, M., Markmann, S., Morelle, W., Schweizer, M., Hermans-Borgmeyer, I., Röchert, A. K., Pohl, S., Lübke, T., Michalski, J. C., Käkelä, R., Walkley, S. U. & Braulke, T. 2012. Lysosomal dysfunction causes neurodegeneration in mucolipidosis II 'knock-in' mice. *Brain,* 135**,** 2661-2675.
Konkle, A. T. & Mccarthy, M. M. 2011. Developmental time course of estradiol, testosterone, and dihydrotestosterone levels in discrete regions of male and female rat brain. *Endocrinology,* 152**,** 223-35.
Kontaxi, C., Piccardo, P. & Gill, A. C. 2017. Lysine-Directed Post-translational Modifications of Tau Protein in Alzheimer's Disease and Related Tauopathies. *Front Mol Biosci,* 4**,** 56.
Koopmans, F., Pandya, N. J., Franke, S. K., Phillippens, I., Paliukhovich, I., Li, K. W. & Smit, A. B. 2018. Comparative Hippocampal Synaptic Proteomes of Rodents and Primates: Differences in Neuroplasticity-Related Proteins. *Front Mol Neurosci,* 11**,** 364.
Korovila, I., Hugo, M., Castro, J. P., Weber, D., Hohn, A., Grune, T. & Jung, T. 2017. Proteostasis, oxidative stress and aging. *Redox Biol,* 13**,** 550-567.
Korvatska, O., Strand, N. S., Berndt, J. D., Strovas, T., Chen, D. H., Leverenz, J. B., Kiianitsa, K., Mata, I. F., Karakoc, E., Greenup, J. L., Bonkowski, E., Chuang, J., Moon, R. T., Eichler, E. E., Nickerson, D. A., Zabetian, C. P., Kraemer, B. C., Bird, T. D. & Raskind, W. H. 2013. Altered splicing of ATP6AP2 causes X-linked parkinsonism with spasticity (XPDS). *Hum Mol Genet,* 22**,** 3259-68.
Koudritsky, M. & Domany, E. 2008. Positional distribution of human transcription factor binding sites. *Nucleic Acids Res,* 36**,** 6795-805.
Kouser, L., Madhukaran, S. P., Shastri, A., Saraon, A., Ferluga, J., Al-Mozaini, M. & Kishore, U. 2015. Emerging and Novel Functions of Complement Protein C1q. *Front Immunol,* 6**,** 317.

Krapfenbauer, K., Engidawork, E., Cairns, N., Fountoulakis, M. & Lubec, G. 2003. Aberrant expression of peroxiredoxin subtypes in neurodegenerative disorders. *Brain Research,* 967**,** 152-160.

Kumar, V., Sami, N., Kashav, T., Islam, A., Ahmad, F. & Hassan, M. I. 2016. Protein aggregation and neurodegenerative diseases: From theory to therapy. *Eur J Med Chem,* 124**,** 1105-1120.

Kurd, N. & Robey, E. A. 2016. T-cell selection in the thymus: a spatial and temporal perspective. *Immunol Rev,* 271**,** 114-26.

Kuroda, Y., Kimura, Y., Uehara, T., Kosaki, K. & Kurosawa, K. 2019. The refinement of 16p13.3 microdeletion syndrome from a case presentation of a girl with epilepsy and intellectual disability. *Congenit Anom (Kyoto)*.

Labbadia, J. & Morimoto, R. I. 2015. The biology of proteostasis in aging and disease. *Annu Rev Biochem,* 84**,** 435-64.

Lahiri, S., Chao, J. T., Tavassoli, S., Wong, A. K., Choudhary, V., Young, B. P., Loewen, C. J. & Prinz, W. A. 2014. A conserved endoplasmic reticulum membrane protein complex (EMC) facilitates phospholipid transfer from the ER to mitochondria. *PLoS Biol,* 12**,** e1001969.

Lambert, S. A., Jolma, A., Campitelli, L. F., Das, P. K., Yin, Y., Albu, M., Chen, X., Taipale, J., Hughes, T. R. & Weirauch, M. T. 2018. The Human Transcription Factors. *Cell,* 172**,** 650-665.

Lasar, D., Rosenwald, M., Kiehlmann, E., Balaz, M., Tall, B., Opitz, L., Lidell, M. E., Zamboni, N., Krznar, P., Sun, W., Varga, L., Stefanicka, P., Ukropec, J., Nuutila, P., Virtanen, K., Amri, E. Z., Enerback, S., Wahli, W. & Wolfrum, C. 2018. Peroxisome Proliferator Activated Receptor Gamma Controls Mature Brown Adipocyte Inducibility through Glycerol Kinase. *Cell Rep,* 22**,** 760-773.

Lazennec, G., Ediger, T. R., Petz, L. N., Nardulli, A. M. & Katzenellenbogen, B. S. 1997. Mechanistic aspects of estrogen receptor activation probed with constitutively active estrogen receptors: correlations with DNA and coregulator interactions and receptor conformational changes. *Mol Endocrinol,* 11**,** 1375-86.

Lean, J. M., Murphy, C., Fuller, K. & Chambers, T. J. 2002. CCL9/MIP-1gamma and its receptor CCR1 are the major chemokine ligand/receptor species expressed by osteoclasts. *J Cell Biochem,* 87**,** 386-93.

Lee, C. Y. & Landreth, G. E. 2010. The role of microglia in amyloid clearance from the AD brain. *J Neural Transm (Vienna),* 117**,** 949-60.

Lee, E. H., Lim, S. S., Yuen, K. H. & Lee, C. Y. 2019. Curcumin and a hemi-analogue with improved blood-brain barrier permeability protect against amyloid-beta toxicity in Caenorhabditis elegans via SKN-1/Nrf activation. *J Pharm Pharmacol,* 71**,** 860-868.

Lee, E. M., Lee, S. S., Tripathi, B. N., Jung, H. S., Cao, G. P., Lee, Y., Singh, S., Hong, S. H., Lee, K. W., Lee, S. Y., Cho, J. Y. & Chung, B. Y. 2015a. Site-directed mutagenesis substituting cysteine for serine in 2-Cys peroxiredoxin (2-Cys Prx A) of Arabidopsis thaliana effectively improves its peroxidase and chaperone functions. *Ann Bot,* 116**,** 713-25.

Lee, H. R., Kim, T. H. & Choi, K. C. 2012. Functions and physiological roles of two types of estrogen receptors, ERalpha and ERbeta, identified by estrogen receptor knockout mouse. *Lab Anim Res,* 28**,** 71-6.

Lee, J. A., Son, H. J., Choi, J. W., Kim, J., Han, S. H., Shin, N., Kim, J. H., Kim, S. J., Heo, J. Y., Kim, D. J., Park, K. D. & Hwang, O. 2018. Activation of the Nrf2 signaling pathway and neuroprotection of nigral dopaminergic neurons by a novel synthetic compound KMS99220. *Neurochem Int,* 112**,** 96-107.

Lee, S. P., Hwang, Y. S., Kim, Y. J., Kwon, K. S., Kim, H. J., Kim, K. & Chae, H. Z. 2001. Cyclophilin a binds to peroxiredoxins and activates its peroxidase activity. *J Biol Chem,* 276**,** 29826-32.

Lee, S. S., Jung, H. S., Park, S.-K., Lee, E. M., Singh, S., Lee, Y., Lee, K. O., Lee, S. Y. & Chung, B. Y. 2015b. Enhancement of Chaperone Activity of Plant-Specific Thioredoxin through γ-Ray Mediated Conformational Change. *International journal of molecular sciences,* 16**,** 27302-27312.

Lee, Y. M., Park, S. H., Shin, D. I., Hwang, J. Y., Park, B., Park, Y. J., Lee, T. H., Chae, H. Z., Jin, B. K., Oh, T. H. & Oh, Y. J. 2008. Oxidative modification of peroxiredoxin is associated with drug-induced apoptotic signaling in experimental models of Parkinson disease. *J Biol Chem,* 283**,** 9986-98.

Lein, E. S., Hawrylycz, M. J., Ao, N., Ayres, M., Bensinger, A., Bernard, A., Boe, A. F., Boguski, M. S., Brockway, K. S., Byrnes, E. J., Chen, L., Chen, L., Chen, T. M., Chin, M. C., Chong, J., Crook, B. E., Czaplinska, A., Dang, C. N., Datta, S., Dee, N. R., Desaki, A. L., Desta, T., Diep, E., Dolbeare, T. A., Donelan, M. J., Dong, H. W., Dougherty, J. G., Duncan, B. J., Ebbert, A. J., Eichele, G., Estin, L. K., Faber, C., Facer, B. A., Fields, R., Fischer, S. R., Fliss, T. P., Frensley, C., Gates, S. N., Glattfelder, K. J., Halverson, K. R., Hart, M. R., Hohmann, J. G., Howell, M. P., Jeung, D. P., Johnson, R. A., Karr, P. T., Kawal, R., Kidney, J. M., Knapik, R. H., Kuan, C. L., Lake, J. H., Laramee, A. R., Larsen, K. D., Lau, C., Lemon, T. A., Liang, A. J., Liu, Y., Luong, L. T., Michaels, J., Morgan, J. J., Morgan, R. J., Mortrud, M. T., Mosqueda, N. F., Ng, L. L., Ng, R., Orta, G. J., Overly, C. C., Pak, T. H., Parry, S. E., Pathak, S. D., Pearson, O. C., Puchalski, R. B., Riley, Z. L., Rockett, H. R., Rowland, S. A., Royall, J. J., Ruiz, M. J., Sarno, N. R., Schaffnit, K., Shapovalova, N. V., Sivisay, T., Slaughterbeck, C. R., Smith, S. C., Smith, K. A., Smith, B. I., Sodt, A. J., Stewart, N. N., Stumpf, K. R., Sunkin, S. M., Sutram, M., Tam, A., Teemer, C. D., Thaller, C., Thompson, C. L., Varnam, L. R., Visel, A., Whitlock, R. M., Wohnoutka, P. E., Wolkey, C. K., Wong, V. Y., et al. 2007. Genome-wide atlas of gene expression in the adult mouse brain. *Nature,* 445**,** 168-76.

Leppek, K., Das, R. & Barna, M. 2017. Functional 5′ UTR mRNA structures in eukaryotic translation regulation and how to find them. *Nature Reviews Molecular Cell Biology,* 19**,** 158.

Leppek, K., Das, R. & Barna, M. 2018. Functional 5' UTR mRNA structures in eukaryotic translation regulation and how to find them. *Nat Rev Mol Cell Biol,* 19**,** 158-174.

Levine, B. & Kroemer, G. 2019. Biological Functions of Autophagy Genes: A Disease Perspective. *Cell,* 176**,** 11-42.

Leyfer, O. T., Tager-Flusberg, H., Dowd, M., Tomblin, J. B. & Folstein, S. E. 2008. Overlap between autism and specific language impairment: comparison of Autism Diagnostic Interview and Autism Diagnostic Observation Schedule scores. *Autism Res,* 1**,** 284-96.

Li, H. L., Lin, H. R. & Xia, J. H. 2017. Differential Gene Expression Profiles and Alternative Isoform Regulations in Gill of Nile Tilapia in Response to Acute Hypoxia. *Mar Biotechnol (NY),* 19**,** 551-562.

Li, J., Liu, R., Feng, H., Zhang, J., Wang, D., Wang, Y., Zeng, J. & Fan, Y. 2018. Novel TBC1D24 Mutations in a Case of Nonconvulsive Status Epilepticus. *Front Neurol,* 9**,** 623.

Li, W., Zhang, H., Nie, A., Ni, Q., Li, F., Ning, G., Li, X., Gu, Y. & Wang, Q. 2016. mTORC1 pathway mediates beta cell compensatory proliferation in 60 % partial-pancreatectomy mice. *Endocrine,* 53**,** 117-28.

Li, Y., Li, W., Liu, C., Yan, M., Raman, I., Du, Y., Fang, X., Zhou, X. J., Mohan, C. & Li, Q. Z. 2014. Delivering Oxidation Resistance-1 (OXR1) to Mouse Kidney by Genetic Modified

Mesenchymal Stem Cells Exhibited Enhanced Protection against Nephrotoxic Serum Induced Renal Injury and Lupus Nephritis. *J Stem Cell Res Ther,* 4.
Liao, G., Wen, Z., Irizarry, K., Huang, Y., Mitsouras, K., Darmani, M., Leon, T., Shi, L. & Bi, X. 2010. Abnormal gene expression in cerebellum of Npc1-/- mice during postnatal development. *Brain Res,* 1325c**,** 128-40.
Licausi, F., Weits, D. A., Pant, B. D., Scheible, W. R., Geigenberger, P. & Van Dongen, J. T. 2011. Hypoxia responsive gene expression is mediated by various subsets of transcription factors and miRNAs that are determined by the actual oxygen availability. *New Phytol,* 190**,** 442-56.
Liddelow, S. A. & Barres, B. A. 2017. Reactive Astrocytes: Production, Function, and Therapeutic Potential. *Immunity,* 46**,** 957-967.
Liddelow, S. A., Guttenplan, K. A., Clarke, L. E., Bennett, F. C., Bohlen, C. J., Schirmer, L., Bennett, M. L., Munch, A. E., Chung, W. S., Peterson, T. C., Wilton, D. K., Frouin, A., Napier, B. A., Panicker, N., Kumar, M., Buckwalter, M. S., Rowitch, D. H., Dawson, V. L., Dawson, T. M., Stevens, B. & Barres, B. A. 2017. Neurotoxic reactive astrocytes are induced by activated microglia. *Nature,* 541**,** 481-487.
Lie, P. P. Y. & Nixon, R. A. 2018. Lysosome trafficking and signaling in health and neurodegenerative diseases. *Neurobiol Dis*.
Lim, Y. Y., Site, M., Maruff, P., Getter, C., Salloway, S., Ott, B. R., Schindler, R. & Snyder, P. J. 2014. Evidence of neuroinflammation in the retina in presymptomatic Alzheimer's disease. *Alzheimer's & Dementia: The Journal of the Alzheimer's Association,* 10**,** P429.
Lindner, A. B. & Demarez, A. 2009. Protein aggregation as a paradigm of aging. *Biochim Biophys Acta,* 1790**,** 980-96.
Link, K. A., Chou, F.-S. & Mulloy, J. C. 2010. Core binding factor at the crossroads: determining the fate of the HSC. *Journal of cellular physiology,* 222**,** 50-56.
Linnartz-Gerlach, B., Bodea, L. G., Klaus, C., Ginolhac, A., Halder, R., Sinkkonen, L., Walter, J., Colonna, M. & Neumann, H. 2018. TREM2 triggers microglial density and age-related neuronal loss. *Glia*.
Liu, K. X., Edwards, B., Lee, S., Finelli, M. J., Davies, B., Davies, K. E. & Oliver, P. L. 2015. Neuron-specific antioxidant OXR1 extends survival of a mouse model of amyotrophic lateral sclerosis. *Brain,* 138**,** 1167-81.
Liu, Q., Zhang, Y., Liu, S., Liu, Y., Yang, X., Liu, G., Shimizu, T., Ikenaka, K., Fan, K. & Ma, J. 2019. Cathepsin C promotes microglia M1 polarization and aggravates neuroinflammation via activation of Ca(2+)-dependent PKC/p38MAPK/NF-kappaB pathway. *J Neuroinflammation,* 16**,** 10.
Liu, Y., Beyer, A. & Aebersold, R. 2016. On the Dependency of Cellular Protein Levels on mRNA Abundance. *Cell,* 165**,** 535-50.
Liu, Y. & O'flaherty, C. 2017. In vivo oxidative stress alters thiol redox status of peroxiredoxin 1 and 6 and impairs rat sperm quality. *Asian J Androl,* 19**,** 73-79.
Lobsiger, C. S., Boillée, S., Pozniak, C., Khan, A. M., Mcalonis-Downes, M., Lewcock, J. W. & Cleveland, D. W. 2013. C1q induction and global complement pathway activation do not contribute to ALS toxicity in mutant SOD1 mice. *Proc Natl Acad Sci U S A,* 110**,** E4385-92.
Longtine, M. S., Chen, B., Odibo, A. O., Zhong, Y. & Nelson, D. M. 2012. Villous trophoblast apoptosis is elevated and restricted to cytotrophoblasts in pregnancies complicated by preeclampsia, IUGR, or preeclampsia with IUGR. *Placenta,* 33**,** 352-9.
Lopez, M. E., Klein, A. D., Hong, J., Dimbil, U. J. & Scott, M. P. 2012. Neuronal and epithelial cell rescue resolves chronic systemic inflammation in the lipid storage disorder Niemann-Pick C. *Hum Mol Genet,* 21**,** 2946-60.

Love, J. E., Hayden, E. J. & Rohn, T. T. 2015. Alternative Splicing in Alzheimer's Disease. *J Parkinsons Dis Alzheimers Dis,* 2.
Lowry, J. R. & Klegeris, A. 2018. Emerging roles of microglial cathepsins in neurodegenerative disease. *Brain Res Bull,* 139**,** 144-156.
Lu, Y., Zhang, X. S., Zhang, Z. H., Zhou, X. M., Gao, Y. Y., Liu, G. J., Wang, H., Wu, L. Y., Li, W. & Hang, C. H. 2018. Peroxiredoxin 2 activates microglia by interacting with Toll-like receptor 4 after subarachnoid hemorrhage. *J Neuroinflammation,* 15**,** 87.
Lüthy, K., Mei, D., Fischer, B., De Fusco, M., Swerts, J., Paesmans, J., Parrini, E., Lubarr, N., Meijer, I. A., Mackenzie, K. M., Lee, W. T., Cittaro, D., Aridon, P., Schoovaerts, N., Versees, W., Verstreken, P., Casari, G. & Guerrini, R. 2019. TBC1D24-TLDc-related epilepsy exercise-induced dystonia: rescue by antioxidants in a disease model. *Brain*.
Luzio, J. P., Hackmann, Y., Dieckmann, N. M. & Griffiths, G. M. 2014. The biogenesis of lysosomes and lysosome-related organelles. *Cold Spring Harb Perspect Biol,* 6**,** a016840.
Luzio, J. P., Pryor, P. R. & Bright, N. A. 2007. Lysosomes: fusion and function. *Nat Rev Mol Cell Biol,* 8**,** 622-32.
Lyly, A., Marjavaara, S. K., Kyttala, A., Uusi-Rauva, K., Luiro, K., Kopra, O., Martinez, L. O., Tanhuanpaa, K., Kalkkinen, N., Suomalainen, A., Jauhiainen, M. & Jalanko, A. 2008. Deficiency of the INCL protein Ppt1 results in changes in ectopic F1-ATP synthase and altered cholesterol metabolism. *Hum Mol Genet,* 17**,** 1406-17.
Lyly, A., Von Schantz, C., Heine, C., Schmiedt, M. L., Sipila, T., Jalanko, A. & Kyttala, A. 2009. Novel interactions of CLN5 support molecular networking between Neuronal Ceroid Lipofuscinosis proteins. *BMC Cell Biol,* 10**,** 83.
Lyons, A., Lynch, A. M., Downer, E. J., Hanley, R., O'sullivan, J. B., Smith, A. & Lynch, M. A. 2009. Fractalkine-induced activation of the phosphatidylinositol-3 kinase pathway attentuates microglial activation in vivo and in vitro. *J Neurochem,* 110**,** 1547-56.
Ma, Q. 2013. Role of nrf2 in oxidative stress and toxicity. *Annu Rev Pharmacol Toxicol,* 53**,** 401-26.
Ma, Z., Zhu, P., Shi, H., Guo, L., Zhang, Q., Chen, Y., Chen, S., Zhang, Z., Peng, J. & Chen, J. 2019. PTC-bearing mRNA elicits a genetic compensation response via Upf3a and COMPASS components. *Nature,* 568**,** 259-263.
Maday, S. & Holzbaur, E. L. 2014. Autophagosome biogenesis in primary neurons follows an ordered and spatially regulated pathway. *Dev Cell,* 30**,** 71-85.
Maday, S. & Holzbaur, E. L. 2016. Compartment-Specific Regulation of Autophagy in Primary Neurons. *J Neurosci,* 36**,** 5933-45.
Man, S. M., Ma, Y. R., Shang, D. S., Zhao, W. D., Li, B., Guo, D. W., Fang, W. G., Zhu, L. & Chen, Y. H. 2007. Peripheral T cells overexpress MIP-1alpha to enhance its transendothelial migration in Alzheimer's disease. *Neurobiol Aging,* 28**,** 485-96.
Mantione, K. J., Kream, R. M., Kuzelova, H., Ptacek, R., Raboch, J., Samuel, J. M. & Stefano, G. B. 2014. Comparing bioinformatic gene expression profiling methods: microarray and RNA-Seq. *Med Sci Monit Basic Res,* 20**,** 138-42.
Marini, J. C., Reich, A. & Smith, S. M. 2014. Osteogenesis imperfecta due to mutations in non-collagenous genes: lessons in the biology of bone formation. *Curr Opin Pediatr,* 26**,** 500-7.
Martin, L., Latypova, X. & Terro, F. 2011. Post-translational modifications of tau protein: implications for Alzheimer's disease. *Neurochem Int,* 58**,** 458-71.
Mary, S., Kulkarni, M. J., Malakar, D., Joshi, S. R., Mehendale, S. S. & Giri, A. P. 2017. Placental Proteomics Provides Insights into Pathophysiology of Pre-Eclampsia and Predicts Possible Markers in Plasma. *J Proteome Res,* 16**,** 1050-1060.

Mattoo, R. U. & Goloubinoff, P. 2014. Molecular chaperones are nanomachines that catalytically unfold misfolded and alternatively folded proteins. *Cell Mol Life Sci,* 71**,** 3311-25.
Maxson, M. E. & Grinstein, S. 2014. The vacuolar-type H⁺-ATPase at a glance – more than a proton pump. *Journal of Cell Science,* 127**,** 4987.
Mcquade, A. & Blurton-Jones, M. 2019. Microglia in Alzheimer's Disease: Exploring How Genetics and Phenotype Influence Risk. *J Mol Biol,* 431**,** 1805-1817.
Mecca, C., Giambanco, I., Donato, R. & Arcuri, C. 2018. Microglia and Aging: The Role of the TREM2-DAP12 and CX3CL1-CX3CR1 Axes. *Int J Mol Sci,* 19.
Medeiros, M. S., Schumacher-Schuh, A., Cardoso, A. M., Bochi, G. V., Baldissarelli, J., Kegler, A., Santana, D., Chaves, C. M., Schetinger, M. R., Moresco, R. N., Rieder, C. R. & Fighera, M. R. 2016. Iron and Oxidative Stress in Parkinson's Disease: An Observational Study of Injury Biomarkers. *PLoS One,* 11**,** e0146129.
Mendez, M. G. & Janmey, P. A. 2012. Transcription factor regulation by mechanical stress. *Int J Biochem Cell Biol,* 44**,** 728-32.
Merkulova, M., Paunescu, T. G., Azroyan, A., Marshansky, V., Breton, S. & Brown, D. 2015. Mapping the H(+) (V)-ATPase interactome: identification of proteins involved in trafficking, folding, assembly and phosphorylation. *Sci Rep,* 5**,** 14827.
Merkulova, M., Paunescu, T. G., Nair, A. V., Wang, C. Y., Capen, D. E., Oliver, P. L., Breton, S. & Brown, D. 2018. Targeted deletion of the Ncoa7 gene results in incomplete distal renal tubular acidosis in mice. *Am J Physiol Renal Physiol,* 315**,** F173-F185.
Messeguer, X., Escudero, R., Farre, D., Nunez, O., Martinez, J. & Alba, M. M. 2002. PROMO: detection of known transcription regulatory elements using species-tailored searches. *Bioinformatics,* 18**,** 333-4.
Michaelis, E. K. 2012. Selective neuronal vulnerability in the hippocampus: Relationship to neurological diseases and mechanisms for differential sensitivity of neurons to stress. *The clinical neurobiology of the hippocampus: An integrative view.* New York, NY, US: Oxford University Press.
Miller, A. F. 2012. Superoxide dismutases: ancient enzymes and new insights. *FEBS Lett,* 586**,** 585-95.
Miller, S. J., Zhang, P. W., Glatzer, J. & Rothstein, J. D. 2017. Astroglial transcriptome dysregulation in early disease of an ALS mutant SOD1 mouse model. *J Neurogenet,* 31**,** 37-48.
Mink, J. W., Blumenschine, R. J. & Adams, D. B. 1981. Ratio of central nervous system to body metabolism in vertebrates: its constancy and functional basis. *American Journal of Physiology - Regulatory, Integrative and Comparative Physiology,* 241**,** R203-R212.
Mironczuk-Chodakowska, I., Witkowska, A. M. & Zujko, M. E. 2018. Endogenous non-enzymatic antioxidants in the human body. *Adv Med Sci,* 63**,** 68-78.
Mishina, N. M., Markvicheva, K. N., Bilan, D. S., Matlashov, M. E., Shirmanova, M. V., Liebl, D., Schultz, C., Lukyanov, S. & Belousov, V. V. 2013. Visualization of intracellular hydrogen peroxide with HyPer, a genetically encoded fluorescent probe. *Methods Enzymol,* 526**,** 45-59.
Miyamoto, A., Wake, H., Ishikawa, A. W., Eto, K., Shibata, K., Murakoshi, H., Koizumi, S., Moorhouse, A. J., Yoshimura, Y. & Nabekura, J. 2016. Microglia contact induces synapse formation in developing somatosensory cortex. *Nat Commun,* 7**,** 12540.
Mol, B. W. J., Roberts, C. T., Thangaratinam, S., Magee, L. A., De Groot, C. J. M. & Hofmeyr, G. J. 2016. Pre-eclampsia. *The Lancet,* 387**,** 999-1011.
Mole, S. E. & Williams, R. E. 2013. Neuronal Ceroid-Lipofuscinoses. *In:* ADAM, M. P., ARDINGER, H. H., PAGON, R. A., WALLACE, S. E., BEAN, L. J. H., STEPHENS, K. &

AMEMIYA, A. (eds.) *GeneReviews((R)).* Seattle (WA): University of Washington, Seattle
University of Washington, Seattle. GeneReviews is a registered trademark of the University of Washington, Seattle. All rights reserved.
Montano, A. M., Lock-Hock, N., Steiner, R. D., Graham, B. H., Szlago, M., Greenstein, R., Pineda, M., Gonzalez-Meneses, A., Coker, M., Bartholomew, D., Sands, M. S., Wang, R., Giugliani, R., Macaya, A., Pastores, G., Ketko, A. K., Ezgu, F., Tanaka, A., Arash, L., Beck, M., Falk, R. E., Bhattacharya, K., Franco, J., White, K. K., Mitchell, G. A., Cimbalistiene, L., Holtz, M. & Sly, W. S. 2016. Clinical course of sly syndrome (mucopolysaccharidosis type VII). *J Med Genet,* 53**,** 403-18.
Monteiro, S., Roque, S., Marques, F., Correia-Neves, M. & Cerqueira, J. J. 2017. Brain interference: Revisiting the role of IFNgamma in the central nervous system. *Prog Neurobiol,* 156**,** 149-163.
Moon, J. C., Hah, Y. S., Kim, W. Y., Jung, B. G., Jang, H. H., Lee, J. R., Kim, S. Y., Lee, Y. M., Jeon, M. G., Kim, C. W., Cho, M. J. & Lee, S. Y. 2005. Oxidative stress-dependent structural and functional switching of a human 2-Cys peroxiredoxin isotype II that enhances HeLa cell resistance to H2O2-induced cell death. *J Biol Chem,* 280**,** 28775-84.
Moors, T., Paciotti, S., Chiasserini, D., Calabresi, P., Parnetti, L., Beccari, T. & Van De Berg, W. D. 2016. Lysosomal Dysfunction and alpha-Synuclein Aggregation in Parkinson's Disease: Diagnostic Links. *Mov Disord,* 31**,** 791-801.
Moreno-Gonzalez, I. & Soto, C. 2011. Misfolded protein aggregates: mechanisms, structures and potential for disease transmission. *Semin Cell Dev Biol,* 22**,** 482-7.
Morey, J. S., Ryan, J. C. & Van Dolah, F. M. 2006. Microarray validation: factors influencing correlation between oligonucleotide microarrays and real-time PCR. *Biological procedures online,* 8**,** 175-193.
Mucha, B. E., Banka, S., Ajeawung, N. F., Molidperee, S., Chen, G. G., Koenig, M. K., Adejumo, R. B., Till, M., Harbord, M., Perrier, R., Lemyre, E., Boucher, R. M., Skotko, B. G., Waxler, J. L., Thomas, M. A., Hodge, J. C., Gecz, J., Nicholl, J., Mcgregor, L., Linden, T., Sisodiya, S. M., Sanlaville, D., Cheung, S. W., Ernst, C. & Campeau, P. M. 2018. A new microdeletion syndrome involving TBC1D24, ATP6V0C, and PDPK1 causes epilepsy, microcephaly, and developmental delay. *Genet Med*.
Mucha, B. E., Hennekam, R. C. M., Sisodiya, S. & Campeau, P. M. 2017. TBC1D24-Related Disorders. *In:* ADAM, M. P., ARDINGER, H. H., PAGON, R. A., WALLACE, S. E., BEAN, L. J. H., STEPHENS, K. & AMEMIYA, A. (eds.) *GeneReviews((R)).* Seattle (WA): University of Washington, Seattle GeneReviews is a registered trademark of the University of Washington, Seattle. All rights reserved.
Mukherjee, A. B., Appu, A. P., Sadhukhan, T., Casey, S., Mondal, A., Zhang, Z. & Bagh, M. B. 2019. Emerging new roles of the lysosome and neuronal ceroid lipofuscinoses. *Mol Neurodegener,* 14**,** 4.
Murphy, K. C. & Volkert, M. R. 2012. Structural/functional analysis of the human OXR1 protein: identification of exon 8 as the anti-oxidant encoding function. *BMC Mol Biol,* 13**,** 26.
Myers, R. H. 2004. Huntington's disease genetics. *NeuroRx,* 1**,** 255-62.
Nakamura, T. & Lipton, S. A. 2013. Emerging role of protein-protein transnitrosylation in cell signaling pathways. *Antioxid Redox Signal,* 18**,** 239-49.
Nakashima, M., Negishi, Y., Hori, I., Hattori, A., Saitoh, S. & Saitsu, H. 2019. A case of early-onset epileptic encephalopathy with a homozygous TBC1D24 variant caused by uniparental isodisomy. *Am J Med Genet A*.

Narciso, L., Parlanti, E., Racaniello, M., Simonelli, V., Cardinale, A., Merlo, D. & Dogliotti, E. 2016. The Response to Oxidative DNA Damage in Neurons: Mechanisms and Disease. *Neural Plast,* 2016**,** 3619274.

Navarro-Yepes, J., Zavala-Flores, L., Anandhan, A., Wang, F., Skotak, M., Chandra, N., Li, M., Pappa, A., Martinez-Fong, D., Del Razo, L. M., Quintanilla-Vega, B. & Franco, R. 2014. Antioxidant gene therapy against neuronal cell death. *Pharmacol Ther,* 142**,** 206-30.

Nelson, K. J. & Parsonage, D. 2011. Measurement of peroxiredoxin activity. *Curr Protoc Toxicol,* Chapter 7**,** Unit7 10.

Nelson, P. T., Dickson, D. W., Trojanowski, J. Q., Jack, C. R., Boyle, P. A., Arfanakis, K., Rademakers, R., Alafuzoff, I., Attems, J., Brayne, C., Coyle-Gilchrist, I. T. S., Chui, H. C., Fardo, D. W., Flanagan, M. E., Halliday, G., Hokkanen, S. R. K., Hunter, S., Jicha, G. A., Katsumata, Y., Kawas, C. H., Keene, C. D., Kovacs, G. G., Kukull, W. A., Levey, A. I., Makkinejad, N., Montine, T. J., Murayama, S., Murray, M. E., Nag, S., Rissman, R. A., Seeley, W. W., Sperling, R. A., White Iii, C. L., Yu, L. & Schneider, J. A. 2019. Limbic-predominant age-related TDP-43 encephalopathy (LATE): consensus working group report. *Brain,* 142**,** 1503-1527.

Ngkelo, A., Meja, K., Yeadon, M., Adcock, I. & Kirkham, P. A. 2012. LPS induced inflammatory responses in human peripheral blood mononuclear cells is mediated through NOX4 and Giα dependent PI-3kinase signalling. *Journal of inflammation (London, England),* 9**,** 1-1.

Nguyen, J. T., Ray, C., Fox, A. L., Mendonca, D. B., Kim, J. K. & Krebsbach, P. H. 2018. Mammalian EAK-7 activates alternative mTOR signaling to regulate cell proliferation and migration. *Sci Adv,* 4**,** eaao5838.

Nguyen, T. A., Hoivik, D., Lee, J. E. & Safe, S. 1999. Interactions of nuclear receptor coactivator/corepressor proteins with the aryl hydrocarbon receptor complex. *Arch Biochem Biophys,* 367**,** 250-7.

Nilsson, M. E., Vandenput, L., Tivesten, A., Norlen, A. K., Lagerquist, M. K., Windahl, S. H., Borjesson, A. E., Farman, H. H., Poutanen, M., Benrick, A., Maliqueo, M., Stener-Victorin, E., Ryberg, H. & Ohlsson, C. 2015. Measurement of a Comprehensive Sex Steroid Profile in Rodent Serum by High-Sensitive Gas Chromatography-Tandem Mass Spectrometry. *Endocrinology,* 156**,** 2492-502.

Nimse, S. B. & Pal, D. 2015. Free radicals, natural antioxidants, and their reaction mechanisms. *RSC Advances,* 5**,** 27986-28006.

Niraula, A., Sheridan, J. F. & Godbout, J. P. 2017. Microglia Priming with Aging and Stress. *Neuropsychopharmacology,* 42**,** 318-333.

Nishihara, E., Yoshida-Komiya, H., Chan, C. S., Liao, L., Davis, R. L., O'malley, B. W. & Xu, J. 2003. SRC-1 null mice exhibit moderate motor dysfunction and delayed development of cerebellar Purkinje cells. *J Neurosci,* 23**,** 213-22.

Nishimura, A. L., Mitne-Neto, M., Silva, H. C., Richieri-Costa, A., Middleton, S., Cascio, D., Kok, F., Oliveira, J. R., Gillingwater, T., Webb, J., Skehel, P. & Zatz, M. 2004. A mutation in the vesicle-trafficking protein VAPB causes late-onset spinal muscular atrophy and amyotrophic lateral sclerosis. *Am J Hum Genet,* 75**,** 822-31.

Nixon, R. A. 2017. Amyloid precursor protein and endosomal-lysosomal dysfunction in Alzheimer's disease: inseparable partners in a multifactorial disease. *FASEB J,* 31**,** 2729-2743.

Norden, D. M. & Godbout, J. P. 2013. Review: microglia of the aged brain: primed to be activated and resistant to regulation. *Neuropathology and applied neurobiology,* 39**,** 19-34.

O'leary, N. A., Wright, M. W., Brister, J. R., Ciufo, S., Haddad, D., Mcveigh, R., Rajput, B., Robbertse, B., Smith-White, B., Ako-Adjei, D., Astashyn, A., Badretdin, A., Bao, Y.,

Blinkova, O., Brover, V., Chetvernin, V., Choi, J., Cox, E., Ermolaeva, O., Farrell, C. M., Goldfarb, T., Gupta, T., Haft, D., Hatcher, E., Hlavina, W., Joardar, V. S., Kodali, V. K., Li, W., Maglott, D., Masterson, P., Mcgarvey, K. M., Murphy, M. R., O'neill, K., Pujar, S., Rangwala, S. H., Rausch, D., Riddick, L. D., Schoch, C., Shkeda, A., Storz, S. S., Sun, H., Thibaud-Nissen, F., Tolstoy, I., Tully, R. E., Vatsan, A. R., Wallin, C., Webb, D., Wu, W., Landrum, M. J., Kimchi, A., Tatusova, T., Dicuccio, M., Kitts, P., Murphy, T. D. & Pruitt, K. D. 2016. Reference sequence (RefSeq) database at NCBI: current status, taxonomic expansion, and functional annotation. *Nucleic Acids Res,* 44**,** D733-45.

Oki, S., Ohta, T., Shioi, G., Hatanaka, H., Ogasawara, O., Okuda, Y., Kawaji, H., Nakaki, R., Sese, J. & Meno, C. 2018. ChIP-Atlas: a data-mining suite powered by full integration of public ChIP-seq data. *EMBO Rep,* 19.

Olah, M., Patrick, E., Villani, A. C., Xu, J., White, C. C., Ryan, K. J., Piehowski, P., Kapasi, A., Nejad, P., Cimpean, M., Connor, S., Yung, C. J., Frangieh, M., Mchenry, A., Elyaman, W., Petyuk, V., Schneider, J. A., Bennett, D. A., De Jager, P. L. & Bradshaw, E. M. 2018. A transcriptomic atlas of aged human microglia. *Nat Commun,* 9**,** 539.

Oliver, P. L., Finelli, M. J., Edwards, B., Bitoun, E., Butts, D. L., Becker, E. B., Cheeseman, M. T., Davies, B. & Davies, K. E. 2011. Oxr1 is essential for protection against oxidative stress-induced neurodegeneration. *PLoS Genet,* 7**,** e1002338.

Orre, M., Kamphuis, W., Osborn, L. M., Melief, J., Kooijman, L., Huitinga, I., Klooster, J., Bossers, K. & Hol, E. M. 2014. Acute isolation and transcriptome characterization of cortical astrocytes and microglia from young and aged mice. *Neurobiol Aging,* 35**,** 1-14.

Ott, M., Gogvadze, V., Orrenius, S. & Zhivotovsky, B. 2007. Mitochondria, oxidative stress and cell death. *Apoptosis,* 12**,** 913-22.

Pankratz, N., Pauciulo, M. W., Elsaesser, V. E., Marek, D. K., Halter, C. A., Wojcieszek, J., Rudolph, A., Shults, C. W., Foroud, T., Nichols, W. C. & Parkinson Study Group, P. I. 2006. Mutations in DJ-1 are rare in familial Parkinson disease. *Neurosci Lett,* 408**,** 209-13.

Papadopoulos, C. & Meyer, H. 2017. Detection and Clearance of Damaged Lysosomes by the Endo-Lysosomal Damage Response and Lysophagy. *Curr Biol,* 27**,** R1330-R1341.

Papaioannou, V. E. & Behringer, R. R. 2012. Early embryonic lethality in genetically engineered mice: diagnosis and phenotypic analysis. *Vet Pathol,* 49**,** 64-70.

Paramanik, V. & Thakur, M. K. 2010. Interaction of Estrogen Receptor Associated Protein (ERAP) 140 with ER beta decreases but its expression increases in aging mouse cerebral cortex. *Cell Mol Neurobiol,* 30**,** 961-6.

Parente, M. K., Rozen, R., Cearley, C. N. & Wolfe, J. H. 2012. Dysregulation of gene expression in a lysosomal storage disease varies between brain regions implicating unexpected mechanisms of neuropathology. *PLoS One,* 7**,** e32419.

Park, J. J., Gondre-Lewis, M. C., Eiden, L. E. & Loh, Y. P. 2011. A distinct trans-Golgi network subcompartment for sorting of synaptic and granule proteins in neurons and neuroendocrine cells. *J Cell Sci,* 124**,** 735-44.

Park, S. A., Ahn, S. I. & Gallo, J. M. 2016. Tau mis-splicing in the pathogenesis of neurodegenerative disorders. *BMB Rep,* 49**,** 405-13.

Parmigiani, R. B., Xu, W. S., Venta-Perez, G., Erdjument-Bromage, H., Yaneva, M., Tempst, P. & Marks, P. A. 2008. HDAC6 is a specific deacetylase of peroxiredoxins and is involved in redox regulation. *Proc Natl Acad Sci U S A,* 105**,** 9633-8.

Parsonage, D., Youngblood, D. S., Sarma, G. N., Wood, Z. A., Karplus, P. A. & Poole, L. B. 2005. Analysis of the Link between Enzymatic Activity and Oligomeric State in AhpC, a Bacterial Peroxiredoxin(,). *Biochemistry,* 44**,** 10.1021/bi050448i.

Patel, R., Zenith, R. K., Chandra, A. & Ali, A. 2017. Novel Mutations in the Crystallin Gene in Age-Related Cataract Patients from a North Indian Population. *Mol Syndromol,* 8**,** 179-186.

Patten, D. A., Germain, M., Kelly, M. A. & Slack, R. S. 2010. Reactive oxygen species: stuck in the middle of neurodegeneration. *J Alzheimers Dis,* 20 Suppl 2**,** S357-67.

Pearson, P., Lewis, S. A., Britton, J., Young, I. S. & Fogarty, A. 2006. The pro-oxidant activity of high-dose vitamin E supplements in vivo. *BioDrugs,* 20**,** 271-3.

Pedersen, J. T. & Heegaard, N. H. 2013. Analysis of protein aggregation in neurodegenerative disease. *Anal Chem,* 85**,** 4215-27.

Pembroke, W. G., Babbs, A., Davies, K. E., Ponting, C. P. & Oliver, P. L. 2015. Temporal transcriptomics suggest that twin-peaking genes reset the clock. *Elife,* 4.

Perry, V. H. & Holmes, C. 2014. Microglial priming in neurodegenerative disease. *Nat Rev Neurol,* 10**,** 217-24.

Persson, T., Popescu, B. O. & Cedazo-Minguez, A. 2014. Oxidative stress in Alzheimer's disease: why did antioxidant therapy fail? *Oxid Med Cell Longev,* 2014**,** 427318.

Pervouchine, D. D., Djebali, S., Breschi, A., Davis, C. A., Barja, P. P., Dobin, A., Tanzer, A., Lagarde, J., Zaleski, C., See, L. H., Fastuca, M., Drenkow, J., Wang, H., Bussotti, G., Pei, B., Balasubramanian, S., Monlong, J., Harmanci, A., Gerstein, M., Beer, M. A., Notredame, C., Guigo, R. & Gingeras, T. R. 2015. Enhanced transcriptome maps from multiple mouse tissues reveal evolutionary constraint in gene expression. *Nat Commun,* 6**,** 5903.

Phalen, T. J., Weirather, K., Deming, P. B., Anathy, V., Howe, A. K., Van Der Vliet, A., Jonsson, T. J., Poole, L. B. & Heintz, N. H. 2006. Oxidation state governs structural transitions in peroxiredoxin II that correlate with cell cycle arrest and recovery. *J Cell Biol,* 175**,** 779-89.

Pieper, A., Rudolph, S., Wieser, G. L., Gotze, T., Miessner, H., Yonemasu, T., Yan, K., Tzvetanova, I., Castillo, B. D., Bode, U., Bormuth, I., Wadiche, J. I., Schwab, M. H. & Goebbels, S. 2019. NeuroD2 controls inhibitory circuit formation in the molecular layer of the cerebellum. *Sci Rep,* 9**,** 1448.

Pierce, A., Podlutskaya, N., Halloran, J. J., Hussong, S. A., Lin, P. Y., Burbank, R., Hart, M. J. & Galvan, V. 2013. Over-expression of heat shock factor 1 phenocopies the effect of chronic inhibition of TOR by rapamycin and is sufficient to ameliorate Alzheimer's-like deficits in mice modeling the disease. *J Neurochem,* 124**,** 880-93.

Pislar, A., Tratnjek, L., Glavan, G., Zivin, M. & Kos, J. 2018. Upregulation of Cysteine Protease Cathepsin X in the 6-Hydroxydopamine Model of Parkinson's Disease. *Front Mol Neurosci,* 11**,** 412.

Poole, L. B., Hall, A. & Nelson, K. J. 2011. Overview of peroxiredoxins in oxidant defense and redox regulation. *Curr Protoc Toxicol,* Chapter 7**,** Unit7 9.

Powis, K., Schrul, B., Tienson, H., Gostimskaya, I., Breker, M., High, S., Schuldiner, M., Jakob, U. & Schwappach, B. 2013. Get3 is a holdase chaperone and moves to deposition sites for aggregated proteins when membrane targeting is blocked. *J Cell Sci,* 126**,** 473-83.

Prince, M., Bryce, R., Albanese, E., Wimo, A., Ribeiro, W. & Ferri, C. P. 2013. The global prevalence of dementia: a systematic review and metaanalysis. *Alzheimers Dement,* 9**,** 63-75 e2.

Przedborski, S. 2007. Peroxiredoxin-2 links Cdk5 to neurodegeneration. *Nat Med,* 13**,** 907-909.

Raj, D., Yin, Z., Breur, M., Doorduin, J., Holtman, I. R., Olah, M., Mantingh-Otter, I. J., Van Dam, D., De Deyn, P. P., Den Dunnen, W., Eggen, B. J. L., Amor, S. & Boddeke, E. 2017.

Increased White Matter Inflammation in Aging- and Alzheimer's Disease Brain. *Front Mol Neurosci,* 10**,** 206.
Randall, L. M., Manta, B., Hugo, M., Gil, M., Batthyany, C., Trujillo, M., Poole, L. B. & Denicola, A. 2014. Nitration transforms a sensitive peroxiredoxin 2 into a more active and robust peroxidase. *J Biol Chem,* 289**,** 15536-43.
Raninga, P. V., Di Trapani, G. & Tonissen, K. F. 2017. The Multifaceted Roles of DJ-1 as an Antioxidant. *Adv Exp Med Biol,* 1037**,** 67-87.
Ransohoff, R. M. 2016. How neuroinflammation contributes to neurodegeneration. *Science,* 353**,** 777-83.
Rapanelli, M., Frick, L. R. & Pittenger, C. 2017. The Role of Interneurons in Autism and Tourette Syndrome. *Trends Neurosci,* 40**,** 397-407.
Rashid, H. O., Yadav, R. K., Kim, H. R. & Chae, H. J. 2015. ER stress: Autophagy induction, inhibition and selection. *Autophagy,* 11**,** 1956-1977.
Reed, T. T. 2011. Lipid peroxidation and neurodegenerative disease. *Free Radic Biol Med,* 51**,** 1302-19.
Reed, T. T., Pierce, W. M., Jr., Turner, D. M., Markesbery, W. R. & Butterfield, D. A. 2009. Proteomic identification of nitrated brain proteins in early Alzheimer's disease inferior parietal lobule. *J Cell Mol Med,* 13**,** 2019-29.
Rehman, A. U., Santos-Cortez, R. L., Morell, R. J., Drummond, M. C., Ito, T., Lee, K., Khan, A. A., Basra, M. A., Wasif, N., Ayub, M., Ali, R. A., Raza, S. I., University of Washington Center for Mendelian, G., Nickerson, D. A., Shendure, J., Bamshad, M., Riazuddin, S., Billington, N., Khan, S. N., Friedman, P. L., Griffith, A. J., Ahmad, W., Riazuddin, S., Leal, S. M. & Friedman, T. B. 2014. Mutations in TBC1D24, a gene associated with epilepsy, also cause nonsyndromic deafness DFNB86. *Am J Hum Genet,* 94**,** 144-52.
Reichel, C. A., Rehberg, M., Lerchenberger, M., Berberich, N., Bihari, P., Khandoga, A. G., Zahler, S. & Krombach, F. 2009. Ccl2 and Ccl3 mediate neutrophil recruitment via induction of protein synthesis and generation of lipid mediators. *Arterioscler Thromb Vasc Biol,* 29**,** 1787-93.
Rhee, S. G. 2016. Overview on Peroxiredoxin. *Mol Cells,* 39**,** 1-5.
Rhee, S. G. & Woo, H. A. 2011. Multiple functions of peroxiredoxins: peroxidases, sensors and regulators of the intracellular messenger H(2)O(2), and protein chaperones. *Antioxid Redox Signal,* 15**,** 781-94.
Robelin, L. & Gonzalez De Aguilar, J. L. 2014. Blood biomarkers for amyotrophic lateral sclerosis: myth or reality? *Biomed Res Int,* 2014**,** 525097.
Rock, R. B., Hu, S., Deshpande, A., Munir, S., May, B. J., Baker, C. A., Peterson, P. K. & Kapur, V. 2005. Transcriptional response of human microglial cells to interferon-gamma. *Genes Immun,* 6**,** 712-9.
Rosenbloom, K. R., Sloan, C. A., Malladi, V. S., Dreszer, T. R., Learned, K., Kirkup, V. M., Wong, M. C., Maddren, M., Fang, R., Heitner, S. G., Lee, B. T., Barber, G. P., Harte, R. A., Diekhans, M., Long, J. C., Wilder, S. P., Zweig, A. S., Karolchik, D., Kuhn, R. M., Haussler, D. & Kent, W. J. 2013. ENCODE data in the UCSC Genome Browser: year 5 update. *Nucleic Acids Res,* 41**,** D56-63.
Rossler, O. G. & Thiel, G. 2017. Specificity of Stress-Responsive Transcription Factors Nrf2, ATF4, and AP-1. *J Cell Biochem,* 118**,** 127-140.
Roy, M., Sorokina, O., Mclean, C., Tapia-Gonzalez, S., Defelipe, J., Armstrong, J. D. & Grant, S. G. N. 2018. Regional Diversity in the Postsynaptic Proteome of the Mouse Brain. *Proteomes,* 6.
Rudzka, D. A., Cameron, J. M. & Olson, M. F. 2015. Reactive oxygen species and hydrogen peroxide generation in cell migration. *Commun Integr Biol,* 8**,** e1074360.

Rusinova, I., Forster, S., Yu, S., Kannan, A., Masse, M., Cumming, H., Chapman, R. & Hertzog, P. J. 2013. Interferome v2.0: an updated database of annotated interferon-regulated genes. *Nucleic Acids Res,* 41**,** D1040-6.

Ryskalin, L., Lazzeri, G., Flaibani, M., Biagioni, F., Gambardella, S., Frati, A. & Fornai, F. 2017. mTOR-Dependent Cell Proliferation in the Brain. *Biomed Res Int,* 2017**,** 7082696.

Saccon, R. A., Bunton-Stasyshyn, R. K. A., Fisher, E. M. C. & Fratta, P. 2013. Is SOD1 loss of function involved in amyotrophic lateral sclerosis? *Brain : a journal of neurology,* 136**,** 2342-2358.

Sakai, A., Nakato, R., Ling, Y., Hou, X., Hara, N., Iijima, T., Yanagawa, Y., Kuwano, R., Okuda, S., Shirahige, K. & Sugiyama, S. 2017. Genome-Wide Target Analyses of Otx2 Homeoprotein in Postnatal Cortex. *Front Neurosci,* 11**,** 307.

Salzano, S., Checconi, P., Hanschmann, E. M., Lillig, C. H., Bowler, L. D., Chan, P., Vaudry, D., Mengozzi, M., Coppo, L., Sacre, S., Atkuri, K. R., Sahaf, B., Herzenberg, L. A., Herzenberg, L. A., Mullen, L. & Ghezzi, P. 2014. Linkage of inflammation and oxidative stress via release of glutathionylated peroxiredoxin-2, which acts as a danger signal. *Proc Natl Acad Sci U S A,* 111**,** 12157-62.

Sanada, Y., Asai, S., Ikemoto, A., Moriwaki, T., Nakamura, N., Miyaji, M. & Zhang-Akiyama, Q. M. 2014. Oxidation resistance 1 is essential for protection against oxidative stress and participates in the regulation of aging in Caenorhabditis elegans. *Free Radic Res,* 48**,** 919-28.

Sanchez-Lopez, F., Tasset, I., Aguera, E., Feijoo, M., Fernandez-Bolanos, R., Sanchez, F. M., Ruiz, M. C., Cruz, A. H., Gascon, F. & Tunez, I. 2012. Oxidative stress and inflammation biomarkers in the blood of patients with Huntington's disease. *Neurol Res,* 34**,** 721-4.

Sasahara, K., Shikimi, H., Haraguchi, S., Sakamoto, H., Honda, S., Harada, N. & Tsutsui, K. 2007. Mode of action and functional significance of estrogen-inducing dendritic growth, spinogenesis, and synaptogenesis in the developing Purkinje cell. *J Neurosci,* 27**,** 7408-17.

Seo, W. & Taniuchi, I. 2016. Transcriptional regulation of early T-cell development in the thymus. *Eur J Immunol,* 46**,** 531-8.

Seo, Y., Kim, H. S., Kang, I., Choi, S. W., Shin, T. H., Shin, J. H., Lee, B. C., Lee, J. Y., Kim, J. J., Kook, M. G. & Kang, K. S. 2016. Cathepsin S contributes to microglia-mediated olfactory dysfunction through the regulation of Cx3cl1-Cx3cr1 axis in a Niemann-Pick disease type C1 model. *Glia,* 64**,** 2291-2305.

Shao, W., Halachmi, S. & Brown, M. 2002. ERAP140, a conserved tissue-specific nuclear receptor coactivator. *Mol Cell Biol,* 22**,** 3358-72.

Sharma, M., Burre, J. & Sudhof, T. C. 2011. CSPalpha promotes SNARE-complex assembly by chaperoning SNAP-25 during synaptic activity. *Nat Cell Biol,* 13**,** 30-9.

Shepherd, G. M. 2004. *The Synaptic Organization of the Brain*, Oxford University Press, USA.

Shi, S., Wang, C., Acton, A. J., Eckert, G. J. & Trippel, S. B. 2015. Role of sox9 in growth factor regulation of articular chondrocytes. *J Cell Biochem,* 116**,** 1391-400.

Shiraki, T., Kondo, S., Katayama, S., Waki, K., Kasukawa, T., Kawaji, H., Kodzius, R., Watahiki, A., Nakamura, M., Arakawa, T., Fukuda, S., Sasaki, D., Podhajska, A., Harbers, M., Kawai, J., Carninci, P. & Hayashizaki, Y. 2003. Cap analysis gene expression for high-throughput analysis of transcriptional starting point and identification of promoter usage. *Proc Natl Acad Sci U S A,* 100**,** 15776-81.

Shkolnik, K., Ben-Dor, S., Galiani, D., Hourvitz, A. & Dekel, N. 2008. Molecular characterization and bioinformatics analysis of Ncoa7B, a novel ovulation-associated and reproduction system-specific Ncoa7 isoform. *Reproduction,* 135**,** 321-33.

Shurtleff, M. J., Itzhak, D. N., Hussmann, J. A., Schirle Oakdale, N. T., Costa, E. A., Jonikas, M., Weibezahn, J., Popova, K. D., Jan, C. H., Sinitcyn, P., Vembar, S. S., Hernandez, H., Cox, J., Burlingame, A. L., Brodsky, J. L., Frost, A., Borner, G. H. & Weissman, J. S. 2018. The ER membrane protein complex interacts cotranslationally to enable biogenesis of multipass membrane proteins. *Elife,* 7.

Simic, G., Babic Leko, M., Wray, S., Harrington, C., Delalle, I., Jovanov-Milosevic, N., Bazadona, D., Buee, L., De Silva, R., Di Giovanni, G., Wischik, C. & Hof, P. R. 2016. Tau Protein Hyperphosphorylation and Aggregation in Alzheimer's Disease and Other Tauopathies, and Possible Neuroprotective Strategies. *Biomolecules,* 6**,** 6.

Siskova, Z. & Tremblay, M. E. 2013. Microglia and synapse: interactions in health and neurodegeneration. *Neural Plast,* 2013**,** 425845.

Skoumalova, A. & Hort, J. 2012. Blood markers of oxidative stress in Alzheimer's disease. *J Cell Mol Med,* 16**,** 2291-300.

Sluchanko, N. N. & Gusev, N. B. 2017. Moonlighting chaperone-like activity of the universal regulatory 14-3-3 proteins. *FEBS J,* 284**,** 1279-1295.

Small, G. W., Siddarth, P., Li, Z., Miller, K. J., Ercoli, L., Emerson, N. D., Martinez, J., Wong, K. P., Liu, J., Merrill, D. A., Chen, S. T., Henning, S. M., Satyamurthy, N., Huang, S. C., Heber, D. & Barrio, J. R. 2018. Memory and Brain Amyloid and Tau Effects of a Bioavailable Form of Curcumin in Non-Demented Adults: A Double-Blind, Placebo-Controlled 18-Month Trial. *Am J Geriatr Psychiatry,* 26**,** 266-277.

Smith, M. & Wilkinson, S. 2017. ER homeostasis and autophagy. *Essays Biochem,* 61**,** 625-635.

Somyajit, K., Gupta, R., Sedlackova, H., Neelsen, K. J., Ochs, F., Rask, M. B., Choudhary, C. & Lukas, J. 2017. Redox-sensitive alteration of replisome architecture safeguards genome integrity. *Science,* 358**,** 797-802.

Spittau, B. 2017. Aging Microglia-Phenotypes, Functions and Implications for Age-Related Neurodegenerative Diseases. *Front Aging Neurosci,* 9**,** 194.

Stashi, E., Lanz, R. B., Mao, J., Michailidis, G., Zhu, B., Kettner, N. M., Putluri, N., Reineke, E. L., Reineke, L. C., Dasgupta, S., Dean, A., Stevenson, C. R., Sivasubramanian, N., Sreekumar, A., Demayo, F., York, B., Fu, L. & O'malley, B. W. 2014. SRC-2 is an essential coactivator for orchestrating metabolism and circadian rhythm. *Cell Rep,* 6**,** 633-45.

Stoka, V., Turk, V. & Turk, B. 2016. Lysosomal cathepsins and their regulation in aging and neurodegeneration. *Ageing Res Rev,* 32**,** 22-37.

Strazisar, B. G., Neubauer, D., Paro Panjan, D. & Writzl, K. 2015. Early-onset epileptic encephalopathy with hearing loss in two siblings with TBC1D24 recessive mutations. *Eur J Paediatr Neurol,* 19**,** 251-6.

Strobbe, D., Robinson, A. A., Harvey, K., Rossi, L., Ferraina, C., De Biase, V., Rodolfo, C., Harvey, R. J. & Campanella, M. 2018. Distinct Mechanisms of Pathogenic DJ-1 Mutations in Mitochondrial Quality Control. *Front Mol Neurosci,* 11**,** 68.

Study, G. 2016. Global, regional, and national incidence, prevalence, and years lived with disability for 310 diseases and injuries, 1990-2015: a systematic analysis for the Global Burden of Disease Study 2015. *Lancet,* 388**,** 1545-1602.

Sun, L., Zhao, Y., Zhou, K., Freeze, H. H., Zhang, Y. W. & Xu, H. 2013. Insufficient ER-stress response causes selective mouse cerebellar granule cell degeneration resembling that seen in congenital disorders of glycosylation. *Mol Brain,* 6**,** 52.

Sun-Wada, G., Murata, Y., Yamamoto, A., Kanazawa, H., Wada, Y. & Futai, M. 2000. Acidic endomembrane organelles are required for mouse postimplantation development. *Dev Biol,* 228**,** 315-25.

Sunico, C. R., Sultan, A., Nakamura, T., Dolatabadi, N., Parker, J., Shan, B., Han, X., Yates, J. R., 3rd, Masliah, E., Ambasudhan, R., Nakanishi, N. & Lipton, S. A. 2016. Role of sulfiredoxin as a peroxiredoxin-2 denitrosylase in human iPSC-derived dopaminergic neurons. *Proc Natl Acad Sci U S A,* 113**,** E7564-E7571.

Svistunova, D. M., Simon, J. N., Rembeza, E., Crabtree, M., Yue, W. W., Oliver, P. L. & Finelli, M. J. 2018. Oxidation resistance 1 regulates post-translational modifications of peroxiredoxin 2 in the cerebellum. *Free Radic Biol Med,* 130**,** 151-162.

Sztal, T. E., Mckaige, E. A., Williams, C., Ruparelia, A. A. & Bryson-Richardson, R. J. 2018. Genetic compensation triggered by actin mutation prevents the muscle damage caused by loss of actin protein. *PLoS Genet,* 14**,** e1007212.

Tabula Muris, C., Overall, C., Logistical, C., Organ, C., Processing, Library, P., Sequencing, Computational Data, A., Cell Type, A., Writing, G., Supplemental Text Writing, G. & Principal, I. 2018. Single-cell transcriptomics of 20 mouse organs creates a Tabula Muris. *Nature,* 562**,** 367-372.

Tahara, Y. & Shibata, S. 2016. Circadian rhythms of liver physiology and disease: experimental and clinical evidence. *Nat Rev Gastroenterol Hepatol,* 13**,** 217-26.

Tai, Y. F., Pavese, N., Gerhard, A., Tabrizi, S. J., Barker, R. A., Brooks, D. J. & Piccini, P. 2007. Microglial activation in presymptomatic Huntington's disease gene carriers. *Brain,* 130**,** 1759-1766.

Takahashi, H. & Kamio, Y. 2018. Acoustic startle response and its modulation in schizophrenia and autism spectrum disorder in Asian subjects. *Schizophr Res,* 198**,** 16-20.

Tal, O., Lim, H. Y., Gurevich, I., Milo, I., Shipony, Z., Ng, L. G., Angeli, V. & Shakhar, G. 2011. DC mobilization from the skin requires docking to immobilized CCL21 on lymphatic endothelium and intralymphatic crawling. *J Exp Med,* 208**,** 2141-53.

Tang, Y. & Le, W. 2016. Differential Roles of M1 and M2 Microglia in Neurodegenerative Diseases. *Mol Neurobiol,* 53**,** 1181-94.

Thannickal, V. J. & Fanburg, B. L. 2000. Reactive oxygen species in cell signaling. *American Journal of Physiology - Lung Cellular and Molecular Physiology,* 279**,** L1005-L1028.

Theurey, P. & Pizzo, P. 2018. The Aging Mitochondria. *Genes (Basel),* 9.

Thielens, N. M., Tedesco, F., Bohlson, S. S., Gaboriaud, C. & Tenner, A. J. 2017. C1q: A fresh look upon an old molecule. *Mol Immunol,* 89**,** 73-83.

Thorvaldsdottir, H., Robinson, J. T. & Mesirov, J. P. 2013. Integrative Genomics Viewer (IGV): high-performance genomics data visualization and exploration. *Brief Bioinform,* 14**,** 178-92.

Tian, Y., Wang, W., Xu, L., Li, H., Wei, Y., Wu, Q. & Jia, J. 2019. Activation of Nrf2/ARE pathway alleviates the cognitive deficits in PS1V97L-Tg mouse model of Alzheimer's disease through modulation of oxidative stress. *J Neurosci Res,* 97**,** 492-505.

Tona, R., Chen, W., Nakano, Y., Reyes, L. D., Petralia, R. S., Wang, Y. X., Starost, M. F., Wafa, T. T., Morell, R. J., Cravedi, K. D., Hoffmann, J., Miyoshi, T., Munasinghe, J. P., Fitzgerald, T. S., Chudasama, Y., Omori, K., Pierpaoli, C., Banfi, B., Dong, L., Belyantseva, I. A. & Friedman, T. B. 2019. The phenotypic landscape of a Tbc1d24 mutant mouse includes convulsive seizures resembling human early infantile epileptic encephalopathy. *Hum Mol Genet*.

Toth, M. E., Szegedi, V., Varga, E., Juhasz, G., Horvath, J., Borbely, E., Csibrany, B., Alfoldi, R., Lenart, N., Penke, B. & Santha, M. 2013. Overexpression of Hsp27 ameliorates symptoms of Alzheimer's disease in APP/PS1 mice. *Cell Stress Chaperones,* 18**,** 759-71.

Trivisano, M., Bellusci, M., Terracciano, A., De Palma, L., Pietrafusa, N., Valeriani, M., Vigevano, F. & Specchio 2017. TBC1D24 gene mutations are associated with high risk of sudden unexpected death. *Epilepsy Behav,* 72**,** 208-209.

Tserel, L., Kolde, R., Rebane, A., Kisand, K., Org, T., Peterson, H., Vilo, J. & Peterson, P. 2010. Genome-wide promoter analysis of histone modifications in human monocyte-derived antigen presenting cells. *BMC Genomics,* 11**,** 642.

Vaahtomeri, K., Brown, M., Hauschild, R., De Vries, I., Leithner, A. F., Mehling, M., Kaufmann, W. A. & Sixt, M. 2017. Locally Triggered Release of the Chemokine CCL21 Promotes Dendritic Cell Transmigration across Lymphatic Endothelia. *Cell Rep,* 19**,** 902-909.

Van Den Berg, R., Kooijman, S., Noordam, R., Ramkisoensing, A., Abreu-Vieira, G., Tambyrajah, L. L., Dijk, W., Ruppert, P., Mol, I. M., Kramar, B., Caputo, R., Puig, L. S., De Ruiter, E. M., Kroon, J., Hoekstra, M., Van Der Sluis, R. J., Meijer, O. C., Willems Van Dijk, K., Van Kerkhof, L. W. M., Christodoulides, C., Karpe, F., Gerhart-Hines, Z., Kersten, S., Meijer, J. H., Coomans, C. P., Van Heemst, D., Biermasz, N. R. & Rensen, P. C. N. 2018. A Diurnal Rhythm in Brown Adipose Tissue Causes Rapid Clearance and Combustion of Plasma Lipids at Wakening. *Cell Rep,* 22**,** 3521-3533.

Van Der Reest, J., Lilla, S., Zheng, L., Zanivan, S. & Gottlieb, E. 2018. Proteome-wide analysis of cysteine oxidation reveals metabolic sensitivity to redox stress. *Nat Commun,* 9**,** 1581.

Vanier, M. T. & Millat, G. 2003. Niemann-Pick disease type C. *Clin Genet,* 64**,** 269-81.

Vanlandingham, P. A. & Ceresa, B. P. 2009. Rab7 regulates late endocytic trafficking downstream of multivesicular body biogenesis and cargo sequestration. *J Biol Chem,* 284**,** 12110-24.

Varvagiannis, K., Hanquinet, S., Billieux, M. H., De Luca, R., Rimensberger, P., Lidgren, M., Guipponi, M., Makrythanasis, P., Blouin, J. L., Antonarakis, S. E., Steinfeld, R., Kern, I., Poretti, A., Fluss, J. & Fokstuen, S. 2018. Congenital Neuronal Ceroid Lipofuscinosis with a Novel CTSD Gene Mutation: A Rare Cause of Neonatal-Onset Neurodegenerative Disorder. *Neuropediatrics,* 49**,** 150-153.

Veal, E. A., Underwood, Z. E., Tomalin, L. E., Morgan, B. A. & Pillay, C. S. 2018. Hyperoxidation of Peroxiredoxins: Gain or Loss of Function? *Antioxid Redox Signal,* 28**,** 574-590.

Verkhratsky, A. & Nedergaard, M. 2018. Physiology of Astroglia. *Physiol Rev,* 98**,** 239-389.

Villa, A., Vegeto, E., Poletti, A. & Maggi, A. 2016. Estrogens, Neuroinflammation, and Neurodegeneration. *Endocr Rev,* 37**,** 372-402.

Vivekanantham, S., Shah, S., Dewji, R., Dewji, A., Khatri, C. & Ologunde, R. 2015. Neuroinflammation in Parkinson's disease: role in neurodegeneration and tissue repair. *Int J Neurosci,* 125**,** 717-25.

Volkert, M. R., Elliott, N. A. & Housman, D. E. 2000. Functional genomics reveals a family of eukaryotic oxidation protection genes. *Proc Natl Acad Sci U S A,* 97**,** 14530-5.

Volkert, M. R., Wang, J. Y. & Elliott, N. A. 2008. A functional genomics approach to identify and characterize oxidation resistance genes. *Methods Mol Biol,* 477**,** 331-42.

Von Bergen, M., Barghorn, S., Li, L., Marx, A., Biernat, J., Mandelkow, E. M. & Mandelkow, E. 2001. Mutations of tau protein in frontotemporal dementia promote aggregation of paired helical filaments by enhancing local beta-structure. *J Biol Chem,* 276**,** 48165-74.

Von Bernhardi, R., Eugenin-Von Bernhardi, L. & Eugenin, J. 2015. Microglial cell dysregulation in brain aging and neurodegeneration. *Front Aging Neurosci,* 7**,** 124.

Von Bernhardi, R., Heredia, F., Salgado, N. & Muñoz, P. 2016. Microglia Function in the Normal Brain. *In:* VON BERNHARDI, R. (ed.) *Glial Cells in Health and Disease of the CNS.* Cham: Springer International Publishing.

Wafer, R., Tandon, P. & Minchin, J. E. N. 2017. The Role of Peroxisome Proliferator-Activated Receptor Gamma (PPARG) in Adipogenesis: Applying Knowledge from the Fish Aquaculture Industry to Biomedical Research. *Front Endocrinol (Lausanne),* 8**,** 102.

Wagh, D. A., Rasse, T. M., Asan, E., Hofbauer, A., Schwenkert, I., Durrbeck, H., Buchner, S., Dabauvalle, M. C., Schmidt, M., Qin, G., Wichmann, C., Kittel, R., Sigrist, S. J. & Buchner, E. 2006. Bruchpilot, a protein with homology to ELKS/CAST, is required for structural integrity and function of synaptic active zones in Drosophila. *Neuron,* 49**,** 833-44.

Walloe, S., Pakkenberg, B. & Fabricius, K. 2014. Stereological estimation of total cell numbers in the human cerebral and cerebellar cortex. *Front Hum Neurosci,* 8**,** 508.

Walsh, C. A., Qin, L., Tien, J. C., Young, L. S. & Xu, J. 2012. The function of steroid receptor coactivator-1 in normal tissues and cancer. *Int J Biol Sci,* 8**,** 470-85.

Walther, T. V. & Maddalo, D. 2012. Intracellular refolding assay. *J Vis Exp*.

Wang, B., Liu, Y., Huang, L., Chen, J., Li, J. J., Wang, R., Kim, E., Chen, Y., Justicia, C., Sakata, K., Chen, H., Planas, A., Ostrom, R. S., Li, W., Yang, G., Mcdonald, M. P., Chen, R., Heck, D. H. & Liao, F. F. 2017a. A CNS-permeable Hsp90 inhibitor rescues synaptic dysfunction and memory loss in APP-overexpressing Alzheimer's mouse model via an HSF1-mediated mechanism. *Mol Psychiatry,* 22**,** 990-1001.

Wang, J., Lin, W., Popko, B. & Campbell, I. L. 2004. Inducible production of interferon-gamma in the developing brain causes cerebellar dysplasia with activation of the Sonic hedgehog pathway. *Mol Cell Neurosci,* 27**,** 489-96.

Wang, Q., Liu, Y. & Zhou, J. 2015. Neuroinflammation in Parkinson's disease and its potential as therapeutic target. *Transl Neurodegener,* 4.

Wang, W., Le, A. A., Hou, B., Lauterborn, J. C., Cox, C. D., Levin, E. R., Lynch, G. & Gall, C. M. 2018. Memory-Related Synaptic Plasticity Is Sexually Dimorphic in Rodent Hippocampus. *J Neurosci,* 38**,** 7935-7951.

Wang, X. & Michaelis, E. K. 2010. Selective neuronal vulnerability to oxidative stress in the brain. *Front Aging Neurosci,* 2**,** 12.

Wang, X., Zaidi, A., Pal, R., Garrett, A. S., Braceras, R., Chen, X. W., Michaelis, M. L. & Michaelis, E. K. 2009. Genomic and biochemical approaches in the discovery of mechanisms for selective neuronal vulnerability to oxidative stress. *BMC Neurosci,* 10**,** 12.

Wang, Y., Chen, J., Tang, W., Zhang, Y. & Li, X. 2017b. Rapamycin inhibits the proliferation of endothelial cells in hemangioma by blocking the mTOR-FABP4 pathway. *Biomed Pharmacother,* 85**,** 272-279.

Wang, Y. C., Lauwers, E. & Verstreken, P. 2017c. Presynaptic protein homeostasis and neuronal function. *Curr Opin Genet Dev,* 44**,** 38-46.

Wang, Y. T., Piyankarage, S. C., Williams, D. L. & Thatcher, G. R. 2014. Proteomic profiling of nitrosative stress: protein S-oxidation accompanies S-nitrosylation. *ACS Chem Biol,* 9**,** 821-30.

Wang, Z., Berkey, C. D. & Watnick, P. I. 2012. The Drosophila protein mustard tailors the innate immune response activated by the immune deficiency pathway. *J Immunol,* 188**,** 3993-4000.

Wang, Z., Hang, S., Purdy, A. E. & Watnick, P. I. 2013. Mutations in the IMD pathway and mustard counter Vibrio cholerae suppression of intestinal stem cell division in Drosophila. *MBio,* 4**,** e00337-13.

Watters, R. J., Hartmaier, R. J., Osmanbeyoglu, H. U., Gillihan, R. M., Rae, J. M., Liao, L., Chen, K., Li, W., Lu, X. & Oesterreich, S. 2017. Steroid receptor coactivator-1 can regulate osteoblastogenesis independently of estrogen. *Mol Cell Endocrinol,* 448**,** 21-27.

Whyte-Fagundes, P., Kurtenbach, S., Zoidl, C., Shestopalov, V. I., Carlen, P. L. & Zoidl, G. 2018. A Potential Compensatory Role of Panx3 in the VNO of a Panx1 Knock Out Mouse Model. *Front Mol Neurosci,* 11**,** 135.

Widmer, C., Gebauer, J. M., Brunstein, E., Rosenbaum, S., Zaucke, F., Drogemuller, C., Leeb, T. & Baumann, U. 2012. Molecular basis for the action of the collagen-specific chaperone Hsp47/SERPINH1 and its structure-specific client recognition. *Proc Natl Acad Sci U S A,* 109**,** 13243-7.

Wilke, S. A., Hall, B. J., Antonios, J. K., Denardo, L. A., Otto, S., Yuan, B., Chen, F., Robbins, E. M., Tiglio, K., Williams, M. E., Qiu, Z., Biederer, T. & Ghosh, A. 2012. NeuroD2 regulates the development of hippocampal mossy fiber synapses. *Neural Dev,* 7**,** 9.

Williams, T. W., Dumas, K. J. & Hu, P. J. 2010. EAK proteins: novel conserved regulators of C. elegans lifespan. *Aging (Albany NY),* 2**,** 742-7.

Williamson, M. G., Finelli, M. J., Sleigh, J. N., Reddington, A., Gordon, D., Talbot, K., Davies, K. E. & Oliver, P. L. 2019. Neuronal over-expression of OXR1 is protective against ALS-associated mutant TDP-43 mislocalisation in motor neurons and neuromuscular defects in vivo. *In press*.

Winter, M., Moser, M. A., Meunier, D., Fischer, C., Machat, G., Mattes, K., Lichtenberger, B. M., Brunmeir, R., Weissmann, S., Murko, C., Humer, C., Meischel, T., Brosch, G., Matthias, P., Sibilia, M. & Seiser, C. 2013. Divergent roles of HDAC1 and HDAC2 in the regulation of epidermal development and tumorigenesis. *EMBO J,* 32**,** 3176-91.

Wolfe, M. S. 2009. Tau mutations in neurodegenerative diseases. *J Biol Chem,* 284**,** 6021-5.

Wu, M. V. & Tollkuhn, J. 2017. Estrogen receptor alpha is required in GABAergic, but not glutamatergic, neurons to masculinize behavior. *Horm Behav,* 95**,** 3-12.

Wu, Y., Davies, K. E. & Oliver, P. L. 2016. The antioxidant protein Oxr1 influences aspects of mitochondrial morphology. *Free Radic Biol Med,* 95**,** 255-67.

Wyss-Coray, T. 2016. Ageing, neurodegeneration and brain rejuvenation. *Nature,* 539**,** 180-186.

Xu, P., Cao, X., He, Y., Zhu, L., Yang, Y., Saito, K., Wang, C., Yan, X., Hinton, A. O., Jr., Zou, F., Ding, H., Xia, Y., Yan, C., Shu, G., Wu, S. P., Yang, B., Feng, Y., Clegg, D. J., Demarchi, R., Khan, S. A., Tsai, S. Y., Demayo, F. J., Wu, Q., Tong, Q. & Xu, Y. 2015. Estrogen receptor-alpha in medial amygdala neurons regulates body weight. *J Clin Invest,* 125**,** 2861-76.

Yang, M., Lin, X., Rowe, A., Rognes, T., Eide, L. & Bjoras, M. 2015. Transcriptome analysis of human OXR1 depleted cells reveals its role in regulating the p53 signaling pathway. *Sci Rep,* 5**,** 17409.

Yang, M., Luna, L., Sorbo, J. G., Alseth, I., Johansen, R. F., Backe, P. H., Danbolt, N. C., Eide, L. & Bjoras, M. 2014. Human OXR1 maintains mitochondrial DNA integrity and counteracts hydrogen peroxide-induced oxidative stress by regulating antioxidant pathways involving p21. *Free Radic Biol Med,* 77**,** 41-8.

Yang, Y., Luo, Z., Hao, Y., Ba, W., Wang, R., Wang, W., Ding, X. & Li, C. 2017. mTOR-mediated Na(+)/Ca(2+) exchange affects cell proliferation and metastasis of melanoma cells. *Biomed Pharmacother,* 92**,** 744-749.

Yang, Y., Van Der Klaauw, A. A., Zhu, L., Cacciottolo, T. M., He, Y., Stadler, L. K. J., Wang, C., Xu, P., Saito, K., Hinton, A., Jr., Yan, X., Keogh, J. M., Henning, E., Banton, M. C., Hendricks, A. E., Bochukova, E. G., Mistry, V., Lawler, K. L., Liao, L., Xu, J., O'rahilly, S., Tong, Q., Consortium, U. K., Ines, B., O'malley, B. W., Farooqi, I. S. & Xu, Y. 2019. Steroid receptor coactivator-1 modulates the function of Pomc neurons and energy homeostasis. *Nat Commun,* 10**,** 1718.

Yao, J., Taylor, M., Davey, F., Ren, Y., Aiton, J., Coote, P., Fang, F., Chen, J. X., Yan, S. D. & Gunn-Moore, F. J. 2007. Interaction of amyloid binding alcohol dehydrogenase/Aβ

mediates up-regulation of peroxiredoxin II in the brains of Alzheimer's disease patients and a transgenic Alzheimer's disease mouse model. *Molecular and Cellular Neuroscience,* 35**,** 377-382.
Yelamanchili, S. V., Chaudhuri, A. D., Flynn, C. T. & Fox, H. S. 2011. Upregulation of cathepsin D in the caudate nucleus of primates with experimental parkinsonism. *Mol Neurodegener,* 6**,** 52.
Yim, Y. I., Sun, T., Wu, L. G., Raimondi, A., De Camilli, P., Eisenberg, E. & Greene, L. E. 2010. Endocytosis and clathrin-uncoating defects at synapses of auxilin knockout mice. *Proc Natl Acad Sci U S A,* 107**,** 4412-7.
Yin, B., Barrionuevo, G., Batinic-Haberle, I., Sandberg, M. & Weber, S. G. 2017. Differences in Reperfusion-Induced Mitochondrial Oxidative Stress and Cell Death Between Hippocampal CA1 and CA3 Subfields Are Due to the Mitochondrial Thioredoxin System. *Antioxid Redox Signal,* 27**,** 534-549.
Ying, Y. & Tao, Q. 2009. Epigenetic disruption of the WNT/ss-catenin signaling pathway in human cancers. *Epigenetics,* 4**,** 307-312.
Yoon, J., Hwang, Y. S., Lee, M., Sun, J., Cho, H. J., Knapik, L. & Daar, I. O. 2018. TBC1d24-ephrinB2 interaction regulates contact inhibition of locomotion in neural crest cell migration. *Nat Commun,* 9**,** 3491.
Yu, C. P., Lin, J. J. & Li, W. H. 2016. Positional distribution of transcription factor binding sites in Arabidopsis thaliana. *Sci Rep,* 6**,** 25164.
Yu, H., Yuan, B., Chu, Q., Wang, C. & Bi, H. 2019. Protective roles of isoastilbin against Alzheimer's disease via Nrf2mediated antioxidation and antiapoptosis. *Int J Mol Med,* 43**,** 1406-1416.
Yu, L., Croze, E., Yamaguchi, K. D., Tran, T., Reder, A. T., Litvak, V. & Volkert, M. R. 2015. Induction of a unique isoform of the NCOA7 oxidation resistance gene by interferon beta-1b. *J Interferon Cytokine Res,* 35**,** 186-99.
Zang, S., Ali, Y. O., Ruan, K. & Zhai, R. G. 2013. Nicotinamide mononucleotide adenylyltransferase maintains active zone structure by stabilizing Bruchpilot. *EMBO Rep,* 14**,** 87-94.
Zarate, S., Stevnsner, T. & Gredilla, R. 2017. Role of Estrogen and Other Sex Hormones in Brain Aging. Neuroprotection and DNA Repair. *Front Aging Neurosci,* 9**,** 430.
Zarouchlioti, C., Parfitt, D. A., Li, W., Gittings, L. M. & Cheetham, M. E. 2018. DNAJ Proteins in neurodegeneration: essential and protective factors. *Philos Trans R Soc Lond B Biol Sci,* 373.
Zhang, J., Perry, G., Smith, M. A., Robertson, D., Olson, S. J., Graham, D. G. & Montine, T. J. 1999. Parkinson's disease is associated with oxidative damage to cytoplasmic DNA and RNA in substantia nigra neurons. *Am J Pathol,* 154**,** 1423-9.
Zhang, L., Hu, L., Chai, Y., Pang, X., Yang, T. & Wu, H. 2014a. A dominant mutation in the stereocilia-expressing gene TBC1D24 is a probable cause for nonsyndromic hearing impairment. *Hum Mutat,* 35**,** 814-8.
Zhang, X., Zhang, S., Liu, X., Wang, Y., Chang, J., Zhang, X., Mackintosh, S. G., Tackett, A. J., He, Y., Lv, D., Laberge, R. M., Campisi, J., Wang, J., Zheng, G. & Zhou, D. 2018. Oxidation resistance 1 is a novel senolytic target. *Aging Cell***,** e12780.
Zhang, Y., Chen, K., Sloan, S. A., Bennett, M. L., Scholze, A. R., Keeffe, S., Phatnani, H. P., Guarnieri, P., Caneda, C., Ruderisch, N., Deng, S., Liddelow, S. A., Zhang, C., Daneman, R., Maniatis, T., Barres, B. A. & Wu, J. Q. 2014b. An RNA-sequencing transcriptome and splicing database of glia, neurons, and vascular cells of the cerebral cortex. *The Journal of Neuroscience,* 34**,** 11929.

Zhou, J., Qu, J., Yi, X. P., Graber, K., Huber, L., Wang, X., Gerdes, A. M. & Li, F. 2007. Upregulation of gamma-catenin compensates for the loss of beta-catenin in adult cardiomyocytes. *Am J Physiol Heart Circ Physiol,* 292**,** H270-6.

Zhou, Q., Lin, Y., Ye, J., Li, L., Hu, N., Wang, D. & Wang, Y. 2017a. Homozygous TBC1D24 Mutation in a Case of Epilepsia Partialis Continua. *Front Neurol,* 8**,** 750.

Zhou, S., Han, Q., Wang, R., Li, X., Wang, Q., Wang, H., Wang, J. & Ma, Y. 2016. PRDX2 protects hepatocellular carcinoma SMMC-7721 cells from oxidative stress. *Oncol Lett,* 12**,** 2217-2221.

Zhou, X., Han, T. L., Chen, H., Baker, P. N., Qi, H. & Zhang, H. 2017b. Impaired mitochondrial fusion, autophagy, biogenesis and dysregulated lipid metabolism is associated with preeclampsia. *Exp Cell Res,* 359**,** 195-204.

Zwirowski, S., Klosowska, A., Obuchowski, I., Nillegoda, N. B., Pirog, A., Zietkiewicz, S., Bukau, B., Mogk, A. & Liberek, K. 2017. Hsp70 displaces small heat shock proteins from aggregates to initiate protein refolding. *EMBO J,* 36**,** 783-796.